Cleavage and cell fates in Phoronida

D i s s e r t a t i o n

zur Erlangung des akademischen Grades

d o c t o r r e r u m n a t u r a l i u m

(Dr. rer. nat.)

im Fach Biologie

eingereicht an der

Lebenswissenschaftlichen Fakultät

der Humboldt-Universität zu Berlin

von

Mag. rer. nat. Markus Pennerstorfer

Präsident der Humboldt-Universität zu Berlin

Prof. Dr. Jan-Hendrik Olbertz

Dekan der Lebenswissenschaftlichen Fakultät

Prof. Dr. Richard Lucius

Gutachter/innen: 1. Prof. Dr. Gerhard Scholtz

2. PD Dr. Carsten Lüter

3. Dr. Andreas Hejnol

Tag der mündlichen Prüfung: 29. Juni 2015

Index

1. Introduction

1.1. Phoronida

Phoronida Hatschek, 1888 (also called horseshoe worms) is a group of exclusively marine invertebrates. The taxon is currently classified in two genera, *Phoronis* Wright, 1856 and *Phoronopsis* Gilchrist, 1907, which comprise some seven or eight and three valid species, respectively[*] (Emig 1974a, 1982; Hirose et al. 2014). Yet, the taxonomy is under debate, and there are indications that these numbers may underestimate the actual diversity (Santagata and Zimmer 2002; Santagata and Cohen 2009; Temereva 2009).

Adult phoronids are sessile tubicolous suspension feeders, with a rather uniform morphology (e.g., Hyman 1959; Emig 1982; Emig and de Mittelwihr 1999; Lüter et al. 2013). They occur worldwide, except in the polar seas, and live infaunal, from the intertidal to a maximum water depth of 400 meters. Their vermiform body is enclosed in a secreted chitinous tube, which is covered with substratum elements (e.g., sediment grains, detritus) (Fig. 1A-B,D-E). The anterior body end carries a characteristic tentacle apparatus, the so-called "lophophore" (Fig. 1C,F,I), the tentacles of which embrace the mouth, but not the likewise anterior anus of the animal (Hyman 1959). The lophophore serves for feeding and respiration and can be extended into the water current (Fig. 1A,G-H), or retracted inside the tube. The animal is anchored inside the tube with its thicker posterior body region, the "ampulla" (Fig. 1B,E). Phoronids live solitarily or in colonies of many individuals, and can be found embedded vertically in soft sediment or encrusting on, or buried in, hard substrata (Emig 1982). Ichnofossils interpreted as phoronid burrows or borings are known since the Devonian (Voigt 1975; Emig 1982, 2010). A molecular clock analysis suggested an origin of the group even not later than the Early Cambrian (Santagata and Cohen 2009).

Phoronids are either hermaphrodites or gonochoristic (e.g., Silén 1954; Emig 1977, 1982; Temereva and Malakhov 2012). The germ cells develop in gonads situated within a special "vasoperitoneal" tissue in the posterior body region. Mature gametes are freely floating within the trunk coelom (Fig. 1B-C), before they are released through the anterior nephridiopores. Fertilization seems to be internal and cross-fertilization appears to be the rule (Emig 1982). In

[*] For convenience, in the present study, *Phoronis* is abbreviated with "*P.*", whereas *Phoronopsis* is abbreviated with "*Ph.*".

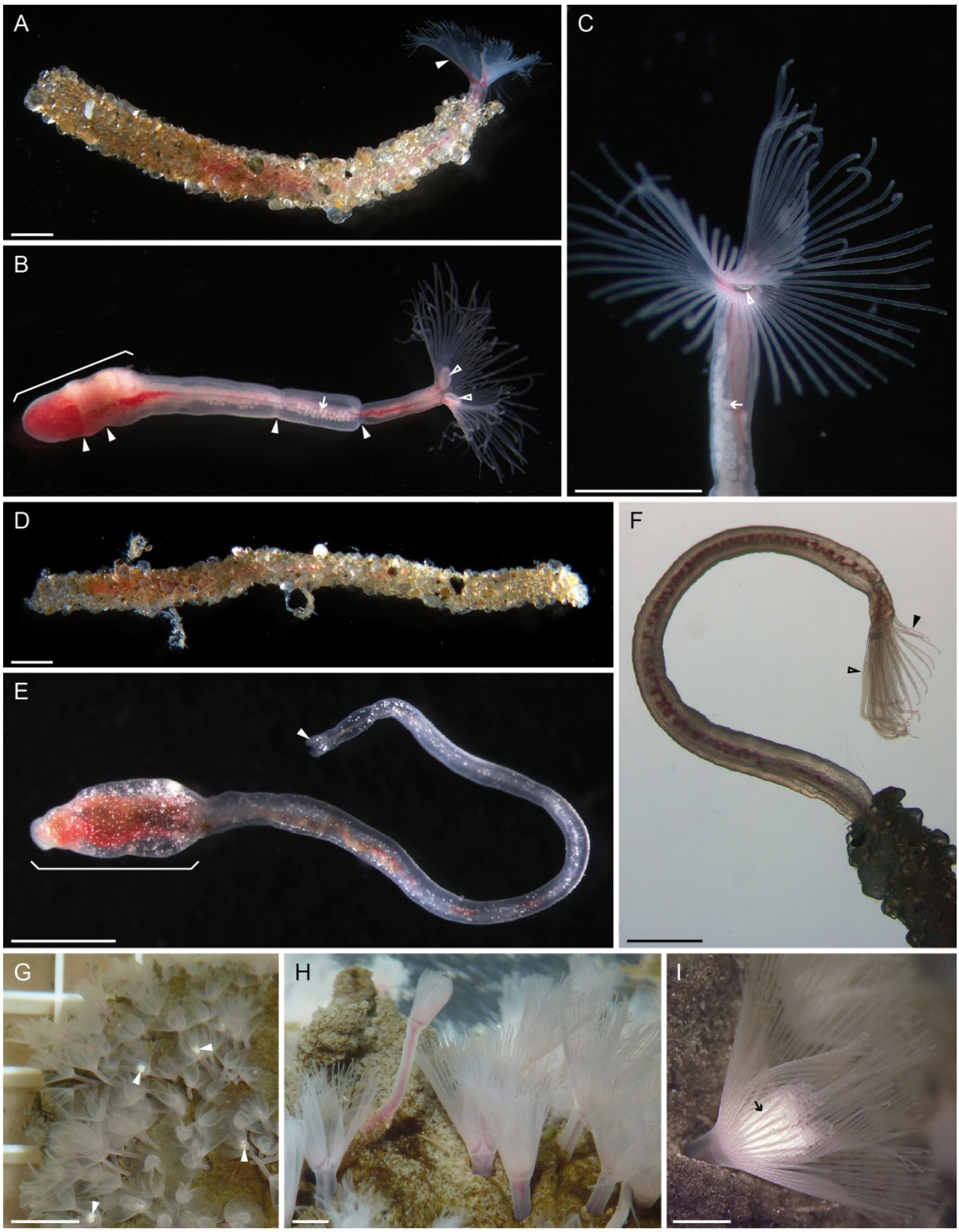

Fig. 1. Phoronid species investigated in this study. *P. pallida* (A-C), *P. muelleri* (D-F), and *P. vancouverensis* (G-I; photographs G and H by courtesy of Gerhard Scholtz). Scale bars in A-F and H-I: 1 mm; scale bar in G: 10 mm.
A. *P. pallida* specimen inside its tube, with the lophophore extended outside (arrowhead). **B**. *P. pallida* freed from the tube; the body zonation by externally distinct sphincter muscles (arrowheads) is characteristic for the species. The ampulla (indicated with bracket) and the lophophoral organs (open arrowheads) are visible. Eggs are floating freely within the coelom (arrow). **C**. Anterior end and lophophore of reproductive *P. pallida* specimen in oral view. Mouth opening (open arrowhead) and epistome (directly above) are visible; eggs lie within the coelom (arrow). **D**. *P. muelleri* specimen inside the tube (its posterior end lies to the left). **E**. *P. muelleri* freed from the tube. The ampulla is visible (indicated with bracket); the lophophore (arrowhead) is in

different species, the zygotes are either spawned freely and cleavage and development take place in the open seawater, or they are retained inside the parental tube or the lophophore until an early larval stage (Fig. 1I) (see Silén 1954; Emig 1977).

Except one species (*P. ovalis*), phoronids develop via a characteristic larva known as Actinotrocha or actinotroch (e.g., Silén 1954; Hyman 1959; Emig 1982). This larva is characterized by a preoral hood, which overhangs the mouth (and bears a ciliated band along its edge and long cilia at its anterior apical plate), a postoral ridge carrying a collar of tentacles, and an elongated posterior trunk with a perianal ciliated ring and a terminal anus. The Actinotrocha undergoes a phase of planktotrophic development, and can occur in high abundances in marine zooplankton, before finally developing into the vermiform adult via a so-called "catastrophic" metamorphosis, which involves a rapid and drastic change in the body organization.

1.2. Phylogenetic background

Phoronida have traditionally been allied with Brachiopoda and Bryozoa (= Ectoprocta) – based on the presence of a similar tentacle apparatus or lophophore – into a taxon named Tentaculata (Hatschek 1888) or Lophophorata (Hyman 1959). Tentaculata, however, always has been a group with controversial internal and external phylogenetic affinities (see Lüter 2004).

On the one hand, the monophyly of Tentaculata – which had explicitly been established as a provisional grouping (see Hatschek 1888) – was often doubted. For example, some authors regarded them to be a paraphyletic group (e.g., Ax 2001), while others suggested them to be polyphyletic, with Phoronida and Brachiopoda standing apart from Bryozoa (Nielsen 2001, 2002). On the other hand, the position of tentaculates – monophyletic or paraphyletic – within Bilateria remained debated. While early students of animal morphology and development often considered them to be protostomes (Fig. 2A) (e.g., Kowalewsky 1867 after Leuckart 1869; Hatschek 1888; Grobben 1908; Hyman 1940; Marcus 1958), many zoologists especially in the second half of the twentieth century associated them closer with

regeneration in this specimen. **F**. Anterior end and lophophore of *P. muelleri* specimen in transmitted light; characteristic for this species, the tentacles are shorter at the oral side (arrowhead) than at the aboral side of the lophophore (open arrowhead). **G**. Part of colony of *P. vancouverensis*. Reproductive specimens are recognizable by carrying brood masses at their lophophores (arrowheads). **H**. Close-up of the same colony. The specimens extend their lophophores into the ambient seawater. **I**. Lophophore of reproductive *P. vancouverensis* specimen, with attached brood mass at the base of the lophophoral cavity (arrow).

deuterostomes (Fig. 2C) (e.g., Zimmer 1973; Emig 1984; Schram 1991; Ax 1995, 2001; Nielsen 2001, 2005). Others left the question undecided (Fig. 2B) (Gruner 1980), or included tentaculates in the archicoelomates, a paraphyletic grouping comprising parts of protostomes and deuterostomes (e.g., Kaestner 1969; Ulrich 1972; Siewing 1980).

A new approach to these questions was possible by the implementation of gene sequence data and computer-based cladistic algorithms for resolving animal phylogenetic relationships. In 1995, an analysis based on 18S ribosomal DNA sequences suggested not only the polyphyly of Tentaculata, but also allied all three tentaculate groups – Phoronida, Brachiopoda, and Bryozoa – with Annelida and Mollusca among protostomes, forming the new taxon Lophotrochozoa* (Halanych et al. 1995). Since then, these findings have been corroborate by many phylogenetic studies, using such different markers as ribosomal genes (e.g., Mackey et al. 1996; Mallatt and Winchell 2002; Paps et al. 2009a), mitochondrial genomes (e.g., Helfenbein and Boore 2004; Jang and Hwang 2009), nuclear genes (e.g., Helmkampf et al. 2008a; Paps et al. 2009b), Hox genes (e.g., de Rosa et al. 1999; Passamaneck and Halanych 2004), and recently, by combined data and EST data analyses (e.g., Dunn et al. 2008; Helmkampf et al. 2008b; Baguñà et al. 2008; Bourlat et al. 2008; Hausdorf et al. 2010; Nesnidal et al. 2010; but see Hejnol et al. 2009; Nesnidal et al. 2013).

The internal relationships within Lophotrochozoa (or more generally, Spiralia; see below) – based on our knowledge not long ago – are given by Hejnol (2010), and here reproduced in Fig. 2D. Therein, Phoronida appears deeply nested within the group. In fact, this is based on several studies, which consistently place Phoronida in close affinity to Brachiopoda and, notably, the three spiralian trochozoan groups Mollusca, Annelida, and Nemertea: often Phoronida resolve in a clade together with Nemertea and Brachiopoda – forming the so-called Kryptrochozoa (Giribet et al. 2009) –, which represents the sister group to Annelida, and all together form the sister taxon to Mollusca (see Fig. 2D) (e.g., Dunn et al. 2008; Helmkampf et al. 2008b; Hausdorf et al. 2010; Nesnidal et al. 2010). Other analyses found different internal relationships, but still revealed the monophyly of a clade comprising these five taxa (e.g., Baguñà et al. 2008; Paps et al. 2009a,b). Hence, Hejnol (2010) subsumed Mollusca, Annelida, Nemertea, Brachiopoda, and Phoronida as the Trochozoa among Lophotrochozoa (Fig. 2D).

* Lophotrochozoa was defined as "the last common ancestor of the three traditional lophophorate taxa, the mollusks, and the annelids, and all of the descendants of that common ancestor" (Halanych et al. 1995: 1642).

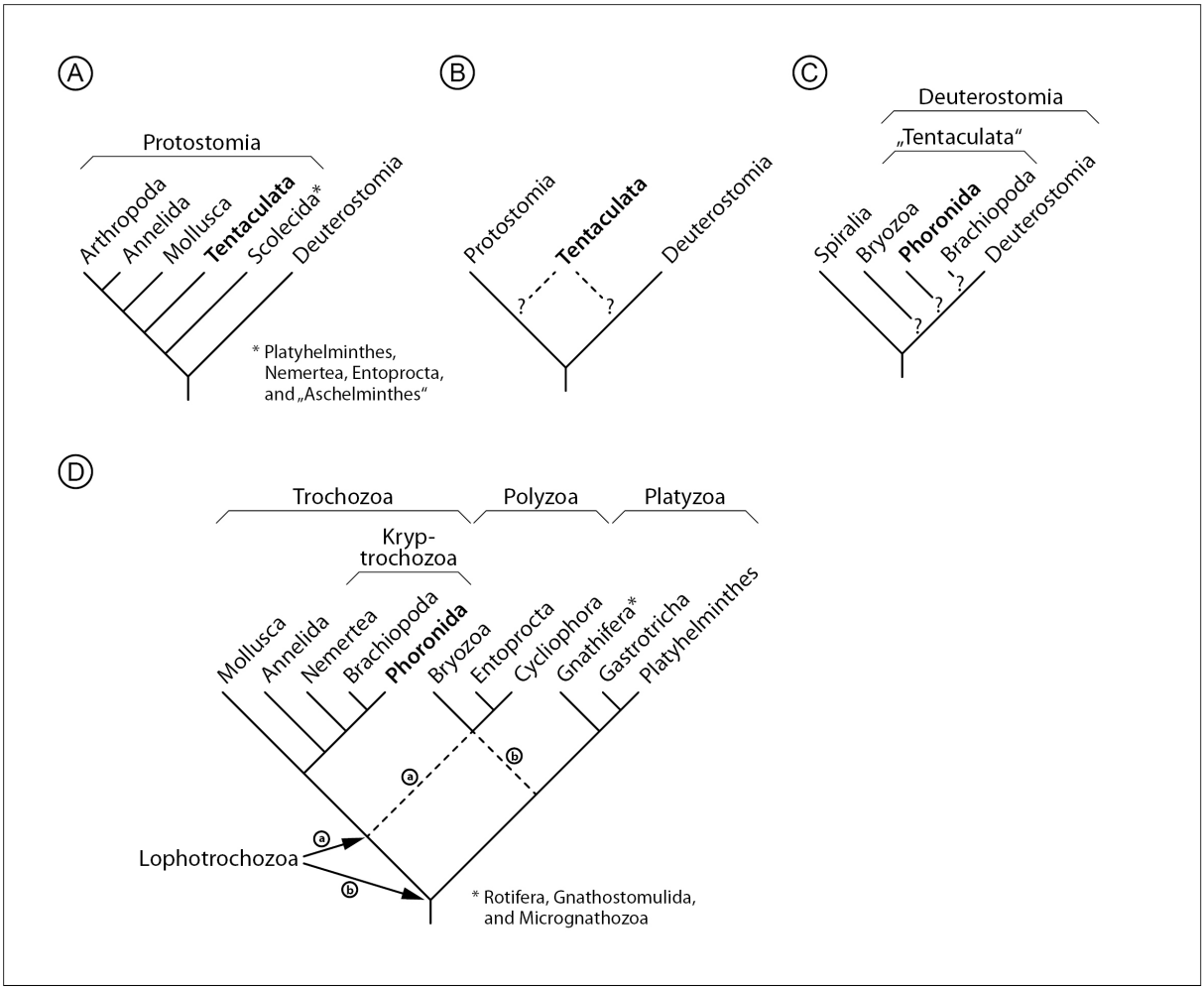

Fig. 2. Phylogenetic position of Phoronida. Selected traditional hypotheses on the placement of Phoronida relative to other bilaterians (A-C), and phylogenetic position as resolved by current molecular studies (D). **A**. Phoronida included in Tentaculata (a traditional grouping comprising Phoronida, Brachiopoda, and Bryozoa), which are a group among Protostomia (modified after Grobben 1908). **B**. Phoronida included in Tentaculata and in unresolved affinity between Protostomia and Deuterostomia (modified after Gruner 1980). **C**. Phoronida as part of paraphyletic "Tentaculata", which represent unresolved offshoots from the lineage leading to Deuterostomia (modified after Ax 1995, 2001). **D**. Phoronida as taxon within Lophotrochozoa among Protostomia. The phylogeny gives the relationships within the Spiralia, as they are resolved in recent molecular analyses (modified after Hejnol 2010; references therein). The position of Polyzoa, as sister group to either Trochozoa or Platyzoa, is unresolved (indicated by dashed lines: 'a' vs. 'b'), yet decisive of the taxonomic level of the clade Lophotrochozoa and its possible identity with the taxon Spiralia (topology 'b'). Phoronida are deeply nested within the Spiralia, and represent a member of Kryptrochozoa among Trochozoa.

1.3. Developmental background

While the protostomian – and more particular, the lophotrochozoan – affinity of Phoronida is thus well established on the base of molecular data, only few morphological or developmental characters are known, which may support this affinity. The new phylogenetic conception, on the other hand, has triggered new studies on phoronids and led to new evaluations of former knowledge and new surprising findings (e.g., Bartolomaeus 2001; Santagata 2002; Freeman

and Martindale 2002; Gruhl et al. 2005; Grobe 2007; Temereva 2012; Temereva and Wanninger 2012; Sonnleiter et al. 2013; Temereva and Tsitrin 2013).

Importantly, a position of Phoronida nested within Lophotrochozoa – and even more, allied with Mollusca, Annelida, and Nemertea – has fundamental consequences for our understanding of the phoronid mode of development. Interestingly, it implies that the phoronid cleavage and development are related to – and derived from – the so-called "spiral cleavage".

1.3.1. Spiral cleavage

Spiral cleavage is a complex mode of development that is best known for representatives of the taxa Mollusca, Annelida (including Sipunculida and Echiura), Nemertea, Platyhelminthes, and Entoprocta (e.g., Nielsen 2004, 2005, 2012; Dohle 2013). Spiral cleavage is generally characterized as a combination of (i) a specific cell division pattern during the early cleavage process, and (ii) certain cell fates of the blastomeres in the early embryo, that is, a specific fate map (e.g., Siewing 1969; Henry and Martindale 1999; Nielsen 2010, 2012).

(i) The spiral early cleavage pattern is characterized by oblique orientations of the mitotic cleavage spindles with respect to the embryo's animal-vegetal axis, and cleavage divisions that (at least from the third cleavage cycle onward) pass obliquely and in alternating orientations with every round of division (e.g., Siewing 1969; Nielsen 2012; Dohle 2013). In very most spiralian embryos, the third cleavage divisions are oriented in a dextral direction (also called "dexiotropic"), while the fourth cleavage is oriented in a sinistral ("laeotropic") direction, and so forth. Hence, the vegetal blastomeres of the embryo (the so-called "macromeres") give off daughter cells toward animal (the "micromeres"), in a specific pattern of alternately clockwise and counterclockwise directions, when the embryo is seen from the animal pole. This leads to embryos in which the blastomeres are arranged in so-called "quartets" – that is, tiers of four cells each –, which are shifted against each other, so that the single blastomeres are positioned in the gaps between the blastomeres of neighboring quartet(s). The cleavage divisions pass in a highly stereotypic pattern, and the cleavage process is so similar between different spiralians that a common notation system can be used to address the single blastomeres, and thus the individual cell lineages, in the embryo (see Conklin 1897).

(ii) On the other hand, certain blastomeres in the spiralian embryo give rise to particular body regions, cells of different germ layers, and structures in the later animal. These fate maps are highly corresponding between representatives of the above-mentioned spiralian groups (e.g., Marcus 1939 after Nielsen 2005; Boyer et al. 1998; Henry and Martindale 1998; Henry et al. 2004; Maslakova et al. 2004; Ackermann et al. 2005; Hejnol et al. 2007; Meyer et al. 2010). For example, the individual cells at the 4-cell stage – representing the four embryonic quadrants, and named "A" to "D" in the spiral notation system – typically will give rise to the roughly the left (A quadrant), the ventral/anterior (B quadrant), the right (C quadrant), and the dorsal/posterior body regions (D quadrant), respectively (and hence the first cleavage plane bears a constant relationship relative to the later bilateral symmetry plane), the mesoderm originates from two different sources (so-called "ectomesoderm" and "endomesoderm"), and only a single cell coming from the D quadrant gives rise to the endomesoderm (the so-called "mesentoblast").

In total, the spiral cleavage mode of development is a complex character set. This complexity led to the conclusion that spiral cleavage is of unique evolutionary origin, and to the establishing of a taxon Spiralia to include all animal groups that develop via spiral cleavage (Schleip 1929). At current knowledge, the validity of the new taxon Lophotrochozoa (which per definition includes Mollusca and Annelida from Spiralia) – besides the older taxon Spiralia – depends on the unresolved position of Polyzoa (a clade that includes the tentaculate Bryozoa) (Hejnol 2010). The group of animals defined as Lophotrochozoa (Halanych et al. 1995) represents either a subtaxon of Spiralia or equals Spiralia (see Fig. 2D). In the latter case, the older name Spiralia has to be preferred over the new name Lophotrochozoa (see Hejnol 2010).
Besides the typical spiralian taxa Mollusca, Annelida, Nemertea, and Platyhelminthes, the "current phylogeny" places several other animal groups within the Spiralia/Lophotrochozoa (Fig. 2D), for which only some (e.g., Gnathostomulida, Rotifera) or even none (e.g., Brachiopoda) of the above characteristics are known to resemble the situation in spiral cleavage (see chapter 4.3.).

1.3.2. Cleavage in phoronids

Nowadays, most textbooks and review articles agree that the phoronid early cleavage is radial, rather than spiral (e.g., Zimmer 1973, 1997; Emig 1977, 1982, 1990; Herrmann 1996;

Ax 2001; Brusca and Brusca 2003; Ruppert et al. 2004; Nielsen 2005; Temereva and Malakhov 2012; but see Dohle 2013).

Radial cleavage is generally characterized by spindle orientations at right angle or parallel to the animal-vegetal axis of the embryo, and blastomere divisions that pass in alternating equatorial and meridional direction starting with the third cleavage cycle (e.g., Siewing 1969; Nielsen 2012). From the 16-cell stage on, this pattern of divisions leads to blastomeres arrangements in so-called "octets" – that is, tiers of eight cells each. These octets are not shifted against each other (as in spiral cleavage), but juxtaposingly aligned so that single cells face the cells of adjacent octet(s) in direct animal-vegetal oppositions. Also, these cell tiers double with every second round of division. In contrast to spiral cleavage, which results in a quartet of four cells encircling the animal and the vegetal pole of the embryo, in radial 16- and 32-cell embryos typically a ring of eight cells encircles each pole (e.g., Siewing 1969).

However, taking a closer look in the literature reveals that the conceptions of the phoronid cleavage, in fact, have been controversial throughout the history of research.

Already among the first contributions on the phoronid development – which mostly addressed the cleavage process only briefly – some reported the presence of radial cleavage divisions (Masterman 1900; Roule 1900; Ikeda 1901; de Selys-Longchamps 1904, 1907), whereas others mentioned observations of oblique cell divisions (Foettinger 1882; Brooks and Cowles 1905). In a review summarizing the knowledge of this period, this ambiguity led Cori (1939) to the notion that the phoronid cleavage is radial with certain tendencies toward the spiral type.

In 1954, Rattenbury published a detailed study on the embryology of *Ph. harmeri*[*], which was based on her earlier dissertation (Rattenbury 1951), and was the most meticulous and comprehensive contribution available at that time. Therein, the author described the observation of a cleavage process that is characterized by mitotic spindles, which become aligned obliquely with respect to the embryo's animal-vegetal axis, and subsequent cell divisions that pass in these oblique directions (Rattenbury 1951, 1954). Moreover, she found that the orientations of these cell divisions alternate with every cleavage cycle, and that this sequence starts with a dextral orientation of the third cleavage; consequently, the animal cells are formed in alternately clockwise and counterclockwise directions, and the cells in the

[*] The original subject of Rattenbury's studies was *Ph. viridis*, which now is generally accepted as conspecific with – and a junior synonym of – *Ph. harmeri* (e.g., Marsden 1959; Emig 1967, 1982).

embryo are organized as shifted blastomere quartets (Rattenbury 1951, 1954). As such a pattern of divisions and cell arrangements is typical for spiral cleavage (see above), Rattenbury suggested that the cleavage of *Ph. harmeri* – and possibly of phoronids in general – follows the mode of spiral cleavage, and proposed a spiralian affinity of Phoronida (Rattenbury 1951, 1954). Also, textbooks on comparative embryology such as those by Siewing (1969), Schwartz (1973), and Ivanova-Kazas (1977) adopted this view.

Since then, the perspective has changed considerably. Nearly all studies on phoronid development after Rattenbury described the early cleavage to be of a radial or a biradial pattern[*] (e.g., Zimmer 1964; Emig 1974b; Herrmann 1986; Malakhov and Temereva 2000; Santagata 2001; Temereva and Malakhov 2007; but see Santagata 2012). This radial (or biradial) cleavage pattern was seen as an argument supporting a closer deuterostome affinity of the group (e.g., Zimmer 1964, 1997; Emig 1977; Herrmann 1996; Nielsen 2001, 2005).
Despite these characterizations as radial or biradial, however, many of the studies mentioned variation between individual embryos, and also reported observations of spindles or cell divisions that were oriented obliquely with respect to the animal-vegetal axis, of embryos that showed cell intercalations between the cell tiers, or generally of non-radial but apparent spiral blastomere arrangements (Zimmer 1964; Herrmann 1981, 1986; Freeman 1991; Temereva and Malakhov 2007; Santagata 2012). For *P. muelleri*, for example, Herrmann (1981, 1986) described that the third and the fourth cleavage spindles can be aligned obliquely (and even in alternating oblique orientations, respectively), and that the blastomeres in the resulting embryos are not necessarily aligned in juxtaposing oppositions. Similarly, for *P. vancouverensis*, Zimmer (1964) observed frequent instances of embryos with shifted cell alignments, some of which the author described to appear as having been derived by spiral cleavage divisions.
In spite of such observations, the studies rejected the meaningfulness of any correspondences to similar findings reported by Rattenbury (1951, 1954). In contrast, many authors discussed the encountered phenomena either as examples of variation or of abnormalities within a radial cleavage mode, or interpreted them to represent artifacts (see Zimmer 1964, 1973; Emig 1974b, 1977, 1990; Herrmann 1981, 1986; Temereva and Malakhov 2007, 2012). For example, it was argued that the apparent spiral cell arrangements would result from secondary re-alignments of the blastomeres, which would glide into the gaps between neighboring cells,

[*] The characterization as "biradial" was given by Zimmer (1964) and was regarded as variant of a radial cleavage mode (see chapter 4.1.2.).

only after they had passed through proper equatorial or meridional cleavage divisions (Zimmer 1964; Herrmann 1981); this could result from a compression of the embryo under diverse effects (Zimmer 1964, 1973; Emig 1974b, 1977, 1990). Or it was suggested that shifted cell alignments would represent erroneous impressions, which would arise from some optical effects due the high magnification necessary to study the small phoronid embryos (Herrmann 1986). Such views even found their way into textbooks (e.g., Brusca and Brusca 2003). Consequently, also Rattenbury's (1951, 1954) findings of a phoronid cleavage very similar to the pattern of spiral early cleavage was interpreted along such lines of arguments, and seriously doubted by later authors (Zimmer 1964; Emig 1977, 1982, 1990; Herrmann 1986).

1.3.3. Cell fates in phoronids

Reliable data on the cell fates in phoronid embryos are scarce. Although Rattenbury (1954) tried to follow groups of cells through the development and up to the larva, based on live observations and fixation series, this approach is probably somewhat error-prone (for example, the embryos lack good landmarks and they begin to move with the onset of ciliation, there are different rates of cell proliferation within the embryo, and cells become internalized with gastrulation; see Rattenbury 1954).
A more reliable method to gain data on cell fates is to label individual blastomeres in early embryos with dye, and to analyze the distribution of the cells that inherited the dye in later developmental stages. For phoronids, cell fate studies following this standard are only available for *P. vancouverensis* (Freeman 1991; Freeman and Martindale 2002).

Interestingly, these studies revealed an origin of the mesodermal germ layer from endodermal as well as ectodermal sources (Freeman and Martindale 2002), similar to the situation in spiralian embryos, and in general contradiction to many former descriptions of a merely endodermal origin of mesoderm (e.g., Rattenbury 1954; Emig 1974b; Zimmer 1980; Herrmann 1986; Malakhov and Temereva 2000). On the other hand, the studies found many differences to a typical spiral cleavage pattern, as for example, the absence of unique blastomere identities at least up to the 16-cell stage, the absence of a constant relationship between the first cleavage plane and the later plane of bilateral symmetry, or the absence of a single mesentoblastic cell (Freeman 1991; Freeman and Martindale 2002).

1.4. Subjects and structure of study

In this study, the development of three representatives of Phoronida is studied: *P. pallida*, *P. muelleri*, and *P. vancouverensis*[*].

In *P. pallida* and *P. muelleri* embryos, the cleavage process is investigated using two different methodical approaches: (i) the study of living embryos by means of a 4D microscopy system, and (ii) the study of specimens that are fixed at subsequent time points during the cleavage, and analyzed using fluorescent and immunocytochemical staining techniques in combination with confocal laser scanning microscopy. For both species, the cleavage is analyzed until the 64-cell stage (chapters 3.1.1., 3.2.). For *P. vancouverensis*, the cleavage process is studied on fixed and immunostained embryos only, and analyzed until the 32-cell stage (chapter 3.3.). This is the first time such methods are used to investigate the phoronid cleavage.
The approach chosen for *P. pallida* and *P. muelleri* is conducted also to deal with the objections that observations on the cleavage pattern may be distorted by artificial effects (e.g. Zimmer 1964; Emig 1977; Herrmann 1981, 1986). As, admittedly, it can never be excluded that a certain method produces to some extend artificial results, the two approaches (4D microscopy and fixation series) may serve as mutual controls of the results of each other. To deal with the problem of variation encountered by previous authors (e.g., Zimmer 1964; Herrmann 1981), quantifiable features of the cleavage process (such as, the inclinations of the mitotic spindles and the axes of cell division, the numbers of pole-encircling blastomeres, and the abundance of polar furrows) are taken on many specimens, and the findings on individual embryos and cells are evaluated over all the analyzed samples.

In addition, the cell fates in early *P. pallida* embryos are studied (chapter 3.1.2.). Single blastomeres at the 2-cell and at the 4-cell stage, respectively, are traced up to a late stage of gastrulation. This investigation is done by means of fluorescent dye in-vivo labelings in combination with confocal laser scanning microscopy.

The discussion is organized in three parts:
In a first chapter, the results on the early cleavage process are discussed, and compared to literature data on the phoronid cleavage (chapter 4.1.). Based on the present findings, former

[*] *P. vancouverensis* is treated as a valid phoronid species herein; however, some authors regard it to be conspecific with *P. ijimai* (see chapter 2.1.).

descriptions and the reliability of observations of oblique cleavage spindles or cell divisions and of non-radial cell arrangements in these animals are re-evaluated. General characteristics of the phoronid cleavage are identified, and differences between different species highlighted. The presence of different cleavage patterns in the group is concluded, and this is discussed in respect of the different types of development present in phoronids. Based on available information on the internal relationships within the clade a reconstruction of the early cleavage pattern that was part of the ground pattern in Phoronida is performed.

In a second chapter, the data gained on the cell fates in *P. pallida* are compared to the literature data on *P. vancouverensis* embryos (chapter 4.2.). Based on correspondences and differences between these species, general conclusions on the axial properties in the developing phoronid embryo, on the relationship between the first cleavage plane and the later plane of bilateral symmetry, and on the contributions of the four embryonic quadrants to the different germ layers and their derivatives are drawn.

In a third chapter, the two aspects of development are discussed in an evolutionary and phylogenetic context (chapter 4.3.). Based on the constant molecular support for a spiralian affinity of Phoronida, the early cleavage and the cell fates in phoronids are compared to the situation in spiral cleaving embryos. Previous objections against a spiral nature of the phoronid cleavage are discussed, and it is found that the early cleavage process in some phoronids shows more correspondences to the cleavage pattern in spiralians, than has been previously recognized. However, the similarities are not displayed by all phoronid species, and the cell fates, on the other hand, show general differences to a spiral cleavage situation. Finally, the correspondences and the differences to between phoronid development and spiral cleavage are discussed in the context of the establishment of cell fates and embryonic axes in these animals.

2. Material and Methods

2.1. Animals and embryos

Phoronis pallida (Schneider, 1862) Silén, 1952 (see Fig. 1A-C) and *Phoronis muelleri* de Selys-Longchamps, 1903 (see Fig. 1D-F) were sampled with support from the Biologische Anstalt Helgoland (BAH) in the North Sea around the island of Heligoland (Germany). Animals of both species live solitarily in tubes, which are encrusted with grains of sand and are embedded vertically in the sediment of the seabed (Fig. 1A,D) (Emig 1969, 1970, 1982). *P. pallida* was sampled at a location around 8 km west of Heligoland (at approximately 54°09'N and 7°46'E) between July and September 2010 and 2011, respectively. *P. muelleri* was collected at a spot somewhat farther from the island (at approximately 54º10'N and 7º42'E) in the same months in 2008 and 2009, respectively. At the sampling sites the water depth is between 30 and 40 meters. From a ship of the BAH, the sediment samples were taken with a bottom grabber. The samples were immediately sieved, and the gathered tubes containing phoronids were sorted out. They were kept in aquaria under running seawater at 10° to 15°C.

P. pallida as well as *P. muelleri* belong to a group of phoronids, which spawn their eggs directly into the ambient seawater (developmental type 1 after Silén 1954, and type 3 after Emig 1977). For the present investigation, however, the development is not studied on freely spawned eggs, but on experimentally gained ones. Therefore, single animals were carefully freed from the tubes using forceps, and checked for the presence of eggs in their coelom under a stereomicroscope. Egg bearing animals were ripped open to release the eggs into a petri dish. In *P. pallida* – which often bears a high number of eggs per animal (see Fig. 1B-C) – for most samples only a single specimen was opened; the thereby released eggs apparently were already fertilized, as they started to develop. In *P. muelleri* – which usually bears fewer eggs – several animals were opened and their eggs were lumped together. After about one hour, the gained eggs were transferred into a new petri dishes with sterile filtered Heligoland seawater (0.22 µm Rotilabo-syringe filters) and developed therein at about 15°C.

Phoronis vancouverensis Pixell, 1912 (Fig. 1G-I) was sampled with support from the Friday Harbor Laboratories on San Juan Island (Washington, USA). In contrast to the former two species, *P. vancouverensis* lives in cushion-like colonies, which encrust to rocky substrata and consist of numerous individual animals, the tubes of which are curved and highly intertwined

with each other (Pixell 1912; Emig 1971, 1982). In July 2011, some colonies were collected at Garrison Bay in the northwest of San Juan Island during low water; this was done under the collection permit SAJH-2008-SCI-0006 from the U.S. National Park Service to Richard Strathmann. The colonies were brought to the laboratory and kept in an aquarium under running seawater at about 13°C (Fig. 1G).

It has to be mentioned that the taxonomical validity of *P. vancouverensis* is under dispute and still unsettled. In a comparative study, Emig (1971) found the adult animals of this species, which occurs at the Eastern coast of the Pacific Ocean (type locality on Vancouver Island, Canada), to be morphologically indistinguishable from animals of *P. ijimai* Oka, 1897, a species known from the Western Pacific coast (type locality close to Misaki, Japan). Consequently, he proposed *P. vancouverensis* to be conspecific with – and a junior synonym of – *P. ijimai* (e.g., Emig 1971, 1974a, 1982). Other authors did not follow this conspecifity and pointed to a lack of information on the Western Pacific form (Santagata and Zimmer 2002; Santagata and Cohen 2009). In a recent study on phoronid larvae, Temereva (2009) found new differences between the two forms: whereas the actinotroch of *P. ijimai* has two blood corpuscle masses, *P. vancouverensis* actinotrochs possess only a single ventral corpuscle mass. Based on this it is possible to distinguish the two phoronid forms. Hence, in this study, they are treated as separate species, and the herein employed animal is referred to as *P. vancouverensis*[*].

P. vancouverensis belongs to a group of phoronids, which do not spawn freely, but which retain their eggs in brood masses that are attached to their lophophore – cleavage and development takes place in these masses (developmental type 2 after Silén 1954 and Emig 1977). By carrying such masses reproductive animals can be easily recognized within a colony (Fig. 1G,I). The tight packing of the brood masses results in a compression of the individual embryos, and it is known that this can distort the cleavage pattern (see Rattenbury 1951; Zimmer 1964). Therefore – and like in the other two species – the early cleavage was examined on eggs that were experimentally obtained from the coelom of the animals. As reproductive animal normally carries only a small number of coelomic eggs, mostly several specimens were freed from the tubes and – lumped together – ripped open to release their eggs into a petri dish. Later, these eggs were transferred into sterile filtered San Juan seawater (0.22 µm Rotilabo-syringe filters) and developed therein at about 13°C.

[*] Note, however, that recently published data on bar-coding genes do not contradict the conspecifity of *P. vancouverensis* with *P. ijimai* sensu Emig (Hirose et al. 2014).

2.2. 4D microscopy and analyses

For *P. pallida* and *P. muelleri*, the process of early cleavage was studied using a 4D microscopy system. For this purpose early developmental stages (*P. pallida*: zygotes, 2-cell, or 4-cell embryos; *P. muelleri*: 2-cell or 4-cell embryos) were placed into a drop of sterile filtered Heligoland seawater on a microscope slide, and covered with a small cover slip (10 x 10 mm). By placing plasticine spacers between slide and slip it could be ensured that the developing embryo was not exposed to any pressure from the cover. The cover was sealed to the slide with petroleum jelly ("Vaseline"), which was applied with a fine brush, so as to avoid evaporation of the water. In this pool, the embryos developed and could survive for several days[*]. The cleavage process of the mounted embryos was recorded at 17°C by means of a Zeiss Axioplan 2 imaging microscope in a 4D microscopy system (Schnabel et al. 1997). This automatic system allows capturing z-stacks of DIC photographs of the embryo in different focal planes (*P. pallida*: stacks comprised of 25, 30 or 40 images; *P. muelleri*: stacks of 25 or 40 images) and for taking these stacks in definable time intervals (*P. pallida*: every 40 or 60 seconds; *P. muelleri*: every 40 seconds). Thus, a spatial and temporal sequence of the cleavage process in the recorded embryo is obtained. In total, the cleavage process of 32 *P. pallida* embryos, and of 6 *P. muelleri* embryos was recorded.

The data gained with 4D microscopy were processed using the program SIMI°BioCell 4.0 (Simi Reality Motion Systems). This software allows visualizing – and scaling through – the 4D data stack, tracing and lineaging single cells and nuclei throughout space and time, and hence analyzing the process as well as the timing and sequence of cleavage in great detail. Twenty recordings of *P. pallida* embryos and four recordings of *P. muelleri* embryos were lineaged in SIMI°BioCell.

The recorded embryos were analyzed for the presence of polar furrows during the cleavage process. Herein, for the 4-cell stage, a polar furrow is defined as a line of cell contact, which is formed between two oppositely situated non-sister blastomeres in the embryo and which is visible at the embryo's pole. For the 8-cell stage and beyond, it is generally defined as a line of cell contact, which – in embryos that have four blastomeres located at a pole – is visible between two oppositely situated ones of these four blastomeres. An X-furrow, in contrast, is

[*] Later post-cleavage stages were found to move actively and unrestricted beneath the cover slips (personal observation; data not shown).

defined as a central cell contact between all four blastomeres at a pole (do not confuse an X-furrow with a cross furrow; see chapter 4.3.1.).

For the third and the fourth cleavage cycles, the inclinations of the axes of cell divisions relative to the animal-vegetal axis of the embryo were measured (for later cleavage cycles, the cleavage axes were evaluated on the observed division processes, but without detailed measurements). Since in the recordings the mitotic spindles, and also the nuclei directly prior and after a division, could not be seen through the cytoplasm, the division axes were inferred from the positions of the centers of two sister cells immediately after they had divided. With SIMI°BioCell these points were located in the recorded z-stacks and marked in their positions, which enables their representation as a spatial model of dots. Since other landmarks are missing in these models, only embryos that were perfectly aligned along the animal-vegetal axis – that is, the animal or vegetal pole was directly facing toward the camera during the recording process – were used for these analyses; this left 12 embryos for *P. pallida*, and 4 embryos in *P. muelleri* for these analyses. In their respective models, the animal-vegetal axis is easily tilted in a vertical orientation (animal pole: up; vegetal pole: down) by a single rotation in a step of 90°. Finally, the models were rotated along the equator and so brought into the necessary positions to measure the inclination of a division axis – as the line between two sister cell dots – against the vertical animal-vegetal axis.
Division axes that passed in an inclination between +10° and –10° along the animal-vegetal axis were characterized as “equatorial”, those in an inclination between +80° and +90° or between –80° and –90° with respect to the animal-vegetal axis as “meridional”. Divisions passing in an angle higher than +10° and lower than +80° to the animal-vegetal axis were characterized as “dextral”, those in an angle lower than –10° and higher than –80° as “sinistral”. Note that these categories are arbitrary and serve only as guidelines.

2.3. Embryo relaxation, fixation, and sample storage

In all three species, the early cleavage was studied on fixed material. For this purpose series of embryos were preserved in different cell stages – e.g., 2-, 4-, 8-, etc. cell embryos –, as well as during different cleavage cycles – that is, with cells in mitosis and/or cytokinesis to the next cell stage. Embryos of *P. pallida* were fixed in a solution of 2.5% or 4% paraformaldehyde in sterile filtered Heligoland seawater. Embryos of *P. muelleri* were fixed either in 2.5 or 4% paraformaldehyde in sterile filtered Heligoland seawater, or in a solution

of 3.7% formaldehyde in PBS buffer (= Phosphate Buffered Saline (protocol after Patel 1994): 18.6 mM NaH_2PO_4, 84.1 mM Na_2HPO_4, and 1750 mM NaCl in 1000 ml dH_2O; this 10x PBS solution is diluted 1:10 in dH_2O and the pH is adjusted to 7.4). Embryos of *P. vancouverensis* were fixed in 4% paraformaldehyde in sterile filtered San Juan seawater. The embryos were directly transferred into the respective fixative and stored therein at 4°C until analysis.

Embryos at the state of gastrulation – those were processed following the cell marking experiments performed in P. *pallida* – tended to shrink during the fixation process. For this reason they were relaxed prior to fixation. Depending on the age of the embryos different relaxation agents gave better results. For the one-day-old mid gastrula stage a solution of $KMnO_4$ in sterile filtered seawater (one small crystal dissolved in 1 ml seawater), for the two-day-old late gastrula a solution of CO_2 in sterile seawater (solution prepared with a soda-club maker) was most effective. The embryos were transferred into the respective relaxant, and kept therein until they stopped moving (about 30 to 60 seconds). Subsequently, they were fixed in 4% paraformaldehyde in sterile filtered Heligoland seawater, and stored therein at 4°C.

2.4. Immunocytochemistry and nuclei stainings

The fixed cleavage samples of *P. pallida* were in parts stained by nuclear markers only (see below), but most of them beforehand were immunostained against tyrosinated α-tubulin, in order to visualize the mitotic spindles.

The immunolabelings were performed with a primary monoclonal mouse antibody (anti-tyrosine tubulin, mouse IgG3 isotype, clone TUB-1A2; Sigma T9028; dilution 1:1000 in PBT+N (protocol see below). From cell cultures it is known that tyrosinated α-tubulin is present in the entire spindle apparatus during all stages of mitosis (Gundersen and Bulinski 1986), and also in the phoronid embryos these stainings gave very good results[*]. As secondary antibody either a Cy-2 conjugated goat antibody (anti-mouse IgG (H+L); Jackson/dianova; dilution 1:50 in PBT+N) or a Cy-3 conjugated goat antibody (anti-mouse IgG (H+L); Jackson/dianova; dilution 1:200 in PBT+N) were used. Prior to staining the fixed

[*] Using instead an antibody against acetylated α-tubulin (monoclonal anti-acetylated tubulin, mouse IgG2b isotype, clone 6-11B-1; Sigma T6793; dilution 1:100 in PBT+N) did not give good spindle stainings, and was therefore not further pursued.

embryos were repeatedly rinsed in PBS*. Subsequently, they were transferred into PBT (= PBS with 0.2% Bovine Serum Albumin ("Albumin Fraction V") and 0.2% Triton X 100; Roth) and washed therein for several times over a course of some hours; afterward, they were washed for two times 30 minutes each in PBT+N (= PBT with 5% Normal Goat Serum; Biozol X0907). The embryos were then transferred into the primary antibody, and incubated therein for one to three nights at 4°C. After a second round of washing in PBT and PBT+N following the same times as given above, the samples were incubated in the secondary antibody for one night at 4°C. Following the immunostaining, the embryos were repeatedly rinsed in PBT.

The nuclear counterstaining – as well as the nuclear staining in embryos without an anti-tubulin staining – was done using the fluorescent nucleic acid specific dye Hoechst (bis-benzimide, H33258; invitrogen). The embryos were repeatedly washed in PBS, and subsequently transferred into the dye (dilution 1:1000 in PBS). The incubation time therein was 30 to 60 minutes at room temperature. Following the nuclear staining, unbound dye was removed by repeated rinsing in PBS. Since the cytoplasm of the cells in early embryos exhibited a broad autofluorescence, also the blastomere shapes in the embryos could be visualized with fluorescence microscopy. For *P. pallida*, about 20 to 50 fixed embryos for each cleavage stage were processed this way.

Fixed embryos of *P. muelleri* were only stained for the nuclei. For this purpose either the nucleic acid specific dyes Hoechst, as described above, or Sytox Green (invitrogen) were used. No consistent differences in the staining results were observed; both dyes visualized nuclei and chromosomes, while the cytoplasm displayed a broad autofluorescence. The fixed embryos were repeatedly washed in PBS buffer for Hoechst, or in TBS buffer (Tris-Buffered Saline: 0.9% NaCl and 10 mM Tris-HCl in 1000 ml dH_2O; pH adjusted to 7.4) for Sytox staining. Subsequently, they were transferred into the respective dye (Hoechst: dilution 1:1000 in PBS; Sytox Green: dilution 1:1000 in TBS). The minimum incubation times at room temperature were 30 minutes for the Hoechst and 3 hours for the Sytox stain, yet many samples were left in the dye overnight at 4°C. After staining, unbound dye was removed by several rinsing steps in PBS or TBS, respectively. About 20 to 30 fixed embryos were processed for each cleavage stage in *P. muelleri*.

* Sample storage in the fixative over a period of some months showed no negative effect on the immunostaining results.

The embryos of *P. vancouverensis* were all immunostained against tyrosinated α-tubulin. The same antibodies and protocol as in *P. pallida* were applied. Counterstaining was performed in PBS using either the fluorescent nucleic acid specific dyes DRAQ5 (BioStatus; dilution 1:500 in PBS) or RedDot2 (Biotium; dilution 1:200 in PBS), with an incubation time of about 30 minutes at room temperature. Both these dyes have their emission range in the far-red to infrared region of the electromagnetic spectrum. Although the rather yolk-rich cells of the *P. vancouverensis* embryo display a broad and intense autofluorescence, these emission spectra allowed for a good detectability of the nuclei through the cytoplasm. About 30 to 40 fixed embryos of the early cleavage stages and six embryos of the 32-cell stage were processed in *P. vancouverensis*.

2.5. Single cell in-vivo labelings

To analyze the cell fates in *P. pallida* embryos, single blastomeres of 2-cell or 4-cell stages were injected with the fluorescent in-vivo marker DiI (Molecular Probes D-282). This dye is lipophilic and binds to the cell membrane of the injected cell. By this it is ensured that it is only inherited to the descendants of the marked cell, and thus allows tracing the fate of this cell and the position of its progeny in embryos of later developmental stages. Embryos in the respective cleavage stages were mounted in a drop of sterile filtered Heligoland seawater on a microscopic slide. They were covered with a small cover slip, the corners of which were supported with spacers of petroleum jelly. The embryos were moved and oriented under the cover using an eyelash fixed on a Pasteur pipette. By this, they were rolled to the edge of the slip, where they could be reached with the injection needle, and subsequently, by applying soft pressure on the cover, were slightly squeezed and thus fixed in the desired position.

Suitable needles for injections were pulled from pipettes (outer diameter: 1.00 mm, inner diameter: 0.58 mm; Hilgenberg) with a KOPF 720C puller (David Kopf Instruments). The tips of the pulled needles were opened and sharpened with a horizontal grinder (Narishige); the angles of the cutting edge varied between 15° and 20°. The needles were loaded with DiI (dilution 2 mg/ml in soy oil) using microloaders (Eppendorf). Single cell injections were performed using an inverse microscope equipped with a micromanipulator (Leica DM IRB) and a FemtoJet microinjector (Eppendorf).

Each successfully marked embryo was transferred into a glass embryo dish in fresh sterile filtered Heligoland seawater and reared in the dark at 15°C. About every 12 hours the

embryos were checked with a stereomicroscope under normal light*. Embryos that had stopped developing or that showed obvious malformations were sorted out. For each experimental approach – injection at the 2-cell stage and at the 4-cell stage, respectively – the normally developing embryos were fixed after either one day of development (24-30 hours after injection) or after two days of development (48-54 hours after injection). Prior to fixation they had been relaxed (see chapter 2.3.). In total, 9 and 13 specimens, respectively, were obtained from the 2-cell injections, and 7 and 13 specimens, respectively, from the 4-cell injections.

Nuclei counterstainings of the marked specimens were performed in PBS using either the fluorescent nucleic acid specific dyes Hoechst (bis-benzimide, H33258; invitrogen; dilution 1:1000 in PBS) or DAPI dihydrochloride (invitrogen; dilution 1:1000 in PBS), and following the same principal protocol as already described (chapter 2.4.). Incubations times for the counterstain were between 20 and 60 minutes at room temperature. Both dyes gave good staining results.

Additionally – as reference for the marked samples –, some one-day-old and two-day-old gastrulation stages of *P. pallida* – which had not been injected and had developed without any treatment – were immunostained against tyrosinated α-tubulin. This was done to visualize the apical plate and the cell shapes in the gastrulating embryos. The same antibodies and protocol as described above were applied (see chapter 2.4.). Nuclear counterstaining of these embryos was done using the Hoechst dye with an incubation time of about 30 minutes.

2.6. Fluorescence microscopy, 3D reconstructions, and analyses

All stained samples were mounted on microscope slides in the anti-fade medium SlowFade Gold (invitrogen) and covered with cover slips, which were supported with plasticine spacers at their corners as to prevent squeezing the embryo. The samples were analyzed and documented using an epifluorescence microscope (Zeiss Axioskop 2 plus) and a confocal laser-scanning microscope (Leica DM IRE2). The data stacks gained with the confocal microscope normally were taken with a distance of 1 µm between two successive scans.

* Repeated inspections under fluorescence exposure apparently caused phototoxicity, as they led to malformations (personal observation).

These data were processed with the software Imaris, version 5.5.3 or 7.1.1 (Bitplane), and analyzed on 3D reconstruction and representations made therein.

In embryos that had been fixed during the third or the fourth cleavage division, the exact inclinations of the division axes with respect to the animal vegetal axis were measured (in later divisions, the axes were evaluated without detailed measurements). In embryos that only had been stained by nuclear markers (*P. pallida*; *P. muelleri*), the axes of divisions were inferred from the positions of the chromosomes in cells that were in anaphase or telophase of mitosis, and from the positions of the nuclei in cells that were in cytokinesis. In embryos that additionally had been stained against α-tubulin (*P. pallida*; *P. vancouverensis*), the division axes were directly taken on the mitotic spindles in cells that were in metaphase, anaphase or telophase of mitosis, and inferred from the nuclei positions in cells in cytokinesis. By rotating the virtual embryo in the proper position with the Imaris software (animal pole: up; vegetal pole: down), the inclination of a division axis can be measured against the animal-vegetal axis of the embryo. The categorization of the cleavage divisions as either "equatorial", "meridional", "dextral", or "sinistral" followed the same angles as given in the 4D microscopy section (chapter 2.2.).
In some embryos without a contrasting tubulin staining, the high autofluorescence of the cytoplasm obscured the visibility of the nuclear signal. This problem could be overcome by highlighting the nuclei in the respective scan using the "Contour Surface" tool of the Imaris software (the nuclear signal was labeled, a surface object of the labeled area was created, the original channel was masked with that surface to a new channel of the nuclear signal only, and finally, this nuclear channel was assigned to a different color).

2.7. Data representation

In the results chapter, the figure plates and the tables are given at the end of each section.

Specimens recorded with the 4D microscopy system are documented in plates, which show successive states during the cleavage process of individual embryos (see e.g., Fig. 3). Most of the images were made from some (two to six) overlying photographs of one z-stack taken at the respective time point (all these photographs showed the region of interest, but at slightly different focal planes). These photographs were merged into one single focused image using the software Helicon Focus 4.75 or 5.3.7 (Helicon Soft). Some images of the 8-cell stage are

full-focal projections of all the photographs of a z-stack merged into one image, to show the blastomere arrangement in the complete embryo (see e.g., Fig. 3G-H).
Specimens processed with confocal laser-scanning microscopy (cleavage stages and single cell labeled embryos) are documented by snapshots taken with the Imaris software (see e.g., Fig. 7). When successive images are connected with a white bar (see e.g., Fig. 7D to E, or F to I), this indicates that they show the same specimen, but form different perspectives (which are specified in the captions). Volume projections of scanned specimens are presented in either Blend mode or MIP mode, as they are implemented in the Imaris software. In images of cleavage stages, often the polar bodies were removed, to show the underlying cell contacts at the animal pole (see e.g., Fig. 7D-E). This was done with the "Contour Surface" tool of the Imaris software (a surface object of the polar bodies was made, from this object a new channel of the polar body signal only was created, and this channel than was deactivated). Some images give virtual sections through individual cells or embryos, made with the "Clipping Plane" tool of Imaris (see e.g., Figs. 7F-I, 13C-D).
Generally, the program Adobe Photoshop CS3 or CS5 was used to improve the global brightness, the contrast, and the levels of the images. All plate layouts were made using the software Adobe Illustrator CS5 (Adobe Systems).

The provided cell lineages and data on the timing of the cleavage process (see e.g., Fig. 6) are based on analyses of 4D-recorded embryos with the SIMI°BioCell software. In the presented lineages beyond the 4-cell stage, if a cell division passed somehow in the animal-vegetal axis (equatorially or obliquely), the upper line after a division event represents the daughter cell that is situated (given off) closer to the embryo's animal pole, and the lower line represents the daughter cell that is situated closer to the vegetal pole; in case a division passed perpendicularly to the animal-vegetal axis, no distinction was made in the lineage.

The quantitative data of the cleavage axes in the third and the fourth cleavage cycles are represented in bar charts (see e.g., Fig. 8). All angles of inclinations that were measured in individual cells (see chapters 2.2., 2.6.) were combined in groups along 5°-steps. The abscissas give the inclination angles: positive values represent inclinations that generally are oriented in a clockwise direction when the embryo is seen from the animal pole, and negative values represent inclinations oriented in a counterclockwise direction. Beneath the abscissas, the categories of cleavage axes, as given in chapter 2.2., are indicated (dex: dextral, eq: equatorial, mer: meridional, sin: sinistral). The ordinates of the charts – and the heights of the

bars – give the relative frequency in which the cleavage inclinations were encountered; the numbers in the bars give the absolute numbers of cells in a respective group. In tables, the data on the cleavage orientations additionally are provided on the level of complete embryos (see e.g., Table 2) – in contrast, to the level of individual cells represented in the bar charts.

The time-lapse videos provided in the Supplementary Material are based on 4D microscopy recordings of individual *P. pallida* and *P. muelleri* embryos. They were made from photographs, which were taken from consecutive z-stacks of a recording. Depending on the position of the chosen photographs within the z-stack, the videos can show the cell divisions in different focal planes within the embryo. The software Adobe Premiere Pro 2.0 or 7.0 (Adobe Systems) was used to convert the temporal sequences of photographs into movies and to arrange the videos. The dot models inserted in the videos give three-dimensional representations of the nuclei in the respective embryo. They were made with the SIMI°BioCell software.

3. Results

3.1. Cleavage and cell fates in *P. pallida*

3.1.1. Cleavage process in *P. pallida*

3.1.1.1. Basic characteristics and timing of cleavage

Zygotes of *P. pallida* are of spherical or somewhat ovoid shape and have a diameter of about 65 to 70 µm (Figs. 3A, 4A). They are surrounded by a delicate fertilization membrane, which, especially in embryos that are compacted between two successive cleavage cycles, has an undulating appearance (e.g., Figs. 3C,E,H, 5C,F). In more advanced stages, this membrane is often difficult to see, and the later blastula starts rotating and swimming movements without an observable hatching event. The formation of the polar bodies was not directly observed, but at the latest at the 2-cell stage normally three polar bodies are found at the embryo's animal pole, both in the 4D-recorded embryos as well as in the fixed material. Cleavage is holoblastic. Initially, it results in approximately equal sized blastomeres, but from the 32-cell stage on, the cells of the embryo's vegetal hemisphere often are slightly larger than the animal ones (see below).

The timing and the lineage of the cleavage process were analyzed on 20 4D-recorded embryos. The first division takes place about 1.5 to 2 hours after releasing the eggs from the coelom. Subsequently, the blastomeres divide every 30 to 40 minutes at 17°C, with the intervals becoming longer following the fourth and, more pronounced, the fifth cell cycle (Fig. 6). In most embryos, the initial division cycles proceed approximately synchronously, but the cleavage process becomes more asynchronously the more cells there are in the embryo (Fig. 6A-C). No consistent pattern in the sequence of the divisions could be identified between different embryos. In some cases, more or less pronounced asynchronies could be observed already during the initial cleavage cycles (Fig. 6D); yet this did not seem to negatively affect the development, as also these embryos formed normally appearing gastrulation stages. Such early asynchronies result in embryos with intermediate blastomere numbers, and such embryos (e.g., 3-, 7-, 14-, 21-cell stages) could also be observed in the fixed material, though they were not abundant.

3.1.1.2. First and second cleavage cycles and resulting embryos

The division planes of the first two cleavage cycles run perpendicularly to each other and both pass through the animal-vegetal axis of the egg. In the 4-cell embryo, the polar bodies always are found at the central junction between the four blastomeres, at one side of the embryo; they are thus good indicators for the animal pole (e.g., Figs. 3D, 7C-D). These first two meridional cleavages divide the egg into two and four approximately equal sized blastomeres, respectively, which lie in one plane (Figs. 3B,D, 4B-C, 5A-B, 7A,C). In rare cases, the second cleavage cycle is not synchronous, but delayed in one blastomere, resulting in the formation of an intermediate 3-cell stage (12% of 17 recorded embryos) (Fig. 7B).

Following each division cycle the embryo compacts. In this process, the cells, which are rather roundish in shape and in minimal contact with each other directly after the divisions, become flattened against each other, and thus increase their contact areas (Fig. 3B-E; Supplementary Material Video_S1-S6). At the 4-cell stage, all cells draw closer to the central animal-vegetal axis (Figs. 3D-E, 5B-C). In some embryos, this can result in the formation of a central cell contact between two oppositely situated non-sister blastomeres – a polar furrow (Table 1; Fig. 5C') –, whereas in most embryos, a small opening persists between the four blastomeres (Figs. 3E, 5C). This opening can be very small (Fig. 7D-E), and in some specimens, all four blastomeres rather seemed to touch each other at the central axis – forming an X-furrow (Table 1). When a polar furrow is present, it always reaches along the entire animal-vegetal axis – from the animal pole to the vegetal pole – and thus completely separates the two remaining cells. No embryo with a second polar furrow between the second pair of non-sister blastomeres – thus, two perpendicularly running polar furrows – was observed. Before the next cell cycle, the cells gain a more spherical shape again and the furrow, if present, dissolves.

3.1.1.3. Third cleavage cycle and 8-cell embryo

The third cleavage cycle starts with a conspicuous process of blastomere elongations. Thereby, the cells expand obliquely to the animal-vegetal axis in a lateral view (Fig. 4D), and elongate in a twisted manner at their poles; the cells' apices get drawn out pointing in a clockwise direction at the animal pole, and in a counterclockwise direction at the vegetal pole, when the embryo is seen in an animal view (Figs. 3F, 5D). Data from fixed embryos suggest

that these twisted elongations are only established when the cells are already in the anaphase state of mitosis (Fig. 7O-P). Generally, the elongations are differently distinct in different cells and embryos (Supplementary Material Video_S1-S6).

The third cleavage divisions follow the direction of the elongations and pass obliquely and with a dextral orientation in most blastomeres (Figs. 3F-G, 4D-F, 5D-E). This pattern of divisions was consistently observed in the analyses of the 4D-recorded embryos (Fig. 8A) as well as of embryos that had been fixed during the division process (Fig. 8B) – thus, in two independent sets of data. Yet, both datasets also reveal the presence of variation in the exact inclination of the cleavage axis (Fig. 8A-B). Also, the dextrality of the third cleavage generally is not very pronounced: the vast majority of cells display inclinations lower than +20°, and of these cells, most ones show inclinations lower than +10°, though still higher than 0°, that is, in principle with a dextral orientation (Fig. 8A-B). Interestingly, the data gained from the fixed embryos show more variability (Fig. 8B). Only in this dataset single cells have very high spindle inclinations; such cases yet are found only in low frequencies, and the deviating spindles are oriented in various angles over nearly the whole range possible (Fig. 8B).

Following the categorization made in the Material and Methods section (chapter 2.2.), the observed variation leads to diverse patterns of cleavage orientations on the level of complete embryos (Table 2A). While only in some embryos the inclinations are pronouncedly dextral in all four blastomeres (Figs. 3G), in most cases, single cells divide only weakly inclined and are thus characterized as equatorial (Table 2A; Figs. 5E, 7R in embryo in Fig. 7O-T, 12A,K). In some embryos, such weak inclinations are even found in all four cells (Table 2A; Fig. 7J-N). Single cells with deviating sinistral or meridional spindles were encountered rarely, and only in the fixed material (Table 2A; Fig. 7I in embryo in Fig. 7F-I).

The 8-cell embryo is composed of an animal and a vegetal tier of four cells each (Fig. 9A-T). At this stage, a first small blastocoel is present. The observed blastomere arrangements roughly seem to reflect the variation encountered in the cleavage inclinations. When a blastomere divides dextrally, the animal cell comes to lie clockwise of its vegetal sister cell, when the embryo is seen from the animal pole. In some embryos, this alignment is found in all four animal/vegetal sister cell pairs; thus the whole animal cell tier is oriented clockwise with respect to the vegetal tier, although the shift is often not very pronounced (Figs. 2G, 4F, 5E, 9C-F). Repeatedly, however, also single sister cell pairs were encountered, which were positioned on top of each other in a juxtaposing alignment along the animal-vegetal axis; in

the fixed material, such arrangements were observed often in two or even three of the sister cell pairs, while the other(s) were aligned shifted clockwise (Fig. 9J-M). In some cases, even all of the animal cells were juxtaposing the vegetal ones (Fig. 9P-S).
The juxtaposing sister cell alignments, in some cases, might be a consequence of third cleavage divisions that had passed in a quite equatorial direction (see above). On the other hand, the 4D-recordings reveal that juxtaposing cell alignments can also result from the compactation of the embryo: it was observed that animal/vegetal sister blastomeres, which are in a dextrally shifted alignment directly after the cell divisions, come into a more juxtaposing alignment during the compactation (Figs. 3G-H, 5E-F). Apparently, compactation can obscure de facto oblique cleavage divisions.

Similar as in the 4-cell stage, the compactation process, which follows the cleavage divisions, leads also to a narrowing of the blastomeres toward the central axis (Figs. 3G-H, 5E-F). At the poles of some 8-cell embryos, this can establish a polar furrow (Figs. 3H, 9T). In the material, polar furrows were found variably either only at the animal pole, or only at the vegetal pole, or at both poles; and in the last case, the two polar furrows were oriented either perpendicularly or parallel to each other (Table 1). Most 8-cell embryos, on the other hand, even after compactation, display a small opening centrally between the animal cells as well as between the vegetal cells (Figs. 5F, 9A-B,G-I,N).

3.1.1.4. Fourth cleavage cycle and 16-cell embryo

At the onset of the fourth cleavage cycle the close cell contact dissolves, and again, the blastomeres elongate somewhat twisted; this time, however, oriented more in a counterclockwise direction, when seen from the animal pole (Figs. 3I, 4G, 5G; Supplementary Material Video_S1-S6).
Subsequently, the cells divide obliquely and with a sinistral orientation, thus the animal blastomeres come to lie counterclockwise to their vegetal sister cells, when the embryo is viewed from animal (Figs. 3J, 4H-I, 5H). Again, this pattern was consistently and independently observed in the data from the 4D recordings (Fig. 8C) as well as the fixed embryos (Fig. 8D). Also in the fourth cleavage the exact inclination of the division axis varies between individual cells; generally, the data show that the obliqueness of the fourth cleavage cycle is more pronounced than of the third cleavage (compare Fig. 8A-B and Fig. 8C-D). Again, the encountered variation is higher in the dataset gained from the fixed material; some

fixed cells showed meridionally or even dextrally oriented spindles (Figs. 8D, 10A-T). Separated analyses for the animal and the vegetal cell tiers of the 8-cell embryo show for the animal tier a few more cells with cleavage axes in higher inclinations than in the vegetal tier (Fig. 8C'-C",D'-D").

The evaluation of the cleavage pattern on the level of complete embryos reflects the variation observed on the level of single cells. Most of the recorded embryos show only divisions that can be categorized as sinistral in all their blastomeres; the results from the fixed material are more variable, and nearly no two fixed embryos show the same orientation pattern (Table 2B).

The 16-cell embryo is composed of four tiers of four cells each, and has a blastocoel that occupies about 40% to 50% of the embryo's diameter (Fig. 11A-H). As a consequence of the obliqueness of the fourth cleavage divisions, the four cell tiers are stacked along the animal-vegetal axis – making up animal, animal-equatorial, vegetal-equatorial, and vegetal tiers – and thereby shifted against each other, so that the single cells are situated in the gaps between the cells of the neighboring tier(s) (see alignment of the tiers in pole views in Figs. 3K, 5I, 11A-B,G). Also, the cell tiers are intertwined at the equator of the embryo (Fig. 11C-F).

Since oblique cleavage division result in the location of a tier of four cells at the embryo's animal and vegetal pole, the number of pole-encircling cells is a well-defined difference to a radial cleavage, which typically results in eight cells surrounding the poles (chapter 1.3.). Analyses of 16-cell *P. pallida* embryos actually show that four blastomeres are located at the animal and at the vegetal pole, in nearly half the specimens (Table 3A; Figs. 3K, 5I, 11A-B,G). In the remaining embryos, a higher number of cells encircle either one or sometimes both poles, but in these specimens, the encountered number of pole cells and their combinations are quite variable (Table 3A). The variability is higher for the animal pole, which is surrounded by four cells in 55% of all analyzed 16-cell embryos, but in the remainder has five to seven cells located around the animal pole (Table 3A; Figs. 11K,M, 12D,N). The vegetal pole, in contrast, is encircled by four blastomeres in nearly nine-tenth of the embryos, and deviating cases involve only the rare occurrence of five pole cells (Table 3A; Fig. 11J). The 4D recordings show that more than four pole cells can result from somewhat irregular fourth cleavage division in individual blastomere(s), which divide with a high inclination, thus rather meridionally (Fig. 12B-D,L-N). The data on the pole cell also seem to be in consistence with the observation of somewhat higher inclined division axes in the animal cells, which was encountered during the fourth cleavage (Fig. 8C'-C",D'-D"). On

the other hand, they also suggest that such divisions occur without a consistent pattern between different embryos. Finally, no embryo was observed, in which eight cells were located at a pole (Table 3A).

Again, the compactation process following the cleavage divisions can either establish cell contacts between the pole cells (Fig. 11L) or leave a pole opening, which, however, it often only small in size (Figs. 3K, 5I, 11A-B,G,I). Cell contacts were only observed when the respective pole tier comprised four blastomeres. Embryos with a higher number of pole cells usually display a rather large pole opening (see Figs. 11J-K,M, 12D,N). The data show that polar furrows occur more frequently than in previous stages, and moreover, that in some embryos the four vegetal cells contact in the organization of an X-furrow, rather than of a polar furrow (Table 1). As polar furrows are generally short in length, the discrimination to an X-furrow is sometimes difficult, however. In total, the results indicate that with advancing cleavage the percentage of embryos that have closed cell contacts at the vegetal pole increases (Table 1).

3.1.1.5. Fifth cleavage cycle and 32-cell embryo

The orientations of the next two cleavage cycles were only studied on 4D-recorded embryos. For the fifth cleavage, all blastomeres of the 16-cell stage were analyzed and evaluated separately for the four cell tiers (Table 2C). The results show that most cells of the animal and the vegetal cell tiers – after undergoing clockwise cell elongations (Figs. 3L-M, 4J-K, 5J-K) – divide obliquely with a dextral orientation, so that the animal cells come to lie clockwise of their vegetal sisters, when the embryo is seen from the animal pole (Figs. 3M-O, 4K-L, 5K-L; Supplementary Material Video_S1-S6). Although, in the animal tier, the number of dextrally dividing cells varies, in the majority of embryos it is three blastomeres that undergo dextral divisions and of all analyzed cells about two-thirds do (Table 2C: first column, n = 48). The evaluation of the 4D recordings show that blastomeres that divided with some irregularity in previous cleavage cycles tend to undergo deviating divisions also in the fifth and later cleavages (see Fig. 12E-F,O-P). In the animal-equatorial cell tier, the divisions are more variable, but still about two-fifths of the blastomeres divide dextrally (Table 2C: second column, n = 48). In the vegetal-equatorial tier, in contrast, most cells – and in most embryos all four cells – divide meridionally (Table 2C: third column, n = 48). In the vegetal cell tier, finally, the dextral division pattern is most consistent and shown by almost all cells (Table

2C: fourth column, n = 48). In total, these data suggest that the pattern and process of cleavage are more variable in the embryo's animal hemisphere (animal and animal-equatorial cell tiers) than in its vegetal hemisphere (vegetal and vegetal-equatorial cell tiers). It is due to this variability in the animal hemisphere that no two analyzed embryos exhibit an identical pattern of cleavage orientations in all their blastomeres (Table 2C).

By the 32-cell stage the embryo has developed into a roundish blastula (Fig. 11N-Q). The cells of the vegetal hemisphere are often slightly larger than the cells in the animal hemisphere, and the blastocoel occupies about 50% to 60% of the embryo's diameter. The variability in the cleavage divisions leads to a high degree of variation in the blastomere arrangement at the 32-cell stage. Due to this, no distinct pattern of arrangement could be identified, and the embryos were only analyzed with respect to the numbers of pole-encircling blastomeres.

The analyses of the number of pole-encircling cells in the 32-cell stage give a largely similar picture than in the 16-cell stage, however, it indicates a somewhat increasing variability for the animal pole. Again, four blastomeres surrounding both poles is the most abundant pattern, yet it is shown by only about two-fifth of embryos (Table 3B; Figs. 5M, 11N,Q). In total, four cells are located at the animal pole in a bit less than half of the analyzed embryos, while the same is true in nine-tenth of the embryos for the vegetal pole (Table 3B). Consistent with the previous stage, among the embryos with more than four pole cells, the number of these cells ranges from five to seven for the animal pole and these cases occur with decreasing frequency the higher the deviation from four cells is (Table 3B; Figs. 3P, 11R,T, 12G,Q); whereas, at the vegetal pole rarely five pole cells are encountered (Table 3B; Fig. 11S). The higher variability regarding the animal pole probably results from the somewhat irregular cleavage divisions observed in the animal hemisphere (see above).

Similar to the previous stages, following compactation, the embryo's poles can display a small central opening (Figs. 5M, 11N-O), a polar furrow (Fig. 11Q), or an X-furrow. Most 32-cell embryos have a small opening at the animal pole, but closed cell contacts at the vegetal pole (Table 1). Embryos with more than four pole cells usually display a large pole opening (Figs. 11R-T, 12G,Q).

3.1.1.6. Sixth cleavage cycle and 64-cell embryo

The high variation in the cell arrangements of the 32-cell embryo makes it extremely difficult to trace the sixth cleavage cycle in others than the animal most and the vegetal most tiers of cells. Although several of these blastomeres divide in a sinistral direction (Fig. 5N-Q) – thus, following the pattern of alternating oblique orientations of divisions that is observable from the third cleavage on – the data suggest that the cleavage pattern becomes more variable with this cleavage cycle (Table 2D). Though, it remains more consistent in the vegetal most blastomeres. While in the animal tier only a third of the analyzed cells undergo sinistral divisions and other orientations are abundant (Table 2D: first column, n = 39; Fig. 3Q-S), in the vegetal tier, nearly two-thirds of the cells divide sinistrally, and in half the embryos, three or all of the vegetal cells do (Table 2D: second column, n = 46; Fig. 5O-Q). No two identical patterns of divisions were observed among the analyzed embryos (Table 2D).

The 64-cell stage was only analyzed on 4D-recorded material. The embryo has a big blastocoel surrounded by small and roundish blastomeres (Figs. 3T, 5S).
The number of cells encircling the poles reflects the variation observed during the divisions. Only in few embryos, four blastomeres are located at both poles (Fig. 5R), the most abundant pattern being instead six animal and four vegetal cells (Table 3C; Fig. 12J,T). While in only about a third of the embryos four cells are found at the animal pole, this is the case for the vegetal pole in nearly two-thirds of the embryos (Table 3C). For both poles the range of variation is higher than in previous stages; at the 64-cell stage, the first and only embryo with eight cells surrounding a pole was encountered (Table 3C).

After compactation, three-fourths of the 64-cell embryos exhibit closed cell contacts at the vegetal pole – either organized as a polar furrow (Fig. 5R) or as an X-furrow (Table 1) – and a small opening at the animal pole. Again, if more than four cells are located at a pole, there is a larger central opening present (Figs. 3S, 12J,T).

Fig. 3. Cleavage of a *P. pallida* embryo in animal view from zygote to 64-cell stage. Sequence of DIC images showing the development of one embryo that was 4D-recorded in a view at the animal pole. The polar bodies are oriented toward the observer, and are marked with an asterisk in some images. Lines indicate the sister cells after divisions, and dots mark the sister cell that is located closer to the animal pole. Scale bar in A applies to all: 20 µm.
A. Spherical zygote surrounded by a delicate fertilization membrane (open arrowhead). **B**. 2-cell embryo directly after first cleavage division. The embryo is uncompacted and the cells are of roundish shape; the fertilization membrane displays a straight appearance (open arrowhead). **C**. 2-cell embryo after compactation between first and second cleavage cycles. The cells became flattened against each other; the fertilization membrane has an undulating appearance (open arrowhead). **D**. Uncompacted 4-cell embryo displaying cells of roundish shape directly after second cleavage divisions. **E**. 4-cell embryo compacted between second and third cleavage cycles. The cells flattened against each other and drew closer to the central animal-vegetal axis; a small central opening persists (arrowhead); the fertilization membrane has a more undulating appearance (open arrowhead). **F**. Blastomere elongations prior to third cleavage divisions. The animal apices of the cells became drawn out pointing into clockwise directions, yet differently distinct in different cells (arrowheads indicate pronounced elongations). **G**. Full-focal projection of 8-cell embryo directly after third cleavage divisions. All cells divided with a dextral orientation, and the four animal blastomeres (marked with dots) are aligned shifted clockwise relative to their vegetal sister blastomeres; however, this is differently distinct in different cell pairs. **H**. Full-focal projection of the 8-cell embryo after compactation. During compactation the animal/vegetal sister blastomeres glided into more juxtaposing positions along the animal-vegetal axis; by this, the shifted cell alignment post divisions became obscured. At the animal pole compactation established a polar furrow (arrowhead), at the vegetal pole a small opening is present between the four cells (not shown); the fertilization membrane shows an undulating appearance (open arrowhead). **I-J**. Fourth cleavage cycle in the animal cells of the 8-cell stage: cell elongations prior to divisions (I), and blastomeres directly after divisions (J). All cells divide obliquely and in a sinistral direction; the four cells given off toward the animal pole (marked with dots in J) are positioned counterclockwise relative to their vegetally situated sister cells. **K**. Compacted 16-cell embryo. Four blastomeres (marked with dots) encircle the animal pole, and leave a small opening central between them (not visible as covered by central polar bodies); likewise four blastomeres are located at the vegetal pole, but these cells touch centrally (not shown). **L-O**. Fifth cleavage cycle in the animal cell tier of the 16-cell stage. The images showing successive elongations and slightly asynchronous divisions of cells, and some variation with respect to cleavage orientations: one blastomere divides equatorially (L-M), the other three blastomeres divide in a dextral direction (N-O). Triangle in O marks a blastomere from the animal-equatorial cell tier (see P). **P**. Compacted 32-cell embryo. The irregular equatorial division of one animal blastomere during fifth cleavage led to the animal daughter cell of a blastomere from the 16-cell embryo's animal-equatorial cell tier (marked with triangle in O) to come to lie at the animal pole. Consequently, five cells (marked with dots) encircle a central opening at the animal pole (partially covered by polar bodies); at the vegetal pole four cells are located and these touch centrally (not shown). **Q-S**. Sixth cleavage cycle in the animal tier of cells of the 32-cell stage: successive cell elongations and cell divisions. The cleavage divisions pass irregularly: three cells divide meridionally (two divisions in R and lower division in S), one cell divides equatorially (upper division in S). This results in seven cells (marked with dots in S) to be situated at the animal pole (this hold also through compactation; not shown); four cells forming a polar furrow are located at the vegetal pole (not shown). **T**. Optical section through compacted 64-cell embryo. Small cells surround a large blastocoel (bc).

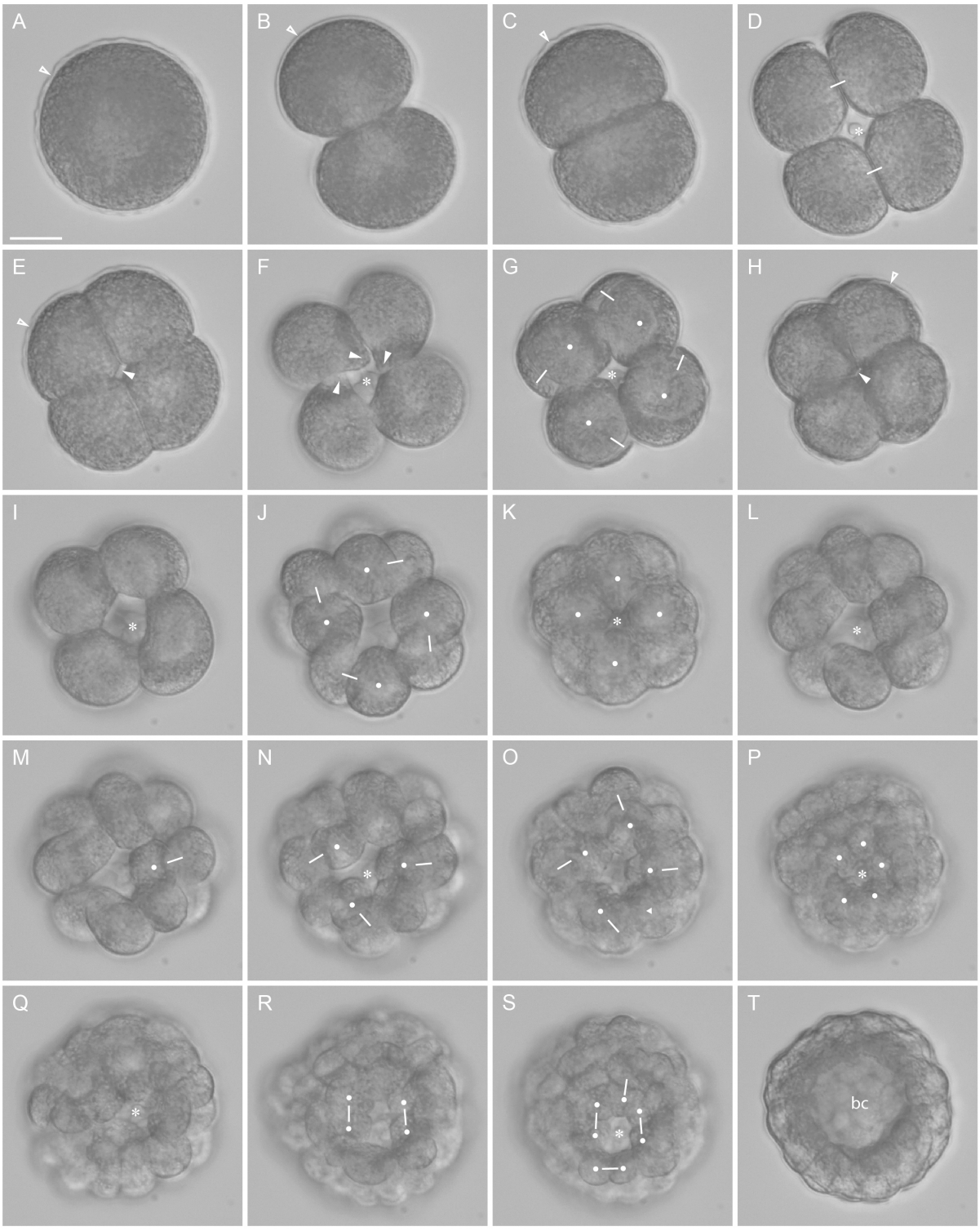

Fig. 3. Cleavage of a *P. pallida* embryo in animal view from zygote to 64-cell stage.

Fig. 4. Cleavage of a *P. pallida* embryo in lateral view from zygote to 32-cell stage. Sequence of DIC images showing the development of one embryo that was 4D-recorded in a lateral view, perpendicularly to the animal-vegetal axis. Asterisks mark the polar bodies visible at the animal pole (A-B), or the position of the animal pole (D-L), respectively; dashed lines indicate the animal-vegetal axis. Sister cells are connected by solid lines. Scale bar in A applies to all: 20 µm.
A. Ovoid zygote surrounded by a delicate fertilization membrane (open arrowhead). **B**. Compacted 2-cell embryo. The left blastomere lies closer to the observer. **C**. Compacted 4-cell embryo. Only three blastomeres are visible (one lies closest to the observer and is marked with a dot); they cover the fourth blastomere that is lying opposite to the observer. **D**. Blastomere elongations shortly prior to third cleavage divisions. The cells elongate somewhat obliquely to the animal-vegetal axis (dashed line). **E-F**. Successive cells divisions during third cleavage cycle, which passes slightly asynchronous in this embryo (division in right cell in E is delayed). All cells divide obliquely and with a dextral orientation; yet, the obliqueness is not strongly pronounced (compare inclination of sister cell pair closest to the observer against animal-vegetal axis). **G**. Blastomere elongations oriented obliquely to the animal-vegetal axis shortly prior to fourth cleavage divisions. **H-I**. Cell divisions in fourth cleavage cycle, passing somewhat asynchronously. The cells divide obliquely and with sinistral orientations; the obliqueness of divisions is more distinct than in third cleavage (see inclinations of sister cell pairs closest to the observer relative to animal-vegetal axis). One blastomere per quadrant comes to lie closest to the animal pole and one blastomere closest to the vegetal pole (marked with dots in H for cells closest to the observed). **J-L**. Successive cell elongations and cell divisions in fifth cleavage cycle. Sister cell relationships only are indicated for the cells closest to the observer; these cells are the descendants of the cell marked with a dot in C. All the cells divide obliquely and with a dextral orientation; however, the inclination of the division differs between the different cells. One blastomere comes to lie closest to the animal pole and one blastomere closest to the vegetal pole (marked with dots in K-L).

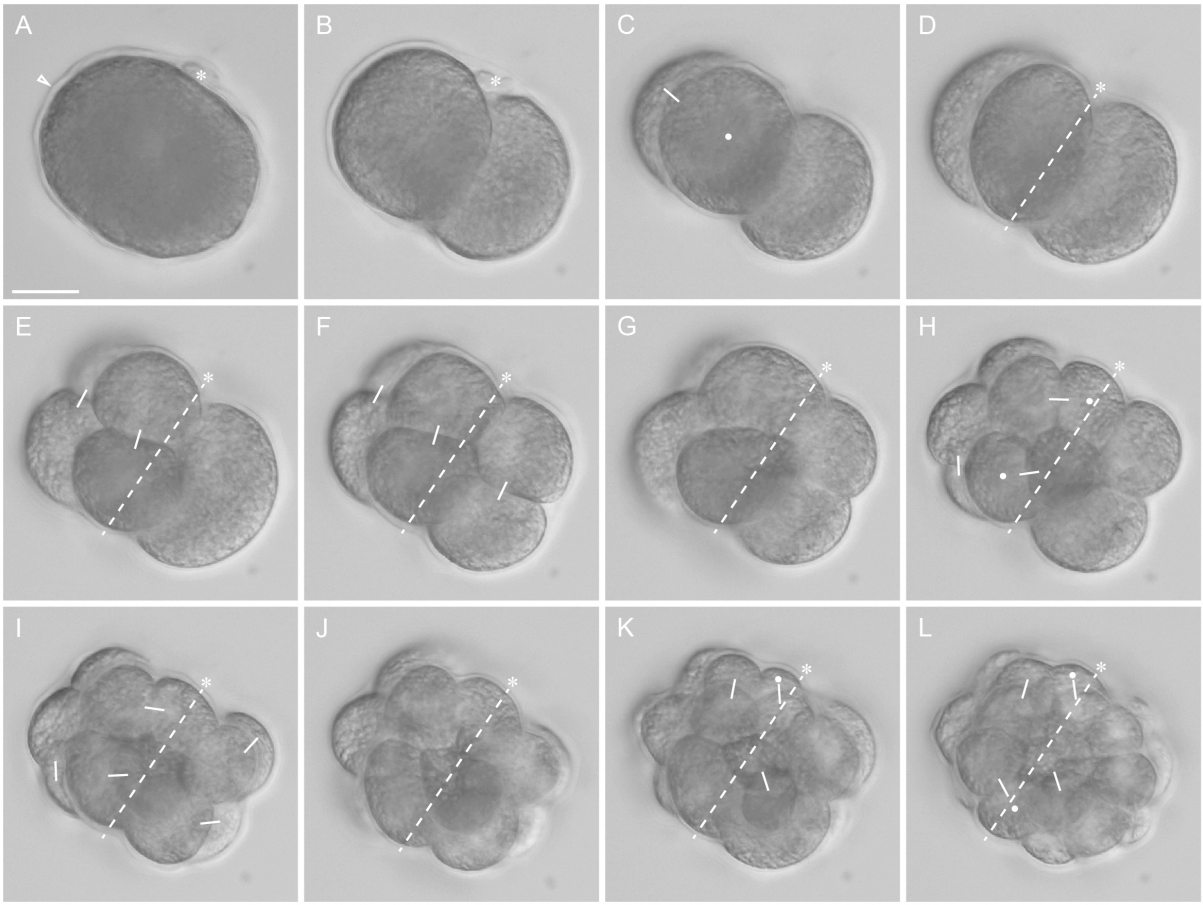

Fig. 4. Cleavage of a *P. pallida* embryo in lateral view from zygote to 32-cell stage.

Fig. 5. Cleavage of a *P. pallida* embryo in vegetal view from 2-cell stage to 64-cell stage. Sequence of DIC images showing the development of one embryo (except C') that was 4D-recorded in a view at the vegetal pole (the animal polar bodies are not visible). Lines indicate the sister cells after divisions, and dots mark the sister cell that is located closer to the vegetal pole. Scale bar in A applies to all: 20 µm.
A. Uncompacted 2-cell embryo directly after first cleavage division. It is surrounded by a delicate fertilization membrane, which has a straight appearance (open arrowhead). **B**. Uncompacted 4-cell embryo directly after second cleavage divisions. **C**. 4-cell embryo after compactation between second and third cleavage cycles. The cells flattened against each other and lost their initial spherical shape (see B); a small opening persists between the four cells (arrowhead); the fertilization membrane displays an undulating appearance (open arrowhead; compare to A-B). **C'**. Compacted 4-cell stage as in C, but of a different specimen: in this embryo a polar furrow between two oppositely situated non-sister cells is formed (arrowhead). **D**. Cell elongations at the blastomeres' vegetal apices prior to third cleavage divisions. The elongations point into clockwise directions, yet note that the embryo is looked at from the vegetal pole; they are differently distinct in different cells (arrowheads indicate pronounced elongations). **E**. Full-focal projection of 8-cell embryo directly after third cleavage divisions. The divisions passed into dextral directions, yet differently distinct in the different cells, and the four vegetal blastomeres (marked with dots) are to different degrees positioned shifted clockwise relative to their animal sister blastomeres (note that the embryo is looked at from the vegetal pole). **F**. Full-focal projection of the 8-cell embryo after the process of compactation. The animal/vegetal sister blastomeres glided into more juxtaposing alignments along the animal-vegetal axis, and now are situated nearly on top of each other. A small opening is present central at the vegetal pole (arrowhead), and the same is the case for the animal pole (not shown). The fertilization membrane has an undulating appearance (open arrowhead). **G-H**. Fourth cleavage cycle in the vegetal blastomeres of the 8-cell stage: cell elongations prior to divisions (G), and cells directly after divisions (H). All cells divide obliquely and in a sinistral direction (note that the embryo is looked at from vegetal). **I**. Compacted 16-cell embryo. The four vegetal blastomeres (marked with dots) leave a small central opening (arrowhead); likewise at the animal pole four blastomeres are located and encircle a small opening (not shown). **J-L**. Fifth cleavage cycle in the vegetal cell tier of the 16-cell embryo: successive cell elongations and cell divisions, all passing obliquely and in a dextral direction. **M**. Compacted 32-cell embryo. Four blastomeres (marked with dots) encircle the vegetal pole, and leave a small opening (arrowhead); likewise four blastomeres are situated at the animal pole (not shown). **N-Q**. Sixth cleavage cycle in the vegetal tier of cells of the 32-cell stage: all four blastomeres successively elongate and divide in a sinistral direction; the four blastomere that come to lie at the vegetal pole (marked with dots in Q) are positioned counterclockwise relative to their sister cells (note that the embryo is looked at from the vegetal pole). **R**. Compacted 64-cell embryo. The vegetal pole is encircled by four blastomeres (marked with dots), between two of them a small polar furrow is established (arrowhead); likewise four blastomeres lie at the animal pole (not shown). **S**. Optical section through compacted 64-cell embryo showing a large blastocoel (bc) surrounded by roundish blastomeres.

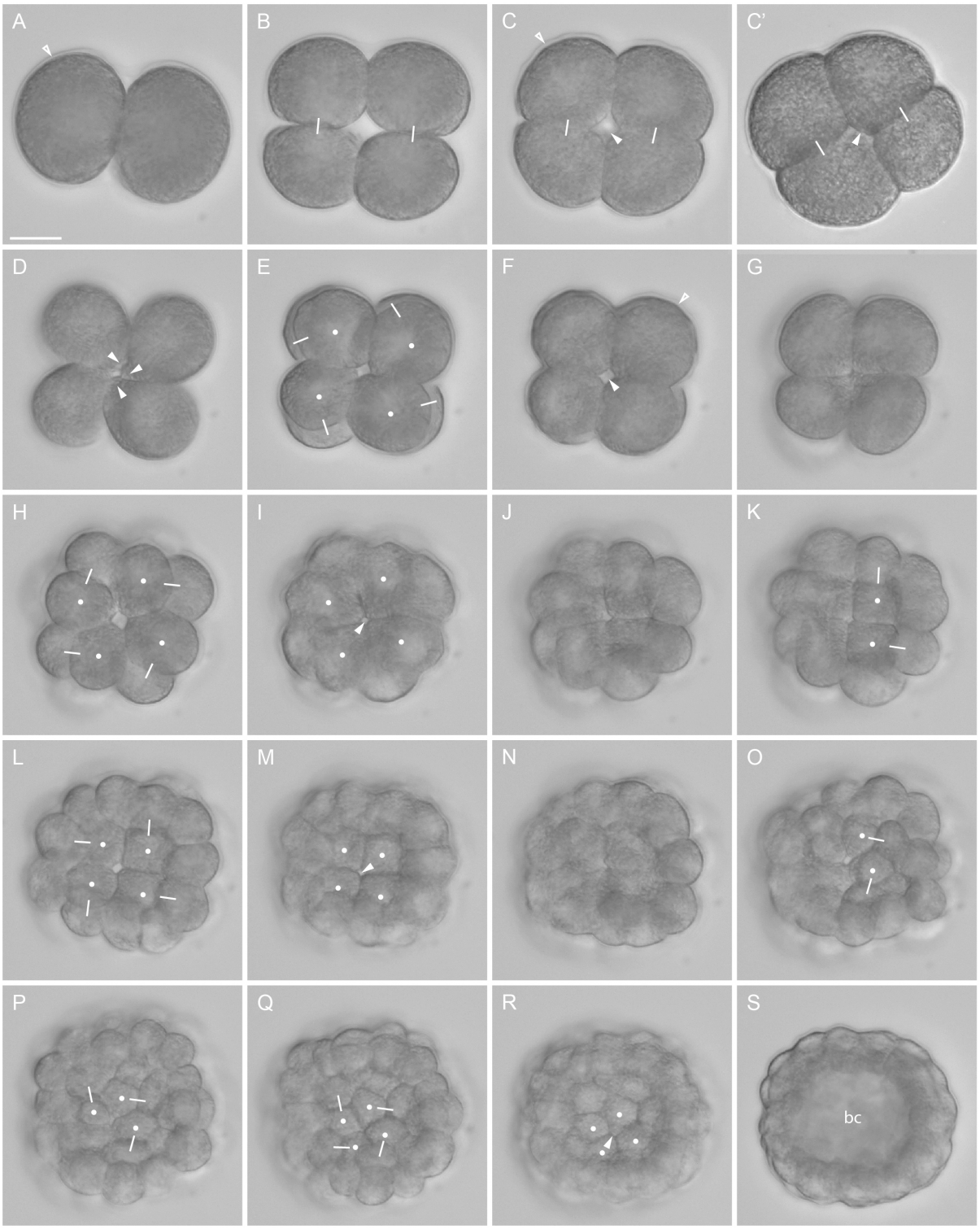

Fig. 5. Cleavage of a *P. pallida* embryo in vegetal view from 2-cell stage to 64-cell stage.

Fig. 6. Timing of cleavage divisions and cell lineage in *P. pallida*. For four different 4D-recorded embryos, the cell lineage up to the sixth cleavage cycle (labeled on top of A for A-C, and on top of D) is given (in lineages A and C, respectively, one cell could not be traced through the sixth division; indicated with dashed line). The recordings started at the zygote in embryos A-C, and at the 2-cell stage in embryo D. Labeled axes beneath each lineage give the timing of the cleavage divisions at 17°C, post egg release by opening of the coelom ('hours pER'). The first division takes place after approximately 1.5 to 2 hours. Subsequently, the time interval between two successive divisions is about 30 to 40 minutes, but it increases following the fourth cleavage cycle. In embryos A-C, the initial cleavage cycles pass approximately synchronous, but the divisions become more asynchronously with increasing cleavage stages. In embryo D, the second cleavage divisions pass markedly asynchronous, resulting in the formation of a transient 3-cell stage; this initial asynchrony is recognizable in the lineage also though later cell cycles (yet, did not seem to negatively effect the embryo's development; see text). The exact timing and the sequence of divisions vary between the different embryos.

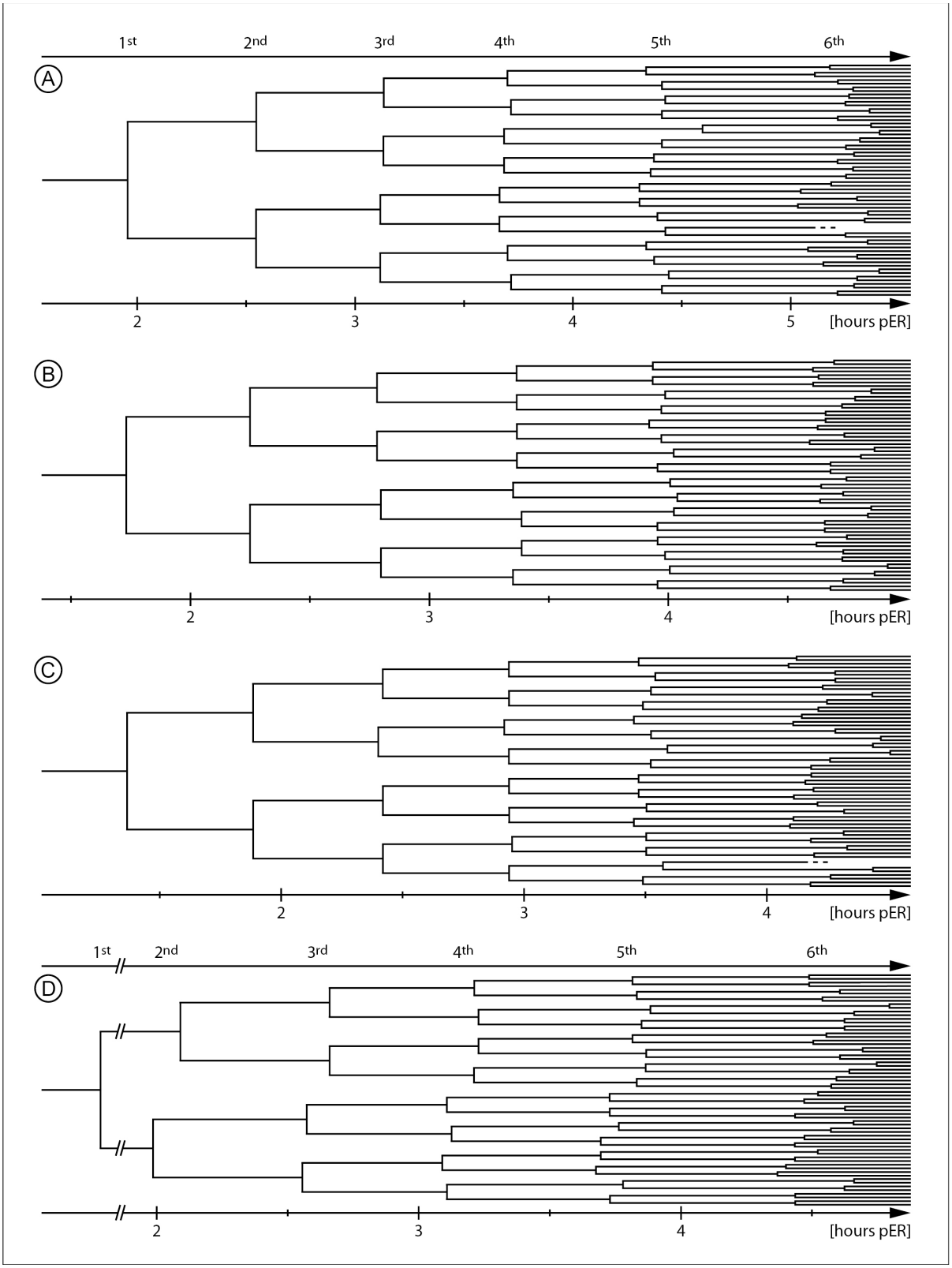

Fig. 6. Timing of cleavage divisions and cell lineage in *P. pallida*.

Fig. 7. *P. pallida* embryos from 2-cell stage to third cleavage cycle. Imaris volume projections (Blend mode; except C and J: MIP mode) of fixed embryos that were stained against α-tubulin (reddish) and for nucleic acids (bright cyan) (except A-B: nuclear stainings only); blastomere shape signals result from autofluorescence of the cytoplasm (dark cyan). Polar bodies are indicated with asterisks; lateral views are oriented with the animal pole to the top (an: animal, vg: vegetal). Images connected with white bars (e.g., D to E, F to I) show the same embryo from different perspectives. Scale bars: 20 µm.
A. 2-cell embryo (animal view). **B**. Transient 3-cell stage (animal view) with large cell on the left not yet divided. **C**. 4-cell embryo shortly after second cleavage divisions (animal view). The chromosomes appear still condensed (indicated by arrowheads); the sister cells pairs within the embryo can be recognized by the midbody residual of the mitotic spindle apparatus (open arrowheads). **D-E**. Compacted 4-cell embryo displaying a closer cell packing (compare to C; animal view). Polar bodies (marked in D) were removed in E to show the small opening between the four blastomeres (arrowhead in E). **F-I**. 4-cell embryo in early metaphase of third cleavage division: the images represent virtual sections through each one of the four blastomeres in the embryo in lateral view, showing the mitotic spindle in each cell (blastomere shapes outlined by dotted lines). The spindle inclinations vary between the cells: they are inclined pronounced dextrally in two cells (F,H), weakly dextrally with an inclination of less than 10° in one cell (G), but sinistrally in the fourth cells (I). **J-N.** Animal (J) and lateral views (K-N) of 4-cell embryo with cells in metaphase (K,L) and anaphase (M,N) of third cleavage division. Again, lateral sections each show the mitotic spindle in one of the four blastomeres (outlined by dotted lines in K-N). In this embryo the spindles are inclined less than 10° in all four cells. **O-T.** Animal (O), vegetal (P), and lateral views (Q-T) of 4-cell embryo in anaphase and beginning cytokinesis of third cleavage cycle (the nuclei signal is not visible). The animal and vegetal apices of the blastomeres are slightly elongated pointing in clockwise directions when looked at from the respective pole (arrowheads in O and P). Lateral sections show the dextrally inclined spindles, and the elongated and likewise dextrally oriented cell shape of each blastomere (outlined by dotted lines in Q-T).

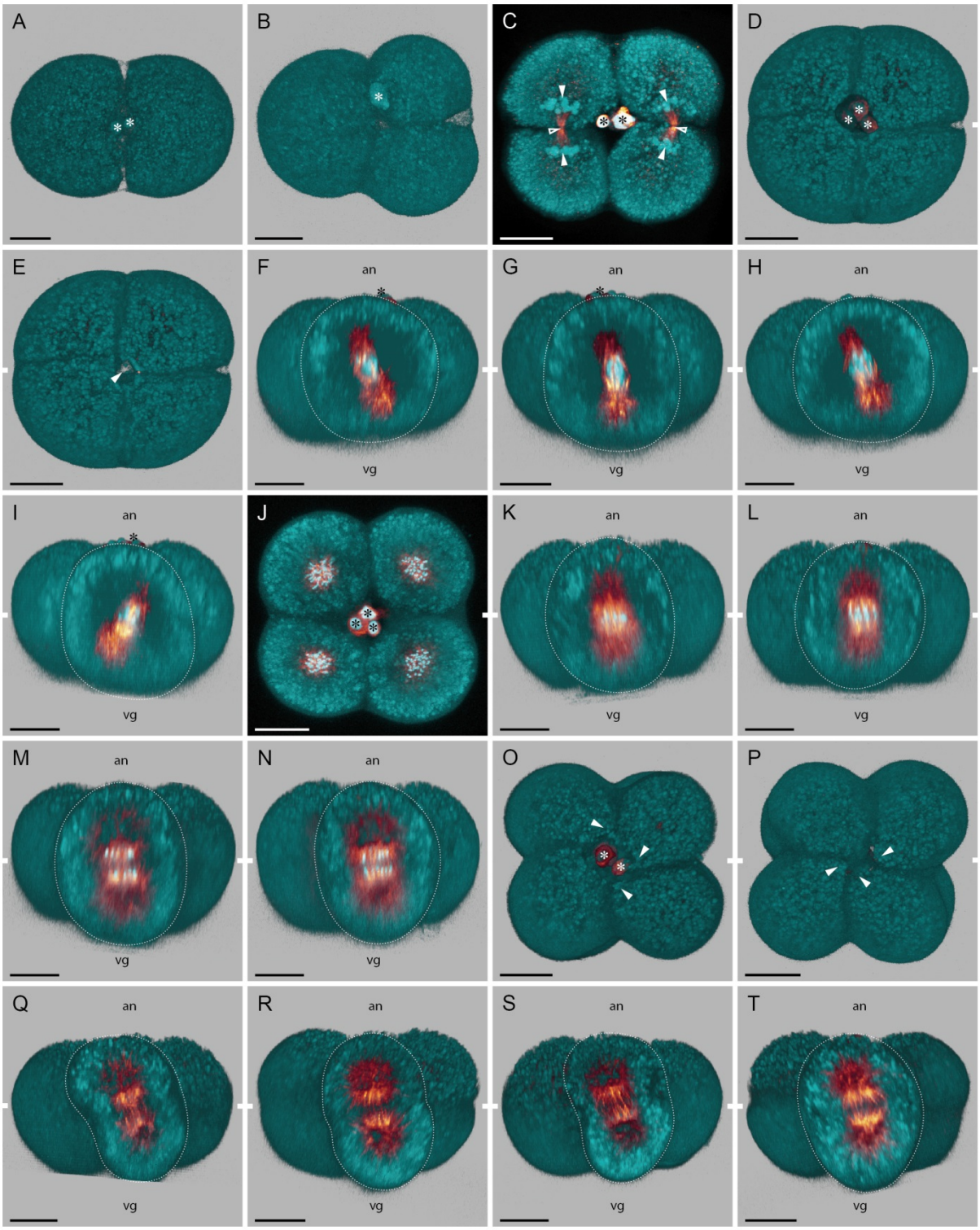

Fig. 7. *P. pallida* embryos from 2-cell stage to third cleavage cycle.

Fig. 8. Inclinations of cleavage axes of third and fourth cleavages in *P. pallida*. The charts give the results of the quantitative analyses of the inclinations of mitotic spindles and cell divisions relative to the animal-vegetal axis in cells during the third (A,B) and the fourth cleavage cycles (C,D); for the latter, separated analyses for cells of the animal cell tier (C',D') and the vegetal cell tier (C",D") of the 8-cell stage are provided. Results obtained from 4D-recorded embryos (left charts: A,C,C',C") and from fixed embryos (right charts: B,D,D',D") are given separately. Abscissas give the angles of inclinations (dex: dextral, eq: equatorial, mer: meridional, sin: sinistral). The heights of the bars give the relative frequencies in which the respective inclinations (grouped in 5°-steps) were observed over all analyzed cells ('n'); the numbers in the bars give the absolute numbers of cells in the respective groups (corresponding half-bars on both ends of the abscissa in C represent inclinations of exactly 90°). In the third cleavage cycle (A,B), the cleavage axes are inclined along positive angles, but the obliqueness is not very distinct. The data from 4D microscopy (A) are more consistent than the data from fixed embryos (B). In the fourth cleavage cycle (C,D), the cleavage axes are inclined sinistrally and generally more pronounced obliquely than in the third cleavage. Data obtained from fixed material (D,D',D") show a higher variability and cases of spindles deviating from the general pattern (see text). In both cleavage cycles, the exact angles of inclination of cleavage axes vary between the analyzed cells in the samples.

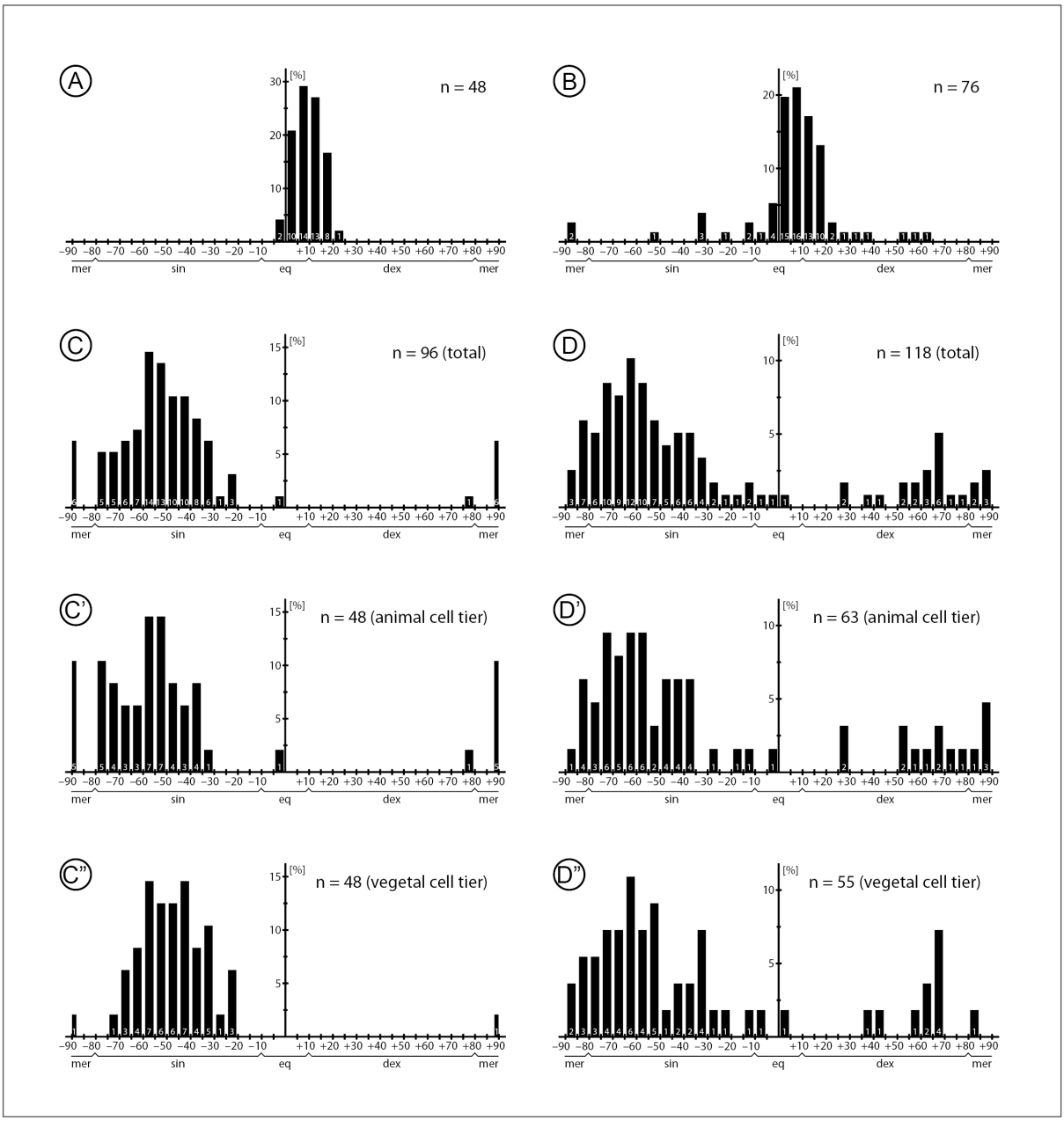

Fig. 8. Inclinations of cleavage axes of third and fourth cleavages in *P. pallida*.

Fig. 9. Different *P. pallida* embryos at the 8-cell stages. Imaris volume projections (Blend mode) of three different 8-cell embryos fixed in a compacted state between the third and fourth cleavage cycles. Specimens in A-G and O-T were stained for nucleic acids, the specimen in H-N additionally against α-tubulin (reddish); blastomere shape signals result from autofluorescence of the cytoplasm (cyan). Each embryo is documented in successive images giving a view on the animal pole (e.g., A-B; for embryos A-G and H-N, two successive images give the animal pole first including the polar bodies (asterisks in A and H), and second (B,I) with removed polar bodies), four lateral views – each shows one of the four animal/vegetal sister cell pairs of the embryo oriented toward the observer (e.g., C-F) –, and a view on the vegetal pole (e.g., G). Polar bodies are indicated with asterisks; lateral views and are oriented with the animal pole to the top (an: animal, vg: vegetal). Scale bars: 20 µm.
Generally, the 8-cell embryo is organized in an animal and a vegetal cell tier of four blastomeres each. However, the embryos differ with respect to the alignment of the individual animal/vegetal sister cell pairs relative to the animal-vegetal axis, and the organization of the embryo's poles. In embryo A-G, the animal blastomere in all four animal/vegetal cell pairs is located clockwise of its vegetal sister blastomere (the upper cell is located left of the lower cell in lateral views C-F), and an opening is present between the four blastomeres at the animal pole as well as at the vegetal pole (arrowheads in B and G). In embryo H-N, a clockwise alignment is apparent in one sister cell pair (J) and only weakly displayed in a second pair (K), while in two animal/vegetal cell pairs the animal blastomere is positioned juxtaposing its vegetal sister blastomere along the animal-vegetal axis (the upper cell is located on top of the lower cell in lateral views L-M); again, an opening is present at the animal and the vegetal pole (arrowheads in I and N). In embryo O-T, finally, in all four animal/vegetal cell pairs the animal blastomere is located juxtaposing its vegetal sister blastomere (P-S); in this embryo a polar furrow is present at the vegetal pole (arrowhead in T).

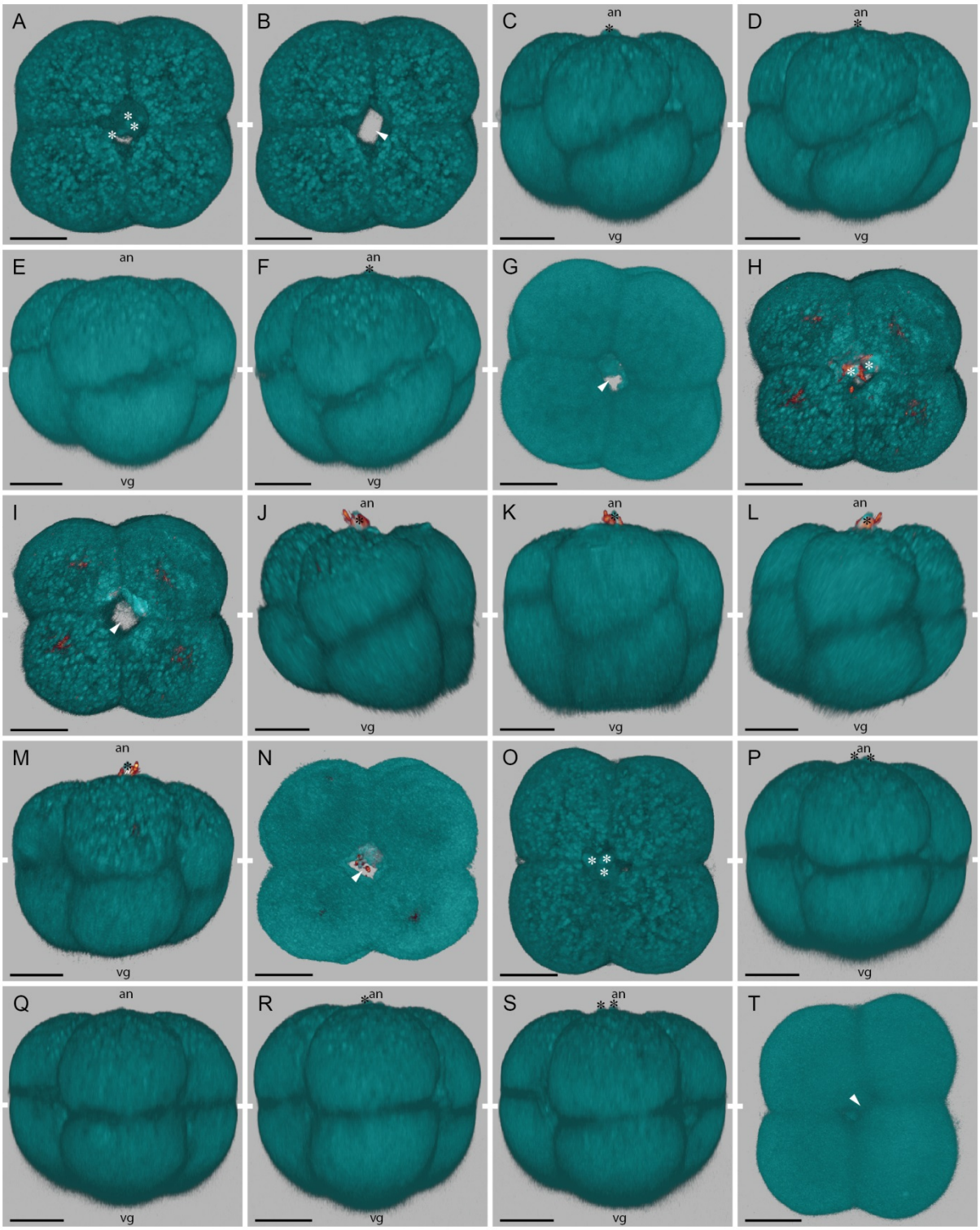

Fig. 9. Different *P. pallida* embryos at the 8-cell stages.

Fig. 10. *P. pallida* embryos at fourth cleavage cycle. Imaris volume projections (Blend mode) of four different 8-cell embryos fixed during the fourth cleavage division. All specimens were stained against tyrosinated α-tubulin (reddish) and for nucleic acids (bright cyan); blastomere shape signals result from autofluorescence of the cytoplasm (dark cyan). In the first three embryos (A-E,F-J,K-O) the cells are in metaphase, in the fourth embryo (P-T) the cells are in anaphase of mitosis. For each embryo, a view on the animal pole (e.g., A) and four successive images representing virtual sections through the animal and vegetal blastomere in each of the four embryonic quadrants (e.g., B-E) are given; the latter images show the mitotic spindles in the individual blastomeres (cell shapes outlined by dotted lines). Polar bodies are indicated with asterisks; lateral views and are oriented with the animal pole to the top (an: animal, vg: vegetal). Scale bars: 20 µm.
The different embryos and their individual blastomeres differ with respect to the exact inclination, and partly even to the orientation, of the mitotic spindles relative to the animal-vegetal axis. In embryos A-E and F-J, most spindles are oriented obliquely and with sinistral orientations (but note dextral spindle orientation in animal blastomere in I). In embryo K-O, the spindles are oriented sinistrally or dextrally in different blastomere. In embryo P-T, the spindles are inclined sinistrally or meridionally.

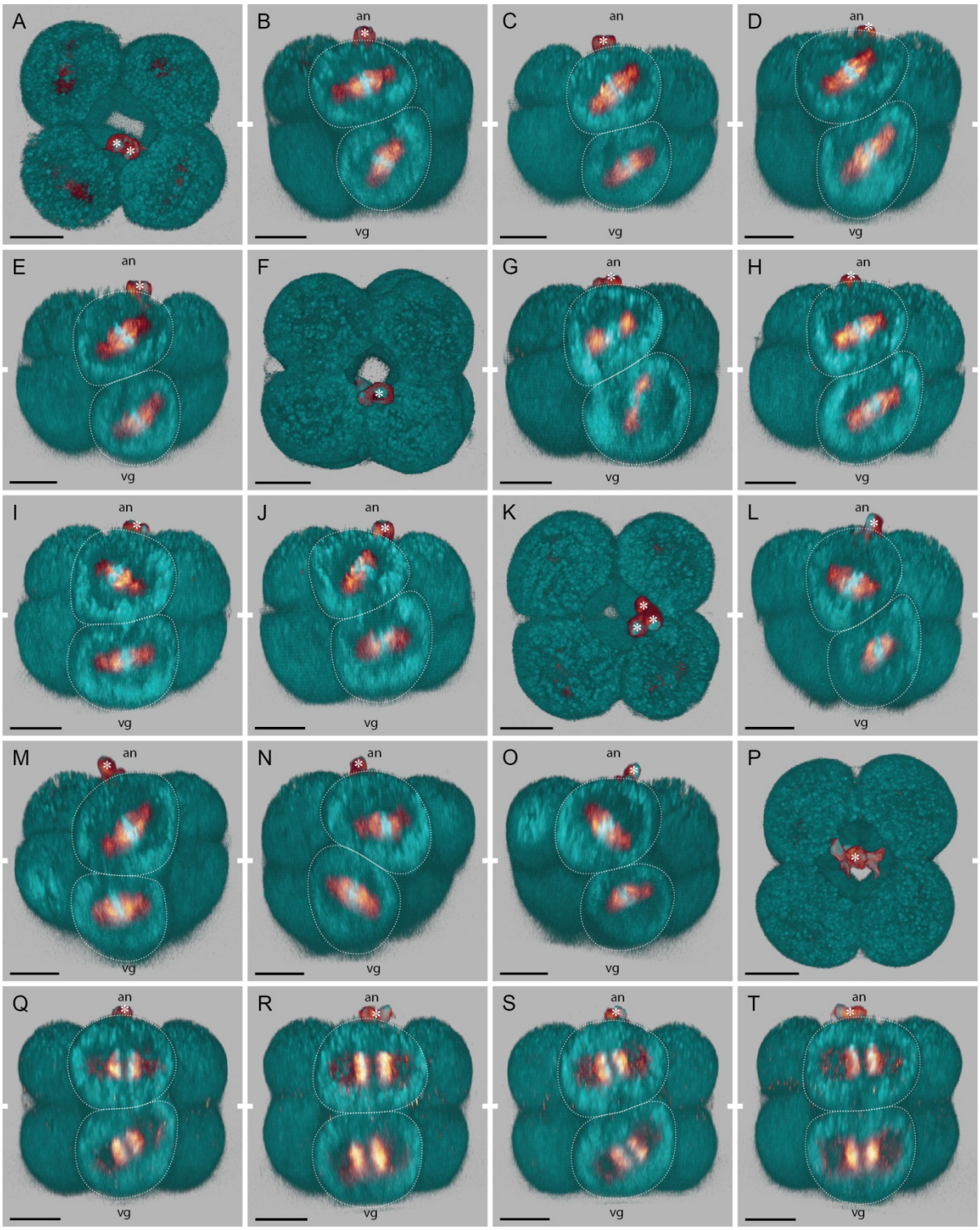

Fig. 10. ***P. pallida*** **embryos at fourth cleavage cycle.**

Fig. 11. *P. pallida* embryos at 16-cell stage and 32-cell stage. Imaris volume projections (Blend mode) of fixed embryos that were stained for nucleic acids (bright cyan) (except M: additional staining against α-tubulin; reddish); blastomere shape signals result from autofluorescence of the cytoplasm (dark cyan). Polar bodies are indicated with asterisks; lateral views are oriented with the animal pole to the top (an: animal, vg: vegetal). Scale bars: 20 µm.
A-H. 16-cell embryo in animal (A-B), lateral (C-F), and vegetal views (G), and a section though the equator area (H). The embryo is composed of four tiers of four blastomeres each. These cell tiers are stacked along the animal-vegetal axis, and thereby shifted against each other: so the individual blastomeres are situated in the gaps between adjacent blastomeres, and the cell tiers are intertwined at the equator of the embryo (indicated by dotted line in C-F). At the equator area a large blastocoel (bc) is surrounded by the eight cells of the animal-equatorial and vegetal-equatorial cell tiers (H). Four blastomeres are situated at the animal (A-B) and at the vegetal (G) pole (pole cells are marked with dots in B-G), and these cells each encircle a small central opening (arrowheads in B and G; polar bodies (asterisks in A) were removed in B). **I-J**. 16-cell embryo in which four blastomeres are located at the animal pole (marked with dots in I), but five cells are situated at the vegetal pole (marked with dots in J). At both poles a small opening is present between the pole cells (arrowheads; in I partly covered by polar bodies). **K-L**. 16-cell embryo in which five cells encircle the animal pole (marked with dots in K), and these cells surround a big opening into the blastocoel (arrowhead in K); at the vegetal pole four blastomeres are located and a small polar furrow is present (marked with dots and arrowhead, respectively, in L). **M**. 16-cell embryo in which with six cells (marked with dots) surround a large opening at the animal pole (arrowhead); in the same embryo four cells are situated at the vegetal pole (not shown). **N-Q**. 32-cell embryo in animal (N-O), lateral (P) and vegetal views (Q). Four blastomeres are situated at the animal as well as the vegetal pole (marked with dots in O and Q); the vegetal cells appear slightly larger than the animal ones (compare Q and O). In lateral view the blastomeres appear highly intertwined (P). At the animal pole a small central opening is present (arrowhead in O; polar bodies (asterisks in N) were removed in O), at the vegetal pole a polar furrow is found (arrowhead in Q). **R-S**. 32-cell embryo in which five cells are located at the animal pole (R) and at the vegetal pole (S; marked with dots); at both poles a small opening is present between the cells (arrowheads; in R partly covered by polar bodies). **T**. 32-cell embryo with six cells encircling an opening at the animal pole (marked with dots and arrowhead, respectively); in the same embryo four cells are situated at the vegetal pole (not shown).

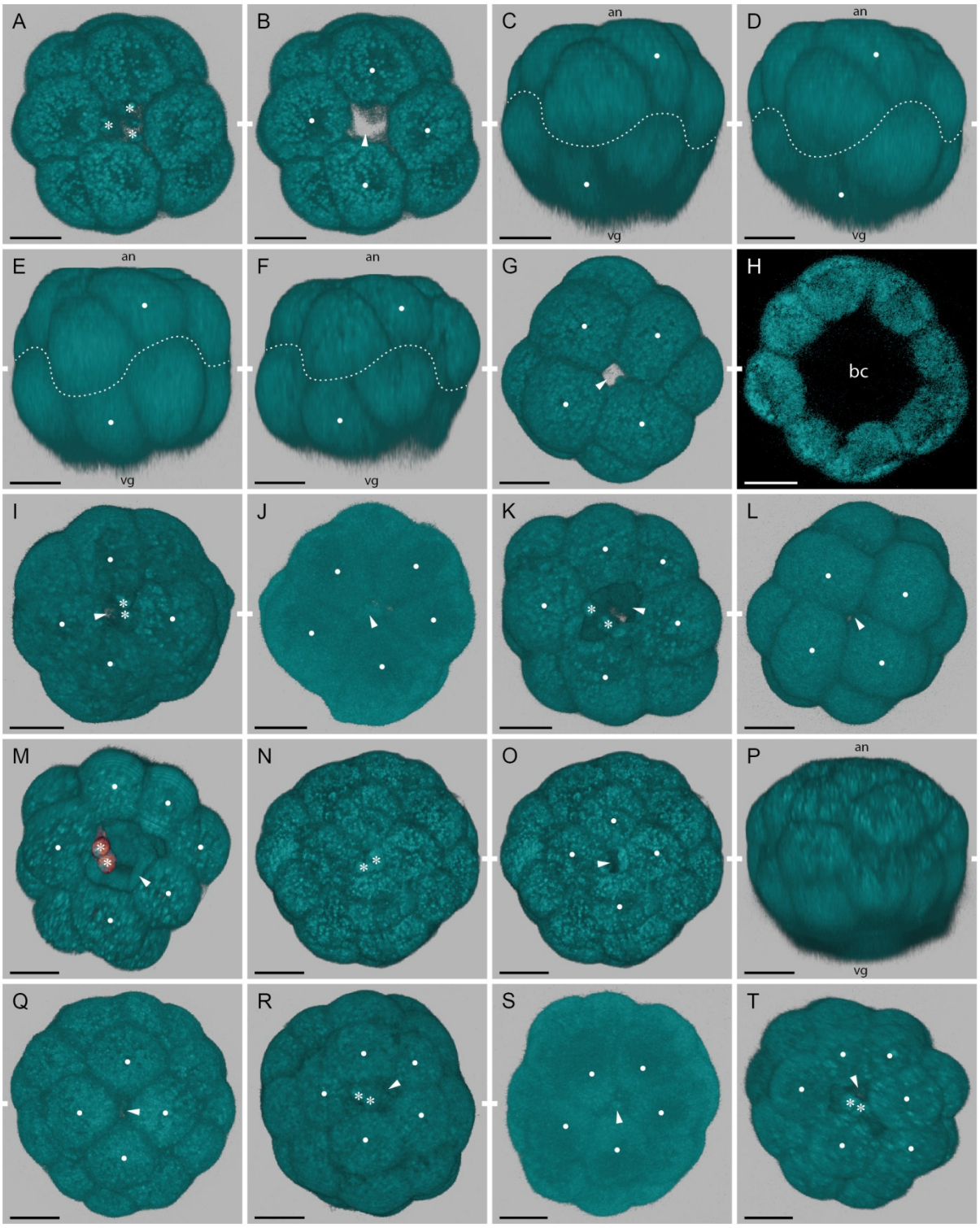

Fig. 11. *P. pallida* embryos at 16-cell stage and 32-cell stage.

Fig. 12. Examples of cleavage variability in two *P. pallida* embryos. Sequence of DIC images showing the development of two different embryos (A-J,K-T), 4D-recorded in a view at the animal pole, from the 8-cell stage to the 64-cell stage. In some images the polar bodies are marked with an asterisk. Lines indicate the sister cells after divisions. Scale bar in A applies to A-J, scale bar in K to K-T: 20 µm.
A. Full-focal projection of 8-cell embryo directly after third cleavage divisions. The animal blastomeres (marked with dots) differently are either aligned clockwise of their vegetal sister blastomeres (upper two cell pairs) or located on top of the vegetal blastomere (lower two cell pairs). **B-C**. Fourth cleavage cycle in the animal cells of the 8-cell stage: cell elongations prior to divisions (B), and blastomeres directly after divisions (C). Three cells divide markedly obliquely and in sinistral directions (left, upper, and right cells in B); their animal daughter cells (marked with dots in C) come to lie aligned counterclockwise relative to their vegetally situated daughter cells. But in one cell (marked with triangle in B) the cleavage division passes with a high inclination and is oriented dextrally; its animal daughter is aligned clockwise relative to its more vegetal daughter (lower sister cell pair in C). The progeny of this cell will display irregularities in divisions up to late cleavage cycles. **D**. 16-cell embryo after compactation. Due to the high inclination of fourth division in the irregular cell (marked with triangle in B), both its daughter cells come to lie at the animal pole; this is therefore encircled by five blastomeres (marked with dots) surrounding a pole opening (arrowhead). In the same embryo only four blastomeres are situated at the vegetal pole (not shown). **E-F**. Fifth cleavage cycle in the animal cells of the 16-cell stage: elongations of cells (E), and blastomeres directly after divisions (F). Three cells divide obliquely and dextrally (left, upper, and right cells in E), and only their animal daughter cells (marked with dots in F) come to lie at the animal pole. In contrast, but both daughter cells of the irregular blastomere (marked with triangles in E) divide equatorially, and their animal daughters both come to lie at the pole (lower/left two sister cell pairs in F). **G**. Compacted 32-cell embryo. As a consequence five blastomeres are situated at the animal pole (marked with dots) and surround a central opening (arrowhead). Only four blastomeres are located the vegetal pole (not shown). **H-I**. Elongations of animal cells (H), and blastomeres directly after sixth cleavage divisions (I). In the different cells, the divisions irregularly pass in sinistral, meridional, or equatorial directions. **J**. Compacted 64-cell embryo. Six blastomeres are located at the animal pole (marked with dots); a small central opening is covered by the polar bodies. At the vegetal pole only four blastomeres are situated (not shown). **K**. Full-focal projection of 8-cell embryo directly after third cleavage divisions. All four animal blastomeres (marked with dots) are aligned clockwise of their vegetal sister blastomeres. **L-M**. Fourth cleavage cycle in the animal cell of the 8-cell stage: cell elongations (L), and cells directly after divisions (M). All blastomeres divide sinistrally, but in two cells (marked with triangles in L) the obliqueness of the divisions is less pronounced than in the other two. Note, the unusually large size of one polar body in this embryo (marked with asterisk). **N**. Compacted 16-cell embryo. The flat inclination of divisions and possibly also the large polar body (asterisk) causes all four daughter cells of the two blastomeres marked with triangles in L to have contact to the animal pole. Hence, the pole is encircled by six blastomeres (marked with dots). In the same embryo, four blastomeres lie at the vegetal pole (not shown). **O-P**. Elongations of animal cells (O), and cells directly after fifth cleavage divisions (P). While two blastomeres divide dextrally, the descendants of the irregular blastomeres (marked with triangles in O) divide equatorially or only weakly pronounced dextrally. **Q**. Compacted 32-cell embryo. Seven blastomeres (marked with dots) encircle the animal pole; centrally between them the large polar body is located (asterisk). At the vegetal pole, only four blastomeres are located (not shown). **R-S**. Successive cell elongations (R) and highly irregular sixth cleavage divisions (S); one cell is not yet divided (cleavage direction indicated by dashed line in S). **T**. Animal pole of compacted 64-cell embryo surrounded by six blastomeres (marked with dots). Again, only four blastomeres encircle the vegetal pole (not shown).

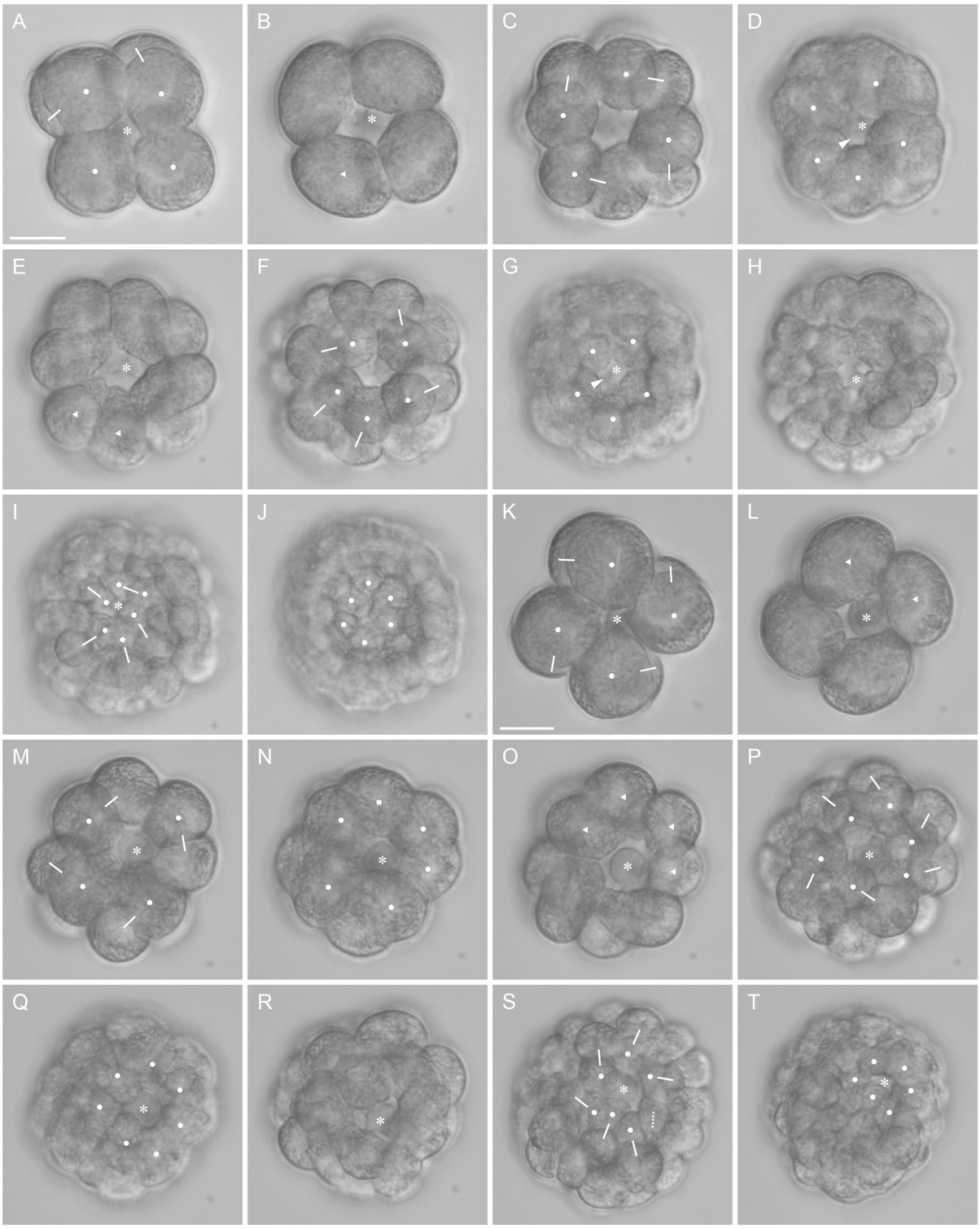

Fig. 12. Examples of cleavage variability in two *P. pallida* embryos.

Table 1. Pole blastomere contacts in *P. pallida* embryos. The four blastomeres of the 4-cell embryo, and the four blastomeres that are located at the animal pole and/or the vegetal pole in many embryos of later cell stages, can show central cell contacts in the organization of a polar furrow or of an X-furrow (polar furrow: contact line between two oppositely situated cells; X-furrow: central contact between all four cells). The table gives the frequency of 4-cell stage to 64-cell stage embryos that have such a cell contact, at only the animal pole, or at only the vegetal pole, or at both poles, over all analyzed embryos ('n'; only embryos in a putatively compacted state, and with (one or both) pole(s) encircled by four blastomeres were included; see Table 3). Per cell stage, the upper row gives the data from 4D-recorded embryos, and the lower row provides data from fixed embryos (for the 64-cell stage, only 4D data are available). All relative numbers are rounded to even. Note, that an embryo that displays a polar furrow at one pole, can have an X-furrow or a small opening between the four pole blastomeres at the opposite pole; but in some cases, it may also have more than four cells located at the opposite pole (Table 3).

Stage	n	Polar Furrow at			X-Furrow at		
		Animal Pole	Vegetal Pole	Both Poles	Animal Pole	Vegetal Pole	Both Poles
4-cell	14			14%[a]			
	13						15%
8-cell	15	7%	13%	7%[b]			
	21		10%	5%[c]			
16-cell	15		27%	7%[b]		20%	
	15	7%	33%				
32-cell	15		47%	7%[b]		13%	
	12	8%	58%				
64-cell	11		64%			7%	

[a] The same polar furrow is visible at both poles (it reaches along the entire animal-vegetal axis)
[b] The animal polar furrow and the vegetal polar furrow are oriented approximately parallel to each other
[c] The animal polar furrow and the vegetal polar furrow are oriented perpendicularly to each other

Table 2. Orientations of cleavage axes in *P. pallida* embryos. From the third to the sixth cleavage cycle, all observed combinations of orientations of cleavage axes in the blastomeres of individual embryos are listed, and the numbers of embryos showing each combination are given. Each line gives a unique combination (the numbers preceding the different cleavage orientations give the number of cells that show such cleavage axes; if cells could not be resolved, as they were not in a proper mitotic state or otherwise not accessible, this is noted as not applicable (n.a.)). For the third and the fourth cleavage cycles (A,B), the numbers of 4D-recorded embryos and of fixed embryos showing each combination are given; for the fifth and sixth cleavage cycles (C,D), only data from 4D recordings were available and each combination was observed only once. Separated evaluations are given for the single cell tiers in the embryo for the fourth and the fifth cleavage cycles (B,C); for the sixth cleavage cycle (D), only the animal and vegetal cell tiers were analyzed.

A. Third cleavage cycle

Cleavage Orientations	Number of Embryos	
	Recorded	Fixed
4 dextral	3	1
3 dextral; 1 equatorial	1	3
3 dextral; 1 sinistral		1
2 dextral; 2 equatorial	2	2
2 dextral; 1 sinistral; 1 equatorial		3
1 dextral; 3 equatorial	3	
1 dextral; 1 sinistral; 2 equatorial		1
1 dextral; 2 equatorial; 1 meridional		1
1 dextral; 2 equatorial; 1 n.a.		2
1 dextral; 2 sinistral; 1 n.a.		1
4 equatorial	3	3
3 equatorial; 1 meridional		1
2 equatorial; 2 n.a.		1
1 equatorial; 3 n.a.		1

B. Fourth cleavage cycle

Cleavage Orientations		Number of Embryos	
Animal Tier	Vegetal Tier	Recorded	Fixed
4 sinistral	4 sinistral	7	2
4 sinistral	3 sinistral; 1 meridional		1
4 sinistral	4 n.a.		1
3 sinistral; 1 meridional	4 sinistral	2	1
3 sinistral; 1 meridional	1 sinistral; 1 dextral; 2 meridional		1
3 sinistral; 1 meridional	2 sinistral; 1 equatorial; 1 n.a.		1
3 sinistral; 1 dextral	4 sinistral	1	1
2 sinistral; 2 meridional	4 sinistral	1	
2 sinistral; 1 meridional; 1 equatorial	3 sinistral; 1 meridional	1	
2 sinistral; 2 dextral	3 dextral; 1 equatorial		1
2 sinistral; 1 dextral; 1 n.a.	3 sinistral; 1 n.a.		1
2 sinistral; 2 n.a.	1 sinistral; 1 meridional; 2 n.a.		1
2 sinistral; 2 n.a.	4 n.a.		1
1 sinistral; 3 meridional	2 sinistral; 2 meridional		1
1 sinistral; 1 dextral; 2 meridional	2 sinistral; 2 dextral		1
1 sinistral; 2 dextral; 1 meridional	3 sinistral; 1 dextral		1
1 sinistral; 2 dextral; 1 equatorial	2 sinistral; 2 dextral		1
1 sinistral; 1 dextral; 2 n.a.	2 sinistral; 2 n.a.		1
1 sinistral; 3 n.a.	1 sinistral; 3 n.a.		1
1 sinistral; 3 n.a.	4 n.a.		1

Table 2. (continuation)

C. Fifth cleavage cycle

Cleavage Orientations			
Animal Tier	**Animal-Equatorial Tier**	**Vegetal-Equatorial Tier**	**Vegetal Tier**
4 dextral	1 dextral; 3 meridional	4 meridional	4 dextral
3 dextral; 1 equatorial	4 dextral	4 meridional	4 dextral
3 dextral; 1 equatorial	3 dextral; 1 equatorial	4 meridional	4 dextral
3 dextral; 1 equatorial	2 dextral; 1 meridional; 1 equatorial	4 meridional	4 dextral
3 dextral; 1 equatorial	2 dextral; 1 meridional; 1 equatorial	1 sinistral; 3 meridional	4 dextral
3 dextral; 1 equatorial	1 dextral; 2 meridional; 1 equatorial	1 sinistral; 3 meridional	4 dextral
3 dextral; 1 sinistral	1 dextral; 3 meridional	3 dextral; 1 meridional	3 dextral; 1 equatorial
3 dextral; 1 meridional	2 dextral; 1 meridional; 1 equatorial	1 dextral; 1 sinistral; 2 meridional	4 dextral
2 dextral; 2 equatorial	1 dextral; 1 meridional; 2 equatorial	1 dextral; 2 meridional; 1 equatorial	4 dextral
2 dextral; 2 equatorial	1 dextral; 1 meridional; 2 equatorial	4 meridional	4 dextral
2 dextral; 2 equatorial	1 dextral; 3 equatorial	4 meridional	4 dextral
1 dextral; 2 meridional; 1 equatorial	1 dextral; 1 meridional; 2 equatorial	4 meridional	4 dextral

D. Sixth cleavage cycle

Cleavage Orientations	
Animal Tier	**Vegetal Tier**
3 sinistral; 1 equatorial	4 sinistral
3 sinistral; 1 meridional	1 sinistral; 1 dextral; 2 meridional
2 sinistral; 1 meridional; 1 equatorial	4 sinistral
2 sinistral; 2 equatorial	2 equatorial; 2 n.a.
1 sinistral; 2 meridional; 1 equatorial	2 sinistral; 2 meridional
1 sinistral; 2 equatorial; 1 n.a.	3 sinistral; 1 equatorial
3 meridional; 1 equatorial	3 sinistral; 1 meridional
2 meridional; 2 dextral	1 sinistral; 3 equatorial
1 meridional; 3 equatorial	3 sinistral; 1 equatorial
3 equatorial; 1 n.a.	3 sinistral; 1 meridional
1 equatorial; 3 n.a.	2 sinistral; 2 equatorial
4 n.a.	1 sinistral; 1 dextral; 2 meridional

Table 3. Number of pole blastomeres in *P. pallida* embryos. For the 16-cell stage to the 64-cell stage, all encountered combinations in the numbers of blastomeres encircling the animal pole and the vegetal pole of individual embryos are listed. For the 16-cell and the 32-cell stages (A,B), the numbers of 4D-recorded embryos and of fixed embryos showing each combination are given separately, and the frequency of the respective pattern (4D-recorded plus fixed specimens) over all embryos ('n') is noted. For the 64-cell stage (C), only data from 4D-recorded embryos were available. All relative numbers are rounded to even. If poles could not be resolved, this is noted as not applicable ('n.a.'). In each table, two bottom lines give the numbers of embryos that have four blastomeres located at either the animal pole or the vegetal pole, irrespective of the respective counter-pole (these include only confirmed cases, and for the 64-cell embryo might be underestimations), as well as the frequencies of these respective patterns (note, that these numbers do not necessarily sum up to 100).

A. 16-cell embryo

Number of Blastomeres at		Number of Embryos		Frequency (n = 33)
Animal Pole	Vegetal Pole	Recorded	Fixed	
4	4	8	8	48%
4	5	1	1	6%
5	4	3	4	21%
5	5		1	3%
6	4	1	3	12%
6	5		1	3%
7	4	2		6%
Animal Pole = 4 Blastomeres		Total: 18		55%
Vegetal Pole = 4 Blastomeres		Total: 29		88%

B. 32-cell embryo

Number of Blastomeres at		Number of Embryos		Frequency (n = 29)
Animal Pole	Vegetal Pole	Recorded	Fixed	
4	4	5	6	38%
4	5	1	1	7%
5	4	4	4	28%
5	5		1	3%
6	4	3	1	14%
7	4	2	1	10%
Animal Pole = 4 Blastomeres		Total: 13		45%
Vegetal Pole = 4 Blastomeres		Total: 26		90%

C. 64-cell embryo

Number of Blastomeres at		Number of Recorded Embryos	Frequency (n = 14)
Animal Pole	Vegetal Pole		
4	4	2	14%
4	7	1	7%
4	n.a.	1	7%
6	4	4	29%
7	4	1	7%
8	n.a.	1	7%
n.a.	4	2	14%
n.a.	5	2	14%
Animal Pole = 4 Blastomeres		Total: 4	29%
Vegetal Pole = 4 Blastomeres		Total: 9	64%

3.1.2. Cell fates in *P. pallida* embryos

At the 2-cell and the 4-cell stage, the blastomeres in the *P. pallida* embryos are of approximately equal size and morphologically indistinguishable (chapter 3.1.1.2.). The fates of these blastomeres were traced by single cell in-vivo labelings; analyses of the distribution and position of the progeny of the labeled cell were carried out after one or after two days of development, when the embryo was in a mid or in a late state of gastrulation, respectively. Before summarizing the results of the labeling experiments, the gross morphology of these gastrula stages is described.

3.1.2.1. Reference morphology

After one day of development the embryo is in the stage of mid gastrula (Fig. 13A-D). In a top view (Fig. 13A: surface of the blastopore; Fig. 13B: surface opposite of the blastopore) this gastrula is roundish, or already slightly elongated in an axis perpendicular to the axis of the archenteron (see e.g., Fig. 14E-F,I-J). It is flattened at the surface of the blastopore (Fig. 13D). The endodermal archenteron is a blind-ending invagination, which displays a shallow pouch-like extension pointing toward one side of the gastrula (Fig. 13D). Inside the gastrula, a blastocoelic cavity is present. It is mainly restricted to the body region of – and around – the blastopore (Fig. 13C), whereas opposing the blastopore, the invaginating archenteron closely reaches to the above lying ectoderm (Fig. 13D), and in many samples even contacts the ectoderm (see Fig. 14). Inside the blastocoel, usually between 30 and 60 mesenchymal cells are found. These mesenchymal cells are situated in a distinct pattern: they are located only in the body region opposite to the archenteral pouch as well as in the adjacent regions on both sides of the archenteron, but not in the body region where the archenteral pouch is located (Fig. 13C-D). The internal organization of these embryos – in comparison to the organization of the embryo at late gastrulation (see next paragraph) – allows to define body axes in the mid gastrula: the site of the blastopore represents the prospective ventral body side, and the location of the majority of mesenchymal cells marks the anterior body end, whereas the location of the archenteral pouch marks the posterior body end (see crosses for orientation in Fig. 13A-D). This is consistent with identifying the elongated body axis found in some mid gastrula embryos (e.g., Fig. 14E-F,I-J) as anterior-posterior axis.

The embryo after two days of development is in a late gastrula stage. It is distinctly elongated in an anterior-posterior axis and shows obvious body axes and a plane of bilateral symmetry (Fig. 13E-H). The later larval body organization is already apparent: the blastopore is located at the ventral body side (Fig. 13E,G) between the anterior preoral hood anlage, which already is protruding ventrally over the blastopore, and the posterior trunk region (Fig. 13F-G); the latter will develop the postoral collar ridge as well as the trunk of the later actinotroch larva (Santagata 2004a). Immunostainings against α-tubulin show an area of tubulin-rich, thickened ectoderm, which consists of columnar shaped cells and is located medianly at the upper surface of the forming preoral hood (Fig. 13H); similar immunostainings at the mid gastrula stage do not give this distinct signal (Fig. 13D). This area is the forming apical plate; it will develop the later center of the larval nervous system (Emig 1977; Temereva and Malakhov 2012). The archenteron extends as a blind-ending sack from the blastopore toward posterior into the trunk (Fig. 13G). In some specimens already an anlage of the hindgut was developed (see e.g., Fig. 15H,L); yet, an anal opening never was observed. Inside the blastocoel, between 60 and 90 mesenchymal cells are found: most of these cells are located inside the hood, others ventrally and laterally of the archenteron within the trunk (Fig. 13G-H).

3.1.2.2. Cell fates of the 2-cell embryo

After the injection of one cell at the 2-cell stage, the progeny of the marked cell always ended up labeling about one half of the later – mid gastrulation or late gastrulation – embryo (Figs. 14, 15). In all cases, the labeled clones included ectodermal as well as endodermal regions, connected via the blastopore. The area of marked endoderm generally was located approximately beneath the area of marked ectoderm; yet in some cases, the endodermal label extended slightly farther than the ectodermal one (see below). In all embryos, some – but never all – of the mesenchymal cells were marked.

The position that the labeled clones occupied in the embryo differed; however, certain distributions were observed repeatedly in the material. These distributions were summarized as different staining patterns, which were characterized according to the position of the labeled clones in relation to the anterior-posterior axes and the right-left axis of the embryos: anterior, anterior-lateral (that is, anterior-right or anterior-left), lateral (that is, right or left), posterior-lateral (that is, posterior-right or posterior-left), and posterior staining patterns were distinguished. With relation to the ventral-dorsal axis of the gastrula, embryos that displayed a more anterior distribution of the label (anterior or anterior-lateral staining patterns) generally

had only a minor region of the dorsal ectoderm marked, whereas a large dorsal region was labeled in those embryos with a more posterior label (posterior or posterior-lateral staining patterns) (see below).
Regarding the position and orientation relative to the main body axes, these staining patterns largely corresponded between the embryos that were at a mid gastrula stage and those at a late gastrula stage. Although no embryo was checked for the presence of the injected dye at both stages of development (from this was refrained due to encountered phototoxicity of DiI under fluorescence exposure), this general correspondence suggests that the labeled clones are stable in position throughout this early course of development. However, possibly due to the small sample size, not each staining pattern was encountered in embryos of both stages.

3.1.2.2.1. Mid gastrula stage

Nine embryos were injected at the 2-cell stage and analyzed after one day of development; in these mid gastrula stages, the descendants of the labeled cell occupied one of the following body regions: anterior, anterior-right, anterior-left, posterior-left, or posterior (Table 4A; Fig. 14).

In embryos showing an anterior staining pattern (2/9 specimens; Fig. 14A-D), the anterior half of the ventral ectoderm was marked (Fig. 14A); this label extended but narrowed toward dorsal, so that the labeled region in the dorsal ectoderm was smaller than in the ventral ectoderm (Fig. 14B). The anterior side of the blastopore and the anterior part of the archenteron were marked (Fig. 14C-D). The label in the endoderm corresponded largely with the labeled ectoderm, yet could also extend some cells more toward posterior. Mesenchymal cells that were located in the area of labeled endoderm and ectoderm were stained; hence, most mesenchymal cells – being located in the anterior half of the blastocoel – were labeled, and only some of the most posterior lateral ones were not (Fig. 14C-D). In one embryo, an unmarked mesenchymal cell was found within the anterior blastocoel region (data not shown).
Most of the embryos displayed an anterior-right staining pattern (4/9 specimens; Fig. 14E-H). In these specimens, the anterior and the right sides of the embryos were marked. At the ventral surface, the border between labeled and unlabeled ectoderm ran obliquely with respect to the embryo's anterior-posterior as well as its left-right axes (Fig. 14E); toward dorsal the labeled region narrowed, and in dorsal view only the anterior and right surfaces of the

ectoderm were labeled (Fig. 14F). The archenteron was likewise marked at the anterior and at the right body side; in some specimens, the label in the endoderm extended a bit farther toward posterior than the ectoderm (Fig. 14G-H). Mesenchymal cells located in the anterior and right regions of the blastocoel – that is, those lying close to labeled endoderm and ectoderm – were marked, mesenchymal cells in the left body region were unmarked (Fig. 14G-H).

The anterior-left staining pattern was only observed in one embryo (1/9 specimens; Fig. 14I-L), and appears to be a rough mirror pattern of the anterior-right staining pattern. The specimen had the anterior and the left regions of the ectoderm (Fig. 14I-J) as well as of the underlying endoderm marked (Fig. 14K); the endodermal label also included the dorsal region of the archenteron (Fig. 14L). Mesenchymal cells that were close to labeled endoderm and ectoderm were marked (Fig. 14K-L), but also two unmarked mesenchymal cells were found in this area (data not shown); mesenchymal cells at the embryo's right side were unlabeled (Fig. 14K).

Likewise, only one embryo showed a posterior-left staining pattern (1/9 specimens; Fig. 14M-P). In this specimen, the posterior and the left regions of the ventral ectoderm were labeled (Fig. 14M); in reaching dorsally the label broadened, and a big region of the dorsal ectoderm – excluding only the most anterior and right surfaces – was marked (Fig. 14N). The archenteron roughly was labeled at the left and at the posterior body regions, yet the staining was not of good quality (Fig. 14O-P). Mesenchymal cells at the left body side were stained; additionally, some marked mesenchymal cells were found in the anterior-right body region (Fig. 14O).

In one embryo a posterior staining pattern was observed (1/9 specimens; Fig. 14Q-T). In this specimen, the central region of the ventral ectoderm posteriorly of the blastopore was marked; this label reached slightly more anteriorly at the left body side (Fig. 14Q). The label broadened toward dorsal and covered a major region of the dorsal ectoderm (Fig. 14R). Only the posterior region and a part of the left side of the archenteron were labeled (Fig. 14S-T). Most mesenchymal cells, lying far from marked endoderm and ectoderm, were unlabeled; however, some of the lateral mesenchymal cells at the left body side were stained (Fig. 14S-T). These marked cells were located somewhat apart from labeled endoderm and ectoderm, yet they appeared to show a cytoplasmic connection to the labeled archenteron (Fig. 14S).

3.1.2.2.2. Late gastrula stage

Thirteen 2-cell injected embryos were analyzed after two days of development. The observed positions of the progeny of the marked cell in these late gastrula stages were: anterior, anterior-right, right, left, posterior-right, posterior-left, and posterior (Table 4A; Fig. 15).

In all embryos showing an anterior staining pattern (3/13 specimens; Fig. 15A-D) the hood ectoderm was marked on its major surfaces. The label reached from an area at the upper hood surface (Fig. 15B) – at which the ectoderm showed thickened cell bodies (Fig. 15D) and which also in position corresponded to the approximate site of the apical plate in the late gastrula stage (compare embryo in Fig. 15D and Fig. 13H) – anterior-ventrally to the blastopore (Fig. 15A), and from both lateral hood surfaces into the lateral-ventral regions of the trunk (Fig. 15A,C). On the other hand, the major dorsal body ectoderm – now, reaching from the upper hood surface toward posterior-dorsally (Fig. 15B-D) – and the embryo's posterior body end were unlabeled (Fig. 15A,C). These patterns suggest that both, labeled and unlabeled ectodermal domains, at the upper hood surface passed through the site of the apical plate (see also below). The found anterior patterns were slightly asymmetrically, insofar as in different specimens the label reached farther toward posterior on the body side right (2 specimens; given in Fig. 15A-D) or on the left body side (1 specimen; not shown). In all specimens, a narrow region of unmarked ectodermal cells extended from the posterior body end up to the blastopore, on the ventral body surface (Fig. 15A). The endodermal archenteron, likewise, was labeled in its anterior part, while its posterior portion was unlabeled (Fig. 15D); the endodermal label included regions of the anterior-dorsal archenteral roof, where the above lying dorsal ectoderm was unlabeled (Fig. 15D). The hindgut-anlage was developed in one embryo and was unmarked (data not shown). Most mesenchymal cells within the hood were labeled – but also some unmarked cells could be found there; most mesenchymal cells in the trunk were unlabeled (Fig. 15D).

In embryos displaying an anterior-right staining pattern (2/13 specimens; Fig. 15E-H), the anterior and the right-sided ectodermal surfaces of the hood (Fig. 15E-F) as well as the right(-ventral) surface of the trunk were labeled (Fig. 15E,G), whereas the left body side, a major part of the dorsal body ectoderm, and the embryo's posterior end were unlabeled (Fig. 15E-G). Again, at the upper hood surface, labeled and unlabeled ectoderm domains passed through the presumptive apical plate site (Fig. 15F,H). The archenteron was stained on the right side (Fig. 15H), but the left side was unmarked. The hindgut-anlage was developed in one

specimen and was unlabeled (Fig. 15H). The mesenchymal cells in the hood were mostly marked, but also some unmarked cells were observed therein; in the trunk, unmarked and marked mesenchymal cells were found in both body sides (Fig. 15H).

Three embryos were characterized as lateral staining pattern (3/13 specimens; Fig. 15I-L). In these specimens, roughly a lateral half of the ectoderm was marked; differently this label was on the left (2 specimens; given in Fig. 15I-L) or on the right body side (1 specimen; not shown). The border between labeled and unlabeled domains, however, did not pass exactly along the anterior-posterior axis: usually, a bit less than exactly one lateral half of the hood was stained (Fig. 15J) – although the label appeared to include a part of the apical plate (Fig. 15J,L) –, while the label at the embryo's posterior body end extended somewhat to the contralateral side (Fig. 15I,K). The archenteron was labeled on the same body side, on which the ectoderm was labeled (Fig. 15L). The hindgut-anlage was developed in one embryo and was marked (Fig. 15L). Stained mesenchymal cells mostly were found within the labeled body side (Fig. 15L); some marked cells were also found within the unlabeled side.

One embryo displayed a posterior-left staining pattern (1/13 specimens; given in Fig. 15M-P), and in two embryos a posterior-right staining pattern (2/13 specimens; not shown) was observed. The latter appeared to be a rough mirror distribution of the former. In these specimens, the hood ectoderm only was labeled laterally on the respective body side (Fig. 15M-N) – but again the label (as well as the unlabeled domain) reached dorsally to the presumptive apical plate site at the upper hood surface (Fig. 15N,P). On the same body side, a major part of the dorsal ectoderm and about half of the ventral surface were marked in the trunk (Fig. 15M-O). The ectodermal label also included the posterior end of the embryo (Fig. 15M,O). The archenteron was stained laterally on the same side as the ectoderm (Fig. 15P). In no specimen, the hindgut-anlage was developed. Mesenchymal cells in the hood and in the trunk were marked mainly on the labeled body side, but some stained cells were also found within the unlabeled body side. Generally, the posterior-lateral staining patterns appear to roughly represent complementary matches of the anterior-lateral patterns (compare labeled clones in Fig. 15M-P and Fig. 15E-H).

In the embryos displaying a posterior staining pattern (2/13 specimens; Fig. 15Q-T), the ectoderm at the posterior body end as well as of the major part of the dorsal body surface were labeled (Fig. 15Q-S). Also in these specimens, the label reached up to the upper hood surface, and hence the presumptive site of the apical plate (Fig. 15R,T). On the ventral surface a narrow region of marked cells extended from the embryo's posterior end up to the blastopore (Fig. 15Q). This region continued as labeled endoderm, and the posterior end of

the archenteron was stained (Fig. 15T). The hindgut-anlage was not yet developed in these embryos. Most mesenchymal cells were unlabeled, however, some labeled cells were observed in the trunk as well as sometimes within the hood region (Fig. 15T). Generally, the posterior staining pattern appears to be a rough complementary match of the anterior staining pattern (compare labeled clones in Fig. 15Q-T and Fig. 15A-D).

3.1.2.3. Cell fates of the 4-cell embryo

When one cell was injected at the 4-cell stage, its progeny marked roughly a quarter of the later embryo, irrespective of the stage (Figs. 16, 17, 18). Like following the injections at the 2-cell stage, in very most samples resulting from the 4-cell stage markings the labeled clones included ectodermal and endodermal regions of the embryo, connected via the blastopore, as well as a part of the mesenchymal cells. However, only following the 4-cell stage experiments, exceptional cases of unambiguous and possibly absent markings of the endoderm and/or the mesenchymal cells were encountered (see below).
The encountered positions of the labeled clones in the embryos varied; again, the distributions were characterized according to the position relative to the anterior-posterior and the left-right axes of the specimens. Almost all observed labelings could be interpreted as a half-pattern of one of the staining patterns, which had been found after the cell injections at the 2-cell stage. An unambiguous assignment to a specific 2-cell staining pattern, however, was not possible: this is because of the presence of variation in the exact distributions of the labeled clones, the small sample size, and the general problem that a half-pattern of a pattern that includes a half of an elongated spherical embryo cannot be differentiated from a half-pattern of a pattern that includes another half, which is aligned roughly perpendicularly to the first half, of the same embryo (see below).

3.1.2.3.1. Mid gastrula stage

Seven embryos were injected at the 4-cell stage and analyzed after one day of development (Fig. 16). The progeny of the marked cell were found to occupy roughly one of the following regions in these mid gastrulae (Table 4B): a section at the right anterior (2/7 specimens; Fig. 16A-C) or at the left anterior of the embryo (2/7 specimens; Fig. 16D-F), a lateral section at the left body side (2/7 specimens; Fig. 16G-L), or a section at the right posterior of the embryo (1/7 specimens; Fig. 16M-O). It should be noted, however, that the exact distributions

of the labeled clones could vary between embryos of these categories (compare labels in embryos in Fig. 16G-I and Fig.16J-L).

Each of the different labelings can be interpreted as a rough half-pattern of one of the 2-cell staining patterns (see chapter 3.1.2.2.1.). The first distribution might represent a half of the anterior staining pattern (compare embryos in Fig. 16A-C and Fig. 14A-C), while the second distribution matches a half of the anterior-right staining pattern (compare embryos in Fig. 16D-F and Fig. 14E-G); however, under the assumed existence of lateral 2-cell staining patterns (those left-sided and right-sided patterns have been found for the late gastrula stages in the respective experiments, but not in the mid gastrula samples; see chapter 3.1.2.2.) both of these labelings could also be interpreted as the anterior half of a respective lateral right or lateral left staining pattern. Similarly, the labeling at the left body side might represent a half of either an anterior-left or a posterior-left 2-cell staining pattern (compare embryos in Fig. 16G-I and Fig. 14I-K, and embryos in Fig. 16J-L and Fig. 14M-O; and vice versa). The right posterior labeling, finally, appears to match a half of the posterior staining pattern (compare embryos in Fig. 16M-O and Fig. 14Q-S). With all this goes that several possible half-patterns of 2-cell staining patterns were not found in the material; possibly, this is due to the small sample size.

Irrespective of the specific section the label occupied, in all studied specimens, the stained ectodermal clone reached from the blastopore to a roughly median and somewhat anterior area at the body surface opposite to the blastopore (Fig. 16B,N; and most evident in the pointed dorsal labels in Fig. 16E,H,K). Only in the specimen with the right posterior labeling, the dorsal ectoderm was marked at a major part (Fig. 16N).

In all, but one, specimen, the label clearly included a portion of the endodermal archenteron (Fig. 16C,F,I,L). The labeled endodermal clone was found roughly in a position underlying the labeled ectoderm; but, repeatedly it was also slightly displaced relative to the ectodermal clone (Fig. 16C,F,I). Only in the specimen with the right posterior labeling, the endodermal marking was doubtful: in this embryo, the labeled clone reached to the rim of the blastopore, but did not unambiguously extend into the archenteron (Fig. 16O). As the exact border between ectoderm and endoderm at the blastopore is not evident, it is arguable whether endodermal cells were marked in this embryo.

Marked mesenchymal cells, finally, were observed in all the embryos (Fig. 16C,F,I,L,O). In some cases, they appear to occur in rough association with labeled endoderm (see Fig.

16C,F,I). Only very few marked mesenchymal cells were found in the embryo with the right posterior labeling pattern (Fig. 16O).

3.1.2.3.2. Late gastrula stage

Thirteen embryos were injected at the 4-cell stage and analyzed after two days of development (Figs. 17, 18). The labelings observed in these late gastrula stages are described after the position, which the stained clones occupied in the specimens (Table 4B), and along the putative correspondence to the staining patterns, which had been observed after the 2-cell injections (see chapter 3.1.2.2.2.).

In some specimens, the labeled ectodermal clone occupied the left-sided surface of the hood and the left ventral surface of the anterior trunk (3/13 specimens; Fig. 17A-D); whereas in others, the label was found at either the right or the left side of the posterior trunk (right: 1/13 specimens: Fig. 17E-H; left: 2/13 specimens, Fig. 17I-L) and also included the ipsilateral dorsal body surface (Fig. 17G,K) as well as a small region on the ventral surface, extending from the posterior body end up to the blastopore (Fig. 17E,I). In all these specimens, the ectodermal label passed through the site of the apical plate at the upper hood surface (Fig. 17B,F,J; see marking of thickened plate ectoderm in Fig. 17D,H,L). The archenteron roughly was labeled in the position where the ectoderm was labeled (Fig. 17D,H,L). Several marked mesenchymal cells were found in the specimens with the anterior-left labeling (Fig. 17D), whereas only few mesenchymal cells were stained in the embryos with the posterior labelings (Fig. 17H,L). These three different labelings can be interpreted as half-pattern of either the anterior or the posterior staining pattern, respectively (compare embryos in Fig. 17 with embryos in Fig. 15A-D,Q-T), but also as half-pattern of either a left or right lateral staining pattern (compare embryos in Fig. 17 with embryo in Fig. 15I-L), as they were described for the 2-cell stage injections (chapter 3.1.2.2.2.).
On the other hand, one specimen was found, in which the ectodermal label occupied only the anterior preoral hood (1/13 specimens; Fig. 18A-D) – from the blastopore (Fig. 18A) to the site of the apical plate (Fig. 18B,D) –; whereas in other specimens, the ectodermal label was restricted to either the right or the left trunk side (right: 4/13 specimens: Fig. 18E-H; left: 1/13 specimens: Fig. 18I-L) – from the ventral mid-area (Fig. 18E,I) toward laterally and including different areas of the ipsilateral trunk and hood region (Fig. 18F-G,J-K). Notably, among the lateral distributions, two specimens were found, in which the ectodermal label did not reach to

the upper hood surface and apparently did not include the site of the apical plate (see Fig. 18F; note thickened but unstained apical plate ectoderm in Fig. 18H). In all specimens of all three labelings, the label extended through the blastopore – which was stained at a portion of its circumference – and the endoderm was marked roughly in the area of the above lying marked ectoderm (Fig. 18D,H,L). Stained mesenchymal cells were found in all the samples, mostly in the region of stained endoderm and ectoderm (Fig. 18D,H,L). In the embryo with the anterior labeling, nearly all the mesenchymal cells in the hood were stained (Fig. 18D). These three different labelings can be interpreted as half-pattern of either the anterior-lateral or the posterior-lateral 2-cell staining pattern, respectively (compare embryos in Fig. 18A-L with embryos in Fig. 15E-H,M-P).

Finally, a single specimen was encountered in which only a major region of the dorsal (and somewhat right-sided) ectoderm, reaching from the embryo's posterior end up to the site of the apical plate, was marked (1/13 specimens; Fig. 18M-P). The label did neither include the ventral surface nor the blastopore (Fig. 18M). Although the sample showed some scattered drops of dye inside the blastocoel and the archenteron, the specimen appeared do have no properly marked endoderm or mesenchymal cells (Fig. 18P). This labeling is difficult to assign to any of the found 2-cell staining patterns; it is included as "posterior" distribution in Table 4B.

Fig. 13. Morphology of *P. pallida* embryos at the states of mid gastrulation and of late gastrulation. Imaris volume projections (Blend mode) and virtual sections of two embryos fixed during gastrulation, and stained against tyrosinated α-tubulin (reddish) and for nucleic acids (cyan). Abbreviations: a: anterior, ap: apical plate, ar: archenteron, bc: blastocoel, bp: blastopore, d: dorsal, ect: ectoderm, end: endoderm, hd: hood, l: left, p: posterior, r: right, tr: trunk, v: ventral. Scale bars: 20 µm.
A-D. Embryo in the state of mid gastrulation (fixed after 25 hours of development) in a view on the blastoporal surface (A; blastopore indicated by dashed line) and on the surface opposite of the blastopore (B), as well as in horizontal (C) and mid-sagittal (D) sections (the tubulin-signal only is given in C and D). The embryo is oriented with the anterior end to the top (A-C) or to the right (D; see labeled crosses for orientation) on the basis of internal features of its organization: the endodermal archenteron is a blind-ending invagination, which has a shallow pouch-like extension oriented toward the posterior body end (arrow in C-D); mesenchymal cells within the blastocoel (marked with arrowheads in C-D) are only located anteriorly and laterally, but not posteriorly, of the archenteron (C-D). **E-H**. Embryo in the state of late gastrulation (fixed after 48 hours of development) in a ventral view (E; location of blastopore indicated by dashed line) and a right lateral view (F), as well as in mid-sagittal sections (G-H; the tubulin-signal only is given in H). The embryo is anterior-posteriorly elongated, has a marked plane of bilateral symmetry (E), and obvious body axes (see labeled crosses for orientation). It shows a separation in an anterior and ventrally protruding hood region and a posterior trunk region (F). The blastopore is located at the ventral body side between these two regions (E,G); the archenteron is a blind-ending sack extending into the trunk (G). Mesenchymal cells are situated within the hood, and ventrally and laterally of the archenteron within the trunk (marked with arrowheads in G). The tubulin signal reveals the thickened ectoderm of the forming apical plate at the upper side of the hood (H), which marks the embryo's anterior body end.

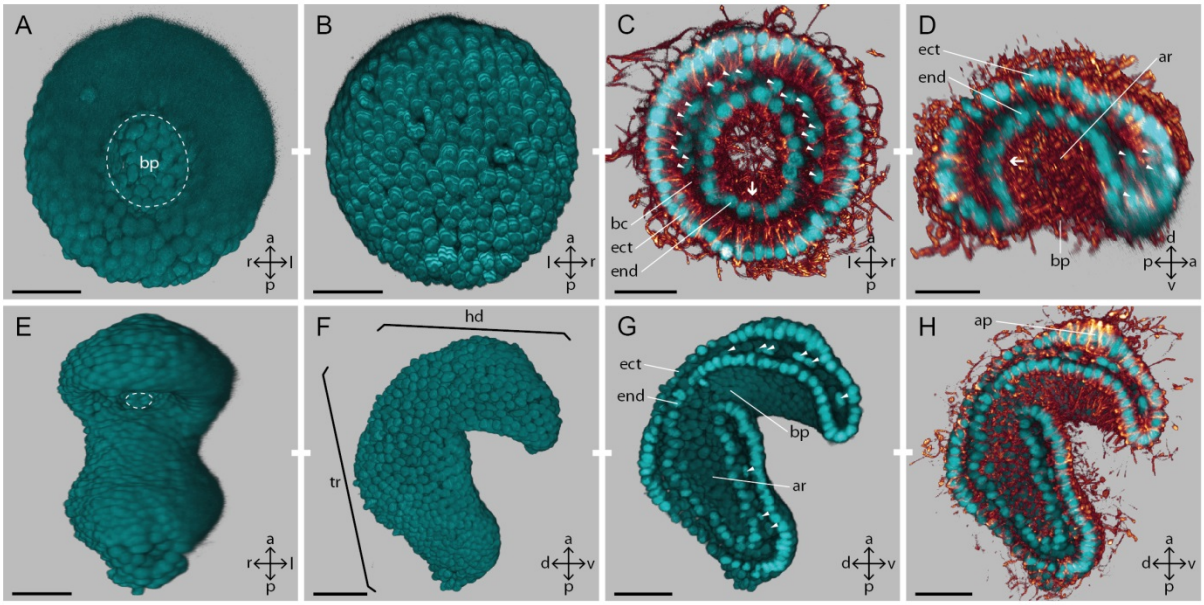

Fig. 13. Morphology of *P. pallida* embryos at the states of mid gastrulation and of late gastrulation.

Fig. 14. Distribution of labeled cells in *P. pallida* embryos at mid gastrulation, after one blastomere was marked at the 2-cell stage. Imaris volume projections (Blend mode) and virtual section. The descendants of the marked blastomere are recognizable by carrying the injected dye (reddish); the embryos were counterstained for nuclei (cyan). The labeled cells make up about a half of the mid gastrula embryo. They occupy a distinct region, but differ in position between the different embryos (see text). Different staining patterns could be identified, and each line gives one specimen representing a certain pattern. Each embryo is documented in successive images showing a view on the blastoporal surface (first column; blastopore indicated by dashed line) and on the surface opposite of the blastopore (second column), as well as a horizontal (third column) and a mid-sagittal (fourth column) section. Labeled crosses indicate the orientation of the specimen (a: anterior, d: dorsal, l: left, p: posterior, r: right, v: ventral). In the virtual sections, the endodermal archenteron and some mesenchymal cells are visible: labeled mesenchymal cells are marked with filled arrowheads, unlabeled mesenchymal cells are marked with open arrowheads (third and fourth columns). For detailed descriptions see text. Scale bars: 20 µm.
A-D. Specimen displaying an anterior staining pattern. **E-H**. Specimen displaying an anterior-right staining pattern. **I-L**. Specimen displaying an anterior-left staining pattern (at the dorsal median body area in J, the labeled archenteron is showing through the ectoderm nuclei layer, but the ectoderm is unlabeled). **M-P**. Specimen displaying a posterior-left staining pattern. **Q-T**. Specimen displaying a posterior staining pattern. The few mesenchymal cells, which are marked, show a cytoplasmic connection to the labeled archenteron (see S).

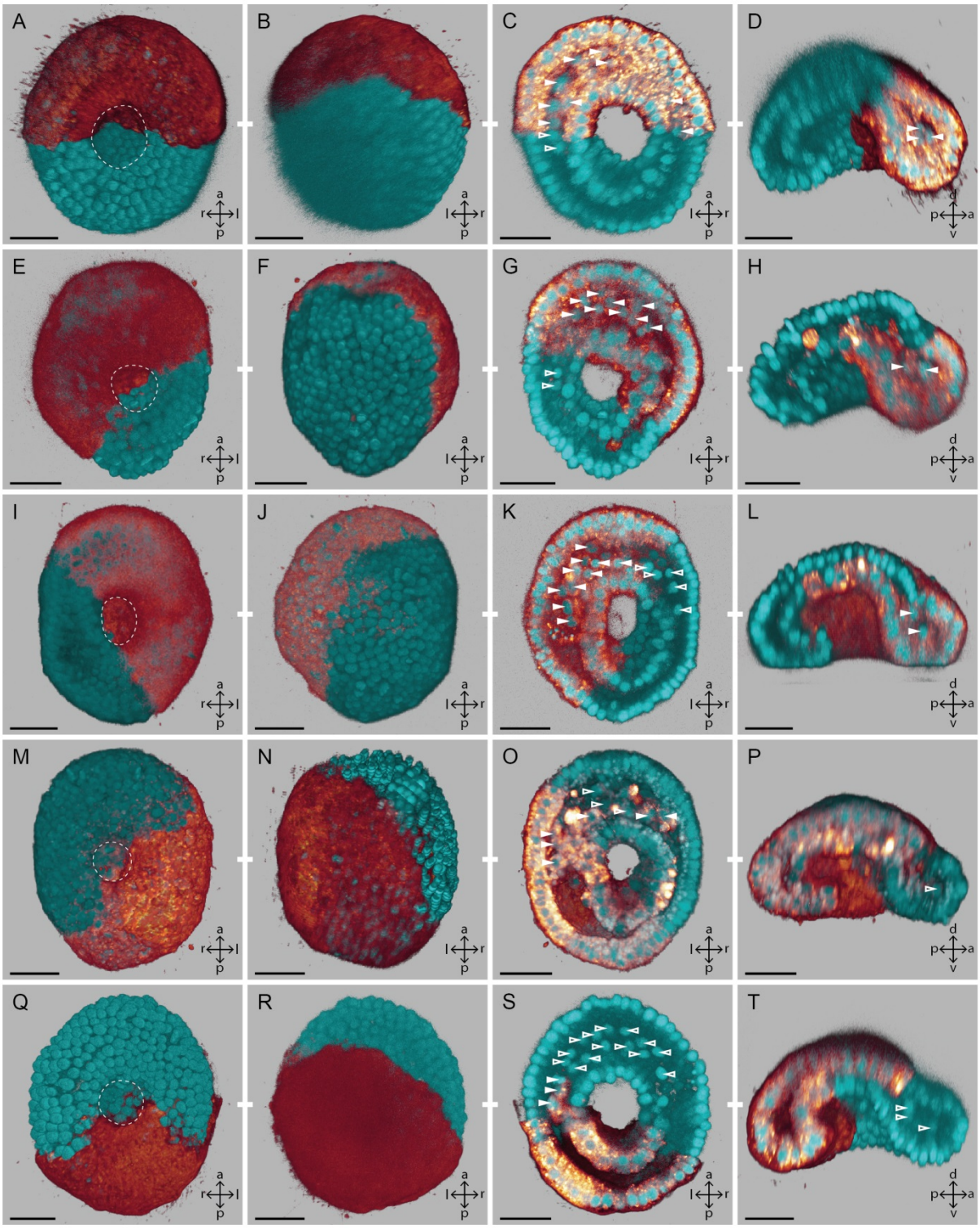

Fig. 14. Distribution of labeled cells in *P. pallida* embryos at mid gastrulation, after one blastomere was marked at the 2-cell stage.

Fig. 15. Distribution of labeled cells in *P. pallida* embryos at late gastrulation, after one blastomere was marked at the 2-cell stage. Imaris volume projections (Blend mode) and virtual section. The descendants of the marked blastomere are recognizable by carrying the injected dye (reddish); the embryos were counterstained for nuclei (cyan). The labeled cells occupy a distinct region in the embryos, which makes up about a half of the late gastrula. The position of the labeled cells differs between different embryos, and different staining patterns could be identified (see text). Each line gives one specimen, representing a certain staining pattern. Each embryo is documented in successive images showing a view on the ventral body surface (first column; blastopore indicated by dashed line), a view on the dorsal surface of the hood (second column), a view on the dorsal surface of the trunk (third column), and a mid-sagittal section (fourth column). Labeled crosses indicate the orientation of the embryos (a: anterior, d: dorsal, l: left, p: posterior, r: right, v: ventral). In all specimens, labeled as well as unlabeled ectodermal domains pass through a median area at the dorsal hood surface (indicated by arrows in second column); this is the presumptive site of the apical plate. In sagittal sections, the thickened ectoderm of the apical plate is visible and labeled in all specimens (indicated by arrows in fourth column). The archenteron and some mesenchymal cells are visible in the sections: labeled mesenchymal cells are marked with filled arrowheads, unlabeled mesenchymal cells are marked with open arrowheads (fourth column). For detailed descriptions see text. Scale bars: 20 µm.
A-D. Specimen displaying an anterior staining pattern. On the ventral surface, a region of unlabeled cells extends from the posterior body end to the blastopore (marked with arrowhead in A). **E-H**. Specimen displaying an anterior-right staining pattern. In this embryo, the hindgut anlage is already developed (marked with star in H) and it is unlabeled. **I-L**. Specimen displaying a lateral left staining pattern. The hindgut anlage in this embryo is labeled (marked with star in L). **M-P**. Specimen displaying a posterior-left staining pattern. Only few mesenchymal cells are visible due to poor scan quality (P). **Q-T**. Specimen displaying a posterior staining pattern. On the ventral surface, a region of labeled cells extends from the posterior body end to the blastopore (marked with arrowhead in Q).

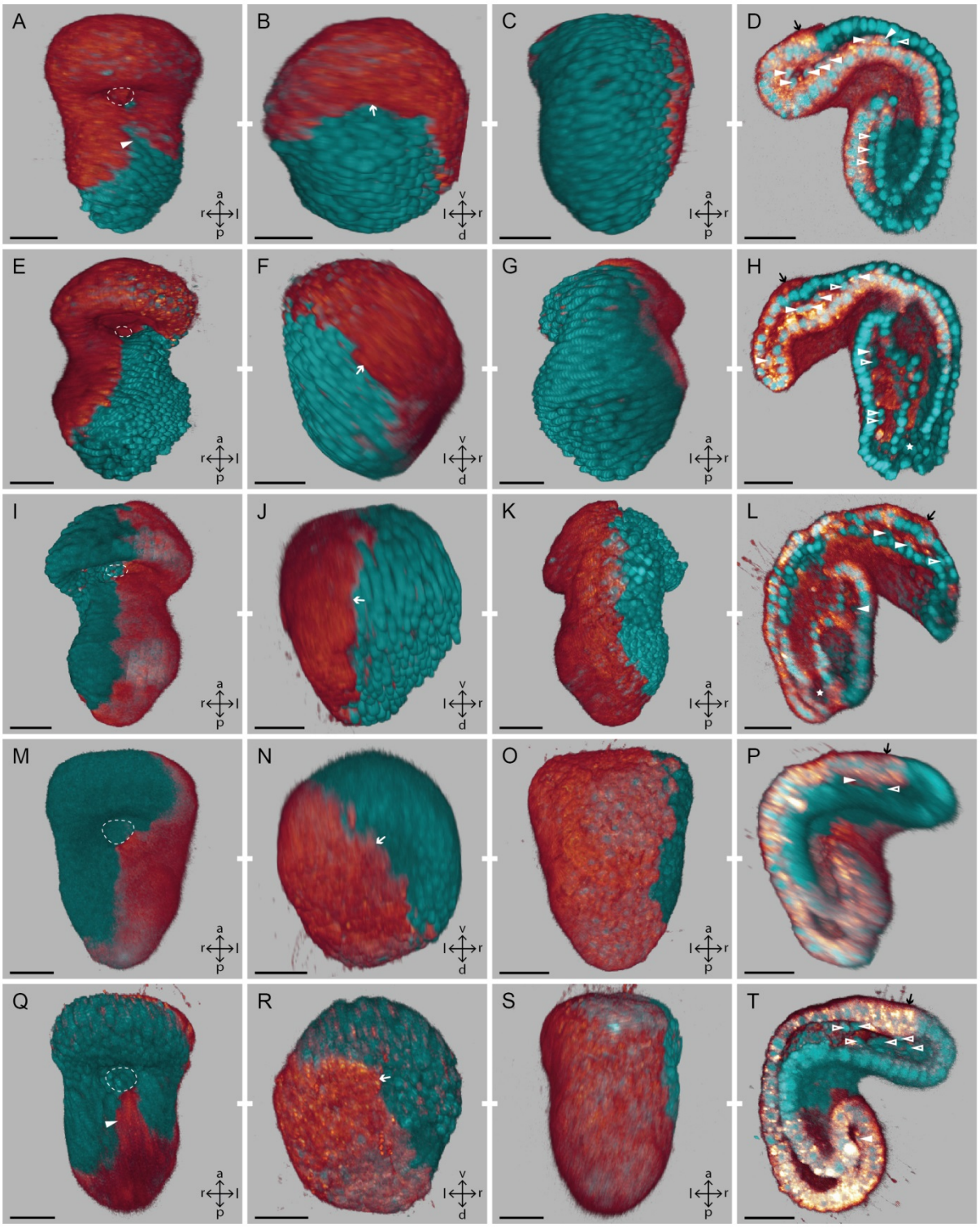

Fig. 15. Distribution of labeled cells in *P. pallida* embryos at late gastrulation, after one blastomere was marked at the 2-cell stage.

Fig. 16. Distribution of labeled cells in *P. pallida* embryos at mid gastrulation, after one blastomere was marked at the 4-cell stage. Imaris volume projections (Blend mode) and virtual section. The descendants of the marked blastomere are recognizable by carrying the injected dye (reddish); the embryos were counterstained for nuclei (cyan). The labeled cells make up about a quarter of the mid gastrula embryo. They occupy a distinct region, but differ in position between the different embryos (see text). Each line shows one specimen documented in successive images of a view on the blastoporal surface (first column; blastopore indicated by dashed line) and a view on the surface opposite of the blastopore (second column), as well as a horizontal (third column). Labeled crosses indicate the orientation of the embryos (a: anterior, d: dorsal, l: left, p: posterior, r: right, v: ventral). In all specimens, the ectodermal label reaches to a region opposite to – and somewhat anterior of – the blastopore (indicated by arrows in second column). In the virtual sections, the endodermal archenteron and some mesenchymal cells are visible: labeled mesenchymal cells are marked with filled arrowheads, unlabeled mesenchymal cells are marked with open arrowheads (third column). In some specimens, the labeled region in the archenteron is somewhat displaced relative to the labeled ectodermal region (indicated by arrows in C,F,I). In the specimen in M-O, the label includes the blastoporal rim (arrow in O), but it does not unambiguously pass onto the endodermal archenteron (see text); only very few mesenchymal cells are stained in this embryo (O). For further descriptions see text. Scale bars: 20 µm.

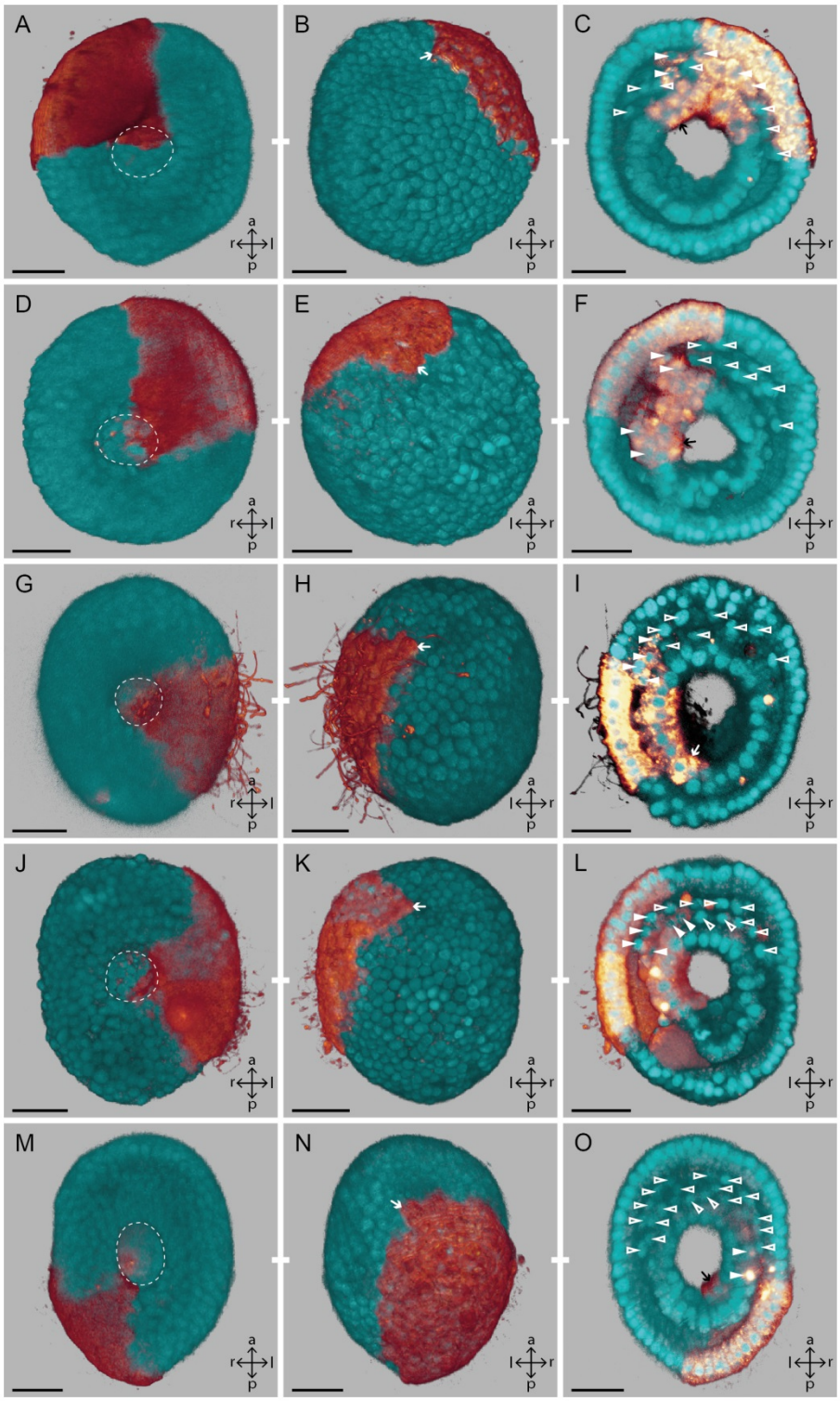

Fig. 16. Distribution of labeled cells in *P. pallida* embryos at mid gastrulation, after one blastomere was marked at the 4-cell stage.

Fig. 17. Distribution of labeled cells in *P. pallida* embryos at late gastrulation, after one blastomere was marked at the 4-cell stage. Imaris volume projections (Blend mode) and virtual section. The descendants of the marked blastomere are recognizable by carrying the injected dye (reddish); the embryos were counterstained for nuclei (cyan). The labeled cells occupy a distinct region in the embryos, which makes up about a quarter of the late gastrula. The position of the labeled cells differs between different embryos (see text): the figure shows specimens with an anterior/left-sided (A-D), a posterior/right-sided (E-H), and a posterior/left-sided (I-L) position of the labeled cells. Each specimen is documented in successive images showing a view on the ventral body surface (first column; blastopore covered by hood in A, but indicated by dashed line in E and I), a view on the dorsal surface of the hood (second column), a view on the dorsal surface of the trunk (third column), and a mid-sagittal section (fourth column). Labeled crosses indicate the orientation of the embryos (a: anterior, d: dorsal, l: left, p: posterior, r: right, v: ventral). In the specimens with posterior/lateral labels (E-H,I-L), a region of labeled ectodermal cells extends from the posterior body end to the blastopore on the ventral trunk surface (marked with arrowhead in E and I). In all specimens, on the dorsal hood surface the ectodermal label reaches to a median area, which is the presumptive site of the apical plate (indicated by arrows in second column). In sagittal sections, the thickened ectoderm of the apical plate is visible and labeled in all specimens (indicated by arrows in fourth column). The archenteron and some mesenchymal cells are visible in the section: labeled mesenchymal cells are marked with filled arrowheads, unlabeled mesenchymal cells are marked with open arrowheads (fourth column). In the embryos in A-D and I-L, the hindgut anlage is already developed (marked with star in D and L); it is unlabeled in the former, and partly labeled in the latter specimen. For further descriptions see text. Scale bars: 20 µm.

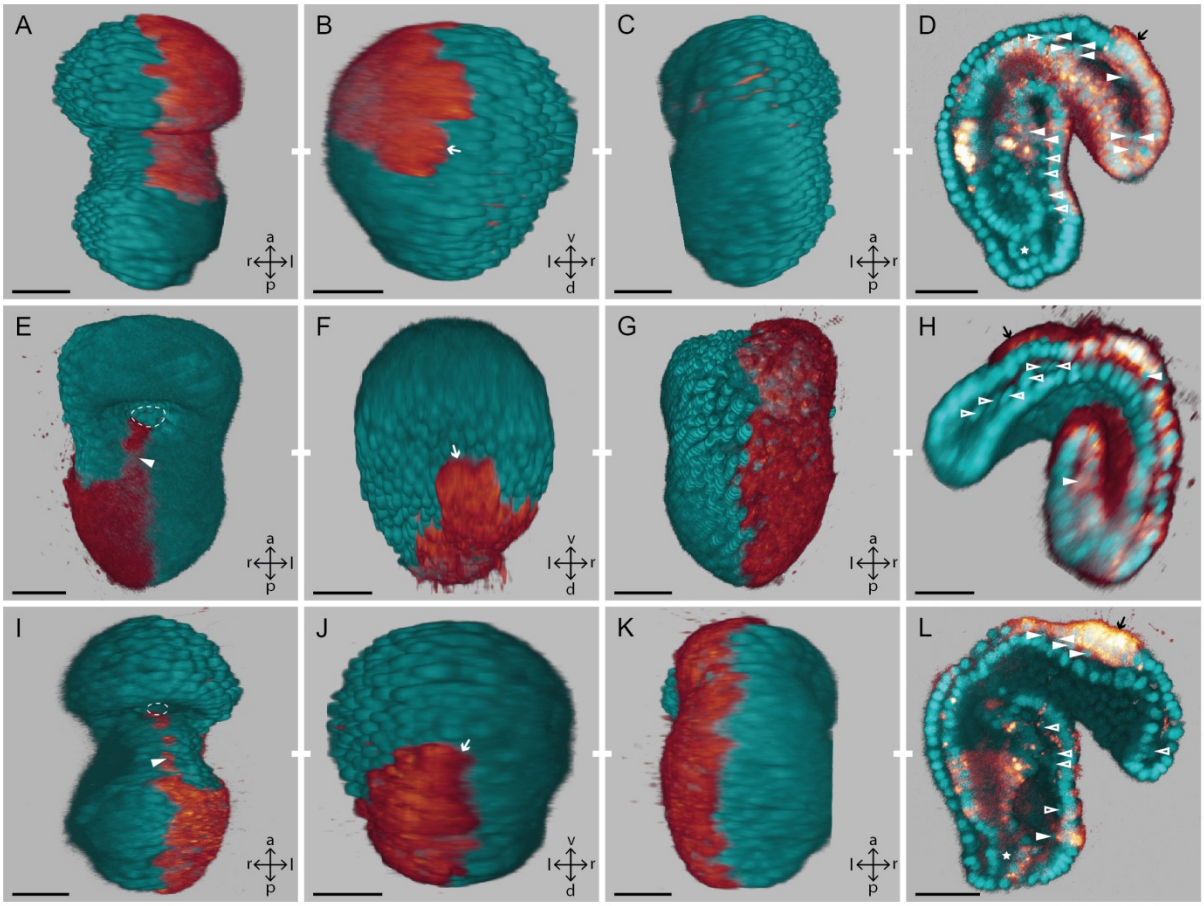

Fig. 17. Distribution of labeled cells in *P. pallida* embryos at late gastrulation, after one blastomere was marked at the 4-cell stage.

Fig. 18. Distribution of labeled cells in *P. pallida* embryos at late gastrulation, after one blastomere was marked at the 4-cell stage. Same as in Fig. 17, but of specimens with an anterior (A-D), a right-sided (E-H), a left-sided (I-L), and a posterior/dorsal (M-P) position of the labeled cells (at the dorsal median trunk area in G and K, the labeled archenteron is showing through the ectoderm nuclei layer, but the ectoderm is unlabeled). The orientation of the embryos is the same as in Fig. 17 (see labeled crosses; a: anterior, d: dorsal, l: left, p: posterior, r: right, v: ventral). In all specimens, except the one in E-H, the ectodermal label reaches to a median area of the dorsal hood surface, which is the presumptive site of the apical plate (indicated by arrows in B,J,N); in the specimen E-H, the label ends more laterally (F). In the sagittal sections, the thickened ectoderm of the apical plate (indicated by arrows in fourth column) is unlabeled in the latter specimen (H), but labeled in the other three (D,L,P). The archenteron and some mesenchymal cells are visible in the sections: labeled mesenchymal cells are marked with filled arrowheads, unlabeled mesenchymal cells are marked with open arrowheads (fourth column). In the embryos in A-D and E-H, the hindgut anlage is already developed and unlabeled (marked with star in D and H). For further descriptions see text. Scale bars: 20 µm.

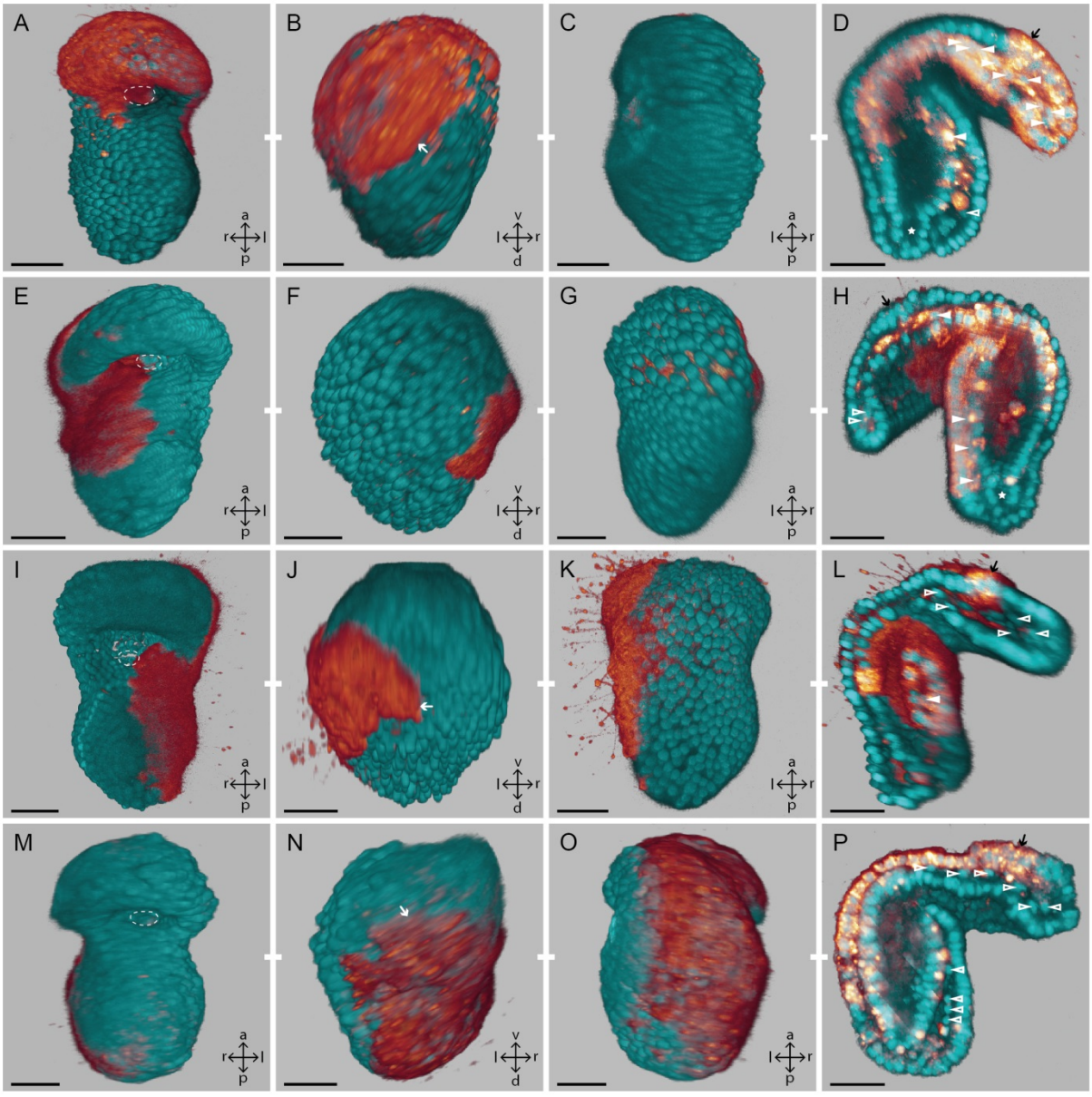

Fig. 18. Distribution of labeled cells in *P. pallida* embryos at late gastrulation, after one blastomere was marked at the 4-cell stage.

Table 4. Abundance of staining patterns observed after single cell labelings of *P. pallida* embryos. For the in-vivo injections of an unselected blastomere at the 2-cell stage (A) and at the 4-cell stage (B), the numbers of mid gastrula and of late gastrula specimens showing different staining patterns are given. The staining patterns, which are specified in the upper two rows of each table, were characterized according to position of the labeled clones with respect to the anterior-posterior and the left-right axes of the embryos (see text). A bottom line in each table gives the total number of embryos displaying each pattern and, in brackets, the frequency of this pattern over all studied embryos ('n'); all relative numbers are rounded to even. If not noted otherwise, cells of all three germ layers were stained, irrespective of the stage of injection and the stage of analysis (see text).

A. 2-cell stage marking

Stage	n	Anterior	Anterior-Lateral		Lateral		Posterior-Lateral		Posterior
			Right	Left	Right	Left	Right	Left	
Mid Gastrula	9	2	4	1				1	1
Late Gastrula	13	3	2		1	2	2	1	2
Total	22	5 (23%)	6 (27%)	1 (5%)	1 (5%)	2 (9%)	2 (9%)	2 (9%)	3 (14%)

B. 4-cell stage marking

Stage	n	Anterior		Posterior		Anterior	Right	Left	Posterior
		Right	Left	Right	Left				
Mid Gastrula	7	2	2	1[a]				2	
Late Gastrula	13		3	1	2	1	4	1	1[b]
Total	20	2 (10%)	5 (25%)	2 (10%)	2 (10%)	1 (5%)	4 (20%)	3 (15%)	1 (5%)

[a] This specimen had an ambiguous staining of the endoderm (see text)
[b] This specimen had no proper endoderm and mesoderm labeling, but only the dorsal ectoderm stained (see text)

3.2. Cleavage process in *P. muelleri*

3.2.1. Basic characteristics and timing of cleavage

Fertilized eggs of *P. muelleri* have a roundish shape and a diameter of about 70 to 80 µm. They are surrounded by a delicate fertilization membrane, which shows an undulating appearance in embryos that are compacted between two successive cleavage cycles (e.g., Fig. 19A,C',F). As in *P. pallida* embryos, no hatching event out from this membrane was witnessed. Polar bodies were observed from the 2-cell stage on, and are found in numbers between one and three, marking the embryo's animal pole. The cleavage is holoblastic and results in blastomeres of approximately equal size; only beginning with the 32-cell stage, and more consistently with the 64-cell stage, the vegetal blastomeres are slightly larger than the animal blastomeres (see below).

The timing and the lineage of the cleavage process were analyzed in four 4D-recorded embryos. The first cleavage division takes place two to three hours after releasing the eggs from the coelom. Subsequently, the blastomeres divide every 35 to 60 minutes at 17°C; yet, similar to *P. pallida*, the intervals become somewhat longer following the fifth cell cycle (Fig. 20) In each cleavage cycle, the cell divisions take place more or less synchronously, however, often they do not pass at the exactly same moment (Fig. 20). With advancing cleavage cycles this asynchrony increases (Fig. 20). No consistent sequence of the divisions between different embryos could be identified. The irregular asynchronies lead to the formation of embryos with all possible intermediate blastomere numbers (e.g., 3-, 6-, 15-, 24-cell stages), but partly already even nuclei numbers (e.g., 4, 8, 16, 32 nuclei); this happens, when all mitoses – yet not all cell divisions – of a respective cycle are completed. Such intermediate embryos are found more abundantly than in *P. pallida*.

3.2.2. First and second cleavage cycles and resulting embryos

The planes of the first two cleavages are perpendicular to each other and both pass through the animal-vegetal axis of the egg, as defined by the animal position of the polar bodies. These meridional divisions result in 2- and 4-cell embryos, respectively, with approximately equal sized blastomeres lying in one plane (Figs. 19A-B, 21A,C). In many embryos, however, the second cleavage cycle is not perfectly synchronous; the division in one blastomere

precedes the other, resulting in the formation of a transient 3-cell stage (75% of 4 recorded embryos) (Fig. 21B).

Shortly after each division cycle the embryo compacts. As in *P. pallida* embryos, during this process, the initially rather spherical blastomeres draw closer and flatten against each other, thus increasing their mutual cell contacts (Fig. 19B-C; Supplementary Material Video_S7-S9). In most 4-cell embryos, the compactation leaves a small opening central to the four blastomeres (Fig. 19C), but in about a quarter of the observed embryos it establishes a polar furrow (Table 5; Figs. 19C', 21D; Supplementary Material Video_S9). As in *P. pallida*, this polar furrow is visible from both poles and it completely separates the two remaining blastomeres; and likewise, no embryo with a second polar furrow was encountered. Prior to the next cleavage cycle, the cells become more roundish again, with the furrow, if present, dissolving.

3.2.3. Third cleavage cycle and 8-cell embryo

Before undergoing the third cleavage divisions, the blastomeres of the 4-cell embryo conspicuously elongate in directions that are preceding the orientations of the following divisions. Thereby, the animal apices of the cells get drawn out pointing in a clockwise direction, whereas the vegetal apices point in a counterclockwise direction, when the embryo is seen from the animal pole (Fig. 19D). This process is differently pronounced in different cells and embryos and appears to be stronger at the vegetal pole (Supplementary Material Video_S7-S9). It is very similar to the observations in *P. pallida*.

Subsequently, in most cells, the divisions pass obliquely and with a dextral orientation (Figs. 19D-E, 21E). This pattern of division was consistently and independently found in the 4D-recorded embryos (Fig. 22A) as well as in the fixed embryos (Fig. 22B). The observed inclinations of the cleavage axes and also the encountered variation are similar in the datasets from both methods (Fig. 22A-B). Only in the fixed material, single deviating inclinations were encountered (Fig. 22B). As in *P. pallida*, the dextrality of the third cleavage is not very distinct, as the oblique division axes are generally more inclined to the animal-vegetal axis, than to the equatorial plane of the embryo; only rarely do cells divide with an inclination higher than +25° (Fig. 22A-B).

The evaluation on the level of complete embryos shows that mostly in two or three blastomeres of the 4-cell embryo the third cleavage axis can be characterized as dextral, while

in the remaining cell(s) the inclination is less pronounced and thus was categorized as equatorial (Table 6A).

The 8-cell embryo is composed of two cell tiers – an animal and a vegetal one – of four cells each, and contains a small central blastocoel. As a result of the dextrality of the third cleavage divisions the blastomeres of the animal tier are located clockwise of their vegetal sister cells, when the embryo is seen from the animal pole (Figs. 19E, 21F-G). This arrangement was observed in more than half of the analyzed 8-cell embryos (50% of 4 recorded embryos, 60% of 15 fixed embryos). In the remainder, the blastomeres of differently one (25% of recorded, 20% of fixed embryos), two (25% of recorded, 13% of fixed embryos), or three (7% of fixed embryos) animal/vegetal sister cell pairs were found to be positioned in a juxtaposing alignment along the animal-vegetal axis (Fig. 21H). This appears to reflect the variation encountered in the data on the third cleavage axes.

After the third cleavage divisions the embryo compacts again. As at the 4-cell stage, this process leads to an increased blastomere contact in the 8-cell embryo (compare cell packing in Fig. 19E and Fig. 19F-G). In some embryos, compactation establishes a polar furrow: polar furrows were found either only at the embryo's animal pole (Fig. 19G) or, in only specimen, at both poles – running perpendicularly to each other (Table 5). In other cases, compactation leaves a small central opening between the four pole cells (Fig. 19F); which, however, in one specimen was so small that it was rated as an X-furrow, that is, a central meeting point of all four cells at the pole (Table 5).

3.2.4. Fourth cleavage cycle and 16-cell embryo

Prior to the fourth cleavage divisions, again, the cells undergo oblique elongations; however this time, they expand into a counterclockwise direction, when the embryo seen in an animal view (Figs. 19H, 23A; Supplementary Material Video_S7-S9). It appears as if this process is more pronounced in *P. muelleri*, than in *P. pallida* embryos.

The subsequent fourth cell division passes obliquely and with a sinistral orientation in most blastomeres; the animal daughter cells are given off in a direction counterclockwise of their vegetal sister cells, when the embryo is seen from the animal pole (Figs. 19I, 21I-J, 23B). Again, this pattern was consistently observed in the 4D-recorded embryos (Fig. 22C) and in the fixed material (Fig. 22D). The data also show that the obliqueness of divisions in the

fourth cleavage cycle is clearly stronger pronounced than in the third cleavage cycle. This is in general correspondence to the cleavage process in *P. pallida*. Although some variation in the exact inclination of the cleavage axes was encountered, the majority of cells divide inclined between –35° and –55° (Fig. 22C-D). Separated analyses for the 8-cell embryos' animal and vegetal cell tiers roughly show a similar distribution (Fig. 22C'-C",D'-D"). In fact, many embryos undergo sinistral divisions in all their blastomeres (Table 6B). An example for variation in the fourth cleavage cycle is given in Fig. 23A and B: here three animal cells divide sinistrally, whereas the cleavage axis in one cell (marked in Fig. 23A) has a stronger inclination and it divides rather meridionally.

The resulting 16-cell embryo is composed of four tiers of four cells each (Fig. 21K-M). The blastocoel forms an extensive cavity occupying almost 50% of the embryo's diameter. Embryos, which have some or all of their polar bodies internalized into the blastocoel, can be found from this stage onward. The single cell tiers are stacked along the animal-vegetal axis – making up an animal, an animal-equatorial, a vegetal-equatorial, and a vegetal tier. More evidently than in the 8-cell stage, the cell tiers are shifted against each other, so that the cells of each tier are aligned in the gaps between the cells of the neighboring tier(s) (see alignment of tiers in pole views in Figs. 19I, 21K,M). Also at the equator of the embryo, the cell tiers are intertwined (Fig. 21L).

The evaluation of the number of pole-encircling blastomeres shows that four cells are located at both poles in nearly two-thirds of the embryos (Table 7A; Figs. 19J, 21K,M). The remaining embryos have a higher – yet variable – number of cells at either the animal pole or at both poles (Table 7A). It appears as if strongly inclined, meridional divisions of individual cell(s) in the fourth cleavage cycle are the reason for such a situation (see Fig. 23A-B: five cells are located at the animal pole in Fig. 23B; note, however, that after compactation (Fig. 23C) one cell got excluded from the pole encircling). As in *P. pallida*, the data reveal a higher variation for the animal pole: while it is surrounded by four cells in about two-thirds of the analyzed embryos, the same is true for the vegetal pole in even nine-tenths of the cases (Table 7A). Among the embryos with more than four cells at a pole, the number of pole blastomeres ranges from five to eight; notably, such embryos roughly appear with decreasing frequency the higher the deviation from four pole cells is (Table 7A; Fig. 21N-P). This suggests that strongly inclined, meridional fourth cleavage divisions happen only rarely – yet more abundantly in the animal cell tier – and without a consistent pattern between the embryos. Only in one embryo eight cells were observed surrounding both poles (Table 7A): the

blastomeres in this embryo, however, appear not to be arranged as true octets, since respectively four of them markedly are protruded more toward each pole (Fig. 21O-P).

Again, the process of compactation following the cleavage divisions, in some 16-cell embryos, can result in the formation of a polar furrow or of an X-furrow (Table 5). Polar furrows are found variably at either only the animal pole or only the vegetal pole, or at both poles (Table 5), but – similar to *P. pallida* – when present they are only short in length (Fig. 19J). In other compacted embryos, a small central opening between the four pole blastomeres is found (Fig. 23C). A larger pole opening is usually present in cases when a pole is encircled by more than four cells (Fig. 21N).

3.2.5. Fifth cleavage cycle and 32-cell embryo

The fifth cleavage cycle was analyzed separately for the four cell tiers of the 16-cell stage (Table 6C). Most blastomeres of the animal and the vegetal tiers divide obliquely and with a dextral orientation, after they have elongated similarly to previous divisions (Figs. 19K-L, 23D-E, 24A,C-D,F; Supplementary Material Video_S7-S9). As a consequence, the animal daughter cells come to lie clockwise of their vegetal sisters, when the embryo is seen in an animal view (Figs. 19L, 23E). However, the results also reveal an increased variability regarding the directions of the cleavage axes, especially in the cells of the two more equatorial cell tiers. The data show that of all analyzed animal tier cells about four-fifths divide dextrally (Table 6C: first column, n = 42), and in the vegetal tier this the case in nearly nine-tenths of the cells (Table 6C: fourth column, n = 44); an example of an irregular division in the animal cell tier, next to proper dextral divisions, is given in Fig. 23D and E. In contrast, the cells of the animal-equatorial tier only in about one-third of the cases undergo dextral divisions; notably, sinistral divisions are equally frequent in this cell tier (Table 6C: second column, n = 39) In the vegetal-equatorial tier, about two-fifths of the cells divide dextrally (Table 6C: third column, n = 41; Fig. 24B,E). Similarly to *P. pallida*, these data seem to indicate that the pattern and process of cleavage is somewhat more variable in the animal hemisphere (animal and animal-equatorial cell tiers) than it is in the vegetal hemisphere (vegetal and vegetal-equatorial cell tiers).

A result of this irregularity is a distinct degree of variation in the blastomere arrangements of 32-cell embryos. The quadrants and the tiers of cells get obscured and, besides the animal

most and the vegetal most cell tiers, no distinct pattern of blastomere arrangements could be identified (Fig. 24G-I).
In embryos at this stage, both poles are encircled by four cells in about half the analyzed cases (Table 7B; Figs. 19M, 24G,I). Of the remaining embryos, more than two-fifths have four cells at one pole, but differently five or six cells at the opposite pole (Fig. 24J), and only in two embryos more than four cells were located at both poles (Table 7B). In total, the animal pole is encircled by four blastomeres in 62% of the analyzed embryos, while for the vegetal pole the same is the case in 76% (Table 7B). This data indicate a higher variability for the animal pole, similar to the 16-cell stage – and also in consistence with the situation found in *P. pallida* cleavage.

The compactation following the cleavage divisions again can establish a short polar furrow, differently at only one pole or at both poles in different 32-cell embryos (Table 5; Fig. 19M). In the latter case, the two polar furrows were found to be differently oriented either perpendicularly or parallel to each other (Table 5). Again, embryos with more than four blastomeres at a pole display a rather large pole opening there (Fig. 24J).

3.2.6. Sixth cleavage cycle and 64-cell embryo

Due to the high variation of cell arrangements in the different 32-cell embryos – as well as the increased asynchrony of cleavage divisions from the fifth cleavage cycle onward (see Fig. 20) – the sixth cleavage divisions could only be analyzed for the animal most and the vegetal most tiers of cells. Most of these cells divide obliquely with a sinistral orientation (Figs. 19N-Q, 23F-H); thus, following the pattern of alternately orientated oblique divisions, which was encountered beginning with the third cell cycle. However, the gained data also point toward a higher variability than in the fifth cleavage cycle, as well as to a higher variability in the cleavage axis of the cells of the animal tier (Table 6D). In the sixth cleavage cycle, 63% of all analyzed animal cells (Table 6D: first column, n = 16), but 77% of the vegetal cells undergo sinistral divisions (Table 6D: second column, n = 22). Although the analyzed sample size is smaller than in *P. pallida*, the data seem to indicate that in *P. muelleri* during the sixth cleavage cycle a pattern of sinistral cleavage orientations is more consistently present.

By the 64-cell stage, the embryo has developed into a blastula, with small roundish cells surrounding an extensive blastocoel (Fig. 19S). In most embryos, the polar bodies are found

internalized into the blastocoel. The cells of the embryo's vegetal hemisphere are slightly larger than the animal cells (Fig. 24K-L). This pattern of size differences can be observed in some 32-cell embryos already, but by the 64-cell stage it is a consistent feature of nearly all embryos.

In most of the analyzed 64-cell embryos, the animal pole is surrounded by four blastomeres (Table 7C; Figs. 23H, 24K), while in the remainders five or six cells are found at this pole; the latter cases, again, occur in decreasing frequency along with the increasing deviation from four cells (Table 7C). The vegetal pole could only be analyzed in the 4D recordings, and is surrounded by four blastomeres in all studied embryos (Table 7C; Fig 19R). In fixed embryos, unfortunately, the lack of proper landmarks does not allow the unambiguous identification of the vegetal pole; however, the fact that also in fixed embryos the vegetal hemisphere is made up of a layer of interlocked blastomeres suggests that four of these cells constitute the vegetal pole encircling (see Fig. 24L).

Similar as in the previous cleavage cycles, the process of compactation following the cleavage divisions – with its narrowing of the blastomeres within the embryo – can lead to the formation of polar furrows; at different poles and in some embryos (Table 5; Fig. 19R).

Fig. 19. **Cleavage of a *P. muelleri* embryo in vegetal view from 2-cell stage to 64-cell stage.** Sequence of DIC images showing the development of one embryo (except C') that was 4D-recorded in a view at the vegetal pole (the animal polar bodies are not visible; except in B). Lines indicate the sister cells after divisions, and dots mark the sister cell that is located closer to the vegetal pole. Scale bar in A applies to all: 20 µm.
A. 2-cell embryo shortly prior to divisions of second cleavage cycle. It is surrounded by a delicate fertilization membrane (open arrowhead). **B**. 4-cell stage directly after second cleavage divisions. The embryo is still uncompacted and the cells are of roundish shape. The polar bodies located at the animal pole, opposite to the observer, are visible (marked with asterisk). **C**. 4-cell embryo after compactation between second and third cleavage cycles. The cells flattened against each other, losing their initial spherical shapes (see B), and drew closer to the central animal-vegetal axis. A small opening between the four blastomeres persists (arrowhead). **C'**. Compacted 4-cell stage as in C, but of a different specimen: in this embryo a polar furrow between two oppositely situated non-sister cells is formed (arrowhead). The fertilization membrane has an undulating appearance (open arrowhead). **D**. Blastomere elongations prior to third cleavage divisions. The vegetal apices of the cells became drawn out pointing into clockwise directions (indicated by arrowheads); yet note that the embryo is looked at from the vegetal pole. **E**. Full-focal projection of 8-cell embryo directly after third cleavage divisions. All cells divided with a dextral orientation; the four vegetal blastomeres (marked with dots) are aligned shifted clockwise relative to their animal sister blastomeres (note that the embryo is looked at from vegetal). **F-G**. 8-cell embryo after compactation (full-focal projection and vegetal pole in F, animal pole in G). A very small opening is present at the vegetal pole (arrowhead in F), but a polar furrow is found at the animal pole (arrowhead in G); the fertilization membrane has an undulating appearance (open arrowhead). **H-I**. Fourth cleavage cycle in the vegetal cells of the 8-cell stage: oblique elongations of cells prior to divisions (H), and blastomeres directly after divisions (I). All cells divide obliquely and in sinistral directions; the four blastomeres at the vegetal pole (marked with dots in I) are positioned counterclockwise relative to their animally situated sister cells (note that the embryo is looked at from the vegetal pole). **J**. Compacted 16-cell embryo. Four blastomeres (marked with dots) are located at the vegetal pole, and a small polar furrow is present (arrowhead); the same situation is found at the animal pole (not shown). **K-L**. Fifth cleavage cycle in the vegetal cell tier of the 16-cell stage: cell elongations prior to divisions (K), and blastomeres directly after divisions (L). All four cells divide obliquely and in dextral directions. **M**. Compacted 32-cell embryo. A tier of four blastomeres (marked with dots) is situated at the vegetal pole, two of them form a small polar furrow (arrowhead); likewise four blastomeres are located at the animal pole (not shown). **N-Q**. Sixth cleavage cycle in the vegetal cell tier of the 32-cell stage: successive cell elongations and cell divisions; all divisions pass in sinistral directions. **R**. Compacted 64-cell embryo. Four blastomeres (marked with dots) are located at the vegetal pole, and a small polar furrow is established (arrowhead); the very same situation is found at the animal pole (not shown). **S**. Optical section through compacted 64-cell embryo. Small roundish blastomeres surround a large blastocoel (bc).

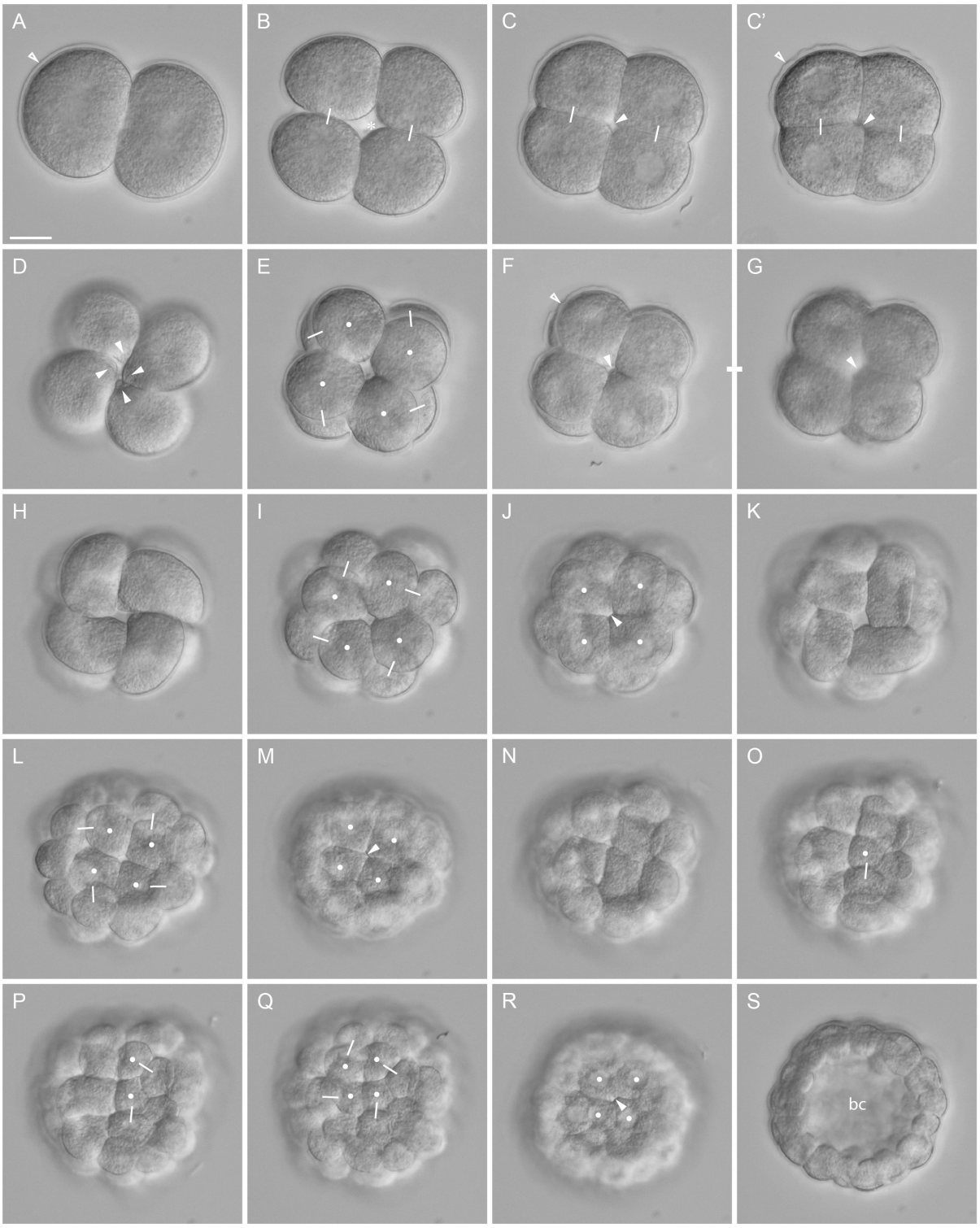

Fig. 19. **Cleavage of a *P. muelleri* embryo in vegetal view from 2-cell stage to 64-cell stage.**

Fig. 20. Timing of cleavage divisions and cell lineage in *P. muelleri*. For three different 4D-recorded embryos (A-C), the cell lineage is given up to the sixth cleavage cycle (labeled on top of A for A-C); for one embryo (D), it is given up to the fifth cleavage cycle (in lineage B, some cells could not be traced through the sixth division; indicated with dashed line). All recordings started at the 2-cell stage. Labeled axes beneath each lineage give the timing of the cleavage divisions at 17°C, post egg release by opening of the coelom ('hours pER'). The cleavage process takes place more or less synchronously; but within individual cleavage cycles often the cells do not divide at exactly the same moment. Early asynchronies are recognizable also though later cell cycles (see lineages in C-D). The time intervals between successive divisions become longer with the fifth cleavage cycle (generally, they lie between 35 and 60 minutes). The exact timing and the sequence of divisions vary between the different embryos.

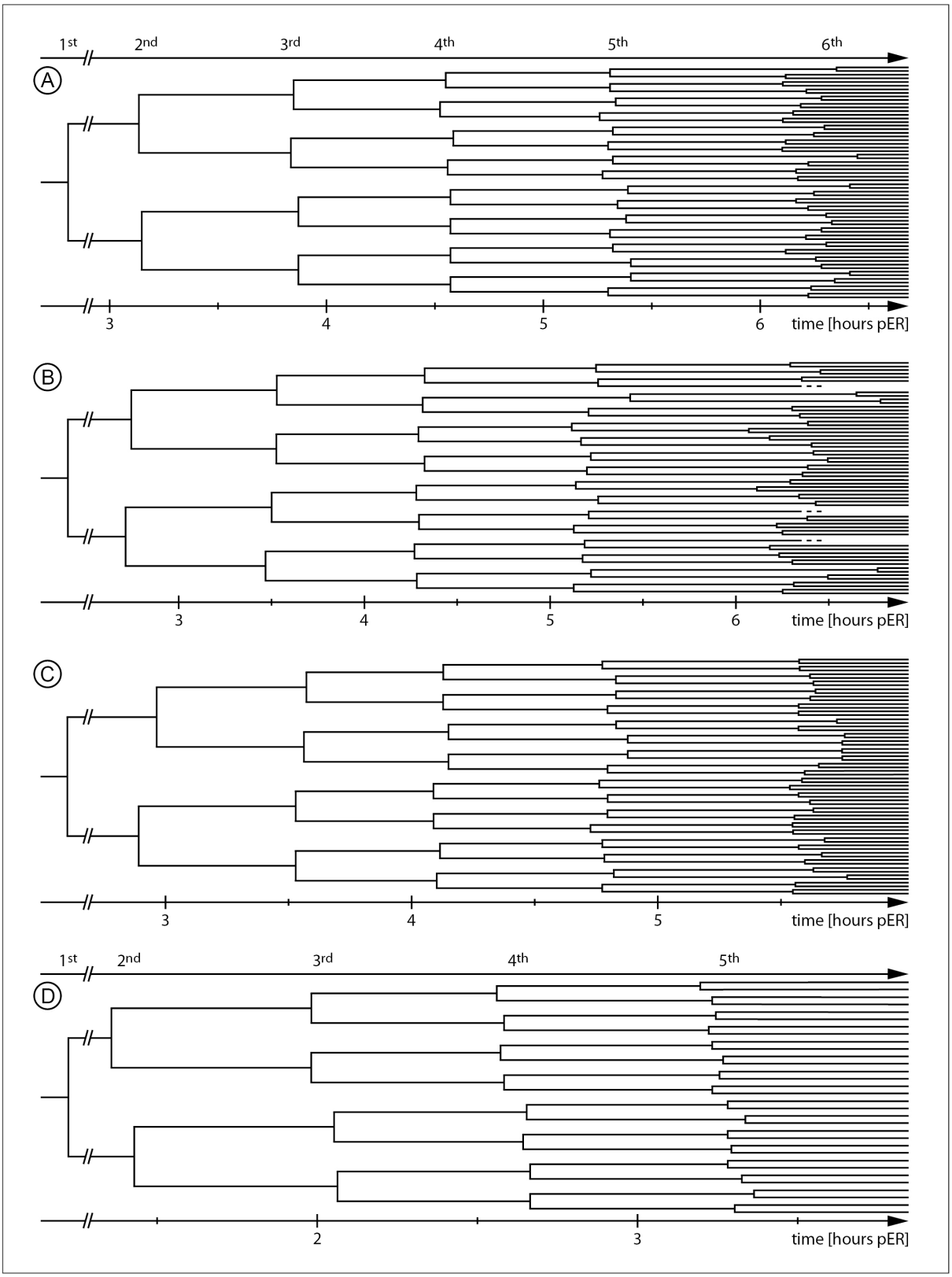

Fig. 20. Timing of cleavage divisions and cell lineage in *P. muelleri*.

Fig. 21. *P. muelleri* embryos from 2-cell stage to 16-cell stage. Imaris volume projections (Blend mode: A,C,E-P; MIP mode: D) and one epifluorescence image (B) of fixed embryos that were stained for nucleic acids. Nuclei are highlighted in gray (e.g., A) or visible in yellow (D,I) or bright blue (B); blastomere shape signals result from autofluorescence of the cytoplasm (reddish; except B: dark blue). Polar bodies are indicated with asterisks; lateral views are oriented with the animal pole to the top (an: animal, vg: vegetal). Scale bars: 20 µm.
A. 2-cell embryo (animal view) with nuclei in anaphase of second cleavage divisions (indicated by open arrowheads in left cell). **B**. Transient 3-cell embryo with already four nuclei. The upper blastomere is not yet divided. **C**. 4-cell embryo shortly after second cleavage divisions (animal view). The nuclei are positioned at the cells' periphery (indicated by open arrowhead in one cell). **D**. 4-cell embryo apparently in a compacted state (animal view). The nuclei are positioned in the center of the blastomeres (indicated by open arrowhead in one cell). A polar furrow is present (arrowhead). **E**. Embryo in cytokinesis of third cleavage cycle (lateral view). The cells are dividing obliquely and with a dextral orientation (indicated by dashed lines). **F-G**. Animal (F) and lateral view (G) of an 8-cell embryo. The blastomeres are organized in two cell tiers, an animal (see F) and a vegetal one; the animal cell tier is shifted against the vegetal cell tier. **H**. 8-cell embryo in which animal and vegetal blastomeres are positioned on top of each other along the animal-vegetal axis (lateral view). **I**. 8-cell embryo with nuclei in anaphase of fourth cleavage divisions (lateral view). The axes of divisions are oriented obliquely and in sinistral directions (indicated by dashed lines). **J**. Embryo in cytokinesis of the fourth cleavage cycle (lateral view). All cells divide obliquely and with sinistral orientations (indicated by dashed lines). **K-M**. 16-cell embryo in animal (K), lateral (L), and vegetal view (M). The blastomeres are organized along the animal-vegetal axis in four tiers of four cells each; the individual cell tiers are shifted against each other: all blastomeres are situated in gaps between adjacent blastomeres, and the cell tiers are intertwined at the embryo's equator (dotted line in L). Four blastomeres are located at the animal and at the vegetal pole (marked with dots in K and M). **N**. 16-cell embryo in which five cells are located at the animal pole (marked with dots) and surround a pole opening (arrowhead). In the same embryo four cells lie at the vegetal pole (not shown). **O-P**. Animal (O) and lateral (P) view of a 16-cell embryo in which eight cells are encircling the animal pole (marked with dots in O) and the vegetal pole (not shown). The blastomeres are not organized in proper octets however: four blastomeres are more protruded toward each pole, respectively (animal most cells marked with dots in P).

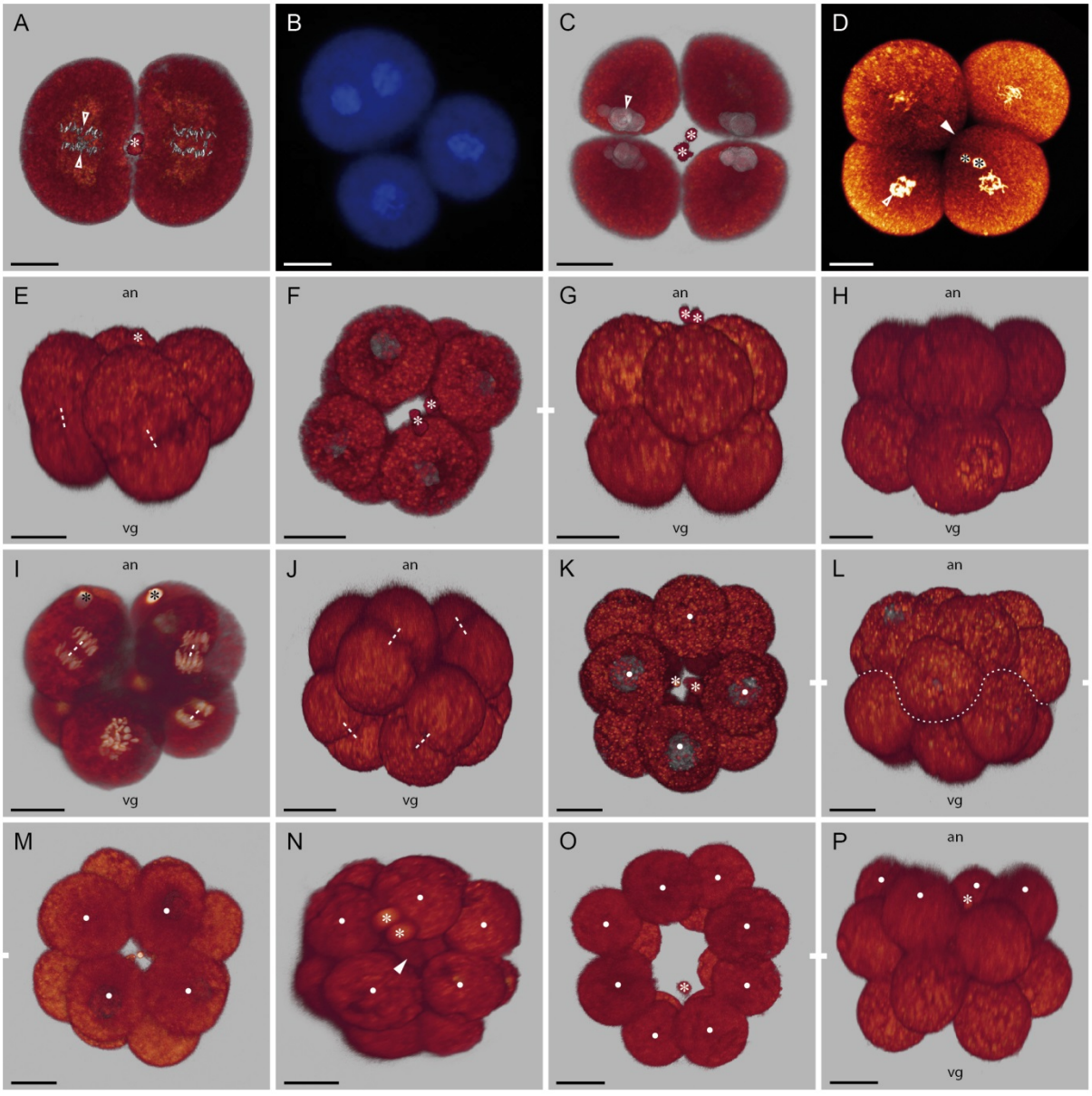

Fig. 21. *P. muelleri* embryos from 2-cell stage to 16-cell stage.

Fig. 22. Inclinations of cleavage axes of third and fourth cleavages in *P. muelleri*. The charts give the results of the quantitative analyses of the inclinations of mitotic spindles and cell divisions relative to the animal-vegetal axis in cells during the third (A,B) and the fourth cleavage cycles (C,D); for the latter, separated analyses for cells of the animal cell tier (C',D') and the vegetal cell tier (C",D") of the 8-cell stage are provided. Results obtained from 4D-recorded embryos (A,C,C',C") and from fixed embryos (B,D,D',D") are given separately. Abscissas give the angles of inclinations (dex: dextral, eq: equatorial, mer: meridional, sin: sinistral). The heights of the bars give the relative frequencies in which the respective inclinations (grouped in 5°-steps) were observed over all analyzed cells ('n'); the numbers in the bars give the absolute numbers of cells in the respective groups. In the third cleavage cycle (A,B), the cleavage axes are inclined along positive angles, that is, dextrally. In the fourth cleavage cycle (C,D), the cleavage axes are inclined sinistrally and generally more pronounced obliquely than in the third cleavage. Both data sets reveal a similar cleavage pattern; yet in both cleavage cycles the measured angles of inclinations vary between the analyzed cells of the samples.

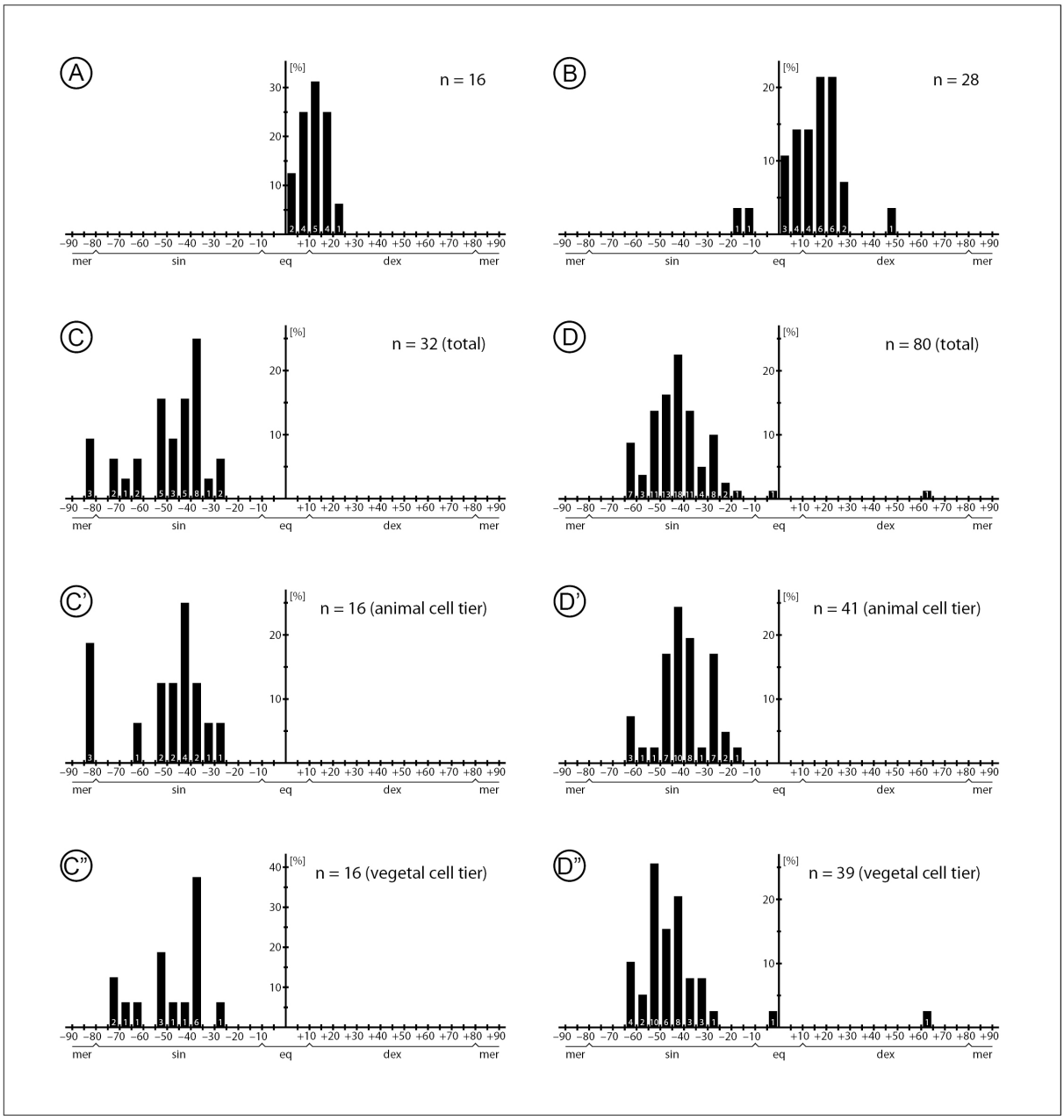

Fig. 22. Inclinations of cleavage axes of third and fourth cleavages in *P. muelleri*.

Fig. 23. Cleavage of a *P. muelleri* embryo in animal view from fourth division cycle to the 64-cell stage. Sequence of DIC images showing the development of one embryo, 4D-recorded in a view at the animal pole. Polar bodies are marked by asterisks in some images. Lines indicate sister cells after divisions, dots mark the sister cell that is located closer to the animal pole. Scale bar in A applies to all: 20 µm.
A-B. Fourth cleavage cycle in the animal cells of the 8-cell stage: cell elongations prior to divisions (A), and blastomeres directly after divisions (B). The divisions in three cells pass markedly obliquely and in sinistral directions, whereas one cell (marked with triangle in A) divides with a high inclination angle and nearly meridionally. The descendants of this cell will display irregularities in the divisions up to the late cleavage cycles. **C**. 16-cell embryo compacted between fourth and fifth cleavage cycles. Only four blastomeres (marked with dots) appear to encircle a small opening (covered by polar bodies) at the animal pole; yet, due to the nearly meridional third division in one blastomere (see A-B), also its second daughter cell (marked with triangle) almost reaches to the pole. In the same embryo four blastomeres are situated at the vegetal pole (not shown). **D-E**. Fifth cleavage cycle in the animal cells of the 16-cell stage: elongations of cells (D), and blastomeres directly after divisions (E). Three cells divide obliquely and in dextral directions, but both descendants of the irregular blastomere divide rather equatorially (marked with triangles in D). Thus, both their animal daughters are located at the pole after the divisions (E). In the same embryo, the divisions pass more regularly in the vegetal cells and a polar furrow is formed by the 32-cell stage (not shown). **F-H**. Successive cell elongations and divisions of the animal cells in sixth cleavage cycle. Only four cells are evaluated: two cells divide clearly sinistrally (divisions in G), one cell very weakly sinistrally (left division in H), and one cells equatorially (marked with triangle in F). The latter is the descendant of the irregular dividing cell in A-B.

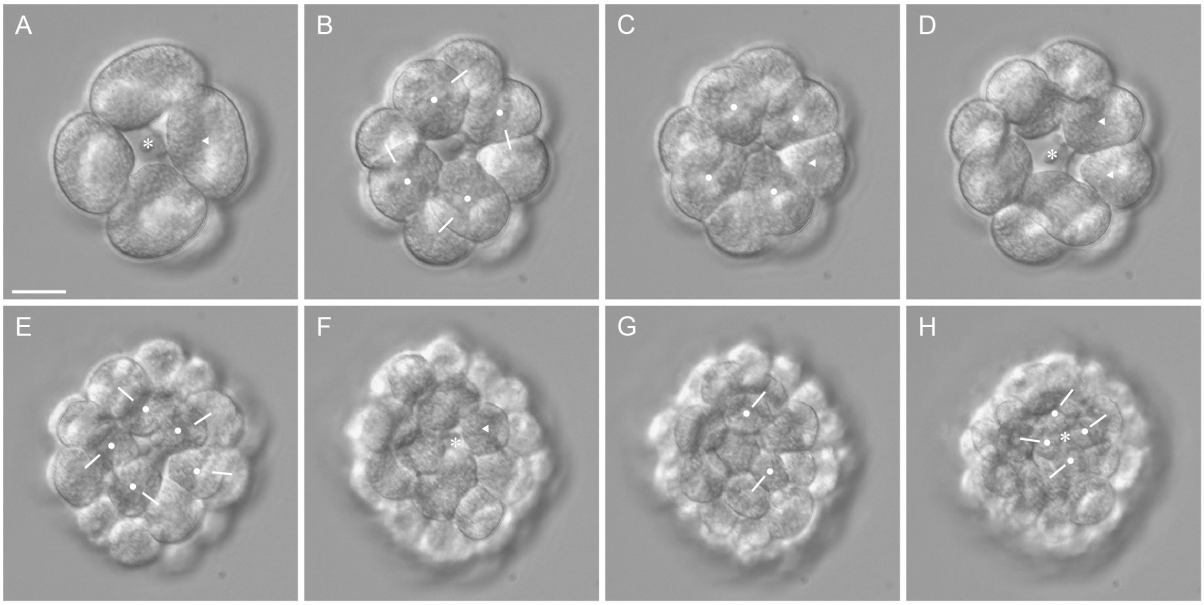

Fig. 23. Cleavage of a *P. muelleri* embryo in animal view from fourth division cycle to the 64-cell stage.

Fig. 24. *P. muelleri* embryos from fifth cleavage cycle to 64-cell stage. Imaris volume projections (Blend mode) of fixed embryos that were stained for nucleic acids. Nuclei are highlighted in gray (e.g., A) or visible in dark yellowish (e.g., G); blastomere shape signals result from autofluorescence of the cytoplasm (reddish). Polar bodies are indicated with asterisks; lateral views are oriented with the animal pole to the top (an: animal, vg: vegetal). Scale bars: 20 µm.
A-C. Animal (A), lateral (B), and vegetal views (C) of 16-cell embryo with nuclei in metaphase and anaphase of fifth cleavage division. The cleavage axes are oriented dextrally (indicated by dashed lines in the animal (A), equatorial (B), and vegetal (C) blastomeres). **D-F**. Animal (D), lateral (E), and vegetal (F) views of 32-nuclei embryo in cytokinesis of fifth cleavage cycle. In this embryo, the animal and vegetal cells divide dextrally but not perfectly synchronously (see F), whereas the divisions in equatorial cells show various orientations (dashed lines indicate cleavage axes of dividing cells in the animal (D), equatorial (E), and vegetal (F) blastomeres). **G-I**. 32-cell embryo in animal (G), lateral (H), and vegetal view (I). Both poles are encircled by four blastomeres (marked with dots in G and I). In lateral view (H) the blastomere are intertwined and the arrangement appear irregular. **J**. 32-cell embryo in which five cells (marked with dots) surround an opening (arrowhead) at the animal pole. In the same embryo four cells are located the vegetal pole (not shown). **K-L**. Animal (K) and vegetal views (L) of 64-cell embryo. Four blastomeres are located at the animal pole (marked with dots in K); the exact position of the vegetal pole cannot be identified due to the lack of proper landmarks (see L). The animal cells appear slightly smaller than the vegetal ones (compare K and L).

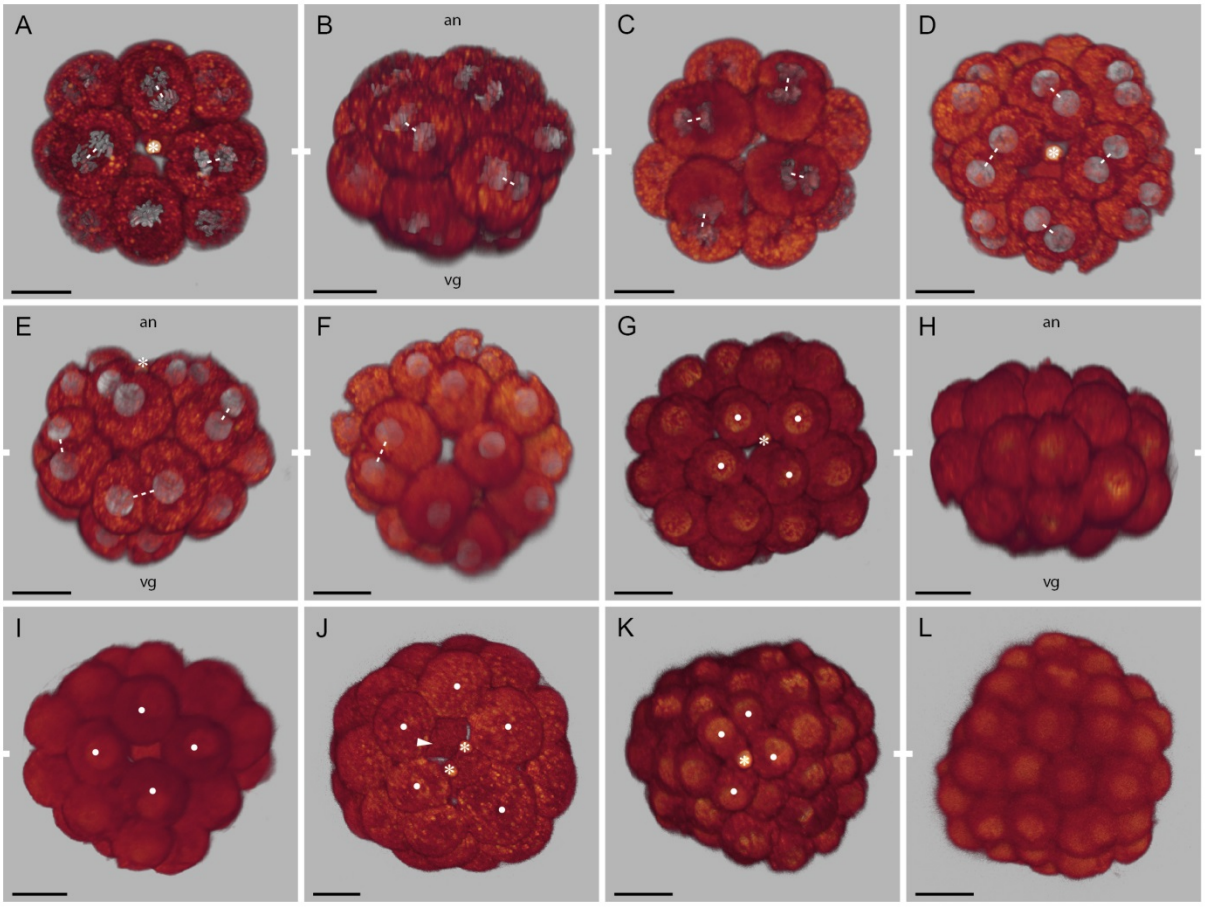

Fig. 24. *P. muelleri* embryos from fifth cleavage cycle to 64-cell stage.

Table 5. Pole blastomere contacts in *P. muelleri* embryos. The four blastomeres of the 4-cell embryo, and the four blastomeres that are located at the animal pole and/or the vegetal pole in many embryos of later cell stages, can show central cell contacts in the organization of a polar furrow or of an X-furrow (polar furrow: contact line between two oppositely situated cells; X-furrow: central contact between all four cells). The table gives the frequency of 4-cell stage to 64-cell stage embryos that have such a cell contact, at only the animal pole, or at only the vegetal pole, or at both poles, over all analyzed embryos ('n'; only embryos in a putatively compacted state, and with (one or both) pole(s) encircled by four blastomeres were included; see Table 7). Per cell stage, the upper row provides the data from 4D-recorded embryos, and the lower row gives data from fixed embryos. All relative numbers are rounded to even. Although the sample size is small, the data indicate against the obligatory presence or absence of polar furrows. Note, that an embryo that displays a polar furrow at one pole, can have an X-furrow or a small opening between the four pole blastomeres at the opposite pole; but in some cases, it may also have more than four cells located at the opposite pole (see Table 7).

Stage	n	Polar furrow at			X-Furrow at		
		Animal Pole	Vegetal Pole	Both Poles	Animal Pole	Vegetal Pole	Both Poles
4-cell	4			25%[a]			
	13			23%[a]			
8-cell	4	50%				25%	
	12	17%		8%[b]			
16-cell	4	25%		25%[c]		25%	
	8		25%				
32-cell	4		25%	50%[b]			
	10	10%		20%[d]			
64-cell	2		50%	50%[b]			
	7	43%					

[a] The same polar furrow is visible at both poles (it reaches along the entire animal-vegetal axis)
[b] The animal polar furrow and the vegetal polar furrow are oriented perpendicularly to each other
[c] The animal polar furrow and the vegetal polar furrow are oriented approximately parallel to each other
[d] The animal polar furrow and the vegetal polar furrow are oriented either perpendicularly or parallel to each other (each in one specimen (10%), respectively)

Table 6. Orientations of cleavage axes in *P. muelleri* embryos. From the third to the sixth cleavage cycle, all observed combinations of orientations of cleavage axes in the blastomeres of individual embryos are listed, and the numbers of embryos showing each combination are given. Each line gives a unique combination (the numbers preceding the different cleavage orientations give the number of cells that show such cleavage axes; if cells could not be resolved, as they were not in a proper mitotic state or otherwise not accessible, this is noted as not applicable (n.a.)). For the third, the fourth, and the sixth cleavage cycles (A,B,D), the numbers of 4D-recorded embryos and of fixed embryos showing each combination are given; in the fifth cleavage cycle (C), each combination was observed only once, and the four upper rows give the data from recorded embryos, the lower rows the data from fixed embryos. Separated evaluations are given for the single cell tiers in the embryo for the fourth and the fifth cleavage cycles (B,C); for the sixth cleavage cycle (D), only the animal and vegetal cell tiers were analyzed.

A. Third cleavage cycle

Cleavage Orientations	Number of Embryos	
	Recorded	Fixed
3 dextral, 1 equatorial	2	2
2 dextral, 2 equatorial	2	1
2 dextral, 2 n.a.		3
1 dextral, 2 sinistral, 1 n.a.		1
1 dextral, 3 n.a.		4
2 equatorial, 2 n.a.		1
1 equatorial, 3 n.a.		1

B. Fourth cleavage cycle

Cleavage Orientations		Number of Embryos	
Animal Tier	Vegetal Tier	Recorded	Fixed
4 sinistral	4 sinistral	2	4
3 sinistral, 1 meridional	4 sinistral	1	
2 sinistral, 2 meridional	4 sinistral	1	
3 sinistral, 1 n.a.	3 sinistral, 1 n.a.		2
3 sinistral, 1 n.a.	2 sinistral, 2 n.a.		1
2 sinistral, 2 n.a.	2 sinistral, 2 n.a.		4
2 sinistral, 2 n.a.	1 sinistral, 1 equatorial, 2 n.a.		1
2 sinistral, 2 n.a.	1 sinistral, 3 n.a.		1
2 sinistral, 2 n.a.	1 dextral, 3 n.a.		1
1 sinistral, 3 n.a.	2 sinistral, 2 n.a.		1
1 sinistral, 3 n.a.	1 sinistral, 3 n.a.		1

Table 6. (continuation)

C. Fifth cleavage cycle

Cleavage Orientations			
Animal Tier	**Animal-Equatorial Tier**	**Vegetal-Equatorial Tier**	**Vegetal Tier**
4 dextral	1 dextral, 2 sinistral, 1 equatorial	2 sinistral, 1 meridional, 1 equatorial	4 dextral
4 dextral	3 sinistral, 1 equatorial	2 dextral, 1 meridional, 1 equatorial	4 dextral
3 dextral, 1 equatorial	2 sinistral, 2 equatorial	3 dextral, 1 sinistral	4 dextral
2 dextral, 2 equatorial	1 sinistral, 3 equatorial	2 dextral, 1 meridional, 1 equatorial	3 dextral, 1 equatorial
4 dextral	2 dextral, 2 sinistral	2 dextral, 2 sinistral	4 dextral
3 dextral, 1 meridional	3 dextral, 1 sinistral	3 dextral, 1 sinistral	2 dextral, 1 equatorial, 1 sinistral
3 dextral, 1 n.a.	3 dextral, 1 n.a.	2 dextral, 1 sinistral, 1 meridional	4 dextral
3 dextral, 1 n.a.	1 dextral, 1 sinistral, 2 n.a.	1 meridional, 1 equatorial, 2 n.a.	4 dextral
2 dextral, 1 meridional, 1 equatorial	2 dextral, 1 equatorial, 1 n.a.	1 sinistral, 1 meridional, 2 n.a.	2 dextral, 2 n.a.
2 dextral, 2 equatorial	2 dextral, 1 sinistral, 1 meridional	2 dextral, 1 sinistral, 1 meridional	3 dextral, 1 meridional
2 dextral, 2 n.a.	1 equatorial, 3 n.a.	1 dextral, 1 sinistral, 1 meridional, 1 n.a.	3 dextral, 1 n.a.
1 dextral, 1 meridional, 2 n.a.	2 sinistral, 2 n.a.	1 sinistral, 1 equatorial, 2 n.a.	2 dextral, 1 meridional, 1 n.a.

D. Sixth cleavage cycle

Cleavage Orientations		Number of Embryos	
Animal Tier	**Vegetal Tier**	**Recorded**	**Fixed**
4 sinistral	4 sinistral	1	
3 sinistral, 1 equatorial	4 sinistral	1	
2 sinistral, 2 dextral	1 sinistral, 1 meridional, 1 dextral, 1 n.a.		1
1 sinistral, 1 equatorial, 2 n.a.	4 n.a.		1
2 meridional, 2 n.a.	2 sinistral, 2 n.a.		1
4 n.a.	2 sinistral, 1 meridional, 1 equatorial		1
4 n.a.	2 sinistral, 2 n.a.		2
4 n.a.	1 sinistral, 1 equatorial, 2 n.a.		1
4 n.a.	1 sinistral, 3 n.a.		1

Table 7. Number of pole blastomeres in *P. muelleri* embryos. For the 16-cell stage to the 64-cell stage, all encountered combinations in the numbers of blastomeres encircling the animal pole and the vegetal poles of individual embryos are listed. The numbers of 4D-recorded embryos and of fixed embryos showing each combination are given separately, and the frequency of the respective pattern (4D-recorded plus fixed specimens) over all embryos ('n') is noted (all relative numbers are rounded to even). If poles could not be resolved, this is noted as not applicable ('n.a.'). In each table, two bottom lines give the numbers of embryos that have four blastomeres located at either the animal pole or the vegetal pole irrespective of the respective counter-pole (these include only confirmed cases, and for the 64-cell embryo might be underestimations), as well as the frequencies of these respective patterns (note, that these numbers do not necessarily sum up to 100).

A. 16-cell embryo

Number of Blastomeres at		Number of Embryos		Frequency (n = 20)
Animal Pole	Vegetal Pole	Recorded	Fixed	
4	4	3	10	65%
5	4		3	15%
6	4	1		5%
7	4		1	5%
8	7		1	5%
8	8		1	5%
Animal Pole = 4 Blastomeres		Total: 13		65%
Vegetal Pole = 4 Blastomeres		Total: 18		90%

B. 32-cell embryo

Number of Blastomeres at		Number of Embryos		Frequency (n = 21)
Animal Pole	Vegetal Pole	Recorded	Fixed	
4	4	3	7	48%
4	5		3	14%
5	4		3	14%
6	4	1	2	14%
8	6		1	5%
9	5		1	5%
Animal Pole = 4 Blastomeres		Total: 13		62%
Vegetal Pole = 4 Blastomeres		Total: 16		76%

C. 64-cell embryo

Number of Blastomeres at		Number of Embryos		Frequency (n = 14)
Animal Pole	Vegetal Pole	Recorded	Fixed	
4	4	2	n.a.	71%
n.a.	4	1	n.a.	
4	n.a.[a]		7	
5	n.a.[a]		3	21%
6	n.a.[a]		1	7%
Animal Pole = 4 Blastomeres		Total: 9		64%
Vegetal Pole = 4 Blastomeres		Total: 3[a]		21% (fixed n.a.)[a]

[a] In fixed embryos, the lack of a landmark does not allow the unambiguous identification of the vegetal pole

3.3. Cleavage process in *P. vancouverensis*

3.3.1. Basic characteristics and timing of cleavage

Zygotes of *P. vancouverensis* are spherical in shape, have a diameter of about 120 µm, and are surrounded by a delicate fertilization membrane (Fig. 25A). Hence, they are considerably larger, and also richer in yolk, than the zygotes of *P. pallida* and *P. muelleri*. The polar bodies are usually easily visible in the fixed material, and are found in numbers of two or three lying at the animal pole of the embryo (e.g., Fig. 25B,E). The cleavage process is holoblastic. From the third cell cycle onward, the divisions are somewhat unequal and generate smaller animal blastomeres (see below).

Data on the timing of the cleavage process are based on live observations under a stereomicroscope, but no 4D recordings, as in *P. pallida* and *P. muelleri* embryos, were performed. At about 13°C, the zygotes undergo the first cleavage division approximately six hours after they had been freed from the coelom; the subsequent divisions pass in intervals of about every two to three hours. The cleavage process appears to proceed largely synchronous: during one cleavage cycle, often all cells in one embryo are in the same state of mitosis (e.g., Fig. 25M-T), and only few embryos with intermediate blastomere numbers have been encountered.

3.3.2. First and second cleavage cycles and resulting embryos

The first and the second cleavage planes pass meridionally and perpendicularly to each other, through the animal-vegetal axis of the egg. They result in 2-cell and 4-cell embryos, respectively, and both cleavages are approximately equal (Fig. 25B,D). Only rarely, a transient 3-cell stage is found (Fig. 25C).

The process of compactation of the embryo – following each division cycle in *P. pallida* and *P. muelleri* cleavage – was not directly witnessed, since no live recordings of the cleavage process were available. However, compactation in *P. vancouverensis* cleavage is described in the literature (see Zimmer 1964; Freeman 1991). Based on these descriptions, putatively uncompacted and putatively compacted embryos in the fixed material at hand are differentiated by the latter's roundish overall shape, their smooth contour, and their generally

packed appearance (compare e.g., embryos in Fig. 25D and Fig. 25E-G; see also documentations of later cell stages); however, not in all cases this discrimination is unambiguous. Apparently, compactation is a very pronounced process in *P. vancouverensis* cleavage, resulting in tight blastomere packings and deformations of individual cell shapes (see also chapters 3.3.4., 3.3.5.).

While in the putatively uncompacted 4-cell embryos a small opening between the four cells is visible (Fig. 25D), in all of the putatively compacted embryos the blastomeres are in contact at the central animal-vegetal axis (Fig. 25E-L). Always, these cell contacts involve a polar furrow (Table 8). Some embryos display a polar furrow only at one pole: that is, either at the animal pole – there often it is covered by on top lying polar bodies (Fig. 25E-F) – or at the vegetal pole (Fig. 25L); at the respective counter-pole of such embryos the four blastomeres leave a central opening (Fig. 25G,K), which however, can be very small and difficult to discriminate against an X-furrow (see Fig. 25G). Other 4-cell embryos display polar furrows at both poles (Table 8). In these specimens, each polar furrow is formed between the cells of one – out of the two – pairs of oppositely situated non-sister cells in the embryo: thus, the embryo has two different polar furrows, which are aligned perpendicularly to each other (Fig. 25H-J). The cells that form the polar furrow at one pole usually are slightly protruded toward this pole, and hence appear larger in the respective pole views (see Fig. 25I-J). No specimen with one polar furrow visible from both poles, thus a cell contact along the entire animal-vegetal axis, as it was found in some *P. pallida* and *P. muelleri* 4-cell embryos, was observed.

3.3.3. Third cleavage cycle and 8-cell embryo

The analysis of embryos that were fixed during the third cleavage division cycle shows that in most cells, the mitotic spindles are roughly aligned along the animal-vegetal axis (Fig. 26A); in individual embryos, however, the spindle's inclinations – and even their orientations – can vary between the cells (Table 9A; Fig. 25M-T). While in nearly 70% of all analyzed cells the spindles are observed in an inclination between –10° and +10°, in the remaining 30% they are inclined in higher angles – either in one or the other direction (Fig. 26A). The third cleavage spindles usually are not located in the center of the blastomeres, but they lie somewhat closer to the animal pole (Fig. 25M-P). This seems to indicate some inequality of the upcoming division. Also, the spindles can be found somewhat tilted to the animal pole (see lateral cells in Fig. 25M; but left lateral cell in Fig. 25N).

The 8-cell embryo consists of an animal and a vegetal cell tier of four cells each – the vegetal blastomeres usually appear slightly larger than the animal ones – and has a first small blastocoel (Fig. 27A-D). The analyses of the blastomere arrangements in different 8-cell embryos show that the cells in most animal/vegetal sister cell pairs are positioned on top of each other, juxtaposingly along the animal-vegetal axis (Fig. 27E,G-I). However, in many embryos, single sister cell pairs are found that are aligned somewhat obliquely with respect to this main axis (Fig. 27F,J). Such arrangements seem to be consistent with the observation of somewhat variable spindle inclinations during the third cleavage divisions (Fig. 26A). Only one embryo was encountered that had the entire animal cell tier arranged shifted clockwise against the vegetal cell tier; the blastomere shapes indicate that this embryo is in an uncompacted state (Fig. 27K-L).

In putatively uncompacted 8-cell embryos, small openings between the four blastomeres at both poles are visible (Fig. 27M-O). In contrast, in all 8-cell embryos in a putatively compacted state, polar furrows are observed (Table 8). In the majority of these specimens, a polar furrow is located only at the embryo's vegetal pole; in other cases it is located only at the animal pole (Table 8). At the respective counter-pole of such embryos, the cells leave a small central opening (Fig. 27A-D) or they all touch centrally, forming an X-furrow (Fig. 27P-Q). In a quarter of the studied 8-cell embryos, polar furrows are found at both poles (Fig. 27R-T). In different specimens, these two polar furrows are yet oriented differently – either perpendicularly or parallel to each other (Table 8).

3.3.4. Fourth cleavage cycle and 16-cell embryo

The analysis of embryos fixed during the fourth cleavage cycle reveals a high variation with respect to the orientation of the mitotic spindles, both between different cells as well as between different embryos (Figs. 26B-B", 28A-J). Except in a range between –20° and +25° along the animal-vegetal axis, spindle inclinations in nearly all possible angles – sinistrally as well as dextrally oriented – are found in the material (Fig. 26B). However, the different spindle inclinations are not equally distributed. Firstly, in many cells, the spindles are inclined in rather high angles, indicating a certain tendency toward meridional fourth cleavage divisions (Fig. 26B); and secondly, over all the analyzed cells, there is a majority of cases in which the spindles are inclined in negative angles, that is, in principle, with a sinistral orientation (Fig. 26B). Separated analyses for the animal and the vegetal cell tiers of the 8-cell

stage reveal that the observed range of spindle inclinations is similar, but the encountered distributions show differences between the two tiers (Fig. 26B'-B"). In the animal cell tier, more cells have spindles that are inclined in rather intermediate angles – that is, obliquely, though differently oriented sinistrally or dextrally (Fig. 26B'); whereas in the vegetal cell tier, more cells have spindles that are inclined in higher angles – that is, oriented rather meridionally (Fig. 26B"). Consistently in both cell tiers, there is a slight majority of cells, which have negatively inclined, and thus in principle sinistral, spindle orientations (Fig. 26B'-B").

This variation is reflected at the level of individual embryos: over all studied embryos, every combination of cleavage axes in individual cells was encountered uniquely (Table 9B). Except for one embryo that displayed sinistral spindle orientations in all its blastomeres (Table 9B), sinistral spindles are found in no more than five cells per embryo (Table 9B).

In putatively uncompacted 16-cell embryos, the blastomeres have a more or less roundish cell shape (Fig. 28K-O). Most 16-cell embryos in the material were in a putatively compacted state. Such compacted embryos appear tightly packed, the blastomeres are rather angular in shape, and the embryo as a whole has a smooth contour and a round, or slightly oval, overall form (Figs. 28P-T, 29). Generally, the blastomeres in the embryo's vegetal hemisphere are slightly larger than those in the animal hemisphere (Fig. 28M), and the blastocoel is small, measuring between 20% and 40% of the embryo's diameter.

Surprisingly, every 16-cell embryo in the material looked different (see Figs. 28M-T, 29). With the absence of 4D microscopy data, the cell arrangements were analyzed on the basis of the midbody residuals of the mitotic spindle apparatuses, which are located between pairs of sister cells in the embryo, and which are visible by their tubulin signal for some time after the cell divisions (see Fig. 28M-N). These midbodies indicate the sister cells alignments within the embryos, and thus allow for a comparative evaluation of the cell arrangements across the material. In the embryos given in Figs. 28M-T and 29A-T (as well as in the 32-cell embryos given in Fig. 30A-T; see chapter 3.3.5.), the sister cells are indicated by connecting lines. Note, however, that the spindle remnants are not visible in the given Imaris Blend mode images, but only when studying the embryos in Imaris MIP mode projections (Fig. 28M-N).

Generally, the 16-cell embryo is organized in four quadrants, each consisting of an animal and a vegetal sister cell pair (Figs. 28M,R, 29D-G). Especially in embryos in a compacted state, the boundaries between the individual quadrants are recognizable as continuous lines of cell

contacts, running from the animal pole to the vegetal pole on the embryo's surface (e.g., Figs. 28Q-T, 29B-G). These lines are well visible in compacted embryos, because the cell contacts between the compacted and angular shaped blastomeres are almost planar in appearance. A further line of cell contacts is recognizable at the equator of the embryo (Figs. 28R-S, 29D-G); it separates the animal and the vegetal blastomeres within each quadrant and hence, in the embryo as a whole, the animal and the vegetal hemisphere, each of which comprising of eight cells. Notably – and very different to the situation found in *P. pallida* and *P. muelleri* –, at least in compacted embryos, the blastomeres of neighboring quadrants are not intertwined at the quadrant boundaries, and neither are the cells at the equator, in *P. vancouverensis* (Figs. 28R,S, 29D-G). However, within each hemisphere and quadrant, the blastomeres can be arranged in various patterns:

In the animal hemisphere, of the two cells per quadrant often one is found to make contact with the animal pole, while the second one – the first one's sister cell – does not (Figs. 28P-Q, 29A-B,K-L,Q-R). Therefore, in the majority of 16-cell embryos, the animal pole is encircled by four blastomeres (Table 10A). In most of these cases, the pole cell extends from the animal pole toward the equator of the embryo; whereas the non-pole cell is restricted to a merely equatorial position (see animal cells in Fig. 29D,F-G). As a consequence, in some embryos, the blastomeres of the animal hemisphere make the first impression of being arranged in two shifted cell layers (e.g., Figs. 28P-Q, 29K-L). A closer look at such embryos, however, reveals that in different quadrants the non-pole cell differently is located either clockwise or counterclockwise of the pole cell (compare sister cell alignments in Fig. 28Q and Fig. 29L; compare alignment of animal cells in lateral views in Fig. 29D vs. Fig. 29F-G). These variable alignments appear to be in principle consistence with the observation of oblique – yet differently oriented – fourth cleavage spindles in the animal cell tier (Fig. 26B'). In other cases – although the quadrant includes an animal pole cell and a non-pole sister cell – the pole cell does not contact the equator, but the non-pole cell is aligned between the pole cell and the equator (see animal cells in Fig. 29E). Such an arrangement is less frequently observed than the former one, although in one embryo it was found in three of its quadrants (see upper right quadrant and lower two quadrants in Fig. 29H-I). Interestingly, such rather animal-vegetal alignments of sister cells do not seem to be in consistence with the data on the cleavage axes, as no spindles with an equatorial orientation were encountered during the fourth cleavage cycle (see Fig. 26B'). It seems possible that such alignments may be the result of secondary cells relocations, which may for example happen during the process of embryo compactation. Finally, in some cases, the quadrant does not consist of a pole and a non-pole cell, but both

animal cells are in contact with the animal pole as well as with the equator (see upper left quadrant in Fig. 29H-I,N-O). In embryos with such alignments, typically more than for blastomeres are surrounding the animal pole (Table 10A; Fig. 29I, O,T).
In the vegetal hemisphere, the cells generally appear somewhat extended in animal-vegetal direction, and always all eight vegetal blastomeres are contacting the equator (see vegetal cells in Fig. 29D-G). This appears to be consistent with the observation of highly inclined and rather meridionally oriented fourth cleavage spindles in the vegetal cell tier (Fig. 26B"). In many embryos, however, – as in the animal hemisphere – only four of these vegetal cells in addition are in contact with the vegetal pole (Table 10A); and in such cases, these four pole blastomeres always belong to the four different quadrants of the embryo (Figs. 28T, 29C,J,M). However, the alignment of pole cell and non-pole cells is different in these embryos. In most cases, the pole and the non-pole cells of neighboring quadrants are located next to each other, and thus, in a vegetal view, two pole cells and two non-pole cells alternate in order (Figs. 28T, 29J). One embryo was found, however, in which instead the pole cells were located next to the non-pole cells in the respective neighboring quadrants, and thus vegetal pole and the non-pole cells directly alternate in a vegetal view (Fig. 29M). In both these alignments, four blastomeres contact the vegetal pole; however, the differences leave the homology of these pole cells between the different embryos debatable. A transition between the two alignments seems comprehensible via an alignment as documented in Fig. 29C: herein, the cells in the two upper quadrants are aligned as in the embryo in Fig. 29J, whereas the cells alignments in the lower quadrants resemble more the situation in Fig. 29M. The irregularity in cell arrangements in the vegetal hemisphere can lead to more than four blastomeres having contact with the vegetal pole, but also make the identification of this pole not always unambiguously possible (Table 10A; Fig. 29P,S).

Similar as in the previous stage, putatively uncompacted 16-cell embryos display a small central opening between the cells at the animal pole and at the vegetal pole (Fig. 28K-L,O), whereas putatively compacted embryos often have closed cell contacts at either one or at both poles. In all compacted embryos with four blastomeres encircling a pole, a polar furrow like cell contact was observed (Table 8; Figs. 28P-Q,T, 29C,J-L) – more often at the vegetal pole –, with the counter-pole displaying either an additional polar furrow, an X-furrow, or a small pole opening (Table 8; Fig. 29A-B,M). Note, however, the already described differences in the alignment of pole cells and non-pole cells in different embryos as well as generally between the animal and the vegetal hemispheres (see above). These circumstances leave the

homologous identity of the polar furrow forming cells between the different embryos debatable. In cases when a pole is encircled by more than four blastomeres, usually a pole opening is present (Fig. 29H-I,N-O,T). In total, in the majority of embryos an animal pole opening and a closed vegetal pole was found (see embryo in Fig. 29A-C), but, also all other combinations of opened and closed animal and vegetal poles, respectively, were encountered (see embryos in Figs. 28P-T, 29K-M and 29N-P).

3.3.5. Fifth cleavage cycle and 32-cell embryo

The fifth cleavage cycle could not be analyzed at the level of spindle orientations, as no embryos fixed during the process of mitosis were available in the material. Some conclusions on the cleavage axes will be drawn on base of the sister cell alignments in the 32-cell embryos (see below).

The 32-cell stage was studied only on few embryos, all of which were in a putatively compacted state. Such putatively compacted embryos are roundish or slightly oval in overall form, have a smooth outside contour, and their cells appear tightly packed and are more or less angular in shape (Fig. 30A-H). Usually, some of the most animal blastomeres in the embryo appear slightly smaller than the other cells in the embryo (see below); the blastomeres in the vegetal hemisphere are all of about the same size. The blastocoel occupies about 30% to 45% of the embryo's diameter.

As the 16-cell stage, the 32-cell embryo is organized in four quadrants; by now each of them comprises four animal and four vegetal blastomeres (Fig. 30E-H). Again, the boundaries between the individual quadrants are recognizable as continuous lines of cell contacts between the angular shaped blastomeres in the compacted embryo, which are running from animal to vegetal on the embryos surface (e.g., Fig. 30B-H). An equator separates the animal and the vegetal blastomeres within each quadrant, and hence the animal and the vegetal hemisphere (e.g., Fig. 30C,E-H). The blastomeres are neither intertwined at the quadrant boundaries nor at the equator (Fig. 30C,K,O,S).

The individual blastomere arrangements are highly variable, and no two 32-cell embryos look identical (see Fig. 30A-T). The analysis of the sister cell alignments – recognizable by the remnants of the spindle apparatuses between sister cells (see above) – reveals that within the animal hemisphere, the sister cells in different quadrants are aligned either differently obliquely (e.g., Fig. 30B,J), or rather along (see e.g., left two quadrants in Fig. 30N), or

perpendicularly (see e.g., upper two quadrants in Fig. 30R) to the animal-vegetal axis. In the vegetal hemisphere, in contrast, the sister cells appear to be mostly aligned along the animal-vegetal axis (e.g. Fig. 30D). This suggests that in the animal hemisphere, the fifth cleavage divisions passed in highly various – and apparently irregular – directions, whereas in the vegetal hemisphere the divisions seem to have passed roughly in equatorial directions. However, an effect of the process of compactation on the cell alignments cannot be excluded (see chapter 3.3.4.).

The identification and homologization of the blastomere arrangements and discrete cell layers between different 32-cell embryos is difficult. Although the general appearance often suggests an arrangement in four blastomere layers along the animal-vegetal axis (e.g., Fig. 30D,O,S), these layers are usually not identifiable along the whole circumference of an embryo (see Fig. 30E-H,K). In addition, due to the variability in cell alignments, especially in the animal hemisphere, the homologous identity of the cells making up these layers in different embryos is debatable (compare e.g., sister cell alignments in Fig. 30O and Fig. 30S). The blastomeres in the vegetal hemisphere can be arranged in two tiers of eight cells each, yet also this arrangement is not universal. Using the poles as landmarks, the analysis shows that in different embryos differently four to six blastomeres encircle the animal or the vegetal pole, and various combinations of these numbers do occur (Table 10B; Fig. 30B-D,J,L,N,P,R,T). Using, on the other hand, the equator as landmark, for both hemispheres the number of blastomeres having contact with the equator differs between eight and ten in different embryos (see embryo in Fig. 30E-H: 10 animal cells and 8 vegetal cells contact the equator) (total data over all embryos: animal hemisphere: 8 cells in 17%, 9 cells in 50%, and 10 cells in 33% of 6 fixed embryos; vegetal hemisphere: 8 cells in 33%, 9 cells in 50%, and 10 cells in 17% of these embryos); likewise, various combinations of these numbers are found in different embryos. Additionally, in most embryos, single blastomeres do neither contact the equator nor a pole (see e.g., upper left animal cell in Fig. 30G and upper right animal cell in Fig. 30H). Also the circumstance of the appearance of some smaller cells among the most animal blastomeres in the embryo does not seem to be a useful landmark; the number of these slightly smaller varied between six and eight in different embryos.

In cases with four pole blastomeres, differently a polar furrow like cell contact (Fig. 30A-B,D,T), an X-furrow (Fig. 30L), or a small central cell opening (Fig. 30J) can be found at the pole (Table 8). Most of the available 32-cell embryos display a small opening between the cells at the animal pole, but a closed vegetal pole (Fig. 30I-J,L,M-N,P,Q-R,T); but in some

specimens, both poles are closed (Fig. 30A-B,D). This reflects the observation that in most embryos the vegetal pole is encircled by four cells, whereas this is less commonly the case for the animal pole (Table 10B).

Fig. 25. *P. vancouverensis* embryos from zygote to third cleavage cycle. Imaris volume projections (A-P: MIP mode; Q-T: Blend mode) of fixed embryos that were stained against α-tubulin (reddish) and for nucleic acids (bright cyan); blastomere shape signals result from autofluorescence of the cytoplasm (dark cyan). Polar bodies are indicated with asterisks; lateral views are oriented with the animal pole to the top (an: animal, vg: vegetal). Images connected with white bars (e.g., E to G) show the same embryo from different perspectives. Scale bars: 20 μm.
A. Spherical zygote with halo representing the fertilization membrane (open arrowhead). **B**. 2-cell embryo (animal view). **C**. 3-cell embryo (animal view) with upper large blastomere not yet divided. Between the two lower sister cells, the midbody residual of the mitotic spindle apparatus is visible (open arrowhead). **D**. 4-cell embryo in a putatively uncompacted state. The blastomeres are rather roundish in shape (compare to E); a small opening is present centrally between them (arrowhead). **E-G**. Animal (E-F) and vegetal (G) views of 4-cell embryo in a putatively compacted state; the blastomeres appear tightly packed (see text). Sister cells are indicated by lines (the midbody residuals indicating the sister cells in the embryo are marked with open arrowheads in G, but poorly visible in the projection). The polar bodies (asterisks in E) are removed in F, to show the small polar furrow at the animal pole (arrowhead in F); at the vegetal pole the four cells leave a very small central opening (arrowhead in G). **H-J**. Putatively compacted 4-cell embryo in which polar furrows are present at the animal pole (arrowhead in I; polar bodies (asterisks in H) were removed in I) as well as the vegetal pole (arrowhead in J). Sister cells are indicated by lines (midbody residuals marked with open arrowheads in I and J). The two polar furrows are established between two different non-sister cell pairs (compare dots in I and J marking the identical blastomeres), and hence are aligned perpendicularly to each other. The polar furrow forming blastomeres appear slightly larger in the respective pole views (see cells with dots in I and cells without dots in J). **K-P**. Animal (K; central polar bodies were removed), vegetal (L), and lateral views (M-P) of 8-cell embryo with cells in metaphase of third cleavage division. The animal pole displays a central opening (arrowhead in K), while a polar furrow is present at the vegetal pole (arrowhead in L). Lateral images show each a view on one of the four blastomeres in the embryo (shape of cell closest to the observer outlined by dotted lines). In three cells the spindles are aligned along the animal-vegetal axis (M-O), in one it is oriented markedly obliquely (P). The mitotic spindles are not positioned centrally in the cells, but somewhat closer to the animal pole (M-P; arrowheads mark metaphase plates at centers of the spindles); in some cells the spindles also are tilted to the animal pole (see lateral cells in M). **Q-T**. Lateral views of a 4-cell embryo with cells in telophase of mitosis and in cytokinesis of third cleavage division. Each images gives a virtual section through one of the four blastomeres in the embryo (cell shapes outlined by dotted lines), showing the differently oriented mitotic spindles and the different directions of cell elongations.

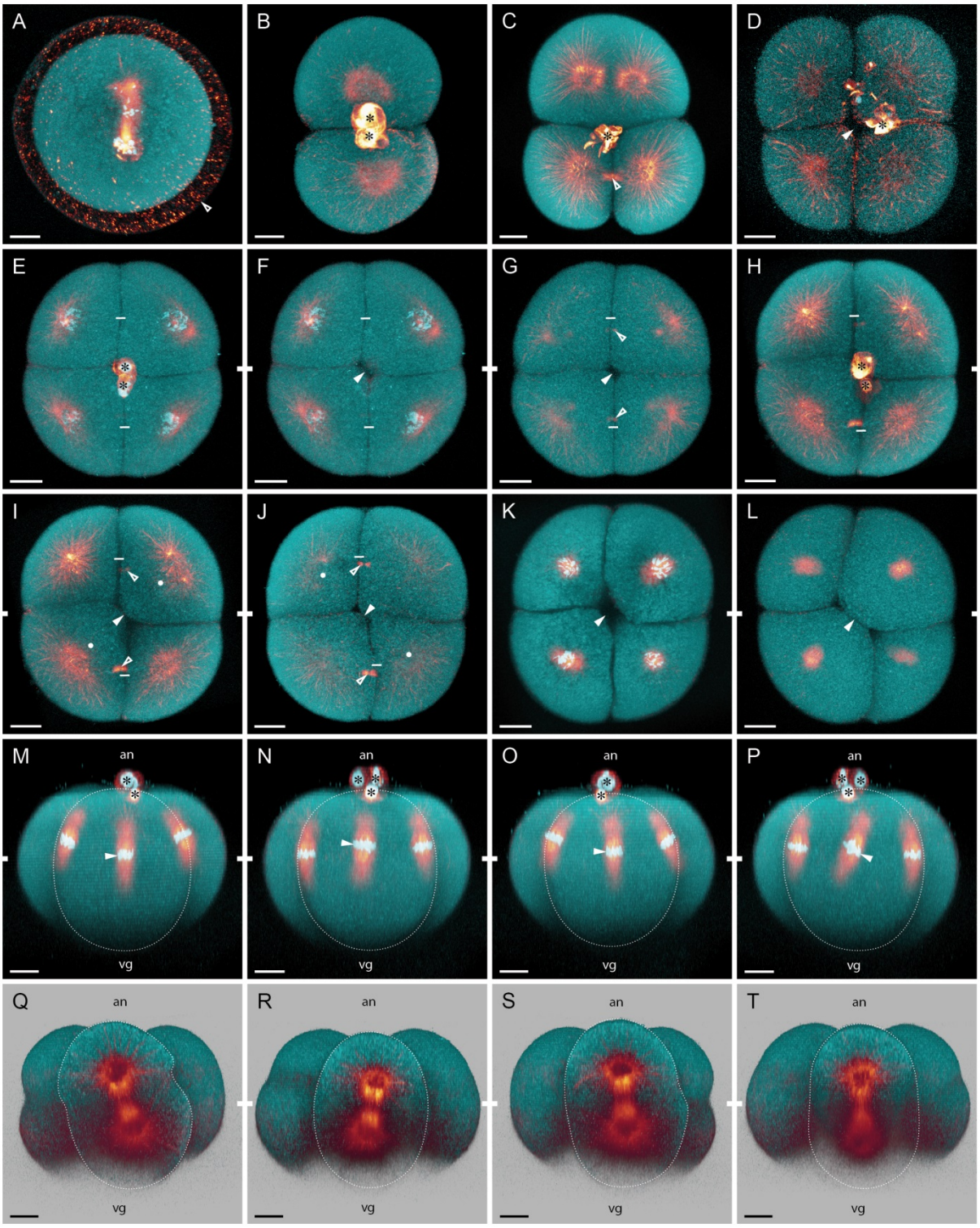

Fig. 25. ***P. vancouverensis*** **embryos from zygote to third cleavage cycle.**

Fig. 26. Inclinations of cleavage axes of third and fourth cleavages in *P. vancouverensis*. The charts give the results of quantitative analyses of the inclinations of the mitotic spindles relative to the animal-vegetal axis in cells during the third (A) and the fourth cleavage cycles (B); for the latter, separated analyses for cells of the animal cell tier (B') and the vegetal cell tier (B") of the 8-cell stage are provided. Only data from fixed embryos were available. Abscissas give the angles of inclinations (dex: dextral, eq: equatorial, mer: meridional, sin: sinistral). The heights of the bars give the relative frequencies in which the respective inclinations (grouped in 5°-steps) were observed over all analyzed cells ('n'); the numbers in the bars give the absolute numbers of cells in the respective groups. In the third cleavage cycle (A), the mitotic spindles are roughly aligned along the animal-vegetal axis, but the exact inclination varies between the analyzed cells. In the fourth cleavage cycle (B), spindle inclinations in various angles are encountered; in many cells the spindles are inclined along high angles. In the animal cells (B') markedly oblique spindle inclinations are frequent; in the vegetal cell tier (B") inclinations in high angles are more abundant. In the analyses of the fourth cleavage cycle, spindle inclinations along negative angles are slightly more abundant than inclination along positive angles (B,B',B").

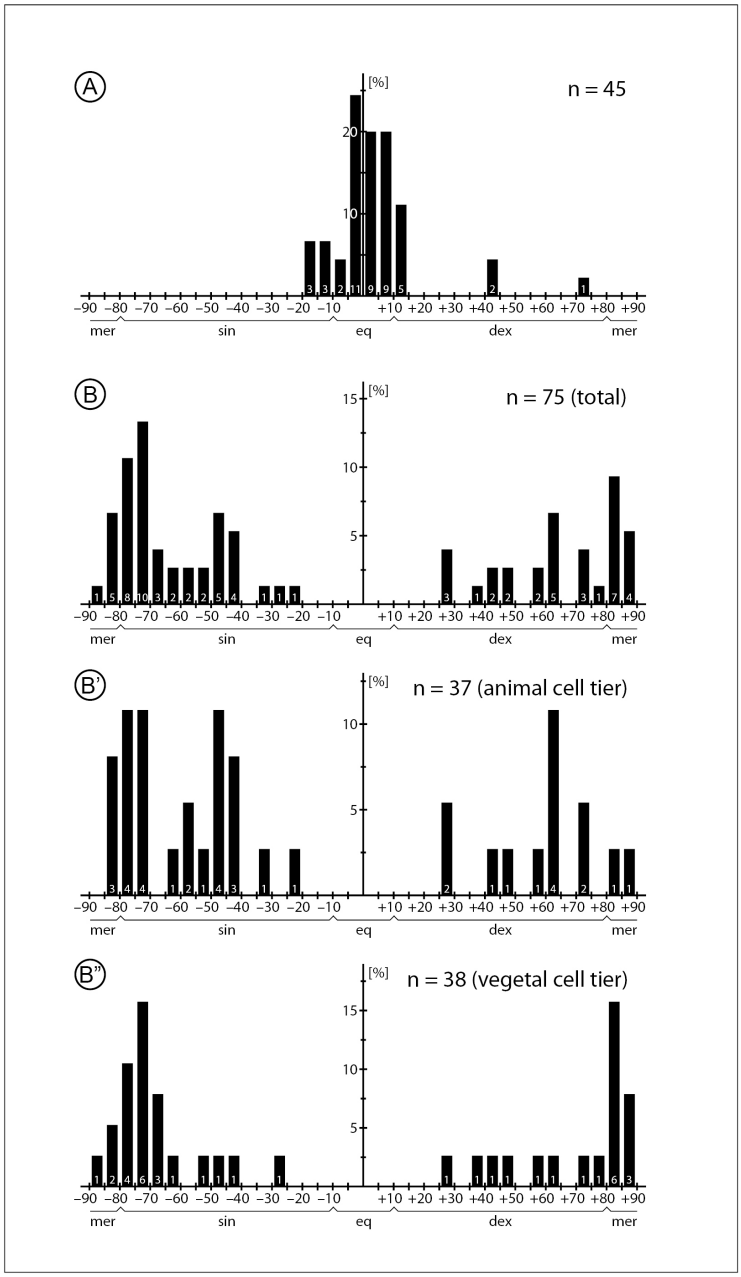

Fig. 26. Inclinations of cleavage axes of third and fourth cleavages in *P. vancouverensis*.

Fig. 27. *P. vancouverensis* embryos at the 8-cell stage. Imaris volume projections (A-D,M-T: MIP mode; E-L: Blend mode) of different 8-cell embryo that were stained against α-tubulin (reddish) and for nucleic acids (bright cyan); blastomere shape signals result from autofluorescence of the cytoplasm (dark cyan). Polar bodies are indicated with asterisks; lateral views are oriented with the animal pole to the top (an: animal, vg: vegetal). Scale bars: 20 µm.
A-D. Embryo in animal (A-B), lateral (C), and vegetal views (D). The 8-cell stage generally is composed of an animal and a vegetal tier of four cells each; the vegetal blastomeres are somewhat larger than the animal blastomeres (see C). In this embryo, a small opening is present at the animal pole (arrowhead in B; polar bodies (asterisks in A) were removed in B), and a polar furrow is found at the vegetal pole (arrowhead in D). The chromosomes are still condensed (indicated on two cells by arrowheads in C); the midbody residual of the mitotic spindle apparatus between sister cells is well visible (indicated for one sister cell pair by open arrowhead in C). **E-H**. Lateral images of an 8-cell embryo, each showing one of the four animal/vegetal sister cell pairs (indicated by lines) oriented toward the observer. The blastomeres are aligned along the animal-vegetal axis in three sister cell pairs (E,G-H), but obliquely and tilted dextrally to this axis in one cell pair (F). **I-J**. Lateral images of an 8-cell embryo showing the alignments in two of the animal/vegetal sister cell pairs: along the animal-vegetal axis (I) and obliquely tilted sinistrally to this axis (J). **K-L**. Animal (K) and lateral (L) views of an 8-cell embryo in which the entire animal cell tier is shifted clockwise against the vegetal cell tier (blastomeres of animal tier marked with dots). **M-O**. Putatively uncompacted 8-cell embryo with a small opening at the animal pole (arrowhead in N; the polar bodies (asterisks in M) were removed) and at the vegetal pole (arrowhead in O). **P-Q**. Animal (P; polar bodies were removed) and vegetal (Q) views of an 8-cell embryo in a putatively compacted state. A polar furrow is present at the animal pole (arrowhead in P) and an X-furrow is present at the vegetal pole (arrowhead in Q). **R-T**. Putatively compacted 8-cell embryo in which a polar furrow is located at the animal pole (arrowhead in S; the polar bodies (asterisks in R) were removed) as well as at the vegetal pole (arrowhead in T).

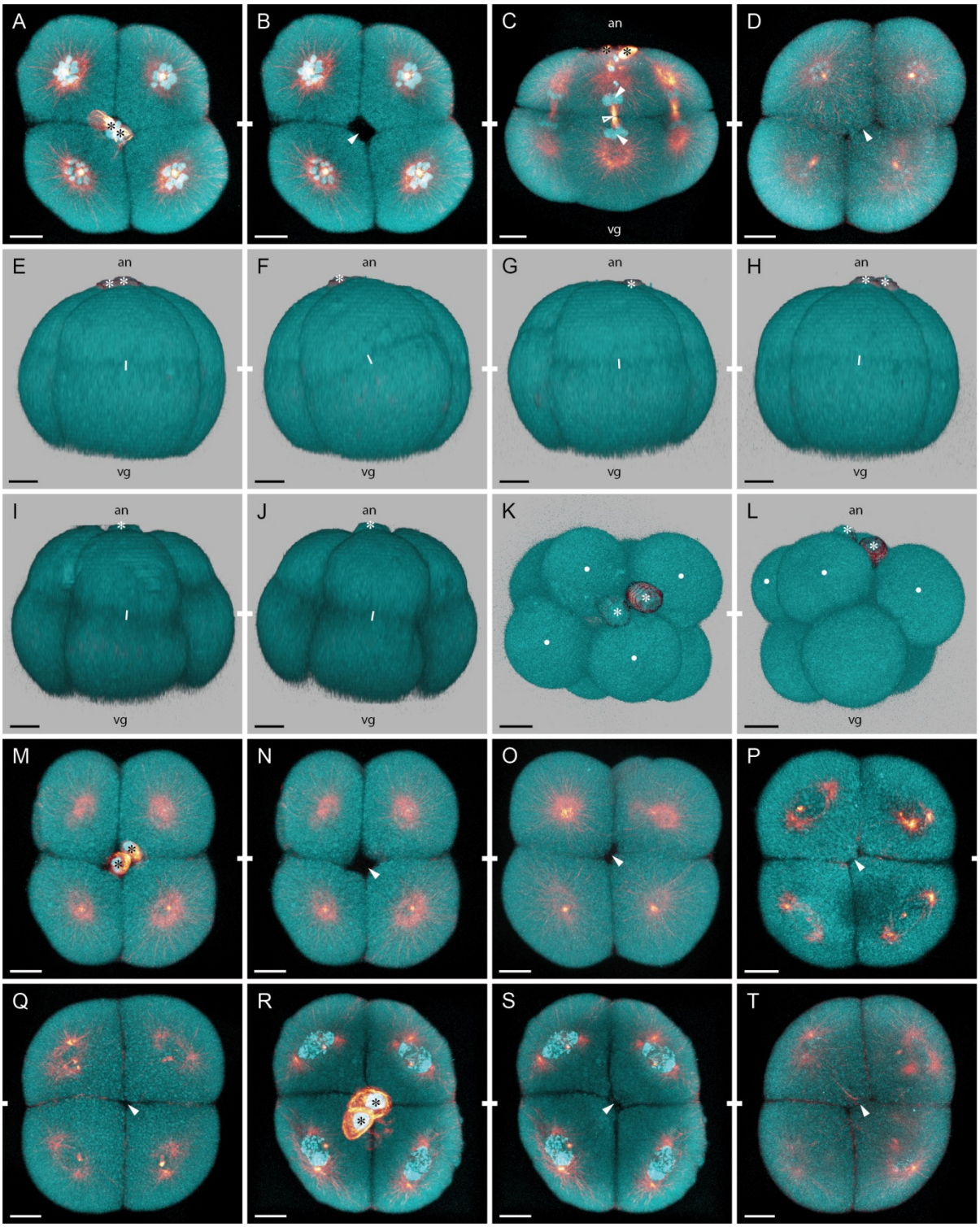

Fig. 27. *P. vancouverensis* embryos at the 8-cell stage.

Fig. 28. *P. vancouverensis* embryos from fourth cleavage cycle to 16-cell stage. Imaris volume projections (MIP mode: A,F,M-N; all others Blend mode) of embryos stained against α-tubulin (reddish) and for nucleic acids (bright cyan); blastomere shape signals result from autofluorescence of the cytoplasm (dark cyan). Polar bodies are indicated with asterisks; lateral views are oriented with the animal pole to the top (an: animal, vg: vegetal). Scale bars: 20 µm.
A-E. 8-cell embryo with cells in metaphase of fourth cleavage division: animal pole view in MIP projection (A), and virtual sections through the animal and vegetal blastomeres in each of the four embryonic quadrants in lateral views (B-E; Blend projections; cell shapes are outlined by dotted lines). The mitotic spindles are well visible. They are oriented obliquely in sinistral direction (e.g., animal blastomeres in B-D) or meridionally (e.g., blastomeres in E) in this embryo. **F-J**. Same representation as in A-E, but of an 8-cell embryo with the cells in late anaphase and telophase of the fourth cleavage. The spindles are oriented obliquely dextrally (e.g., blastomeres in H-I) or meridionally (e.g., vegetal blastomere in G) in this embryo. **K-O**. 16-cell embryo in a putatively uncompacted state; the cells are of more or less roundish shape. The embryo is given in animal view (K-L), two lateral perspectives (M-N; MIP projections), and in a vegetal view (O). The two lateral perspectives give a view on one embryonic quadrant (M) and the border between two neighboring quadrants (N) (quadrant boundaries are indicated by dashed lines, the equator is indicated with a dotted line). The sister cells within the embryo are indicated by lines; the sister cell relationships are deduced from the midbody residuals of the spindle apparatus, that are visible between the cells of sister cell pairs in the MIP projections (M-N; midbodies marked with open arrowheads in M). Four blastomeres that belong to the four different quadrants encircle the animal pole (marked with dots in L) and leave a small central opening (arrowhead in L; polar bodies (asterisks in K) were removed in L); an opening is also present at the vegetal pole (arrowhead in O). **P-T**. Same perspectives as the in K-O, but of a 16-cell embryo in a putatively compacted state (all images are given in Blend projections so show the cell contours): the cells appear tightly packed and are of angular shape; the whole embryo has a smooth overall surface (see also text). Sister cells are indicated by connecting lines (the midbody residuals are yet not visible in the given projections). The embryo is organized in four quadrants and two hemispheres (quadrant boundaries are indicated by dashed lines, the equator is indicated by dotted line). The blastomeres neither appear intertwined between neighboring quadrants, nor between the hemispheres. In this specimen, four cells belonging to the different quadrants are located at the animal pole and at the vegetal pole (marked with dots in Q and T), and both poles display a small polar furrow (arrowheads in Q and T; polar bodies (asterisks in P) were removed in Q).

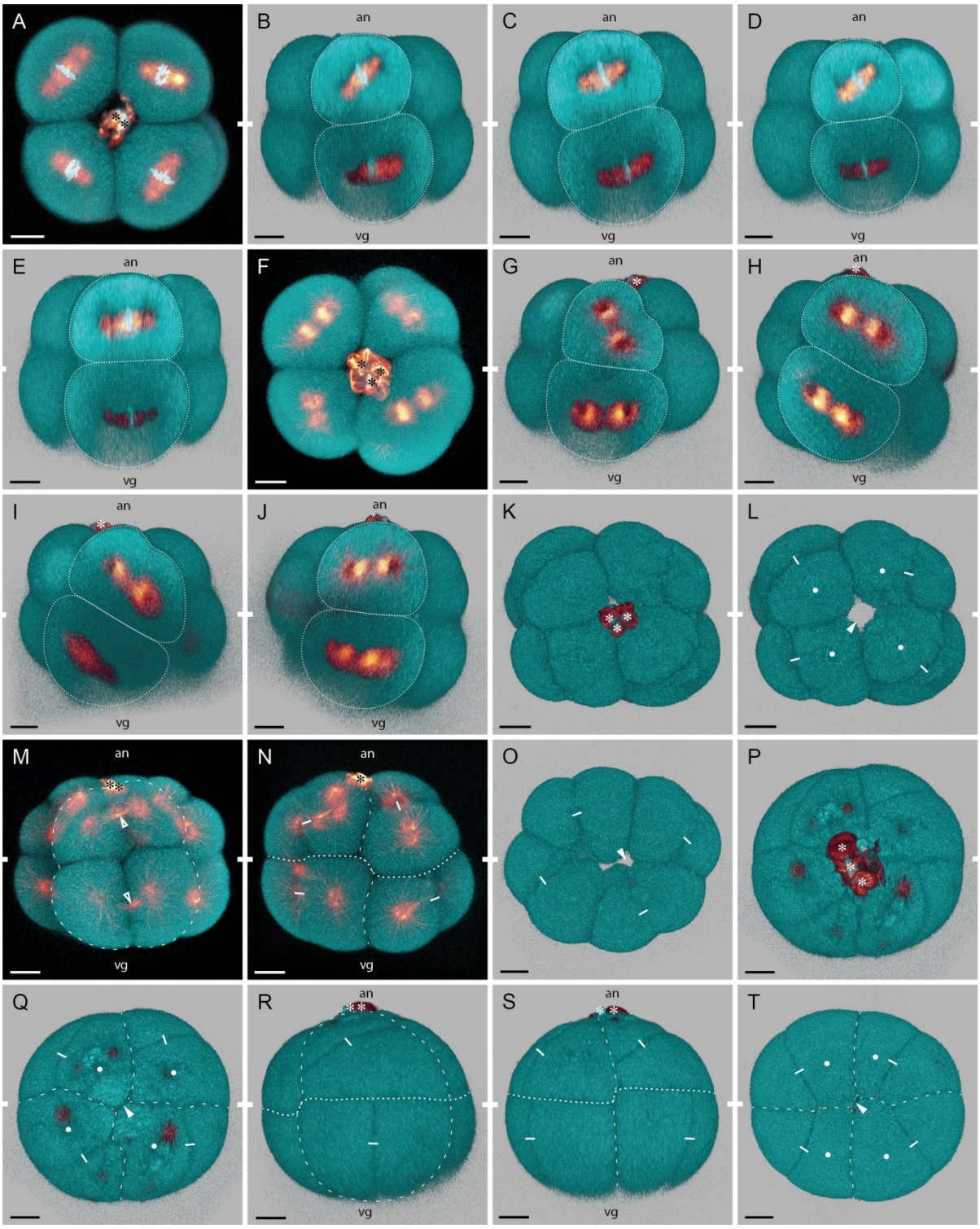

Fig. 28. *P. vancouverensis* embryos from fourth cleavage cycle to 16-cell stage.

Fig. 29. Different *P. vancouverensis* embryos at the 16-cell stage. Imaris volume projections (Blend mode) of six different 16-cell embryos (the images connected with white bars show the same specimen from different perspectives: A-G, H-J, K-M, N-P, Q-S, T) stained against α-tubulin (reddish) and for nucleic acids (bright cyan); blastomere shape signals result from autofluorescence of the cytoplasm (dark cyan). All embryos are in a putatively compacted state: the blastomeres are of more or less angular shape, and the embryos have a roundish or oval overall form and a smooth outside contour (see also text). Every embryo (except embryo T: animal view only) is documented in successive images showing two animal views – one with the polar bodies (indicated by asterisks) (e.g., A,H) and one with removed polar bodies (e.g., B,I) – as well as a vegetal view (e.g., C,J). For the first embryo, additional lateral images show each of the four embryonic quadrants oriented to the observer (D-G). Sister cells are indicated by connecting lines (the midbody residuals allowing for the identification of sister cells within the embryos are not visible in the presented Blend mode projections). Dashed lines running from animal to vegetal on the embryos' surface indicate the boundaries between the four embryonic quadrants (e.g., B-G,I-J); the equator of the embryo is indicated by a dotted line in the lateral views (D-G; the animal pole is oriented to the top; an: animal, vg: vegetal). Dots mark the blastomeres that are located encircling the pole in the respective pole views (animal pole: e.g., B,I; vegetal pole e.g., C,J); arrowheads indicate polar furrows (C,J,L), X-furrow (R), or pole openings (B,I,M,O,T). The blastomere arrangement and the sister cell alignments are different in every embryo. For detailed description see text. Scale bars: 20 µm.

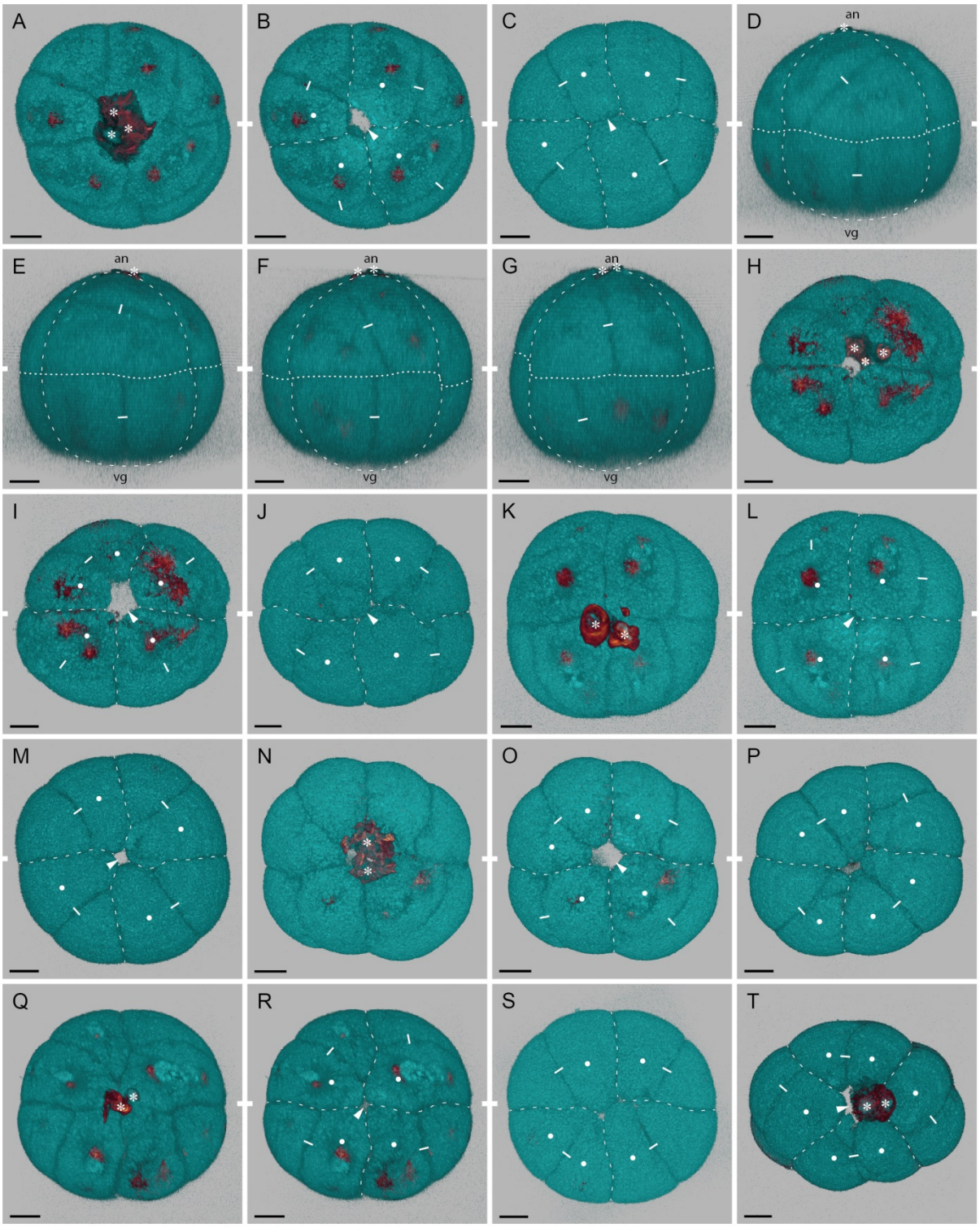

Fig. 29. Different *P. vancouverensis* embryos at the 16-cell stage.

Fig. 30. Different *P. vancouverensis* embryos at the 32-cell stage. Imaris volume projections (Blend mode) of four different 32-cell embryos (A-H, I-L, M-P, Q-T) stained against α-tubulin (reddish) and for nucleic acids (bright cyan); blastomere shape signals result from autofluorescence of the cytoplasm (dark cyan). All embryos display tightly packed and angular shaped blastomeres, and are in a putatively compacted state (see text). Every embryo is documented in successive images showing two animal views – one with the polar bodies (indicated by asterisks) (e.g., A,I) and one with removed polar bodies (e.g., B,J) –, a lateral view looking at the boundary between two embryonic quadrants (e.g., C,K; the animal pole is oriented to the top; an: animal, vg: vegetal), and a vegetal view (e.g., D,L). For the first embryo, additionally, lateral images looking directly at each of the four quadrants are given (E-H; an: animal pole, vg: vegetal pole). Sister cells are indicated by connecting lines (the midbody residuals allowing for the identification of sister cells within the embryos are not visible in the presented Blend mode projections). Dashed lines running from animal to vegetal on the embryos' surface mark the boundaries between the four embryonic quadrants (e.g., B-H,J-L); horizontal dotted lines indicate the equator of the embryo (e.g., C,E-H,K). Dots mark the blastomeres that are located encircling the pole in the respective pole views (animal pole: e.g., B,J; vegetal pole e.g., D,L); arrowheads indicate polar furrows (B,D,T), X-furrow (L), or pole openings (J,N,R). The blastomere arrangement and the sister cell alignments are different in every embryo. The cells of neighboring quadrant are not intertwined at the quadrant boundaries, nor are the blastomeres at the equator. For detailed description see text. Scale bars: 20 µm.

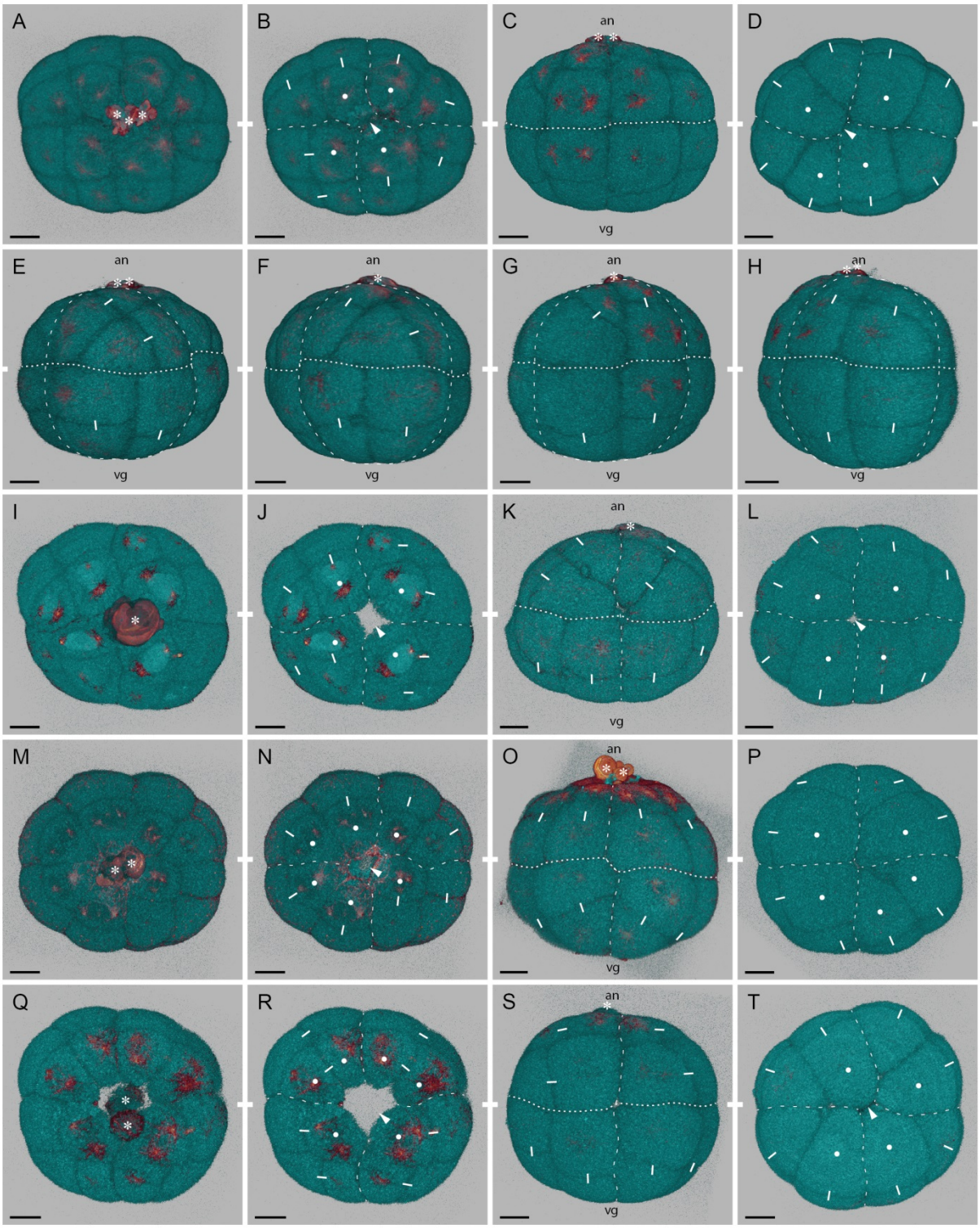

Fig. 30. Different *P. vancouverensis* embryos at the 32-cell stage.

Table 8. Pole blastomere contacts in *P. vancouverensis* embryos. The four blastomeres of the 4-cell embryo, and the four blastomeres that are located at the animal pole and/or the vegetal pole in some embryos of later cell stages, can show central cell contacts in the organization of a polar furrow or of an X-furrow (polar furrow: contact line between two oppositely situated cells; X-furrow: central contact between all four cells). The table gives the frequency of 4-cell stage to 32-cell stage embryos that have such a cell contact, at only the animal pole, or at only the vegetal pole, or at both poles, over all analyzed embryos ('n'; only embryos in a putatively compacted state, and with (one or both) pole(s) encircled by four blastomeres were included; see Table 10). All data are based on fixed material; all relative numbers are rounded to even. Note, that nearly all embryos show (a) polar furrow(s). If a polar furrow is present at only one pole, the opposite pole can display an X-furrow or a small opening between the four pole blastomeres; or the embryo can also have more than four cells located at the opposite pole (Table 10).

Stage	n	Polar furrow			X-furrow		
		Animal Pole	Vegetal Pole	Both Poles	Animal Pole	Vegetal Pole	Both Poles
4-cell	12	25%	33%	42%[a]	8%	15%	
8-cell	16	13%	63%	25%[b]	13%	13%	
16-cell	11	18%	64%	18%	9%		
32-cell	4		50%	25%		25%	

[a] The polar furrow at the animal pole is different from the polar furrow at the vegetal pole; the two furrows are oriented perpendicularly to each other

[b] The animal polar furrow and the vegetal polar furrow are oriented either perpendicularly or parallel to each other (each in two specimens (12.5%), respectively)

Table 9. Orientations of cleavage axes in *P. vancouverensis* embryos. For the third and the fourth cleavage cycles, all observed combinations of orientations of cleavage axes in the blastomeres of individual embryos are listed, and the numbers of embryos showing each combination are given (only data from fixed embryos were available). Each line gives a unique combination (the numbers preceding the different cleavage orientations give the number of cells that show such cleavage axes; if cells could not be resolved, as they were not in a proper mitotic state or otherwise not accessible, this is noted as not applicable (n.a.)). For the fourth cleavage cycle (B), separated evaluations are given for the animal and for the vegetal cell tier, and each combination was observed only once. For comparability, the combinations are given in a similar order as in *P. pallida* (Table 2) and in *P. muelleri* (Table 6) (but see text for differences in the cleavage pattern).

A. Third cleavage cycle

Cleavage Orientations	Number of Fixed Embryos
2 dextral, 2 sinistral	1
2 dextral, 2 n.a.	1
1 dextral, 3 equatorial	2
1 dextral, 1 equatorial, 2 n.a.	2
4 equatorial	3
3 equatorial, 1 sinistral	1
2 equatorial, 2 sinistral	1
2 equatorial, 1 sinistral, 1 n.a.	1
2 equatorial, 2 n.a.	2

B. Fourth cleavage cycle

Cleavage Orientations		Number of Fixed Embryos
Animal Tier	Vegetal Tier	
4 sinistral	4 sinistral	1
3 sinistral, 1 meridional	2 sinistral, 2 meridional	1
3 sinistral, 1 dextral	1 sinistral, 2 dextral, 1 n.a.	1
2 sinistral, 2 meridional	3 sinistral, 1 meridional	1
2 sinistral, 2 meridional	1 sinistral, 1 dextral, 2 meridional	1
2 sinistral, 1 dextral, 1 n.a.	2 sinistral, 1 dextral, 1 n.a.	1
1 sinistral, 3 dextral	2 dextral, 2 meridional	1
1 sinistral, 2 dextral, 1 n.a.	1 sinistral, 2 meridional, 1 n.a.	1
1 sinistral, 1 dextral, 2 n.a.	2 meridional, 2 n.a.	1
1 sinistral, 1 dextral, 2 n.a.	1 sinistral, 1 dextral, 2 n.a.	1
1 sinistral, 3 n.a.	2 sinistral, 2 n.a.	1
2 dextral, 2 n.a.	1 sinistral, 1 dextral, 1 meridional, 1 n.a.	1

Table 10. Number of pole blastomeres in *P. vancouverensis* embryos. For the 16-cell stage and the 32-cell stage, all encountered combinations in the numbers of blastomeres encircling the animal and the vegetal poles of individual embryos are listed. The numbers of embryos showing each combination are given, and the frequency of the respective pattern over all embryos ('n') is noted (all relative numbers are rounded to even). Only data from fixed embryos were available. If poles could not be resolved, this is noted as not applicable ('n.a.'). In each table, two bottom lines give the numbers of embryos that have four blastomeres located at either the animal pole or the vegetal pole, irrespective of the respective counter-pole (these include only confirmed cases, and for the 16-cell embryo might be underestimations), as well as the frequencies of these respective patterns.

A. 16-cell embryo

Number of Blastomeres at		Number of Fixed Embryos	Frequency (n = 21)
Animal Pole	Vegetal Pole		
4	4	5	24%
4	5	3	14%
4	6	1	5%
4	n.a.	3	14%
5	4	4	19%
5	5	1	5%
5	6	2	10%
5	n.a.	1	5%
6	6	1	5%
Animal Pole = 4 Blastomeres		Total: 12	57%
Vegetal Pole = 4 Blastomeres		Total: 9	43%

B. 32-cell embryo

Number of Blastomeres at		Number of Fixed Embryos	Frequency (n = 6)
Animal Pole	Vegetal Pole		
4	4	2	33%
5	6	1	17%
6	4	2	33%
6	5	1	17%
Animal Pole = 4 Blastomeres		Total: 2	33%
Vegetal Pole = 4 Blastomeres		Total: 4	67%

4. Discussion

4.1. Cleavage in phoronids

This first chapter of discussion is structured in three parts. In the first two sections, the results on the early cleavage in the three investigated phoronids are summarized and compared to respective literature data on these species: based on to the large correspondences between the cleavage processes in *P. pallida* and *P. muelleri*, these two species are discussed in one section (chapter 4.1.1.); *P. vancouverensis* is discussed in a subsequent section (chapter 4.1.2.). In a final chapter, the results are discussed with reference to the cleavage literature beyond the three species (for five other phoronids, descriptions are available), allowing for conclusion on the early cleavage in the taxon Phoronida in general (chapter 4.1.3.).

4.1.1. Cleavage in *P. pallida* and *P. muelleri*

4.1.1.1. Former characterizations

For *P. pallida*, only brief descriptions on the cleavage are available (Santagata 2001, 2004a, 2012)[*]. These are somewhat contradictory. In an early description, the *P. pallida* cleavage pattern was characterized as "clearly radial" (Santagata 2001: 12) – the author based this mainly on the observation of cell arrangements in 8-cell and 16-cell embryos, which he described as radial (see below) –, whereas in a recently published abstract, the same author reports that the cleavage "deviates from a typical radial pattern" and describes that the third to the fifth cleavage divisions "alternate between dexiotropic and levotropic spiral divisions" (Santagata 2012: 26.2).

For *P. muelleri*, the first cleavage observations were published by de Selys-Longchamps (1902, 1904); however, they do not go beyond the 8-cell stage. Brooks and Cowles (1905), on the other hand, published a more detailed cleavage description, which – according to them – was done on *P. architecta*; later, however, it was suspected to – in fact – have dealt with embryos of *P. muelleri* (Emig 1990). This study is therefore included in this comparison (but

[*] It should be noted, that all these studies dealt with *P. pallida* specimens from the Eastern Pacific, whereas *P. pallida* for the present study was sampled in the North Sea. There are differences in adult habitat and life history between different – distantly located – *P. pallida* populations, and cryptic speciation is possible (see Santagata 2004b).

see also chapter 4.1.3.). Interestingly, the authors described an oblique third cleavage division, but a meridional fourth cleavage cycle (Brooks and Cowles 1905) (see below). The most recent and most detailed descriptions of the *P. muelleri* cleavage, however, are provided by Herrmann (1981, 1986), who also published a video showing the embryonic development, including the cleavage process, of this species (Herrmann and Inst. Wiss. Film 1980). This author characterized the *P. muelleri* cleavage pattern as "derived radial" (Herrmann 1986: 447). This qualification as "derived" – yet not "properly" radial – seemingly attributes to the author's observation that the blastomeres in 8-cell and 16-cell embryos can be shifted against each other – and hence are not necessarily positioned in juxtaposing, radial, alignments (see below) – (Herrmann 1986), and the same author's previous finding that the third division spindles can be inclined "up to an angle of 45°" obliquely against the animal-vegetal axis (Herrmann 1981: 8), whereas the fourth cleavage is obliquely inclined into the opposite direction (Herrmann 1981). Unfortunately, the author did not specify these observations in reference to the embryo's animal pole, but only speaks of "left" and "right" shifts and inclinations, respectively (Herrmann 1981, 1986). Interestingly, several of the figures and videos provided by Herrmann show processes and cell arrangements that are very similar to what was observed during the present investigation (see below).

Despite these observations, Herrmann (1981, 1986) rejected any correspondences between the cleavage pattern in *P. muelleri* and previous descriptions of alternating oblique cleavage divisions in phoronids, as they had been published for *Ph. harmeri* (Rattenbury 1951, 1954). In contrast, he discussed his observations to represent variations of a radial cleavage pattern, or to be artifacts (Herrmann 1981, 1986). The author argued that the observed non-juxtaposing blastomere arrangements would result from secondary re-alignments of the cells, which would glide into the gaps between adjacent cells only after the cell divisions (Herrmann 1981); and that these divisions therefore had to be understood as passing in proper equatorial and meridional directions alone (Herrmann 1986). Before, a similar argument had been put forward by Zimmer (1964, 1973), yet, it is somewhat astonishing that this author suggested such re-alignments to be the result of a too tight egg membrane (see also chapter 4.1.2.1.), whereas Herrmann (1981) suspected the loose egg membrane of the *P. muelleri* embryo to offer enough space for the cells to glide into such a secondary arrangement. Herrmann (1986) further suggested that the putative artifacts would be statistically detectable, but did not perform the necessary analyses to go after this.

4.1.1.2. Present findings

The present investigation tried to deal with these objections by the application of two different and independent techniques (4D microscopy; study of fixation series), and by comparative analyses of quantitative data on (i) the orientation of the cleavage axes in embryos during the actual cell division process (in particular, data on the inclination of the mitotic spindles and the cell divisions relative to the animal-vegetal axis), as well as on (ii) features of embryos that were in the state in between two successive cleavage cycles (in particular, general blastomere arrangements, data on the number of blastomeres encircling the embryo's poles, and data on the occurrence of polar furrows).
On the one hand, the two techniques – 4D and fixation series – serve as mutual controls: the data gained by one technique can be evaluated against the data gained by the other technique. One the other hand, the two datasets – (i) and (ii) – can be understood as independent of each other, and hence, can be evaluated for consistencies and inconsistencies with respect to the reconstruction of the cleavage pattern. The dataset independence is evident for material from fixation series: different specimens were fixed during a cleavage cycle, and in between cleavage cycles. But also in the 4D recordings, which clearly show the same specimen during as well as in between cleavage cycles, the comparison of the data taken at the different consecutive time points – (i) and (ii), respectively – gives insights in consistencies and inconsistencies, which, for example, allow to evaluate the effect of the compactation process on cell arrangements (see below).

4.1.1.2.1. Cleavage axes

For *P. pallida* as well as *P. muelleri*, the data on the cleavage axes reveal that oblique cleavage orientations do neither represent variational nor artificial abnormalities. On the contrary, the inclination of the mitotic spindles in fixed embryos as well as of the cell divisions in the 4D-recorded embryos consistently show that, beginning with the third cleavage cycle, the cleavage axes are inclined obliquely with respect to the animal-vegetal axis, and, what is more, in both species, these axes are oriented alternately in dextral and sinistral directions, in the subsequent cleavage cycles. Such consistency between the two techniques and over many different embryos one would not expect, if the observed inclinations were the result of mere random variation along equatorial and/or meridional cleavage axes, or if they were artifacts. Although the detailed data reveal that the exact axis of

inclination shows some variation between different cells and different embryos, the pattern of alternating oblique cleavage axes is clearly identifiable across the material. Only in the data on *P. pallida*, the encountered variation is higher in the data obtained from the fixed material, than in the data from the 4D recordings. The reason of this discrepancy is possibly related to differences between the two techniques (see chapter 4.1.1.2.4.).

In both species, in was found that the dextral inclination of the third cleavage axes is not very pronounced, whereas the sinistral inclination of the fourth cleavage axes is more distinct. A third cleavage spindle inclined up to 45 degree, as it was mentioned by Herrmann (1981) for *P. muelleri*, was almost never observed. In the following fifth and the sixth cleavage cycles, dextral and sinistral cleavage axes, respectively, were found mostly in the animal and the vegetal cell tiers of the embryo, whereas the two equatorial cell tiers – which were only analyzed through the fifth cleavage – display more variability in the cleavage orientations. In total, the data indicate that the pattern of alternating oblique divisions becomes more irregular with progressing cleavage cycles. Generally, it is more consistently found in the vegetal blastomeres, but appears to be more variable in the animal cells. The encountered variability in the cleavage divisions is an important characteristic of the cleavage process in *P. pallida* and *P. muelleri*, which clearly has consequences for the cell arrangements in the embryo (see below). This variability might explain why the pattern of alternating oblique divisions was not recognized and identified by previous investigators.

That the cleavage divisions truly pass in oblique orientations is also evident by a conspicuous process of cell elongations, which the blastomeres undergo shortly prior to the actual divisions. Thereby, the cells expand obliquely to the animal-vegetal axis – and alternately into dextral and sinistral directions –, and hence precede the axes of the upcoming division. This process is most conspicuous in the third cleavage cycle, when it also involves the formation of twisted expansions of the cells animal and vegetal apices, pointing into the direction of the division and indicating the positions of the forming daughter cells. Brooks and Cowles (1905) probably described the very same process when they reported that during the third cleavage “the blastomeres become drawn out into a more or less ovoid shape and, as divisions take place, the upper four blastomeres become rotated in the direction of the hands of a watch” (Brooks and Cowles 1905: 78). Interestingly, this process is also documented, but not discussed, by Herrmann (1981, 1986; see also Herrmann and Inst. Wiss. Film 1980). Surprisingly, the author’s earlier contribution shows the blastomeres expanding into a

clockwise direction (Herrmann 1981: Fig. 1e), while the later publication apparently uses the very same picture in a mirrored display, so that the expansions point counterclockwise (Herrmann 1986: Fig. 4b).

4.1.1.2.2. Blastomere arrangements

The findings on the blastomere arrangements in embryos in between two successive cleavage cycles are largely consistent with the data on the cleavage axes. In both species, several 8-cell embryos show a cell arrangement, in which the four animal blastomeres are positioned shifted against their four vegetal sister blastomeres, and thus, the whole animal cell tier is aligned clockwise of the vegetal cell tier, when the embryo is seen from the animal pole. Importantly, this blastomere shift is never very pronounced, and this is consistent with the data, which showed dextrally oriented – yet not very pronouncedly oblique – third cleavage axes. On the other hand, the encountered 8-cell arrangements are variable, insofar as, in both species, also many embryos were found in which individual animal/vegetal sister cell pairs were positioned in a juxtaposing, rather than a shifted, alignment; and in some embryos, even all four animal cells were located on top of the vegetal cells. Consistently, the data on the cleavage axes showed variation between individual cells and embryos.
Herrmann, surprisingly, documented an 8-cell embryo with two shifted cells tiers for *P. muelleri*: while, however, the upper cell tier is aligned clockwise of the lower cell tier in Herrmann (1981: Fig. 1f), it is shifted counterclockwise in Herrmann (1986: Fig. 4c). Importantly – and in contrast to Herrmann's (1981) interpretations of such shifted cell arrangements – the present study found no indication that the blastomeres glide into the shifted alignment only after equatorial cleavage divisions. Quite on the contrary, however, the performed 4D recordings of the *P. pallida* cleavage process show that animal blastomere, which are clearly shifted clockwise of their vegetal sister cells directly after the third dextral cleavage division, can glide into an alignment more juxtaposing the vegetal blastomeres, during the compactation of the 8-cell embryo. Interestingly, for the *P. muelleri* cleavage a similar process is recognizable in a video published by Herrmann and Inst. Wiss. Film (1980). This observation suggests that the process of compactation has the potential to obscure de facto oblique cleavage divisions, and clearly advises caution when evaluating the cleavage pattern merely on the base of blastomere arrangements; in particular, when one works only on fixed material.

Also the cell arrangement of the 16-cell stage is in general consistence with the cleavage axes data. When in an 8-cell embryo the fourth cleavage divisions pass obliquely sinistral – as it is indicated by these data –, this results in a 16-cell stage with four shifted cells tiers along the animal-vegetal axis. In *P. pallida* as well as *P. muelleri*, this is in fact the most common appearance of the 16-cell stage. It is composed of four tiers of four blastomeres each, and these tiers are shifted against each other, so that the blastomere of each tier are aligned in the gaps between the blastomeres of the neighboring tier(s) in the animal-vegetal axis. In such embryos, four blastomeres are encircling the animal pole as well as the vegetal pole. The shifted arrangement of the cell tiers is more evident than at the 8-cell stage, consistent with the finding of a more pronounced oblique nature of the fourth cleavage axes, compared to the third cleavage.

The findings stand in contrast to the previous description of the 16-cell stage, which always include the presence of cell octets. Although, differently, for *P. pallida* the 16-cell stage was described to consist of two rings of eight blastomeres each stacked upon one another (Santagata 2001, 2004a), and for *P. muelleri* it was described to consist of three cell tiers: one vegetal tier comprising eight cells, and one animal and one middle tier of four cells each (Herrmann 1981, 1986). Such arrangements were never observed during the present investigation. On the other hand, a section through the equator of the 16-cell stage shows a blastocoel surrounded by eight cells – these are intertwined animal-equatorial and vegetal-equatorial cell tiers (see Fig. 11H) –, which is similar to a figure given by Santagata (2001: Fig. 1g, 2004a: Fig. 1A). And Herrmann gives a figure of the 16-cell stage, which could also be interpreted to show three shifted cell tiers, which each consist of only four cells (Herrmann 1981: Fig. 2a), similar to the situation found herein.

On the other hand, it is important to note that not all 16-cell embryos display the above-described arrangement. In *P. pallida* and *P. muelleri*, embryos were found, in which more than four cells were encircling the animal – and, in rare cases, the vegetal – pole, and hence, the organization in four four-celled blastomere tiers was obscured. In *P. pallida*, such embryos could have up to seven animal cells, and in *P. muelleri* two exceptional embryos showed even eight pole blastomeres. Importantly, however, among all the specimens, which had more than four pole cells, the numbers and combinations of the pole blastomeres – at the animal and vegetal pole, respectively –varied; and furthermore, the higher the deviation from four pole cells was, the less frequent such embryos were found in the material. The 4D recordings show that deviating numbers of pole blastomeres can result from somewhat irregular divisions of individual blastomeres in the embryo. During the fourth cleavage cycle,

it was observed that such divisions can pass with a high inclination, and thus almost meridionally. The data on the pole blastomere numbers allow identifying such divisions and embryos as variational, as they indicate that such highly inclined divisions occur only rarely and without a consistent pattern between different embryos.

Embryos beyond the 16-cell stage are difficult to analyze. Besides the small polar bodies (which can be internalized into the blastocoel), and the circumstance that the vegetal cells are slightly larger than the animal cells (variably, by the 32-cell stage or only by the 64-cell stage), they lack recognizable landmarks. In addition, in both species, with the fifth cleavage cycle, the (irregular) asynchronies between the cleavage divisions as well as the variability with respect to the cleavage axes increase (see above). Previous authors did not describe these stages, and only Herrmann (1986) mentioned the slight cell size differences in later embryos. Also in the present study, no distinct blastomere arrangements could be identified for the 32-cell and the 64-cell stages. These embryos have the general appearance of a small blastula, and consist of blastomeres, which appear irregularly intertwined against each other. They could only be analyzed for the number of blastomeres that were located at the animal and at the vegetal pole.

Importantly, these evaluations show – for both species – that four blastomeres encircle both poles in many embryos. This frequent observation of cell tiers consisting of four blastomeres at the poles of the 32-cell and 64-cell stages is in consistence with the data on the cleavage axes, which – for the pole tiers – showed a predominant pattern of oblique, and alternately dextral and sinistral, fifth and sixth cleavage cycles, respectively. For a characteristic radial cleavage pattern, in contrast, one would expect to observe a ring of eight blastomeres located at the poles of, at least, the 32-cell stage. Across the material, however, eight cells were only found in one exceptional case, at the animal pole of a 32-cell *P. muelleri* embryo; a further irregular case had even nine animal cells. In contrast, the relative majority of 32-cell embryos have a tier of four blastomeres located at the animal as well as the vegetal pole. In both species, the pattern of four pole blastomeres is more consistently found at the vegetal pole – this is true for the 32-cell as well as the 64-cell embryos; whereas with respect to the animal pole a higher percentage of embryos show a higher blastomere number and also the degree of deviation from four pole cells is higher. Similar to the 16-cell stage, the data show that the cases of deviations from the pattern of four animal and four vegetal pole cells at the 32-cell and 64-cell stages display variable combinations of the pole cell numbers, and occur less frequently in the material the higher the deviation is. Hence, such cases are interpreted as

variational, although it is generally concluded that the blastomere alignment in cell tiers and cell quadrants in embryos beyond the 16-cell stage becomes more irregular and obscured. In general, the data on the pole blastomeres are consistent with the observed increasing variability and irregularity of the cleavage axes with advancing cleavage cycles, but they are also supportive of the observation that the pattern of alternating oblique cleavage divisions is more consistently present in the vegetal blastomeres.

4.1.1.2.3. Polar furrows

In the present study, detailed analyses on the occurrence of polar furrows were performed. Herein, a polar furrow generally is defined as a line of cell contact present between two oppositely situated cells – of the four cells at the 4-cell stage, or of the four cells that constitute a pole cell tier in later cell stages (chapter 2.2.). This focus was set, since Herrmann (1986) emphasized the absence of polar furrows at the 4-cell stage of *P. muelleri* and interpreted this as evidence against a spiral nature of the cleavage (surprisingly, a film published by the same author shows polar furrows in some specimens; see Herrmann and Inst. Wiss. Film 1980). In fact, many spiralian embryos display two perpendicularly oriented polar furrows – one at each pole, respectively (so-called “cross furrows”) – during the early cleavage process (see chapter 4.3.1.). In conflict to Herrmann, Brooks and Cowles (1905) had mentioned a polar furrow at their 4-cell stages, and observed that it was formed as the cells narrow toward each other after the divisions; yet, they did not trace this through later cleavage cycles.

The performed 4D recordings show that polar furrows, in fact, are sometimes established during the compactation of the embryo, between two successive cleavage cycles. In this process, the blastomeres flatten against one another and all cells draw closer to the central animal-vegetal axis, and, in some *P. pallida* and *P. muelleri* 4-cell embryos, this can lead to the formation of a central polar furrow. In all these cases, the polar furrow reached from the animal pole to the vegetal pole along the entire animal-vegetal axis of the embryo; no 4-cell stage with two perpendicularly running polar furrows, one situated at each pole, was encountered. In the majority of 4-cell embryos, however, a small opening persisted centrally between the four blastomeres, even through compactation. Polar furrows also can be found through the next cleavage stages; however, in general, they are usually short in length, and they occur only occasionally, and variably at only one pole or at both poles of different

embryos. Moreover, in case of later embryos, in which a polar furrow was observed at the animal as well as the vegetal pole, these two furrows differently were found to be oriented either perpendicularly or rather parallel to each other. The findings generally contradict previous descriptions (Brooks and Cowles 1905; Herrmann 1986), and reveal that polar furrows do occur, but are no obligatory features of the cleavage process.

For *P. pallida*, the high number of 4D recordings allows an even more detailed picture. This data indicate that with advancing cell stages, polar furrows occur in an increasing frequency. Moreover, from the 16-cell stage on, in some embryos the four pole blastomeres do contact in the organization of an X-furrow – that is, all four blastomeres meet at the central axis (not to confuse with a "cross furrow") – rather than of a polar furrow (however, as polar furrows are often short, it is sometimes difficult to discriminate between a polar furrow and an X-furrow). Importantly, the later the cell stage, the higher the percentage of embryos that display cell contacts – either in the organization of a polar furrow or of an X-furrow – between the pole blastomeres, and this, in particular, is the case for the vegetal pole. It appears as if the smaller the cells are in the embryo – and hence, with advancing cleavage cycles and cell stages –, the more likely the compactation of the embryo will establish a cell contact between the pole blastomeres, and as if the organization of the cell contact (polar furrow or X-furrow) does not further matter. Also, this contact is probably easier established between the cells at the vegetal pole, where no polar bodies are located. At the animal pole, the polar bodies often are intercalated between the pole blastomeres, and thus hinder their central contact. In fact, most *P. pallida* 32- and 64-cell embryos have a closed vegetal pole, and a small opening into the blastocoel centrally between the four blastomeres at the animal pole.

In those embryos, in which more than four blastomeres are located at one (or both) pole(s) (see above), always an opening was observed between these cells. In the rare cases, with a very high number of pole blastomeres (six and more cells), this opening can become rather large and conspicuous. Probably, the same condition was described by Brooks and Cowles, who mentioned a "blastocoel pore" as a feature they had occasionally observed in later embryos; this "pore" however "does not seem to be of constant occurrence nor definite in position" (Brooks and Cowles 1905: 78). As illustration the authors give a figure of what seems to be a 64-cell stage with an opening into the blastocoel surrounded by eight cells (Brooks and Cowles 1905: Fig. 12).

4.1.1.2.4. Methodical remarks

As mentioned earlier, for *P. pallida* the data on the third and the fourth cleavage cycles gained from fixed material exhibit a higher variation in the axes inclinations – and even divergently oriented cleavage axes – than the data from the 4D-recorded embryos. Most plausible the cause for this circumstance has to be sought in differences between the two techniques. In fact, the two datasets represent two different aspects of the cleavage divisions. In the recorded embryos, the cleavage axes were inferred from the positions of the centers of two sister cells immediately after they had divided (see chapter 2.2.); hence, this data represent the orientations and inclinations of actual cell divisions. In the fixed embryos, in contrast, the cleavage axes were taken from cells during mitosis – and, depending on the applied stainings, either directly on the mitotic spindles or inferred from the positions of the chromosomes – or, in some cases, from cells during cytokinesis (see chapter 2.6.); hence, this data represent snapshots of cells some time prior to the actual cell division.

To explain the differences observed between the two datasets it is possible to hypothesize that the orientations of the spindles in the fixed embryos do not always exactly correspond to the axis of the later cell division. For example, this would be the case, if spindles changed their inclination during the process of mitosis. Interestingly, this phenomenon was described for the cleavage in *Ph. harmeri* (Rattenbury 1951, 1954): there, the spindles appear in various directions and, only shortly before the cell divisions, they align along the long axis of the cells, which also in *Ph. harmeri* corresponds to the future division axis. For the studied species herein, the performed recordings and live observations do neither allow to confirm nor to reject such spindle movements, as the spindles during mitosis are not visible through the light-dense yolk of the cells. On the other hand, Rattenbury's description seems to indicate that the cell elongations preceding the divisions are a more reliable indicator for the actual axis of cell divisions, than are the mitotic spindles. Embryos in the state of displaying these cell elongations are hard to find in the fixed material, but in the 4D recordings these cell elongations are well observable (see above).
Secondly, it is also possible that fixation process itself is the cause for the irregularity of the data obtained on the fixed material. The fixing agent takes some time to penetrate and preserve the cells; while additionally, it had probably a somewhat different tonicity than the cytoplasm and hence led to some osmotic pressure on the cells. Hence, it is possible that during the time fixation takes, cells could get distorted and this leads to a distortion or even

displacement of the mitotic spindles. Although, when fixation was done, notable cell distortions were not observed, the possibility that undetected deformations, maybe only within the cytoplasm but nonetheless affected the mitotic spindles, cannot be excluded.
Finally, it is possible that the spindles in fixed embryos correctly indicate the axes of the later cell divisions. This was in fact the approach of the present analyses, when the cleavage axes were measured on and compared between data from fixed embryos and 4D-recorded embryos. If one accepts this, the cells in the fixed material would apparently divide more variably. Although this sounds implausible at first glance, it actually could represent a methodical artifact. This is simply, because embryos, which have been fixed, cannot be studied during the later course of their development. Notably, however, the sometimes highly irregular cleavage divisions that the fixed cells undergo – according to their spindle inclinations – either could have no dramatic effect on the later development, or, on the contrary, could have such an effect, which possibly would have resulted in a misdevelopment or even a termination of development, if the embryos had been allowed to develop further. As the embryos were although fixed, none of these possibilities can be rejected. The fact, however, that such highly irregular divisions were not encountered in the data from the recorded embryos might suggest that such divisions in fact would have had negative consequences. Of all recorded embryos, only those were analyzed that had developed into normally appearing early larvae. Thus, those embryos that had died already during the cleavage process or had obviously misdeveloped later on do not show up in the dataset from the 4D recordings.

It is concluded that 4D recordings and analyses are in general the more reliable method for evaluating the cleavage process, than fixed material is. To the standards applied in the present study (chapter 2.2.), 4D recordings appear to be a proper method to guarantee for the observation of the normal developmental process.

4.1.1.3. Conclusions

The present study gives a more detailed picture of the cleavage process in *P. pallida* and *P. muelleri*, than provided in previous studies. Yet, furthermore, the results shed serious doubt on former characterizations of the cleavage pattern as radial (see Herrmann 1986; Santagata 2001, 2004a). In none of the two species, any indications of a consistent pattern of meridional and equatorial cleavage divisions or of the presence of blastomere arrangements in octets of

cells – both typical for a radial cleavage mode – were observed. On the contrary, for both species, the data gained by the two different techniques (4D microscopy and fixation series), and the data on the cleavage axes in consistency with the data on the blastomere arrangements, reveal a pattern of cleavage that is characterized by oblique divisions, and an identifiable sequence of alternating dextrally and sinistrally oriented cleavage cycles, beginning with a dextral third cleavage. However, the cleavage process in both species also is characterized by certain degree of variability.

Based on the finding, the early cleavage pattern of *P. pallida* and *P. muelleri* should not be characterized as radial. Moreover, there are no indications that the cleavage somehow represents a "derived radial" condition (Herrmann 1986). Morphologically, such a characterization seems not justified by the results. In a phylogenetic context, on the other hand, the term "derived radial" implies that a radial cleavage mode was the plesiomorphic condition for Phoronida. This was to be expected, for example, when Phoronida would be located at the base of deuterostomes, which was in fact argued by some authors (e.g., Herrmann 1986).

The early cleavage process in *P. pallida* and in *P. muelleri* embryos displays surprising correspondences – but also interesting differences – to the cleavage pattern in typical spiralian embryos (see chapter 4.3.).

4.1.2. Cleavage in *P. vancouverensis*

Different than the free-spawning phoronids *P. pallida* and *P. muelleri*, *P. vancouverensis* is a brooding phoronid species. In natural development, its eggs/embryos develop in brood masses within the parental lophophore, and – only after reaching an early actinotroch stage – the offspring break free from the masses and begin their pelagic existence (Zimmer 1964). For the present investigation, eggs had been artificially gained from the coelom of ripe animals, and had left to develop devoid of the pressure exerted within the brood mass.

The present study found general differences between the cleavage in *P. vancouverensis*, on the one hand, and the cleavage in *P. pallida* and *P. muelleri*, on the other hand: in the former species, for example, the eggs are larger and appear richer in yolk, the cleavage divisions start later and they proceed more slowly, the inequality between smaller animal and larger vegetal cells is apparent earlier, and the blastocoel is generally smaller. These general characteristics are in consistence with previous description of the *P. vancouverensis* cleavage (Zimmer 1964, Freeman 1991); and the principle differences between brooding and free-spawning phoronids have often been noted in the literature (e.g., Silén 1954; Emig 1977, 1982; Temereva and Malakhov 2012) (see chapter 4.1.3.4.).

4.1.2.1. Former characterizations

Descriptions of the early cleavage in *P. vancouverensis* were provided by Zimmer (1964) and by Freeman (1991)[*]. Both authors studied the cleavage process on eggs that had been artificially obtained from the coelom of the animals. Both studies reported an essentially radial cleavage pattern, and described that the cell divisions of the third to the fifth cleavage cycles pass in alternating equatorial and meridional directions, and that the blastomeres at the 16-cell and 32-cell stage are arranged in plates of eight cells each or octets (Zimmer 1964; Freeman 1991). Zimmer (1964) characterized the *P. vancouverensis* cleavage pattern of as biradial, which he understood as variant of a radial cleavage. The author used term “biradial” in reference to the “arrangement of the eight cells in each tier of the 16- and 32-cell stages” (Zimmer 1964: 245), and in a later article, specified the cleavage would be “best described as

[*] Cleavage descriptions of *P. ijimai*, a species that is sometimes considered to be conspecific with *P. vancouverensis* (see chapter 2.1.), are discussed in the following section (chapter 4.1.3.).

biradial as the 16-cell stage features two tiers of eight cells each and has only two planes of symmetry through the animal-vegetal axis" (Zimmer 1973: 595).
Interestingly, however, both authors additionally mentioned variation in their material. Zimmer (1964), for example, generally reported that at the 4-cell, the 8-cell, and the 16-cell stages there are "frequently examples of blastomere orientation which do not appear to be of a radial pattern" (Zimmer 1964: 94). In particular, the author mentioned 8-cell embryos that "appear to have been derived by spiral cleavage" (Zimmer 1964: 94), 16-cell and 32-cell stages in which the "cells are frequently arranged irregularly within their respective octets", although both stages "typically have an arrangement into two or tour tiers of eight cells each" (Zimmer 1964: 246). Similarly, Freeman found "frequently some intercalation of blastomeres between [the] two plates [of the 16-cell stage]" (Freeman 1991: 161).
Confronted with this variability, Zimmer (1964) discussed the question whether the cleavage pattern was derived from a radial or from a spiral pattern. The author argued that it would be more probable that the impression of a spiral pattern would derive secondary from a true radial pattern, than the converse (Zimmer 1964). Therefore, he suggested that non-radial blastomere arrangements could result from secondary cell re-alignments after de facto radial cleavage divisions; as cause for such re-alignments Zimmer proposed a forced compression by the egg membrane, which could artificially be too tight, for example, due to the use of ambient seawater of too low tonicity (Zimmer 1964). While radial cell arrangements could be forced into a spiral looking arrangement, the converse would be physically impossible (Zimmer 1964, 1973). Furthermore, the author reasoned that the mere existence of octets would indicate that the cleavage process was radial rather than spiral (Zimmer 1964).

4.1.2.2. Present findings

To deal with the described variability and the objection of artificial effects, the early cleavage of *P. vancouverensis* was evaluated following a similar approach as in the other investigated species (see chapter 4.1.1.). While previous studies judged about the early cleavage pattern based mostly on the observation of blastomere arrangements (see Zimmer 1964; Freeman 1991), the present study combines this approach with detailed analyses of the mitotic spindles during the cleavage divisions (however, the actual cell divisions could not be analyzed, as no 4D recordings of the *P. vancouverensis* cleavage were available). The findings suggest some different interpretations from those in the previous studies. But they also reveal that the early

cleavage process in *P. vancouverensis* is interestingly different to cleavage in *P. pallida* and *P. muelleri*.

4.1.2.2.1. Cleavage axes

The evaluation of the cleavage axes in the third cleavage cycle shows the general presence of variation in the exact inclination of the mitotic spindles between the analyzed cells, somewhat similar to the situation in *P. pallida* and *P. muelleri*. Different from the situation found in these two species, however, the data for *P. vancouverensis* show that the spindles in most cells are roughly aligned along the animal-vegetal axis, that is, in an equatorial orientation. On the other hand, in a minority of cells, oblique spindle orientations were observed, and these were found to be oriented variably in either a dextral or a sinistral orientation. Within individual *P. vancouverensis* embryos, the spindles' inclinations and even their orientation usually vary between the single blastomeres.

Interestingly, for the next fourth cleavage cycle, the encountered variation in spindle inclination between the analyzed cells is even higher, than in the third cleavage. Although the data seem to indicate a tendency toward high angles of inclinations – that is, tending toward meridional orientations –, there is also a majority of cells, in which the spindles principally display sinistral orientations. Separated analyses for the animal and the vegetal cell tier of the 8-cell stage show that in the blastomeres of the animal tier, the spindles are oriented in various directions, and often obliquely, although without an identifiable pattern; whereas in blastomeres of the vegetal tier the spindles are more often inclined in high angles, thus tending toward meridional orientations.

For the fifth cleavage cycle, no data on the mitotic spindles were available, and the cleavage axes only could be evaluated based on sister cell alignments in embryos that already were at the 32-cell stage – and putatively all in a compacted state. These alignments indicate that in the blastomeres of the embryo's animal hemisphere the axes of the cleavage divisions were oriented in highly variable directions, similarly to the fourth cleavage cycle; whereas, in the blastomeres of the vegetal hemisphere the divisions seem to have passed roughly in equatorial directions. However, some effect of the process of compactation on the observed blastomere alignments in the 32-cell stage cannot be excluded (see next section).

4.1.2.2.2. Blastomere arrangements

The *P. vancouverensis* 8-cell stage consists of four animal/vegetal sister cell pairs, and an animal and a vegetal cell tier of four blastomeres each. This general arrangement is similar to the situation found in *P. pallida* and *P. muelleri* 8-cell embryos. In difference to the latter species, however, in the *P. vancouverensis* 8-cell embryos, the blastomeres in the single animal/vegetal sister cell pairs are mostly positioned in a juxtaposing alignment along the animal-vegetal axis. Although, many embryos also included individual cell pairs in which the blastomeres were aligned slightly tilted against this axis – and this, differently in either clockwise or counterclockwise orientation, in the different cell pairs and specimens. Interestingly, one embryo was found, in which the whole animal cell tier was shifted clockwise against the vegetal cell tier, somewhat resembling the situation in *P. pallida* and *P. muelleri*.

It has to be mentioned that that this general appearance of the 8-cell embryo – but moreover, also the encountered variation – are in general accordance with the descriptions of Zimmer (1964). Furthermore, however, the different observed 8-cell arrangements also are in consistence with the data on the third cleavage axes, which had shown spindle inclinations roughly along the animal-vegetal axis in most cases, but in other cases spindles that were inclined more obliquely to this axes – and differently, in dextral or sinistral directions. In contrast to Zimmer (1964), it is therefore concluded that that the cases of shifted blastomere arrangements, which are generally found in *P. vancouverensis* 8-cell samples, are the result of de facto oblique cell division, and cell re-alignments are not needed to explain such patterns.

Most 16-cell embryos and all of the 32-cell embryos, which were available for the analysis of the blastomere arrangements, were on hand in a putatively compacted state. As described for the *P. pallida* and *P. muelleri* cleavage, the process of compactation, which the embryo undergoes between two successive cleavage cycles, leads to a narrowing of the blastomeres toward each other and to the central animal-vegetal axis (chapter 4.1.1.2.) For *P. vancouverensis*, no 4D recordings of the cleavage were performed in the present study, and the compactation process was not directly observed. In the literature, however, it is described that the blastomeres, which are “essentially spherical” immediately after the divisions, “soon flatten against each other at the areas of contact”, and that the resulting compacted “embryo as a whole assumes a nearly spherical shape with a smooth contour” (Zimmer 1964: 92). In the material at hand, in fact most embryos fitted this description, and were therefore rated to be in

a compacted state. Notably, the blastomeres in such putatively compacted 16-cell (and 32-cell) embryos are very tightly packed, and they have almost angular formed cell shapes. Interestingly, such a strongly packed condition was never observed in the *P. pallida* or *P. muelleri* embryos. Apparently, compactation is a very pronounced process in the *P. vancouverensis* cleavage.

Very differently to the situation found in *P. pallida* and *P. muelleri*, in the available 16-cell embryos of *P. vancouverensis*, no cell arrangement in four tiers of four blastomeres each was identifiable. On the other hand, it can be recognized that the embryo is arranged in an animal and a vegetal hemisphere of each eight cells, and in four quadrants – which represent the descendants of the four blastomeres of the 4-cell stage. Especially in the putatively compacted embryos, the boundaries between the hemispheres – and between the quadrants – are apparent as continuous lines of cell contacts, because the blastomeres of the two hemispheres are not intertwined at the embryo's equator, and neither are the blastomeres of neighboring quadrants at the quadrant boundaries. This is very different to the situation in *P. pallida* and *P. muelleri* 16-cell embryos, in which the cell tiers are generally aligned shifted against each other, and hence the blastomeres between different tiers and between the embryo's quadrants are intertwined, and no linear separation of hemispheres and quadrants is apparent. Unfortunately, too few *P. vancouverensis* 16-cell samples in a putatively uncompacted state were available to analyze the exact condition prior to compactation.

Former authors described the 16-cell stage to be generally organized in "two plates of eight cells each" (Zimmer 1964: 93; Freeman 1991: 161), yet they conceded also some irregularity in this arrangement (see above). Zimmer (1964) characterized the cell arrangement – and the *P. vancouverensis* cleavage in general – as "biradial", based on his finding that the "16-cell stage features two tiers of eight cells each and has only two planes of symmetry through the animal-vegetal axis" (Zimmer 1973: 595). The present investigation indicates that the "two plates of eight cells each" refer to the general arrangement in two hemispheres, while the "two planes of symmetry" seem to capture the organization in quadrants and to describe the lines of quadrant boundaries, which are recognizable in the compacted embryo. Notably, however, the former descriptions neglect the great degree of variability that is present with respect to the blastomere arrangements and the individual sister cell alignments within different *P. vancouverensis* embryos. In the material that was available for the present study, no two 16-cell embryos looked the same. Within the animal hemisphere, the sister cell alignments are generally diverse – between different quadrants as well as between different embryos. But

also for the vegetal hemisphere, different cell arrangements can be found. Particularly with regard to the variable animal hemisphere, there are no real “planes of symmetry” present in the 16-cell stage.

Importantly, the finding of highly variable 16-cell stage arrangements is in great general consistence with the data on the fourth cleavage axes: as mentioned, the mitotic spindles were found highly variably and irregularly oriented in the animal cell tier of the 8-cell stage, and rather oriented in angles of inclination in the vegetal cell tier. Congruently with the third cleavage cycle, this suggests that a general process of cell re-alignments is not needed to explain the various blastomere arrangements found in *P. vancouverensis* embryos (contra Zimmer 1964), but that the cleavage divisions in fact do pass in different – and also oblique – directions during cleavage.

On the other hand, it has to be emphasized that a conflict was encountered between the circumstance that same animal sister cell pairs were found to be positioned along the animal-vegetal axis, and circumstance that the data on the fourth cleavage axes did not show spindle inclinations along the animal-vegetal axis. This seems to indicate that to some degree relocations of the blastomeres occur, and that this happens post the cleavage divisions, and probably during the compactation of the embryo – a similar cell displacement during compactation was observed in 4D recordings of the *P. pallida* cleavage (see chapter 4.1.1.2.2.). At all, it appears not unlikely that the process of compactation in *P. vancouverensis* – which apparently is very distinct, leading to tight cell packing and even cell deformations – has an effect on the definitive cell arrangement in the embryo. The reconstruction of cleavage axes and a cleavage pattern on sister cell alignments might then, to some degree, be misleading (see also chapter 4.1.1.2.4.). Clearly, spatiotemporally more detailed data, as for instance by 4D recordings, would be helpful in contribution to this issue.

Only few embryos could be analyzed for the 32-cell stage. Largely similar to the 16-cell stage, the available embryos show an organization in two hemispheres and four quadrants, yet, the individual blastomere arrangements are highly variable, and every embryo looked differently. Previous authors described the 32-cell stage to consist of “octets” (Zimmer 1964: 94f) or “layers of cells” (Freeman 1991: 161) aligned along the animal-vegetal axis. Although 32-cell embryos actually make the general impression to be arranged in layers of cells (in particular, in the vegetal hemisphere), these cell layers are universally identifiable neither within single embryos nor between different embryos. In fact, the performed analysis reveals that the identification of discrete tiers of cells within the 32-cell embryo, and furthermore, the

homologization of a cell arrangement between different embryos is problematic. In the attempt to identify a constant pattern, different landmarks – such as, the embryo's animal and vegetal pole, and the embryo's equator – were evaluated for the number of cells that were positioned contacting these landmarks, and the number of smaller animal blastomeres occurring for the first time in 32-cell embryos was analyzed. All these numbers were variable among the embryos, and hence neither of these approaches gave a consistent pattern of identifiable cell tiers.

Finally, both previous studies mentioned the constant occurrence of an opening surrounded by eight cells at the animal pole of the embryos in 16- and 32-cell stages (Zimmer 1964; Freeman 1991). In contrast, the number of cells encircling the embryos' poles in the material analyzed for this study, neither in the 16-cell stage nor in the 32-cell stage, exceeded six. This questions the presence of proper pol3 octets. Moreover, in the relative majority of embryos from both stages, four blastomeres were located at the animal pole as well as at the vegetal pole. However, there is clearly a much higher percentage of embryos that display different numbers and combinations of pole cell, than it was observed in *P. pallida* or *P. muelleri* embryos. Although it was in fact found that most 16-cell and 32-cell embryos display an opening at the animal pole – which differently is surrounded by four to six cells – and closed cell contacts at the vegetal pole, this is clearly not the case in every specimen, and also all other combinations of opened and closed animal and vegetal poles, respectively, were observed.

4.1.2.2.3. Polar furrows

For *P. pallida* and *P. muelleri*, it was shown that the formation of polar furrows results from the general narrowing of the blastomeres during the process of compactation, apparently as by-products of compactation (chapter 4.1.1.2.3.). Although no 4D recordings of the *P. vancouverensis* cleavage are available, alone the general appearance of putatively compacted *P. vancouverensis* embryos seems to suggest that the same is the case in this species as well.
In fact, every studied putatively compacted *P. vancouverensis* 4-cell embryo had polar furrows. Several specimens were found that displayed two perpendicularly running polar furrows – one at each pole –, in others the polar furrow was restricted to only the animal or only the vegetal pole. In some of the latter specimens, at the opposite pole, the cells sometimes seemed to form an X-furrow, that is, they all contacted at the pole. Surprisingly, 4-

cell specimens with a polar furrow reaching from one pole to the other – as it was found in *P. pallida* and *P. muelleri* embryos – were not encountered in the material. Zimmer (1964) described the same general variability of 4-cell stage central blastomere contacts, and notably, also mentioned specimens with a condition comparable to *P. pallida* and *P. muelleri* embryos. Also in embryos at later cell stages, polar furrows are observed in nearly every specimen (similarly to *P. pallida* and *P. muelleri*, they occur only at poles that are encircled by four cells, while a higher number of pole cells leads to the presence of a pole opening). Generally, they are found more frequently at the vegetal pole, than at the animal pole; in several embryos, they were found at both poles – yet, then, differently oriented either perpendicularly or parallel in different specimens. In this context, however, it is important to repeat that the blastomere arrangements are highly variable in *P. vancouverensis* embryos, and that generally the sister cell alignments between individual quadrants, and between the animal and the vegetal hemisphere, vary greatly within and between different embryos (see above). For this circumstance, a homologization of the polar furrow forming blastomeres (or the polar furrows themselves) between different embryos appears highly problematic.

4.1.2.3. Conclusions

The present investigation shows that previous descriptions of the cleavage pattern in *P. vancouverensis* are, to some degree, simplifications. Importantly, there is a general consistency between the variability that is found in the spindle orientations during the cleavage division, and the variation that is observed in the blastomere arrangements between different embryos of the same cell stage. Based on this consistency the general explanation that the cleavages divisions would at first pass truly radial – that is, in equatorial and meridional directions alone – and only afterwards the cells would shift in the high variety of observed patterns, is rejected (contra Zimmer 1964). In contrast, the data indicate that non-radial and even apparent spiral blastomere arrangements (see Zimmer 1964), in fact, result from cell divisions that passed obliquely to the animal-vegetal axis. On the other hand, some effect of the process of compactation on the definitive cell alignments possibly exists. 4D microscopic studies are needed to go after that.

The early cleavage of *P. vancouverensis* is most similar to a typical radial pattern only until the third cleavage cycle. During the fourth and fifth cleavage cycles, there seems to be some tendency toward meridional and equatorial division axes, respectively, only for the blastomeres in the vegetal hemisphere; while the cleavage in the animal hemispheric

blastomeres appears to be characterized by the presence of variable cleavage axes, which not rarely are oriented obliquely to the animal-vegetal axis. No pattern – neither of alternating meridional and equatorial nor sinistral and dextral cleavage axes – could be identified with respect to these animal cells. Furthermore, no consistent blastomere arrangement in octets of cells is identifiable across different specimens, but the cell alignments generally are highly variable between the embryos.

In total, the early cleavage of *P. vancouverensis* shows more differences to a proper radial cleavage pattern of alternating equatorial and meridional divisions (e.g., Siewing 1969; Nielsen 2012), than it was previously recognized. On the other hand, it should be noted that in the case of enteropneust hemichordates, radial cleavage can include some irregular cell divisions and variational cell arrangements with respect to the animal cell octets (see Colwin and Colwin 1953; Henry et al. 2001).

Interestingly, the early cleavage of *P. vancouverensis* remarkably differs from the cleavage in *P. pallida* and *P. muelleri* (see chapter 4.1.1.). Hence, it appears as if different patterns of cleavage are present in Phoronida (see next chapter).

4.1.3. Cleavage in the taxon Phoronida

Besides the three species investigated in the present study – *P. pallida*, *P. muelleri*, and *P. vancouverensis* – descriptions of the early cleavage process are available for five other phoronid species; four from the genus *Phoronis*, and one from *Phoronopsis*: *P. hippocrepia* (Foettinger 1882), *P. australis* (Masterman 1900; Kume 1953), *P. ijimai* (Ikeda 1901; Wu et al. 1980; Malakhov and Temereva 2000), *P. psammophila* (Emig 1974b), and *Ph. harmeri* (Rattenbury 1951, 1954; Zimmer 1964; Temereva and Malakhov 2007)[*]. In addition, a cleavage description is available for *P. architecta* (Brooks and Cowles 1905). Although this study later was suggested to in fact have dealt with embryos of *P. muelleri* (Emig 1990)[**], it is also respected here (but see also chapter 4.1.1.). A comparison of the present results to these literature data allows some general conclusions on the early cleavage in Phoronida.

4.1.3.1. Basic characteristics and timing of cleavage

In phoronids, the size and the yolk content of the eggs vary between different species (see Zimmer 1964; Emig 1974b, 1977). While *P. pallida*, *P. muelleri* and *Ph. harmeri* have relatively small eggs – generally between 60 and 80 µm in diameter – which are poor of yolk, the eggs of *P. vancouverensis*, *P. hippocrepia*, *P. australis*, *P. ijimai*, *P. psammophila*, and *P. architecta* are more rich in yolk and generally larger – between 80 and 130 µm. The yolk-richest eggs among phoronids are found in *P. ovalis*, measuring about 125 µm. These differences seem to be associated with the "developmental type" of the respective species (see chapter 4.1.3.4.). In all species, the cleavage is holoblastic. The first cleavage division differently takes place between half an hour (*P. psammophila*; Emig 1974b) and six hours (*P. vancouverensis*: present study) after egg release from the coelom. Subsequently, the time interval between two successive cleavage cycles lies between about half an hour (*P. pallida*, *P. muelleri*: present study; *P. australis*: Kume 1953; *Ph. harmeri*: Temereva and Malakhov 2007) and three hours (*P. vancouverensis*: present study; *P. ijimai*; Malakhov and Temereva 2000). There seems to be a tendency that this interval increases with advancing cleavage cycles (see Zimmer 1964; Temereva and Malakhov 2007; present study).

[*] This listing is based on the synonymies of *P. australis* with *P. buskii* (Emig and Marche-Marchad 1969; Emig 1974a, 1982) and of *Ph. harmeri* with *Ph. viridis* (Marsden 1959; Emig 1967).

[**] *P. architecta* itself was proposed to be conspecific with *P. psammophila* (Emig 1969, 1982); for objections against this synonymy see e.g., Santagata and Zimmer (2002) and Santagata and Cohen (2009).

Generally, the early cleavage cycles pass more or less synchronously in phoronids. However, cases in which, during one cleavage cycle, the cells do not divide at the exactly same moment are common. This leads to the formation of transient embryos with intermediate blastomere numbers. Such embryos were observed in all species studied herein, but are likewise mentioned in nearly all studies on phoronid development (e.g., Foettinger 1882; Ikeda 1901; Rattenbury 1954; Zimmer 1964; Emig 1974b; Malakhov and Temereva 2000). Only for *P. australis*, highly synchronous divisions were explicitly claimed (Kume 1953). The more cells there are in the embryo – thus, with progressing cleavage cycles – the more asynchronous the divisions become. This makes the analysis especially of advanced cell stages difficult. The lineage analyses performed herein for *P. pallida* and *P. muelleri* did not reveal any consistent pattern in the temporal sequence of the divisions between different embryos. This was also described for *Ph. harmeri* (Rattenbury 1951, 1954). Thus, it seems likely that the slight and increasing asynchronies observed during the phoronid cleavage represent variational irregularities.

While the first cleavage cycles generally produce cells of approximately equal size, there is a tendency for the animal blastomeres to be slightly smaller than the vegetal ones in later stages, throughout phoronids. This size difference is never very pronounced, however, and in different species becomes manifest at different stages. In *P. vancouverensis*, *P. hippocrepia*, *P. australis*, and *P. psammophila*, smaller animal cells can be identified already at the 8-cell stage (Foettinger 1882; Kume 1953; Emig 1974b; present study), whereas in *P. pallida* and *P. muelleri* the difference becomes apparent only in later stages (present study). The data on *P. ijimai* and *Ph. harmeri* are ambiguous in this respect; different authors observed cell size differences at different stages (see Ikeda 1901; Rattenbury 1954; Zimmer 1964; Malakhov and Temereva 2000; Temereva and Malakhov 2007).

4.1.3.2. Polar furrows

The question whether polar furrows are present during the phoronid cleavage process is a topic that was controversially discussed in the literature (see Rattenbury 1954; Zimmer 1964; Herrmann 1986). The importance of this issue relates to the fact that many equally cleaving spiralian embryos have polar furrows – or more precisely cross furrows, that is, two perpendicularly running polar furrows (see chapter 4.3.1.). Different authors emphasized the absence (Herrmann 1986 for *P. muelleri*) or the obligatory presence (Rattenbury 1954 for *Ph.*

harmeri) of polar furrows during the cleavage, and used this as an argument against or in favor of a spiral nature of the phoronid cleavage, respectively.

The present study evaluated this point in all three analyzed species. It could be shown that polar furrows are neither obligatorily present nor absent, but in contrast, in all three species are structures that do occur only occasionally during the cleavage process. The performed 4D recordings show that polar furrows are by-products of the process of compactation, and variably are established or not established in different embryos of the same stage. Furthermore, data on *P. pallida*, suggest that these structures are formed more frequently the smaller the cell size is in the embryo, thus with progressing cleavage and advancing cell stages.
The literature data on the occurrence of polar furrows in other species are scarce, and limited to information on the 4-cell stage. Interestingly, these data are conflicting, and thus might indicate a variable occurrence of polar furrows as well. Early studies reported the presence of polar furrows in embryos of *P. australis* (Masterman 1900), *P. ijimai* (Ikeda 1901: Fig. 2b), and *P. psammophila* (de Selys-Longchamps 1907: Plate 8, Fig. 18), whereas later re-investigations of the same species did not mention these structures, which are not easily overlooked (*P. australis*: Kume 1953; *P. ijimai*: Malakhov and Temereva 2000; *P. psammophila*: Emig 1974b). Furthermore, also the description of obligatory polar furrows in *Ph. harmeri* (Rattenbury 1954) was not corroborated by a later investigation (Zimmer 1964), leaving them possibly variable in this species as well.

Based on these data, it seems justified to conclude that polar furrows are structures of variable occurrence in the early cleavage process of phoronids in general. Interestingly, this variability makes it unlikely that these structures play any significant role during the development and the establishment of cell fates, as they do in some equal-cleaving spiralian embryos (see chapter 4.3.3.).

4.1.3.3. Cleavage patterns among different species

The nature of the phoronid cleavage mode is subject of a long discussion in the literature (e.g., Cori 1939; Rattenbury 1954; Zimmer 1964; Emig 1977; Herrmann 1986; Malakhov and Temereva 2000; Temereva and Malakhov 2012). Nowadays, it is widely accepted that the phoronid cleavage is of a radial or a biradial type (e.g., Zimmer 1973, 1997; Emig 1977,

1982, 1990; Ax 2001; Ruppert et al. 2004; Nielsen 2005; Temereva and Malakhov 2012). Repeated observations of features deviating from such a radial pattern, such as oblique spindles or division axes and cases of non-radial or shifted blastomere arrangements (e.g., Brooks and Cowles 1905; Rattenbury 1951, 1954; Zimmer 1964; Herrmann 1981, 1986; Temereva and Malakhov 2007), are mostly discussed as variation or abnormalities within the radial cleavage mode, or merely as descriptions of artifacts (see Zimmer 1964, 1973; Emig 1974b, 1977, 1990; Herrmann 1981, 1986; Temereva and Malakhov 2007, 2012).

The present investigation is the first one to analyze the early cleavage of phoronids using different modern morphological methods – enabling a high spatial and temporal resolution of the cleavage process – and to perform detailed, quantitative analyses of the inclinations of the mitotic spindles and the axes of cell divisions, as well as of features of the blastomere arrangements in different cell stages. One of the surprising findings is that in none of the three analyzed species the cleavage divisions run only in equatorial and meridional directions, as it would be typical for a radial cleavage pattern. In contrast, in all species cleavage divisions, which pass obliquely to the animal-vegetal axis of the embryo, were observed. However, there are interesting differences in the cleavage between the investigated species.

On the one hand, the study reveals that the cleavage process in *P. pallida* and *P. muelleri* are greatly corresponding (chapter 4.1.1.). In both species, the cleavage divisions beyond the 4-cell stage are characterized by passing obliquely to the animal-vegetal axis. Consistently in both species, the third cleavage passes obliquely and with a dextral orientation, and the successive divisions run alternately in sinistral and dextral directions. Although in more advanced stages this pattern of alternating oblique divisions is somewhat dissolved and irregularities occur, it can be identified in the animal most and – even more regularly – in the vegetal most blastomeres until at least the sixth cleavage cycle. This cleavage pattern is clearly different to a radial cleavage pattern; however, it shows interesting correspondences to the early cleavage pattern in spiralians (chapter 4.3.1.).
The cleavage in *P. vancouverensis*, on the other hand, is surprisingly different (chapter 4.1.2.). In this species, the third cleavage passes roughly in an equatorial direction, whereas the orientations of the successive divisions differ between the animal and the vegetal blastomeres in the embryo. The vegetal hemispheric cells display a tendency to divide in meridional and equatorial directions, and hence – although some variation was observed – show correspondences to a radial cleavage pattern. The animal hemispheric cells, in contrast,

divide in various directions, and oblique division axes were observed repeatedly; for these cells no cleavage pattern was identifiable. The resulting embryos show various and unique cell arrangements; and no blastomere alignments in proper octets were identifiable.

A comparison of the early cleavage of *P. pallida* and *P. muelleri* to previous investigations of phoronid cleavage reveals the best correspondences to the cleavage process of *Ph. harmeri*, as it was described by Rattenbury (1951, 1954). This author observed that, successively, the cells in the embryo elongate in an axis that is oblique to the animal-vegetal axis, the mitotic spindles get aligned along these elongated axes, and finally the cells divide in these oblique axes, at least from the third cleavage onward (Rattenbury 1951, 1954). Furthermore, she described that these elongation and division axes are oriented in alternating dextral and sinistral directions ("dexiotropic" and "laeotropic" in Rattenbury's terminology), and are starting with a dextrally oriented third cleavage axis (Rattenbury 1951, 1954). Consequently, the cleavage process generates quartets of four cells each, which, in an animal view, are given off toward animal alternately clockwise and counterclockwise; and also a blastomere quartet at each of the embryo's poles (Rattenbury 1951, 1954). This description is highly reminding of the cleavage process observed in *P. pallida* and *P. muelleri*. The main difference lies in the observation of some variability with respect to the cleavage orientations in *P. pallida* and *P. muelleri* embryos, while for *Ph. harmeri* Rattenbury (1951, 1954) generally described that until the sixth cleavage cycle all cells in the embryo divide in the alternating oblique orientation pattern. The author only shortly mentioned that for the third cell cycle the "degree of inclination may vary between the cells of one embryo and the process is not one of great precision or regularity" (Rattenbury 1954: 296), and in her original study in general conceded the observation of "occasional irregularities in the direction of cleavage" (Rattenbury 1951: 114).

The correspondence between the cleavage pattern in *P. pallida* and *P. muelleri*, on the one hand, and the studies of Rattenbury (1951, 1954), on the other hand, are interesting, because later re-investigations of *Ph. harmeri* questioned Rattenbury's findings, and instead claimed the presence of a radial or biradial cleavage mode (Zimmer 1964; Temereva and Malakhov 2007; but see Rimler 2013). These studies, however, came to this characterization, although the authors also observed features, which do not fit with a radial cleavage.

Zimmer (1964) characterized the *Ph. harmeri* cleavage pattern as biradial, and described the divisions to pass only equatorially and meridionally. However, the author also conceded that not all embryos displayed the proper radial or biradial cell arrangements, and described the

presence of "a great variety of cell patterns" in the material, 16-cell stages in which "[f]requently the cells are not arranged in two plaques [that is, octets, M.P.], but rather are jumbled" and occasionally "appear derived from typical spiral cleavage", as well as an increasing "irregularity of cleavage patterns" with later division cycles (Zimmer 1964: 137). Some of the embryos Zimmer (1964) admitted to resemble cell arrangements as they also had been found by Rattenbury (1951, 1954). However, the author proposed that such arrangements might be the result of an artificial compression of the blastomeres (see also chapter 4.1.2.2.1.), and, at the same time, suggested them to represent anomalies from the radial or biradial cleavage pattern (Zimmer 1964).

Temereva and Malakhov (2007), in turn, characterized the *Ph. harmeri* cleavage as radial, but also conceded that the proper division pattern is present only until the third cell cycle. For the fourth and the succeeding cleavages, the authors observed that the "cleavage furrows between sister blastomeres are oblique with respect to the animal-vegetal axis, and the regular radial cleavage pattern is thus distorted", and also described that "blastomeres move apart forming a spacious blastocoel" (Temereva and Malakhov 2007: 59). The authors discussed this as a modification of the radial cleavage mode, and argued that the later divisions would pass obliquely in order to allow for the formation of a blastocoel by the 16-cell stage (Temereva and Malakhov 2007) (see chapter 4.1.3.4.).

Hence, in both studies, there is an ambiguity between the characterization of the cleavage pattern and the actual observations, which is surprising and makes a further re-investigation of the cleavage of *Ph. harmeri* – following the methodical standards of the present study – desirable. On the other hand, these ambiguities, in combination with the finding of an in fact alternating oblique cleavage pattern in *P. pallida* and *P. muelleri* in this study, might shed a new – and more positive – light on the reliability of Rattenbury's (1951, 1954) studies.

An early cleavage process proceeding with alternating oblique divisions was not described for any other phoronid species. However, for three species – *P. hippocrepia*, *P. australis*, and *P. architecta* – there are observations in the literature which seem to suggest that at least the third cleavage cycle does not invariably pass equatorially; that is, in accordance with a strictly radial pattern.

This is the case for *P. hippocrepia*, for which only one very brief cleavage description is available (Foettinger 1882). *P. hippocrepia* is a phoronid species that broods its embryos in tight brood masses, similarly to *P. vancouverensis*. Unfortunately, Foettinger (1882) apparently used embryos from these brood masses, which therefore could have been distorted

(see Rattenbury 1951; Zimmer 1964). In any case, the author's information on the third cleavage cycle is ambiguous. His study gives a figure of an embryo during the cell division process that shows clearly oblique – though somewhat irregular – orientations of the mitotic spindles, as well as a figure of an 8-cell stage in which the animal cells are aligned perfectly juxtaposing the vegetal ones (Foettinger 1882: Figs. 8, 9); unfortunately, it provides no information on the following cleavage cycles.

For *P. australis*, which is likewise a brooding species, only one available study analyzed the cleavage process on eggs that had been liberated from the animals' coelom (Kume 1953; vs. Masterman 1900). It briefly reported an essentially radial division pattern, but surprisingly, a photograph provided for the 8-cell stage shows an embryo that apparently displays shifted blastomere alignments in three of its four animal/vegetal sister cell pairs (Kume 1953: Fig. 9), similar to some of the *P. pallida* and *P. muelleri* embryos encountered in the present study. A picture of the 16-cell stage, in contrast, shows similarities to *P. vancouverensis* embryos (see below).

Finally, the study of Brooks and Cowles (1905) has to be discussed in this context. For the case this description actually dealt with *P. architecta* – and not with *P. muelleri* (contra Emig 1990) – it should be repeated that Brooks and Cowles (1905) observed during the third cleavage cycle an essentially similar – obliquely and dextrally oriented – cell elongation and cell division process, as well as shifted cell arrangement in 8-cell embryos, as it also was found in *P. pallida* and *P. muelleri* cleavage (see chapter 4.1.1.). Only the divisions in the fourth cleavage cycle are described to pass meridionally; yet, unfortunately, no figure of the resulting stage is provided (Brooks and Cowles 1905). *P. architecta* is a non-brooding species (see chapter 4.1.3.4.).

Likewise, the comparison of the early cleavage in *P. vancouverensis* to the cleavage in other phoronid species has to be ambiguous; simply because the presence of cleavage divisions that pass in various – and seemingly irregular – directions, as in the animal hemispheric blastomeres in *P. vancouverensis* cleavage, was not reported for any other species.

As already mentioned, there are similarities between the cleavage in *P. vancouverensis* and in *P. australis*; a species for which a regular radial pattern of alternating equatorial and meridional cell divisions was described (Kume 1953), although the information on the third cleavage cycle is ambiguous (see above). The possible correspondence to *P. vancouverensis* lies in the later divisions, which in the vegetal blastomeres of the *P. vancouverensis* embryo display some tendency to pass meridionally and equatorially (see above). A benefit of Kume's

study is that it provides a photograph of the vegetal hemisphere of a 16-cell embryo (Kume 1953: Fig. 10); this actually shows a cell arrangement that is similar to the situation found in uncompacted *P. vancouverensis* 16-cell embryos (see Fig. 28O). Unfortunately, for the following stages, the quality of the photographs in the study does not allow a meaningful comparison to the present study (Kume 1953). Moreover, it does not give any pictures of the embryos' animal hemisphere; only the author's description of alternating equatorial and meridional divisions (Kume 1953), clearly differs from the situation in the animal blastomeres in *P. vancouverensis*.

There are two further phoronid species – *P. ijimai* and *P. psammophila* – for which a typical radial cleavage passing only with equatorial and meridional divisions was described; the respective studies provide no photographs, but give only schematic drawings of the cleavage stages (Ikeda 1901; Wu et al. 1980; Emig 1974b; Malakhov and Temereva 2000). Correspondences to the *P. vancouverensis* cleavage pattern exist with respect to an equatorial orientation of the third cleavage cycle, but again, in the next cleavage cycles are limited to the vegetal hemispheric cells. In contrast, an animal hemisphere in which eight blastomeres surround perfectly equidistant the animal pole, as it is shown in the illustrations of 16-cell and 32-cell stages of *P. psammophila* (Emig 1974b), was never observed in *P. vancouverensis*.

One noteworthy disparity between the *P. australis*, *P. ijimai*, and *P. psammophila* cleavage pattern is a difference in the orientation of the fifth cleavage cycle. While in *P. australis* and *P. psammophila* these divisions are described to pass equatorially (Kume 1953; Emig 1974b), in *P. ijimai* they are reported to run meridionally (Malakhov and Temereva 2000). Especially with respect to the cells in the animal hemisphere, one can only speculate whether this divergence in the descriptions of a radial cleavage are a result of different attempts to draw conclusions from actually irregularly passing cleavage divisions, maybe similar to *P. vancouverensis*. Clearly, re-investigations of the three species could bring some clarity to this point.

Finally, is has to be repeated that the quantitative analyses performed in the present study revealed – for all three investigated species – the presence of some variability and irregularity during the early cleavage process. This relates, for example, to the exact inclinations of the mitotic spindles or axes of cell divisions, the occurrence of divisions in orientations deviating from any identified pattern, or the number of blastomeres that are encircling the embryo's poles. Generally speaking, different embryos do not cleave exactly identical, however, there is no reason to assume that these embryos do not develop into normal larvae.

Intraspecific variation is only rarely mentioned in former investigations (e.g., Zimmer 1964), but the ambiguities found in some studies could actually indicate the presence of variation (see above). Hence, it is possible that a certain degree of variability and irregularity – and hence, the absence of a strictly stereotypic cleavage pattern – is one further general characteristic of the phoronid cleavage process. To substantiate this point re-investigations, following the methodological standards of the present study, are needed.

To summarize this section, there exist interesting differences between the patterns of division during the early cleavage process between the different phoronid species. In an attempt to generalize these differences, one might speak of the occurrence of at least two different phoronid cleavage patterns:
(i) One – a pattern that is characterized by an oblique and dextrally oriented third cleavage cycle, as well as subsequent division cycles that pass in an identifiable sequence of alternately sinistral and dextral oblique directions – is found in *P. pallida* and *P. muelleri*. There are some indications that this pattern is also present in *Ph. harmeri*.
(ii) The other – a pattern that is characterized be a roughly equatorial third cleavage cycle, and subsequent cleavage divisions that in the vegetal hemispheric cells tend to pass in alternately meridional and equatorial directions, but in the animal hemispheric cells pass in various directions with no identifiable sequence – only is documented for *P. vancouverensis*.
Additionally, the available descriptions of the early cleavage in *P. ijimai*, *P. psammophila*, and also *P. australis* report, in total, more similarities to the *P. vancouverensis* cleavage, than to the cleavage observed in *P. pallida* and *P. muelleri* (see above). Having in mind, moreover, the differences that have been found between the *P. vancouverensis* cleavage as it was observed in the present study and the literature data on the *P. vancouverensis* cleavage (see chapter 4.1.2.), the cleavage pattern in *P. ijimai*, *P. psammophila*, and *P. australis* embryos may cautiously considered to be of the *P. vancouverensis* type as well.

4.1.3.4. Developmental types

The distribution of the different early cleavage patterns among the different phoronid species is interesting, when it is related to the so-called developmental types in phoronids. This concept organizes the phoronid species into three different groups, which share certain reproductive and developmental characteristics (see Silén 1954; Emig 1977).

In this context, it is noteworthy that *P. pallida*, *P. muelleri*, and *Ph. harmeri* all three belong to the same developmental type (type 1 after Silén 1954; type 3 after Emig 1977). Species of this type generally produce relatively small, yolk-poor eggs and are freely spawning: they release their eggs directly into the surrounding seawater, where the cleavage process and the subsequent development will take place. The only other phoronid species for which free-spawning is known – and which therefore is rated to belong to the same development type (see Emig 1977)* – is *P. architecta*; surprisingly, for this species the presence of relatively yolk-rich and large eggs, with a diameter of normally 100 µm, is described (Brooks and Cowles 1905).

The finding of a corresponding cleavage pattern in several species of this developmental type is interesting (see chapter 4.1.3.3.), since the presence of small eggs and a direct egg release have been suggested to be the plesiomorphic condition in Phoronida (Emig 1985). Hence, the presence of an early cleavage pattern characterized by alternating oblique divisions in the freely spawning phoronids could then suggest that this pattern of cleavage is plesiomorphic for Phoronida.

Another explanation for the presence of oblique cleavage division in the species of this developmental type was recently discussed by Temereva and Malakhov (2012). The authors suggested that the cell divisions would pass obliquely tilted with respect to the animal-vegetal axis in order to allow for the formation of a blastocoel by the 16-cell stage; this would promote the buoyancy of the embryo, which in phoronids of this developmental type is pelagic in an early stage of development (Temereva and Malakhov 2012). Although it appears to be the case that embryos of free-spawning species generally have a larger blastocoel, than embryos of brooding species (see e.g., Emig 1977; present study), the significance of this is unclear. It has to be mentioned that the matter filling the blastocoel in phoronids most likely has the same specific weight as seawater, or possibly is seawater. Furthermore, is seems to me as if also the increased buoyancy resulting from the bigger volume of embryos with a larger blastocoel may be negligible in relation to the water currents affecting the embryo. In addition, the explanation of Temereva and Malakhov (2012) raises the question why the cleavage cycles in *P. pallida*, *P. muelleri*, and *Ph. harmeri* – besides passing obliquely – do also correspond with respect to the orientation of the division axes, that is, starting with a dextral direction of the third cleavage.

* This objects to Emig's proposal of a conspecifity of *P. architecta* and *P. psammophila* (Emig 1969); notably, the latter species is not spawning freely (see also Santagata and Zimmer 2002).

All other species for which data on the early cleavage are available – *P. vancouverensis*, *P. hippocrepia*, *P. australis*, *P. ijimai*, and *P. psammophila* – belong to another developmental type (type 2 after Silén 1954 and Emig 1977). Phoronids of this type develop via eggs of moderate size and yolk content and do not spawn freely. In contrast, they show brood protection in such a way that the eggs and developing embryos are kept in tight packings, so-called brood masses, which are attached to the mother animal's lophophore. As already mentioned, this is known to result in a compression of the individual embryos, and in a possible distortion of the cleavage pattern (Rattenbury 1951; Zimmer 1964). Newly released eggs push the older ones upward, and the offspring detaches from the masses' distal end only at gastrulation or as early larva (Silén 1954; Zimmer 1967; Emig 1977). This brooding behavior is achieved by means of nidamental glands, which produce mucus that catches newly shed eggs and maintains the cohesion of the brood (Zimmer 1967; Emig 1977). While these nidamental glands are absent in all species not belonging to this developmental type, interestingly, the structure of the glands as well as the number of formed brood masses (paired or unpaired) is different between species of this type (Emig 1977).
As discussed, it is possible that several of the species of this developmental type show a corresponding cleavage pattern (chapter 4.1.3.3.). The significance of this is unclear. To my knowledge, brooding of developmental type 2 never was suggested to represent the plesiomorphic condition for Phoronida. In contrast, it was proposed to be a derived situation with respect to free-spawning and holopelagic development (Temereva and Malakhov 2012), and also to represent an evolutionary plastic character among phoronids (Santagata and Zimmer 2002; Santagata and Cohen 2009). Whether the cleavage pattern came prior to the developmental type, or the converse was the case, cannot be decided unambiguously.

There is only a single phoronid species, which represents the last developmental type, *P. ovalis* (type 3 after Silén 1954; type 1 after Emig 1977). Unfortunately, for this species no report on the early cleavage exists. *P. ovalis* produces the largest and yolk-richest eggs among phoronids, and differs in many developmental aspects from all other species: it does not shed its eggs through the nephridia, as in the other phoronids, but probably through a body opening formed by the autotomy of the lophophore, it is the only species that displays brood protection by retaining its eggs within the parental tube, and the only one, which does not develop via a planktonic actinotroch larva but via a lecithotrophic slug-like larva without a true pelagic life phase (Silén 1954; Emig 1977). The question whether *P. ovalis* represents either the ancestral or a highly derived condition among phoronids is undecided (see e.g.,

Silén 1952; Emig 1985; Santagata and Zimmer 2002; Grobe 2007). Interestingly, this species is the sister group to all other phoronids in many phylogenies (see next chapter).

4.1.3.5. Ground pattern of phoronid early cleavage

The differences in the early cleavage pattern between the different phoronid species raise the question which cleavage pattern was part of the ground pattern in the taxon Phoronida. This question has to be addressed irrespective of any assumptions about the putative plesiomorphic condition of a certain developmental type (and its possible association with a certain cleavage pattern; see chapter 4.1.3.4.), as well as of any hypotheses about the phylogenetic position of Phoronida within Bilateria. The most reliable approach that allows drawing conclusions about the cleavage ground pattern is to reconstruct this pattern based of on the internal phylogenetic relationships within Phoronida; this, however, brings along additional complications.

First of all, there is no generally accepted phylogeny of Phoronida. Different cladistic analyses resolved contradictory, and in parts very different, relationships between phoronid species (Emig 1985; Grobe 2007; Santagata and Cohen 2009; Hirose et al. 2014)[*]. This is the case for analyses, which were based on morphological character sets (see Fig. 31), but also for analyses, which were built on gene sequence data (see Fig. 32). At present, none of these phylogenies can be preferred over the others.
Furthermore, the different analyses used different species samplings, and not always applied the same taxonomic conceptions. The relatively new species *Ph. malakhovi* and *P. emigi* and the taxonomically disputed species *P. architecta* were only accounted for in some studies (see Figs. 31, 32), and the different authors dealt differently with the taxonomic validity of *P. vancouverensis* and its proposed conspecifity and synonymy with *P. ijimai* (see chapter 2.1.): Emig (1985) and Grobe (2007) followed the conspecifity, but did not specify the origin of their respective specimens (Fig. 31A-B), whereas Santagata and Cohen (2009) did not accept the conspecifity and sampled only specimens from the Eastern Pacific *P. vancouverensis* population (Figs. 31C, 32A-B). Most recently, in the study of Hirose and co-worker (2014), 18S rRNA and *cox1* sequence data from specimens of both populations – the Eastern Pacific *P. vancouverensis* and the Western Pacific *P. ijimai* – were analyzed. The authors found a genetic distance, which they rated as to low to erect two separate species, and thus went with

[*] The same is true for pre-cladistic conceptions about the major subdivisions within Phoronida (see Silén 1952; Marsden 1959; Emig 1974a).

the older species name *P. ijimai* (Hirose et al. 2014; Figs. 31D, 32C-D). Furthermore, due to the lack of available sequence data, none of the molecular analyses included the species *P. psammophila* (Fig. 32), and additionally *P. pallida* was not included in the analyses reproduced in Fig. 32D (Hirose et al. 2014).

Finally, since all comparisons of the present results to the literature data on the phoronid cleavage pattern resulted in some inconsistencies and ambiguities, the coding of the different cleavage patterns for the ground pattern reconstruction has to be ambiguous. Herein, it was decided to follow the generalization suggested above (chapter 4.1.3.3.), and to code only two character states:
(i) One character state represents a cleavage pattern that is characterized by an oblique and dextrally oriented third cleavage cycle, as well as subsequent division cycles that pass in an identifiable sequence of alternately sinistral and dextral oblique directions. It is coded as present for *P. muelleri*, *P. pallida*, and *Ph. harmeri*; and represented by an open circle in the reconstructions (Figs. 31, 32).
(ii) The other character state generally stands for a different cleavage pattern. It is coded present for *P. vancouverensis*, *P. australis*, *P. ijimai*, and *P. psammophila*; and is represented by a filled circle (Figs. 31, 32). These species are coded within the same character state, despite the differences found between the *P. vancouverensis* cleavage and the radial cleavage pattern that was described for the other three species (see chapter 4.1.3.3.). The conservative coding applied herein also compensates for the circumstance that *P. vancouverensis* and *P. ijimai* are not employed as different species in most of the available phoronid phylogenies.
For the remaining species, the data are either insufficient (*P. hippocrepia*), ambiguous with respect to the species that was actually described (*P. architecta*), or missing (all others), and no proper character state can be assigned. This is represented by an interrogation mark in the reconstructions (Figs. 31, 32).

For each of the different phoronid phylogenies the cleavage ground pattern is reconstructed (Figs. 31, 32). These reconstructions are performed by, firstly, mapping the two different character states onto each of the phoronid phylogenies, and by, secondly, tracing the most parsimonious evolution of the states stepwise from node to node back in time, that is, to the base of the respective phylogeny. Thereby, when the two different character states come together at a node, no reconstruction result is obtained, and no discrete state can be assigned to the common ancestor; and whereas when an assigned character state comes together with a

state that is not unambiguously assigned, and thus unknown, the state that is known is reconstructed for the ancestor.

Based on this approach, the following statements can be made:

(i) While none of the morphological phylogenies gives an unambiguous outcome to the ground pattern reconstructions (Fig. 31), three of the four presented molecular phylogenies do; surprisingly, they reveal the cleavage pattern of *P. muelleri*, *P. pallida*, and *Ph. harmeri* as the ground pattern situation in Phoronida (Fig. 32A-B,D). Note, however, that none of the molecular analyses included *P. psammophila*, a species that was coded with the second character state, and the phylogeny in Fig. 32D additionally did not include *P. pallida*. Therefore, it cannot be excluded that the inclusion of this species (these species) would change the topologies, and thus the outcome of the ground pattern reconstructions.
In total, these results show that at present knowledge it cannot unambiguously be decided, which of the two cleavage patterns was part of the ground pattern in Phoronida. On the other hand, however, the reconstructions reveal that it is clearly not justified to reject the possibility that a cleavage process characterized by alternating oblique dextral and sinistral divisions, as it was found in *P. pallida* and *P. muelleri* in the present study, was the ground pattern situation. Importantly, this stands in contrast to the prevailing belief that the phoronid cleavage is beyond doubt of a radial pattern.

(ii) In nearly all the phylogenies, the different species coded with the same character state are positioned on phylogenetically distant branches (Figs. 31, 32A,C). Although the phylogenies are in several parts mutually contradictory, this observation seems to indicate that the early cleavage pattern was subject to evolutionary change within Phoronida.
Some phylogenies suggest that, irrespective of what was the cleavage ground pattern situation, the respective other cleavage pattern evolved at least two times independently in the group. Strikingly, in all morphological analyses, *P. psammophila* is positioned apart from *P. vancouverensis*, *P. ijimai*, and *P. australis*, with the latter forming a monophylum together with *P. hippocrepia* (Fig. 31); and in the molecular analyses, *Ph. harmeri* resolves on a basal branch, distant from *P. pallida* and *P. muelleri* (Fig. 32). These distant positions advise thorough re-investigations of the cleavage process especially for *P. psammophila* and for *Ph. harmeri*. Such studies would be important to evaluate the perception of convergent evolution, on the one hand, but also of the performed character coding, on the other hand. This is

because, if species, which de facto show different cleavage patterns, are coded together in the same character state, the erroneous impression of a convergent evolution will be observed. As it is possible that re-investigations would reveal differences in the cleavage patterns between *P. psammophila* and *P. vancouverensis*, on the one hand, and/or between *Ph. harmeri* and *P. pallida*/*P. muelleri*, on the other hand, such studies are clearly needed for future reconstruction approaches.

Finally, the particular position of *P. ovalis* as sister taxon to all other phoronids in most phylogenies (Figs. 31B-D, 32) advises a study of the cleavage process in this species. Irrespective of the question whether *P. ovalis* represents the ancestral condition or is highly derived among phoronids (see chapter 4.1.3.4.), its phylogenetic position makes this species crucial for any ground pattern reconstruction.

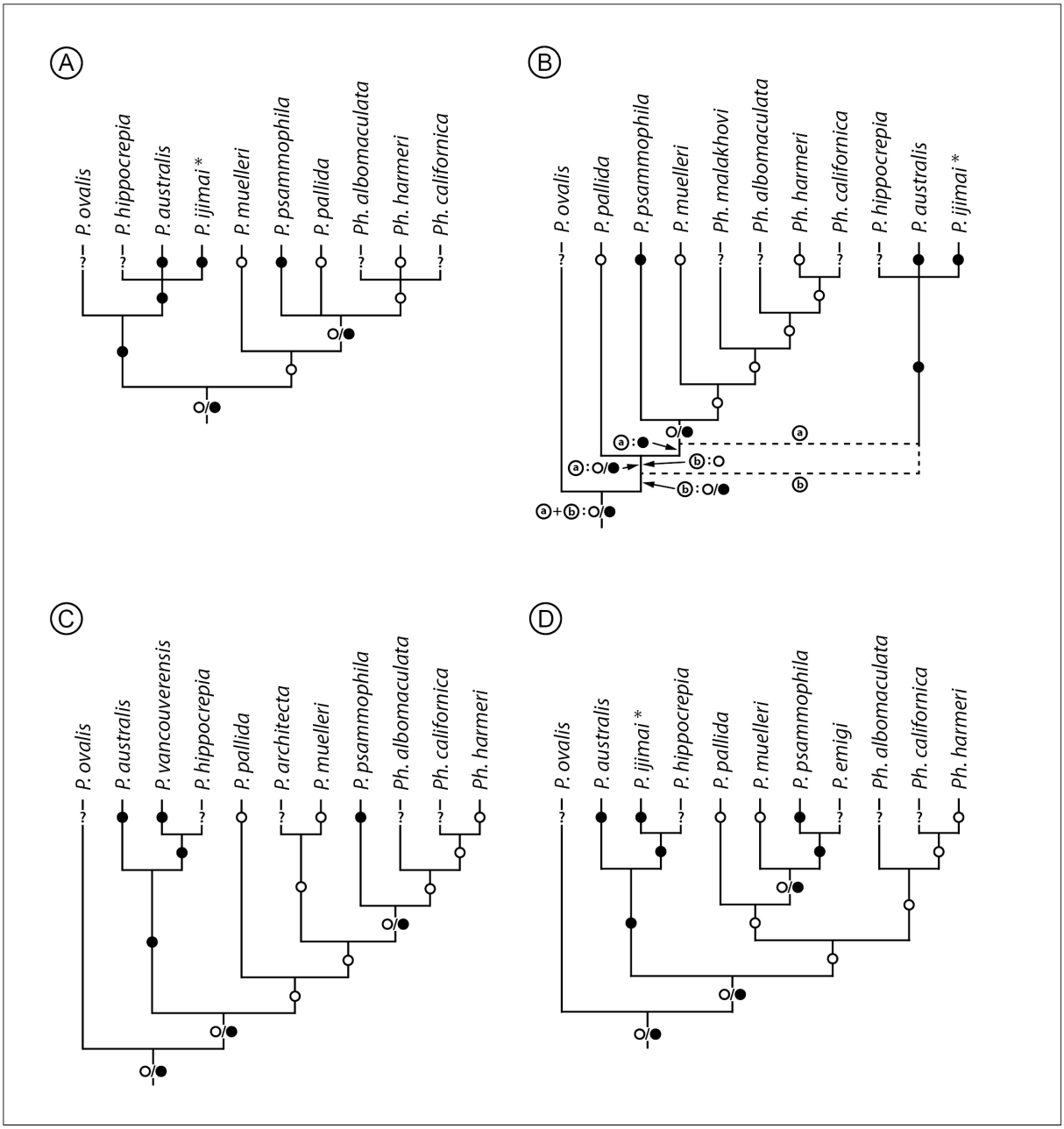

Fig. 31. Phoronid phylogenies based on morphological analyses by different authors and ground pattern reconstruction of cleavage in Phoronida. The different phylogenies show the internal relationships within the taxon Phoronida, as they were resolved in cladistic analyses of morphological datasets by different authors. For each phylogeny the cleavage pattern that was part of the ground pattern of the clade is reconstructed: the cleavage patterns found in different species are coded as two character states and mapped onto the respective topology (open circle for *P. pallida*, *P. muelleri*, *Ph. harmeri*; filled circle for *P. vancouverensis*, *P. ijimai*, *P. australis*, *P. psammophila*; data on other species are insufficient or missing and represented by '?'); subsequently, the most parsimonious evolution of the character states is traced back in time to the base of the topology (for further explanation see text). For none of the phylogenies the reconstruction gives an unambiguous outcome.

A. Phoronid phylogeny after Emig (1985) based on analysis of 11 morphological characters. *: the author considered *P. ijimai* as conspecific with *P. vancouverensis*. **B**. Phoronid relationships after Grobe (2007) based on 43 phoronid-specific and 133 total morphological characters (including outgroups). Dashed lines indicate two alternative topologies ('a' vs. 'b'), differing with respect to the position of the clade (*P. hippocrepia* + *P. australis* + *P. ijimai*) (see Grobe 2007); for each topology the reconstruction results are given. *: same as in A. **C**. Phylogeny after Santagata and Cohen (2009) based on 24 morphological characters. **D**. Phylogeny after Hirose and coworkers (2014) based on 32 morphological characters. *: same as in A.

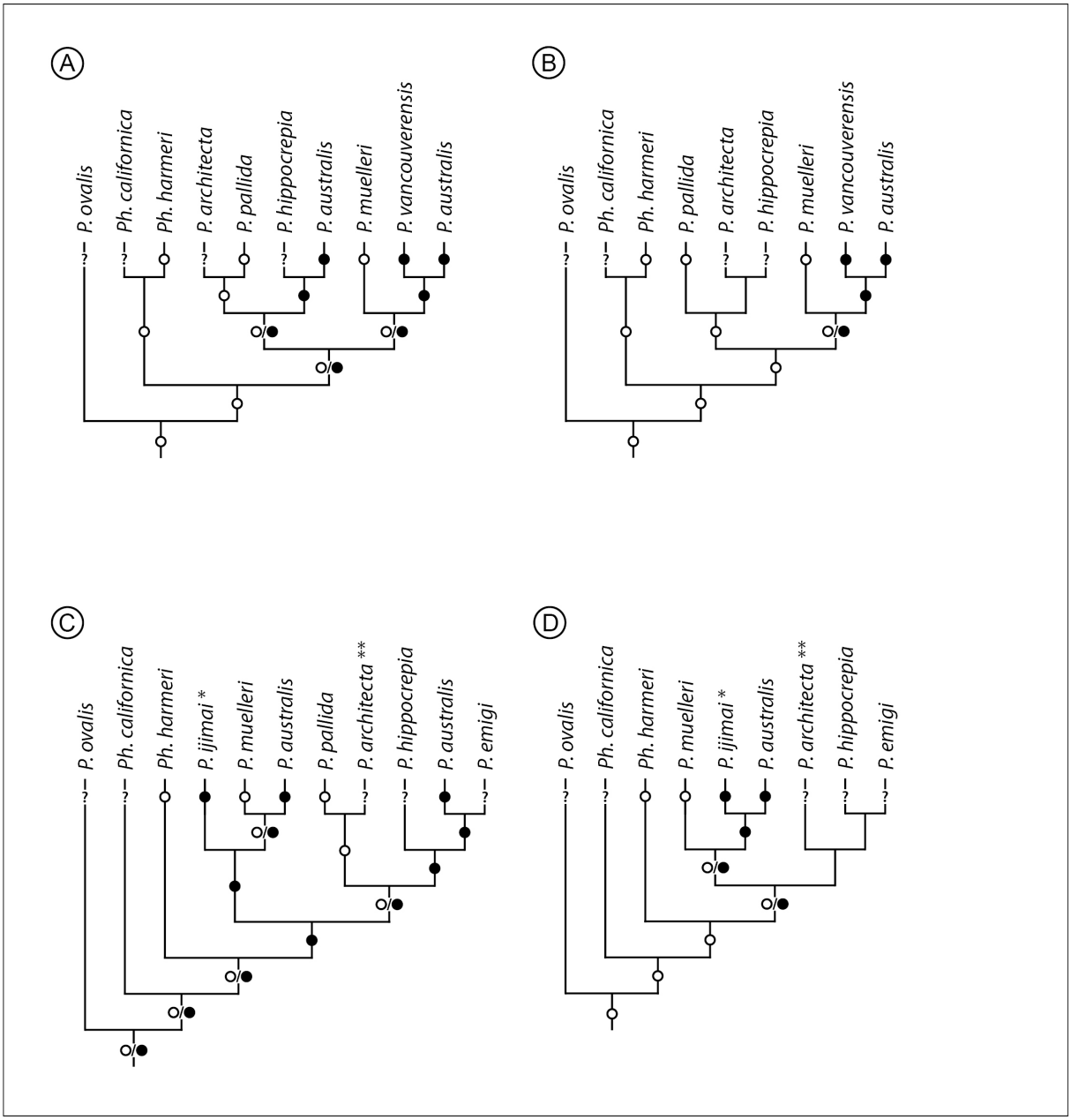

Fig. 32. Phoronid phylogenies based on molecular analyses by different authors and ground pattern reconstruction of cleavage in Phoronida. Same as in Fig. 31, but on phylogenies showing the relationships within Phoronida, as they were resolved in cladistic analyses of 18S, 28S, and *cox1* gene sequence data by different authors. The topologies in A, B, and D result in the *P. pallida*/*P. muelleri*/*Ph. harmeri* cleavage pattern as ground pattern situation for Phoronida; the topology in C gives an ambiguous outcome. Yet, note that none of the analyses included the species *P. psammophila* (see text).
A-B. Phoronid relationships after Santagata and Cohen (2009) based on analyses of 18S and 28S rDNA (A), and of 18S and 28S in combination with *cox1* (B). Note, that *P. australis* resolves as polyphyletic in A. **C-D**. Phoronid relationships after Hirose and coworkers (2014), based on 18S and 28S rRNA (C), and on 18S, 28S and *cox1* (D). Note, that *P. australis* resolves as polyphyletic in C; and that *P. pallida* was not included in D. *: the authors supported the identity of *P. ijimai* with *P. vancouverensis* (see Hirose et al. 2014); **: the authors used sequence data that had been published for *P. architecta* for their analyses, but argued for a conspecifity of *P. architecta* with *P. psammophila* (for objections against this see e.g., Santagata and Zimmer 2002; Santagata and Cohen 2009).

4.2. Cell fates in phoronids

Data on the cell fates in phoronid embryos that are based on modern single cell marking and tracing techniques, rather than observations of living embryos or fixation series (see e.g., Rattenbury 1954), are only provided by few authors and are restricted to a single species, *P. vancouverensis* (Freeman 1991; Freeman and Martindale 2002). These studies injected (or marked) individual cells of *P. vancouverensis* embryos from 2-cell to 16-cell stages, and traced the progeny of these cells up to early larval stages. In the present study, for the first time, a similar approach was used to follow the cell fates in *P. pallida* embryos: individual cells were injected at the 2-cell stage or the 4-cell stage, respectively, and traced through gastrulation: labeled embryos were analyzed at the stage of a mid gastrula after one day of development, or at a late gastrula stage after two days. A comparison of the findings between the two species allows drawing general conclusions on the axial properties in the developing phoronid embryo, the relationship of the first cleavage plane with respect to the later plane of bilateral symmetry, and the contribution of the four embryonic quadrants to the different germ layers.

4.2.1. Animal-vegetal axis and process of gastrulation

The animal-vegetal axis of the phoronid egg is defined by the position of the polar bodies (Fig. 33A): the animal pole is the site where the polar bodies are given off during the maturation division, the vegetal pole is the site directly opposite to the animal pole (see e.g., Rattenbury 1954; Zimmer 1964; Freeman 1991; Malakhov and Temereva 2000). Generally, the first two cleavage divisions pass meridionally along the animal-vegetal main axis in phoronids (Fig. 33B) (e.g., Zimmer 1964; Emig 1977; Herrmann 1986; Freeman 1991; present study). However, with progressing cleavage the polar bodies are often difficult to see (e.g., Zimmer 1964; Freeman 1991), and sometimes even become internalized into the blastocoel (Brooks and Cowles 1905; Santagata 2004a; present study). In the literature, it is widely claimed that the vegetal pole is the site of gastrulation, whereas the animal pole is the site of formation of the apical plate (see e.g., Rattenbury 1954; Zimmer 1964; Emig 1977; Herrmann 1986; Freeman 1991; Temereva and Malakhov 2007, 2012). The appropriate experiments – marking the animal or the vegetal pole of uncleaved eggs after polar body formation, and observing the position of the respective marking at gastrulating stages – has

only been performed for *P. vancouverensis*, and actually confirmed the supposed relationship (Freeman 1991).

In *P. pallida*, when one cell is loaded with dye at the 2-cell stage, about half the body of the later gastrulating embryo is stained; a marking at the 4-cell stage results in a labeling of about a quarter of the later embryo. Generally, the labeled clone of cells spanned from the region of the blastopore to the region of the (prospective) apical plate in the ectoderm (see below), and endoderm was labeled approximately in areas underlying the area of labeled ectoderm. This indicates that the first two cleavage divisions pass along an axis, which goes from the blastopore to the (prospective) apical plate. In combination with the observation that the first two cleavage planes pass through the animal-vegetal axis in *P. pallida* (chapter 3.1.1.), this suggest that one pole of the embryo becomes the site of gastrulation and the other pole becomes the site of apical plate formation. The assignment of the polarity in the animal-vegetal axis cannot be clarified by the performed experiments, however, since all cells at the initially marked stages included both, animal and vegetal, domains. Yet, there is no reason to assume the polarity would not be the same as in *P. vancouverensis* cleavage (see above).

4.2.1.1. Site of gastrulation and prospective ventral surface

The process of gastrulation is similar in all studied phoronid species (see e.g., Masterman 1900; Brooks and Cowles 1905; Rattenbury 1954; Zimmer 1964; Emig 1974b; Herrmann 1986; Freeman 1991; Malakhov and Temereva 2000; Santagata 2001, 2004a; Temereva and Malakhov 2007). Generally, it involves the flattening and thickening of the initially spherical blastula at one surface – forming the so-called "vegetal plate" or "gastral plate" (Fig. 33C-D) – and the subsequent invagination of this area into the blastocoel; this establishes a blastopore and an endodermal archenteron (Fig. 33E). For some species, it was described that in this process the invaginating archenteron virtually obliterates the blastocoel (see Freeman 1991; Malakhov and Temereva 2000), while in others a portion of the blastocoelic cavity remains present (see Rattenbury 1954; Emig 1974b; Herrmann 1986; Temereva and Malakhov 2007). In the analyzed *P. pallida* mid gastrula samples, the blastocoelic cavity mainly expands around the blastopore, whereas oppositely of the blastopore, the archenteron closes to the above lying ectoderm, and in many specimens even contacts the ectoderm. Directly following – or already contemporaneous with – the formation of the archenteron, the embryo begins to elongate in an axis that is perpendicular to the axis of the invagination (Fig. 33F-H). In many

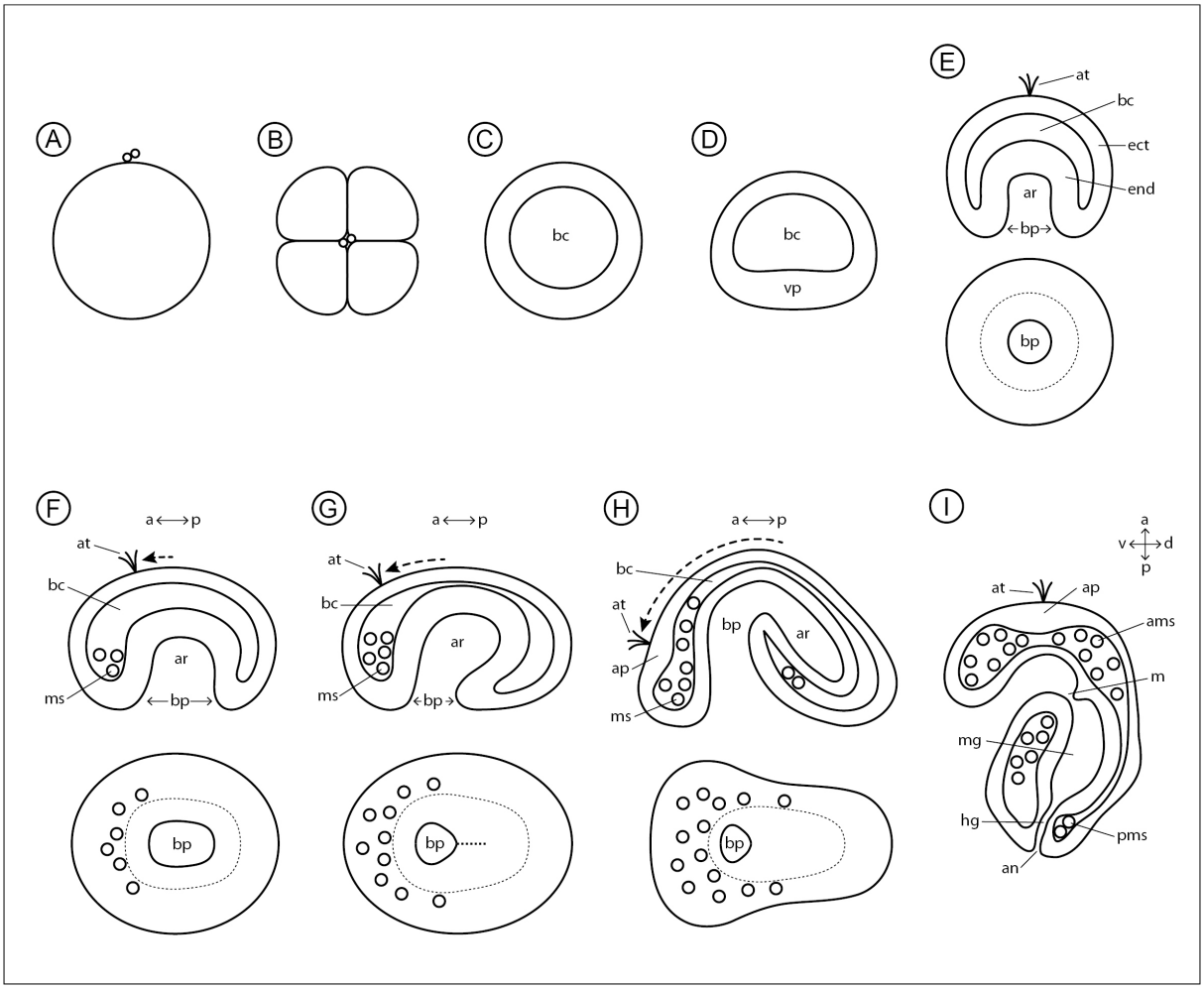

Fig. 33. Generalized scheme of phoronid development. Selected stages and major events from the zygote to the early larval stage are shown (own data and modified after different authors). The diagrams are not to scale. Abbreviations: a: anterior, ams: anterior mesoderm, an: anus, ap: apical plate, ar: archenteron, at: apical tuft, bc: blastocoel (in some species completely obliterated during gastrulation), bp: blastopore, d: dorsal, ect: ectoderm, end: endoderm, hg: hindgut, m: mouth, mg: midgut, ms: mesenchymal cells, p: posterior, pms: posterior mesoderm, v: ventral, vp: vegetal plate.
A. Zygote after giving off of polar bodies at the animal pole (small circles on the top). **B**. Cleavage process, represented by animal view of a 4-cell stage (central polar bodies indicated by small circles). **C-D**. Blastula stages: the animal pole is oriented to the top. **C**. Initial blastula with blastocoel surrounded by outer cell layer. **D**. Blastula after flattening and thickening of the vegetal surface, forming the vegetal plate. **E-H**. Successive stages of gastrulation: each given in sketches of a sagittal section (upper diagrams) and of the vegetal/ventral surface (lower diagrams; dashed line indicates archenteron outline); the apical tuft indicates the position of the animal pole. **E**. Gastrulation via invagination of vegetal plate area: a blastopore (initially located approximately centrally at the vegetal/ventral surface; lower diagram) and an endodermal archenteron are from; in some species, the invaginating archenteron completely obliterated the blastocoel (see text). **F**. Early gastrulation stage: beginning of establishment of anterior-posterior axis (anterior is to the left, posterior to the right) and of the formation of mesoderm (anterior and anteriolateral of the blastopore). The blastopore becomes expanded anterior-posteriorly, and the dorsal apical tuft site site begins to displace toward anterior (dashed arrow in upper diagram) (see text). **G**. Mid gastrulation stage. The apical tuft has further displaced (upper diagram). The blastopore has shifted to an anterior position on the ventral surface; its posterior lips have fused leaving a raphe in some species (indicated by dotted line posterior of blastopore in lower diagram). **H**. Late gastrulation stage: beginning of body regionalization. The forming preoral hood (to the left) protrudes ventrally over the blastopore. The apical tuft (associated with the apical plate) is now positioned at the anterior body end, and thus has widely displaced from its original position (compare positions in E-G; see text). The posterior trunk contains the still blind-ending archenteron. Mesenchymal cells are located within the hood, and ventrally and laterally of the archenteron in the trunk. **I**. Early Actinotrocha larva in diagrammatic sagittal section. The apical plate is situated at the top of the anterior preoral hood (to the top), a through-gut and a terminal anus are established, and the posterior mesodermal cells start to form (see text).

studies, it is described that the surface of the site of gastrulation will become the future ventral surface of the later embryo (and larva), and the elongation process establishes the anterior-posterior axis, and hence the plane of bilateral symmetry in the embryo (e.g., Rattenbury 1954; Zimmer 1964; Emig 1977; Herrmann 1986; Freeman 1991; Santagata 2001; Temereva and Malakhov 2007).

During the elongation of the embryo, the blastopore – that initially is located approximately centrally at the ventral surface (Fig. 33E) – expands anterior-posteriorly, but eventually, it becomes restricted to an anterior position on the ventral surface (Fig. 33F-H). The displacement and the secondary reduction in size, at least in part, take place by a progressive lateral fusion of the blastopore's posterior lips (Freeman 1991). These processes are often reported in the literature (see Caldwell 1885; Masterman 1900; Brooks and Cowles 1905; Rattenbury 1954; Zimmer 1964; Herrmann 1986; Malakhov and Temereva 2000; Santagata 2004a; Temereva and Malakhov 2007). In some species, the line of fusion of the posterior lips can be seen as a raphe extending from the blastopore somewhat posteriorly on the ventral surface (Fig. 33G) (see Caldwell 1885; Ikeda 1901; Brooks and Cowles 1905; Rattenbury 1954; Zimmer 1964; Freeman 1991; Temereva and Malakhov 2007). The posteriorly oriented blind-ending pouch of the archenteron, which was found in the mid gastrula samples of *P. pallida*, is also described in the literature (Masterman 1900; Brooks and Cowles 1905; Rattenbury 1964; Zimmer 1964; Herrmann 1986; Freeman 1991). Eventually, the blastopore's remaining anterior part will become the future mouth of the larva (Fig. 33I) (e.g., Emig 1977; Temereva and Malakhov 2012).

Among the analyzed *P. pallida* embryos, it was often found that the labeling of the blastopore did not include an exact half or quarter of its circumference, following the respective experiments. In particular, in all embryos that displayed a posterior staining pattern less than the respective portion was labeled; in one late gastrula specimen, the ectodermal label did not extend to the blastopore at all. These findings possibly are a result of the elongation of the ventral ectoderm and the progressive fusion of the posterior and lateral blastoporal lips. Although, this fusion was not witnessed during the present investigation, it is known for *P. pallida* gastrulation (Santagata 2001, 2004a). Seemingly, the blastopore closure can displace – and in some cases even totally exclude – posterior ectodermal domains from the late blastopore.

4.2.1.2. Apical plate and prospective posteriodorsal surface

The apical plate is a thickening of the ectoderm, which is associated with a tuft of long cilia; it represents the incipient center of the larval nervous system (see e.g., Emig 1977; Temereva and Wanninger 2012; Temereva and Malakhov 2012). In some phoronid species, the apical plate appears at the animal pole – opposite of the site of gastrulation – at the onset of gastrulation (Brooks and Cowles 1905; Rattenbury 1954; Zimmer 1964; Herrmann 1986); in others, it can be identified only during later stages of gastrulation (Emig 1974b; Freeman 1991; Malakhov and Temereva 2000). In any case, by the time of late gastrulation the apical plate is found medianly at the upper surface of the forming preoral hood, at the anterior end of the embryo (Fig. 33H) (e.g., Rattenbury 1954; Zimmer 1964; Emig 1974b; Herrmann 1986; Malakhov and Temereva 2000; Temereva and Wanninger 2012).
In fixed *P. pallida* embryos, the long cilia of the apical plate are difficult to recognize. Immunostaining against α-tubulin, however, allowed visualizing the columnar shape of the ectoderm cells in the thickened apical plate. Performing such stainings on embryos at a late gastrula stage showed that the apical plate is located at the median upper region of the hood, like in other phoronids. In embryos, that were only at a mid gastrula stage, in contrast, the same stainings did not reveal a thickened ectodermal region yet. This indicates that the apical plate of *P. pallida* is formed at some time between the first and the second day of development.

Different authors have assumed that the positional shift of the apical plate during gastrulation – from a location opposite of the vegetal pole toward a location at the embryo's anterior end – is a consequence of an anterior-posteriorly directed growth process in the ectoderm that lies posterior to the prospective apical plate forming area (e.g., Rattenbury 1954; Zimmer 1964; Herrmann 1986); the resulting expansion would displace the plate into an anterior position, and the expanding ectodermal region itself would become the future dorsal and posterior surface of the later embryo and larva (Fig. 33F-H). Some authors have interpreted this as the bending of the animal-vegetal axis (compare the position of apical tuft relative to blastopore in Fig. 33E-H) (see Rattenbury 1954; Temereva and Malakhov 2007). Importantly, this process implies that the ectoderm that makes up the dorsal side in the late gastrula – thus the surface opposite to the site of gastrulation – stems from an ectodermal region that is initially located posteriorly of the animal-vegetal axis – and thus posterior of the site of gastrulation – before the growth process.

In embryos that were marked for single cell tracings, no additional anti-tubulin stainings was performed; however, the approximate position of the apical plate could be deduced from its location in the immunostained samples. In fact, in nearly all marked embryos that were analyzed at a late gastrula stage, the labeled as well as the unlabeled ectodermal domains passed through the median, upper area of the preoral hood (but see below); hence, indicating a partial marking of the apical plate. In some embryos, the quality of the marking even allowed identifying the columnar cell shapes in the plate. In marked embryos that were analyzed at the mid gastrula stage, on the other hand, – when the apical plate is not yet morphologically identifiable – the dorsal ectodermal label always passed through an area opposite of the blastopore, which was somewhat shifted toward one side of the embryo (the prospective anterior end). Particularly obvious, in such samples marked at the 4-cell stage, the ectodermal label always extended to a median and slightly anterior area of the dorsal surface. These findings seem to indicate that the respective area in the mid gastrula corresponds to the region of the apical plate in later gastrula. Moreover, for both gastrulation stages, the experiments showed that in all those embryos, which generally displayed posterior or posterior-lateral staining patterns, a major region of the dorsal ectoderm was labeled – and in all cases this region spanned from the posterior body end up to the anterior (prospective) apical plate. These observations indicate that the dorsal surface of the embryo in fact stems from a growth of the ectoderm, which is located posteriorly of the apical plate/animal pole, supporting previous morphological descriptions (Rattenbury 1954; Zimmer 1964; Herrmann 1986). In addition, the findings indicate that already at the mid gastrula stage the animal pole (the prospective apical plate) is somewhat displaced toward anterior.

Furthermore, the results suggest that normally all four cell of the 4-cell embryo contribute to the formation of the apical plate. However, there may be rare exceptions. In very few late gastrula samples, and only in those, which have been injected at the 4-cell stage, the ectodermal label of the lateral surface of the hood did not reach up to its median midline; although without anti-tubulin staining the apical plate was not unambiguously identifiable, it appeared as if in these specimens the plate was not marked. Possibly, interactions between the cells in the embryo are involved in initiating the formation of the apical plate. The cleavage process in *P. pallida* normally results in the animal most derivatives of the cells of the 4-cell stage to come to lie at the animal pole of the embryo, however, there is variation in this process (see chapter 3.1.1.). One can only speculate on the possibility that the observed cases without apical plate labeling might represent embryos in which the cleavage divisions had

passed with such a high degree of irregularity that the animal derivatives of the injected cell did not end up in the proper position to receive a putative inductive signal for apical plate formation. Unfortunately, for *P. vancouverensis*, the staining results of the apical plate are not described in detail (see Freeman 1991; Freeman and Martindale 2002). Since in *P. vancouverensis* the cleavage divisions – especially in cells of the animal hemisphere – exhibit a remarkable degree of variability (see chapter 3.3.), staining data on its apical plate would be very interesting to compare to *P. pallida* embryos.

4.2.2. Plane of bilateral symmetry and its relationship to first cleavage plane

With the beginning of the process of elongation that establishes the anterior-posterior axis, and the blastopore that marks the prospective ventral body surface, phoronid embryos possess a plane of bilateral symmetry. Characteristic for the axial properties in phoronid embryos, however, the animal-vegetal axis of the egg and of the early cleavage stages does correspond neither to the future dorsoventral axis nor the future anterior-posterior axis of the gastrulating embryo or later larva. This is due the growth process during gastrulation, which displaces the animal pole from its position initially dorsal and opposite of the vegetal pole toward the anterior body end, while the vegetal pole remains at the ventral body side (chapter 4.2.1.). This has to be kept in mind, when interpreting the results of the in-vivo labelings.

Labeling experiments in which a blastomere is marked at the 2-cell stage enable conclusions on the relationship between the plane of the first cleavage division and the later body axes in the embryo. In *P. pallida*, the region of cells that inherit the dye following such experiments can occupy different positions in the later embryo. These positions corresponded largely between the embryos at mid gastrula and at late gastrula stages, and allowed the identification of different staining patterns. These staining patterns were characterized according to the position of the label relative to the anterior-posterior and the left-right axes of the embryo: anterior, anterior-lateral, lateral, posterior-lateral, and posterior staining patterns were distinguished. Moreover it was found that in embryos that displayed posterior or posterior-lateral patterns a major region of the dorsal(-posterior) ectoderm was labeled, whereas in those with anterior or anterior-lateral staining patterns only a minor, anterior and/or lateral, part of the dorsal ectoderm was marked. Importantly, this asymmetry is a consequence of the mentioned growth process in the dorsal ectoderm (see above), and clearly not of a variable orientation of the first cleavage plane relative to the dorsoventral axis.

Consequently, these results show that the first cleavage plane does pass variably with respect to the anterior-posterior and the left-right axes, and hence the plane of bilateral symmetry, in the later embryo. Respectively two of the observed staining patterns roughly represented complementary pairwise matches: these are the anterior and the posterior, the anterior-right and the posterior-left, the anterior-left and the posterior-right, and the right and the left patterns. From this it can be generalized that the plane of the first cleavage division passed differently either roughly perpendicularly (anterior/posterior patterns), along (right/left patterns), or – in one of two ways – obliquely (anterior-right/posterior-left or anterior-left/posterior-right patterns) relative to the later bilateral symmetry plane. These findings are also supported by the injections performed at the 4-cell stage: nearly all of the resulting labelings could be identified as a half-pattern of one of the staining patterns obtained from the markings at the 2-cell stage.
However, it has to be noted that the observed matches between two complementary staining patterns were not in all cases perfect, and furthermore, the observation was made that markings also in anterior, posterior, and lateral staining patterns were never exactly symmetrical. Due to the low sample size (2-cell stage labeling: n = 22; 4-cell stage: n = 20) it cannot be decided whether these observations are a result of variation in the exact distribution of the labeled cells in the same staining pattern or of individual differences in cell proliferation and growth processes during gastrulation; or whether they indicate the presence of staining patterns, which have not been found in the present investigation.

Although the pattern of early cleavage divisions displays some considerable differences between *P. pallida* and *P. vancouverensis* embryos (see chapter 4.1.), cell fate studies on the latter species have revealed a situation very similar to the results found in the present investigation. Also in *P. vancouverensis*, when a cell is marked at the 2-cell stage, this results in a labeling that can differently occupy an anterior, an anterior-lateral, a lateral, a posterior-lateral, or a posterior position in the later gastrula or early larval stage (Freeman 1991). The described staining patterns even correspond in some details with the patterns observed in *P. pallida* (see Freeman 1991). It can be concluded that in *P. vancouverensis* the first cleavage plane can have the same four general orientations with respect to the later bilateral symmetry plane, as it was observed in *P. pallida*.

One interesting difference between *P. vancouverensis* and *P. pallida*, however, lies in the frequency with which the different staining patterns are observed after a marking at the 2-cell

stage. For *P. vancouverensis*, Freeman found that about 70% of the specimens displayed an anterior or a posterior staining pattern, whereas only 8% were of the lateral patterns, and the rest divided on the different oblique patterns (n = 61 gastrula and n = 32 larval stages; Freeman 1991). Interestingly, the anterior body region (that is, anterior or anterior-lateral staining patterns) was found to be stained 2.8 to 6.3 times more often than the posterior region (that is, posterior or posterior-lateral staining patterns) (different numbers refer to different marking techniques in Freeman 1991). Although the present data on *P. pallida* are based on a smaller sample size (n = 22 mid and late gastrula stages), they seem to indicate that there is no such outstanding correlation between the first cleavage plane and later anterior-posterior axis. In the available samples of 2-cell injected embryos, only about 36% of the specimens displayed an anterior or a posterior staining pattern, while equally abundant an anterior-right or a posterior-left pattern was observed (see Table 4A); the remainders divide on the left/right and the anterior-left/posterior-right patterns, respectively. Hence, in more than 70% of all cases, the prospective anterior-posterior axis (the plane of bilateral symmetry) was oriented either perpendicularly or skewed clockwise relative to the first cleavage plane, in an animal view of the embryo.

Freeman (1991) discussed these findings with regard to the specification of the anterior-posterior axis, and concluded that this axis probably is not specified by the different localization of cytoplasmic factors (otherwise, the anterior and posterior regions would be marked in roughly equal numbers). In contrast, the author suggested that events that happen during the early cleavage process may play a role in positioning the later anterior-posterior axis with reference to the animal-vegetal axis of the embryo; these initial events, however, must be very labile, since the act of marking can bias the result and cause an anterior regional specification (see Freeman 1991). The final determination of the anterior-posterior axis is achieved only after gastrulation and presumably requires cell-cell interactions (Freeman 1991).

If events that take place during the early cleavage are involved in the initial specification of the anterior-posterior axis, the differences, which are encountered in the frequencies of the staining patterns between the two species, might be related to the differences in their cleavage pattern. While in *P. vancouverensis* the third cleavage cycle produces two cell tiers that are aligned roughly along the animal-vegetal axis (see chapter 3.3.), in many *P. pallida* embryos these third divisions generate a clockwise shift of the animal cell tier relative to the vegetal tier, when seen from the animal pole (see chapter 3.1.1.). Possibly, this shift in cell alignments has consequences for the initial positioning of the prospective anterior-posterior axis in

relation to the animal-vegetal axis of the embryo. Despite the small sample size, it should be noted that in the *P. pallida* material, anterior or anterior-lateral staining patterns were encountered only 1.7 times more often than posterior or posterior-lateral patterns. This could suggest that the initial specification process is less labile in *P. pallida*, than in *P. vancouverensis* (see above).

4.2.3. Germ layers

4.2.3.1. Ectoderm

In all marked *P. pallida* embryos, irrespective of the stage of injection, a distinct area of the ectodermal germ layer – the outer epithelium of the gastrula – was stained. The stained regions differed in position between different embryos, and the details were discussed in previous sections (chapters 4.2.1., 4.2.2.). Likewise, for *P. vancouverensis* it was reported that a marking at 2-cell or 4-cell stages in all cases resulted in a stained region in the future ectoderm; only injections at 8-cell and 16-cell stages led, in some cases, to samples without an ectodermal labeling (see Freeman 1991; Freeman and Martindale 2002). These data suggest that all four embryonic quadrants of the phoronid embryos contribute to the generation of the ectoderm.

The apical plate, which is a derivate of the ectoderm, was already discussed (see chapter 4.2.1.2.).

For *P. vancouverensis*, Freeman and Martindale (2002) furthermore could show that also the hindgut (the "intestine" in their terminology) is an ectodermal derivative. Their labeling data indicate that it forms as an ingression of the posterior ectoderm. This contradicted previous authors, who had assumed the hindgut to develop from the archenteron, and hence, to be of endodermal origin (e.g., Masterman 1900; Brooks and Cowles 1905; Rattenbury 1954; Emig 1977). In the analyzed *P. pallida* specimens, a functional through-gut was not yet present, but in some of the late gastrula samples the anlage of the hindgut was already developed. This anlage was labeled only in specimens that displayed a staining at the posterior body region. Since in such specimens, however, the posterior ectoderm as well as the posterior region of the endodermal archenteron was stained, the origin of the hindgut from either of these two germ layers cannot be clarified. On the other hand, it should be mentioned that in some of the given figures the epithelium of the archenteron appears to be continuous with the epithelium

of the forming hindgut (see Figs. 15H,L, 17L, 18D). This could indicate that the hindgut in *P. pallida* forms as outgrow from the posterior archenteron. Notably, however, the given figures are representations of embryos stained only for nuclei (besides the injected staining dye), while the cell shapes and tissues are not visible. Histological sections and stainings could help to solve the origin of the hindgut.

4.2.3.2. Endoderm

At gastrulation, the endodermal germ layer is represented by the invaginating archenteron (Fig. 33E-H). Every *P. pallida* embryo injected at the 2-cell stage showed a later staining in the archenteron (n = 22), and the same was true for very most injection experiments at the 4-cell stage (n = 20). Generally, the labeled clones in the ectoderm reached through the blastopore onto the endoderm, and the endoderm was stained in similar body regions where also the above lying ectoderm was marked (see also Freeman 1991). However, in several embryos, the endoderm label was found slightly displaced of – or extending somewhat farther than – the ectodermal label. This is possibly a result of different growth processes in the two germ layers.

Only following the injections at the 4-cell, one late gastrula specimen was found that did not have a staining in the archenteron (5% of 20 cases); and additionally, in one early gastrula sample the endodermal labeling was ambiguous as it included cells at the blastoporal rim but did not extend into the archenteron (5% of 20 cases). Both these cases were embryos in which generally the posterior and dorsal ectodermal regions were marked.
Interestingly, in *P. vancouverensis*, cases without marking in the endodermal germ layer already were encountered when one cell was marked at the 2-cell stage (22% of n = 32; Freeman 1991); these cases seem to occur irrespective of the ectodermal staining patterns, yet noteworthy, in three out of four embryos that showed the posterior ectoderm stained (see Freeman 1991). After injections at the 4-cell stage even 40% of the later larvae showed no staining of the endoderm (n = 20; Freeman and Martindale 2002). (Injections at the 8-cell and the 16-cell stages led to about 50% larvae without endodermal labeling; n = 32 and n =57, respectively; Freeman and Martindale 2002.)
This is surprising, since in *P. vancouverensis* – as well as in *P. pallida* – the first two cleavage divisions pass along the animal-vegetal axis, and thus all the cells in the injected stages inherit presumptive endodermal (= vegetal) domains (see Freeman and Martindale 2002).

Furthermore, for *P. vancouverensis* it is known that all the cells at the 2-cell and the 4-cell stages have the potential to form endoderm (Zimmer 1964). To explain the cases without endodermal marking Freeman and Martindale (2002) argued that this potential may not always be exhibited, and that under some circumstances cell interactions during the early embryogenesis might prevent certain cells from forming endoderm. The encountered samples without endodermal marking in *P. pallida* could indicate that a similar mechanism is at work. The rare occurrence of such cases, however, may also suggest a generally stricter correlation between the vegetal pole and its de fact contribution to the endoderm in *P. pallida*, than in *P. vancouverensis*.

4.2.3.3. Mesoderm

The mesodermal germ layer is represented by mesenchymal cells, which are found within the blastocoel in embryos during gastrulation (Fig. 33F-H). In *P. pallida* embryos at a mid gastrula stage, mesenchymal cells only were found anteriorly and laterally of the archenteron. At the late gastrula stage, these cells were more numerous and located within the forming preoral hood and ventrally and laterally of the archenteron inside the trunk. More mesenchymal cells were observed than previously has been reported for *P. pallida* gastrulation stages (see Santagata 2004a).

In all but one marked *P. pallida* embryos, irrespective of the stage of injection, stained mesenchymal cells were found; in all embryos, other mesenchymal cells were not stained. This indicates that usually all four embryonic quadrants contribute to the formation of mesodermal cells. Generally, more stained mesenchymal cells were found in embryos that had a labeling of the anterior body region (anterior or anterior-lateral staining patterns), than in those with the posterior body region labeled (see below). The only encountered embryo without a marking of mesenchymal cells also was of a posterior dorsal staining pattern.
In the mid gastrula samples, stained mesenchymal cells generally were found in close proximity to stained endoderm and ectoderm, and as mentioned, only anteriorly and laterally of the archenteron. This suggests that these cells actually originated at (or close to) the sites where they are observed, and is consistent to morphological descriptions on phoronid development, which reported that the mesenchymal cells originate in the regions anteriorly and/or anteriolaterally of the archenteron (see e.g., de Selys-Longchamps 1902; Brooks and Cowles 1905; Rattenbury 1954; Zimmer 1964; Herrmann 1986; Malakhov and Temereva

2000). In the late gastrula samples, in contrast, several marked mesenchymal cells were found close to unlabeled endodermal and ectodermal areas, and vice versa. This suggests that these mesenchymal cells must have migrated within the blastocoel to come to these positions. Such migration of mesenchymal cells is described in many studies (e.g., Brooks and Cowles 1905; Rattenbury 1954; Zimmer 1980; Herrmann 1986; Malakhov and Temereva 2000; Freeman and Martindale 2002).

The question whether mesodermal cells in phoronids originate from cells of the endodermal or the ectodermal germ layer is very interesting. In most embryological studies, it was assumed that the mesenchymal cells that are found at the edges of the blastopore have their origin from the endodermal archenteron (e.g., Rattenbury 1954; Emig 1974b; Zimmer 1980; Herrmann 1986; Malakhov and Temereva 2000; Temereva and Malakhov 2007). In contrast, for *P. vancouverensis* the experiments of Freeman and Martindale (2002) found strong indications that the mesenchymal cells actually originate from ectoderm as well as endoderm, at sites of boundaries between these germ layers in the embryo. Such ectodermal-endodermal boundaries are present at the blastopore, but also at the site of contact between midgut and hindgut. The authors proposed that the contact between ectoderm and endoderm – at site where these two germ layers are juxtaposed – might set up a local signaling system, which would have the morphogenetic effect of changing the behavior of cell on each side of the boundary and causing them to differentiate into mesodermal cells (see Freeman and Martindale 2002). Importantly, their findings suggest that the mesodermal precursors are not specified during the early cleavage process (Freeman and Martindale 2002). Interestingly, these experimental data are in consistence with morphological descriptions that reported two sources of mesoderm in phoronids (Zimmer 1980; Malakhov and Temereva 2000; Temereva and Malakhov 2007; Temereva and Tsitrin 2013). While the anterior mesoderm originates from the wall of the archenteron during gastrulation (Fig. 33F-H), the posterior mesoderm develops only in the almost fully developed larva, at the junction area between midgut and hindgut (Fig. 33I).

In the present study, the origin of the mesodermal cells from either endoderm or ectoderm is difficult to assess, since all cells up to the 4-cell stage inherit presumptive ectodermal as well as endodermal domains (see above). In some mid gastrula samples, however, marked mesenchym cells were found in apparently close association with marked endoderm, in positions where the above lying ectoderm was not marked. This could suggest their origin from the endoderm. On the other hand, one mid gastrula specimen was encountered, which

had a staining in the ectoderm that reached to the blastopore but did not extend into the archenteron (see chapter 4.2.3.2.); as the exact boundary between ectoderm and endoderm at the blastopore is not identifiable, it could be possible that the few stained mesenchymal cells found in this specimen originated from the ectoderm. Clearly, markings in more advanced cell stages are needed to come to more reliable conclusions on this point in *P. pallida*. Since, additionally, the oldest analyzed gastrula samples were just on the verge of developing a hindgut, it is possible that the development of the posterior mesoderm – at the contact zone between midgut and intestine (see Freeman and Martindale 2002; Temereva and Malakhov 2007) – had not yet started. This could explain the difference observed with respect to the number of stained mesenchymal cells between anterior and posterior staining patterns, and might suggest that this asymmetry declines during the later development.

4.3. Phoronid development and spiral cleavage

The present study allowed for new insights in the process of early cleavage as well as the fates of early blastomeres in phoronid embryos (chapters 4.1., 4.2.). In this chapter, these findings are discussed in the context of a close phylogenetic relationship between Phoronida and Spiralia.

As introduced, today there is nearly constant support from molecular phylogenetic reconstructions, that Phoronida belong within the protostomian taxon Lophotrochozoa (which itself possibly is equivalent to the older taxon Spiralia, or a subtaxon of Spiralia; see Hejnol 2010), and there, in particular are nested among the trochzoan spiralian groups Mollusca, Annelida, and Nemertea (see Fig. 1D) (e.g., Dunn et al. 2008; Baguñà et al. 2008; Helmkampf et al. 2008b; Paps et al. 2009a,b; .Hausdorf et al. 2010; Nesnidal et al. 2010).

This phylogenetic position of Phoronida implies that the process of cleavage and the development of phoronids derived from the so-called "spiral cleavage". As mentioned, this stands in contrast to the nowadays predominant perception of the phoronid development as radial or biradial spiral (e.g., Zimmer 1973, 1997; Emig 1977, 1982, 1990; Herrmann 1996; Ax 2001; Brusca and Brusca 2003; Ruppert et al. 2004; Nielsen 2005; Temereva and Malakhov 2012; but see Dohle 2013).

Spiral cleavage is generally characterized as a combination of (i) a specific cell division pattern during the early cleavage process, and of (ii) a specific fate map, with particular fates of individual blastomeres in the early embryo (e.g., Siewing 1969; Henry and Martindale 1999; Nielsen 2010, 2012).

In fact, development along these typical characteristics of spiral cleavage displays large and complex correspondences between embryos of the trochozoan taxa Mollusca, Annelida, and Nemertea, embryos of some groups of Platyhelminthes, as well as of Entoprocta (e.g., Henry and Martindale 1999; Nielsen 2004, 2005, 2012; Hejnol 2010; Dohle 2013). The distribution of these taxa on distant branches of the current Spiralia/Lophotrochozoa suggests that spiral cleavage along these characteristics was the ancestral condition for the entire clade Spiralia/Lophotrochozoa (see Fig. 1D).

In addition, however, the current phylogeny of Spiralia/Lophotrochozoa places several other taxa within the clade (Fig. 1D), for which correspondences to spiral cleavage exist only for some characteristics of the developmental process, or for which no resemblances to spiral cleavage are known at all. Often these taxa are poorly studied and data do not suffice to draw

reliable conclusions. For Gnathostomulida, for example, there is only one publication on the early cleavage and it reports a spiral cleavage pattern (Riedl 1969), however, no information on the cell fates is available. Rotifera and Bryozoa, on the other hand, have an early cleavage that is markedly different from the spiral pattern (Tannreuther 1920; Hyman 1959; Lechner 1966; Boschetti et al. 2005; Nielsen 2012), however, the cell lineages seem to indicate some resemblances to the condition in spiral cleavage (Lechner 1966; Schiemann and Hejnol 2011; Vellutini and Hejnol 2014). The cleavage of Gastrotricha shows differences to the spiral pattern, but different authors disagree whether there are traces of spiral cleavage (see Sacks 1955; Teuchert 1968). And in Brachiopoda, the cleavage pattern as well as the early cell fates show differences between the different subgroups (Freeman 1993, 1995, 1999, 2000, 2003). The brachiopod cleavage and development generally are characterized as radial (e.g., Nielsen 2012); although, in some rhynchonelliform and linguliform species, the axes of cleavage divisions are variable and non-radial or irregular cell arrangements are known (Freeman 1995, 2003), and an early investigator observed a spiral cleavage, at least in some eggs (Conklin 1902).

This allows the conclusion that the spiral cleavage mode of development – despite its conservative nature in some lineages – was modified, and presumably lost, on different levels of its characteristics, in other spiralian/lophotrochozoan lineages (e.g., Boyer and Henry 1998; Henry and Martindale 1999; Hejnol 2010). This can shifts the focus of interest beyond the fascinating correspondences of the spiral cleavage in some animal taxa, toward the question of how the spiral cleavage mode of development evolved in other spiralian groups. Such a broad comparative perspective can allow new insights in the evolution of one of the most fascinating developmental modes found in animals. To cover the various possible evolutionary gains and losses of parts of the spiral cleavage at different levels, it is necessary to “deconstruct” the character complex of spiral cleavage, as is true for all morphological and developmental characters (see Scholtz 2010).

In the herein performed approach, the process of early cleavage and the cell fates in phoronid embryos are treated as separate sub-characters (or better, sub-character sets) of spiral cleavage. In separate sections (chapters 4.3.1., 4.3.2.,), they are compared in their different features to the situation found in spiral cleaving embryos (with an emphasis on the trochozoan spiralians Mollusca, Annelida, Nemertea). Finally, the correspondences and the differences to spiral cleavage are discussed with regard to the process of establishment of cell fates and embryonic axes during development (chapter 4.3.3.).

4.3.1. Cleavage process

One of the most surprising results of the present investigation – and largely contradictory to precious conceptions of phoronid cleavage – is the finding that embryos of the phoronid species *P. pallida* and *P. muelleri* undergo a process of early cleavage which is characterized by alternating oblique orientations of the mitotic spindles with respect to the animal-vegetal axis, a third cleavage cycle that passes in a dextral direction, alternating sinistral and dextral orientations of the subsequent cleavage cycles, 8-cell and 16-cell stages in which the blastomeres are arranged in four shifted cell tiers of four cells each, and the location of a four blastomere tier at both poles in many embryos, at least up to 64-cell stage. In these characteristics, the cleavage pattern of the two phoronids shows remarkable correspondences to the pattern of spiral early cleavage (see also chapter 1.3.1.). As mentioned, for the phoronid species *Ph. harmeri* a very similar cleavage pattern was described and it even was characterized as spiral (Rattenbury 1951, 1954). On the other hand, the present study found that the *P. pallida* and *P. muelleri* cleavage process displays a degree of variability that unknown for typical spiral cleavage (see below). Furthermore, the early cleavage in embryos of *P. vancouverensis* shows surprising differences to the cleavage in *P. pallida* and *P. muelleri*, as well as to the spiral cleavage pattern (see below).

Several authors have argued that observations of spirally appearing blastomere arrangements in phoronid embryos would result from artificial re-alignments of the cells, only after the cell divisions had passed in proper radial equatorial or meridional divisions, and that such re-alignments may be caused by some compression of the embryos and its cells (Zimmer 1964, 1973; Emig 1974b, 1977, 1990; Herrmann 1981, 1986). Herein, this objection is rejected on base of the performed high-resolution 4D analyses (which clearly would have shown such re-alignments), and the large consistency between the observation of oblique cleavage axes, on the one hand, and the cell arrangements in embryos between successive cleavage cycles, on the other hand. However, some effect of the process of compactation on the definitive cell alignments possibly exists (see chapters 4.1.1., 4.1.2.).

Moreover, in the present study, the oblique cleavage pattern could be identified by the analyses of the mitotic spindles – which were aligned in oblique axes with respect to the animal-vegetal axis – as well as the observation of oblique cell divisions following these oblique spindle axes. This situation is markedly different from a so-called “pseudo spiral cleavage” in which the mitotic spindles are aligned in axes along or perpendicular to the

animal-vegetal axis, and, only after undergoing cell divisions along these axes, the blastomeres re-align into a shifted, and apparent spiral, arrangement (this is found in some cnidarians; e.g., Siewing 1969; Tardent 1978). In fact, Herrmann (1986) argued that in phoronids the presence of such a "pseudo spiral cleavage" – over a proper spiral cleavage – could be revealed by statistical evaluations over many different embryos. Such detailed analyses were done in the present study, and in contrast revealed the presence of a pattern of de facto alternating oblique cleavage divisions.

Admittedly, in *P. pallida* as well as in *P. muelleri*, the oblique nature of the third cleavage cycle is not very distinct – the cleavage axes are inclined more to the animal-vegetal axis than the equatorial plane of the embryo, and thus in an angle less than 45 degree –, while only with the fourth cycle, the cleavage divisions become more pronouncedly oblique. Interestingly, such a situation is not without precedent in spiralian embryos. In the annelid *Owenia collaris*, for example, a highly similar pattern, with a very weakly dextrally inclined and somewhat variable third division cycle, but a cleavage that becomes more pronouncedly spiral with the following divisions, is described (Smart and von Dassow 2009). Also among echiurid annelids, the third cleavage axes are not strongly inclined against the animal-vegetal axis (Newby 1932). These examples show that pronouncedly oblique third cleavage divisions – in a proper angle of 45 degree dextral to the animal-vegetal axis – are no essential condition of spiral cleavage.

In this context, it should be noted that even the dextral orientation of the third cleavage cycle is not invariable in spiralians. Among molluscs and annelids, there are examples of embryos, which show a sinistral – instead, of a dextral – third cleavage cycle. In different species, this sinistral orientation either is invariantly present (Arenas-Mena 2007), or different embryos cleave either dextrally or sinistrally (Luetjens and Dorresteijn 1995). Yet, the orientation can even differ between different blastomeres in the embryo (Sandig and Dohle 1988).

Additionally, in both phoronid species, a conspicuous process of cell elongations was found to precede the oblique divisions from the third cleavage onward. Thereby, the blastomeres expand obliquely with respect to the animal-vegetal axis, and their apices get drawn out oriented in the direction of the subsequent cell division. An essentially similar process is described for the spiral cleavage divisions among serpulid annelids (Groepler 1986). Herein – and therein (see Groepler 1986) – these oblique cell elongations are interpreted as a clear indication for an oblique nature of the cleavage divisions.

The circumstance that the phoronid cleavage generally does not generate a 4-cell stage with distinct blastomere size differences, nor very pronouncedly smaller animal blastomeres and larger vegetal blastomeres – thus, literally "micromeres" and "macromeres" – in later cell stages, should not be used as indication against the possible presence of spiral cleavage (see also Rattenbury 1951; Zimmer 1964; Herrmann 1986). Although the cleavage process in many mollusc and annelid embryos, in fact, goes with the formation of an unequal 4-cell stage – with one markedly larger blastomere than the other three – as well as smaller animal micromeres and larger vegetal macromeres (e.g. Nielsen 2004, 2012), the spiral pattern of cleavage is different in this regard between different spiralian lineages.
For example, in several annelid lineages (polychaetes, echiurids, sipunculids), spiral cleavage does not generate pronounced size differences between the blastomeres, up to the 16-cell or even the 32-cell stage (e.g., Mead 1897; Treadwell 1901; Torrey 1903; Woltereck 1904; Newby 1932; Groepler 1986; Nielsen 2005; Arenas-Mena 2007). Some studies related this to the small size and the poor yolk content of the eggs in these animals (see Woltereck 1904; Groepler 1986). Notably, the general appearance and the blastomere arrangements of such early annelid embryos are very similar to the arrangements observed in *P. pallida* and *P. muelleri* embryos. In nemerteans, the cells at the 4-cell stage are generally equally sized, and later cleavage cycles typically generate animal "micromeres" that are even somewhat larger than the vegetal "macromeres" (Maslakova et al. 2004 and references therein). Also in several platyhelminth lineages and generally in entoprocts, the spiral cleavage process does not generate pronounced early cell size differences (Nielsen 2005; Martín-Durán and Egger 2012; Merkel et al. 2012).

Some authors have argued against the presence of spiral cleavage in phoronids also on base of the absence of "cross furrows" and a so-called "spiralian cross" during embryogenesis (Herrmann 1986; Temereva and Malakhov 2012).

In the terminology of the present study, a cross furrow can be defined as two perpendicularly running polar furrows, one at each pole of the embryo. In fact, cross furrows are found in many spiralian embryos (e.g., Nielsen 2012). In these embryos at the 4-cell stage, the blastomeres of one pair of oppositely situated non-sister cells form a polar furrow at one pole, while the blastomeres of the second pair of opposing non-sister cells form a polar furrow at the opposite pole – resulting in two perpendicularly oriented polar furrows, which have a cross like arrangement in a pole view of the embryo, hence, a cross furrow. This cross furrow

– the two perpendicular polar furrows at the two opposing poles – usually persist throughout the spiral early cleavage process, and at least for molluscs and some nemerteans, it also plays an important role in the establishment of quadrant identities and cell fates (van den Biggelaar and Guerrier 1979; van den Biggelaar 1977; Boring 1989; Maslakova et al. 2004) (see chapter 4.3.3.).

In the present study, neither in the *P. pallida* nor the *P. muelleri* 4-cell stage, a cross furrow like arrangement of two polar furrows was observed: some embryos have a single polar furrow reaching from one pole to the other, but most specimens display a central opening between the blastomeres. Although some *P. vancouverensis* specimens displayed two perpendicularly running polar furrows, those occurred only among various other patterns. At later cell stages, two perpendicularly oriented polar furrows were found only very rarely, while generally in all three species polar furrows are structures of variable occurrence, which can be found at only the animal or only the vegetal pole, or at both poles, in different embryos. If present, these furrows are mostly short in length. The performed 4D recordings, moreover, showed that the polar furrows are formed during the compactation of the embryo, between two successive division cycles, apparently as by-products. For *P. pallida*, the data even showed that polar furrows occur more frequently with advancing cleavage cycles and thus decreasing cell sizes (chapter 4.1.1.2.3.).

However, it has to be noted that also among spiralian embryos – even those with equal cleavage divisions – cross furrows are not always present. Among annelids, for example, species with a 4-cell stage having a polar furrow only at the vegetal pole (but a small space at the animal pole) are known (Torrey 1903), and in others the 4-cell embryo differently has either a single polar furrow that reaches from one pole to the other, or it displays a small central opening between the four cells (Groepler 1986 and references therein). Notably, the latter example is very similar to the situation found in *P. pallida* or *P. muelleri* embryos. Among nemerteans, which generally have an equal 4-cell stage, on the other hand, cross furrows are usually lacking, and occur only in few species (Maslakova et al. 2004 and references therein). Therefore, cross furrows or polar furrows are clearly no essential characteristic of a spiral cleavage pattern.

The term “spiralian cross”, on the other hand, refers to certain pattern of blastomeres – which are arranged in the appearance of a cross – that can be found at the animal pole in some trochozoan embryos (Nielsen 2001; Maslakova et al. 2004; Merkel et al. 2012). These spiralian crosses have received attention by many embryologists and are even used in some

morphological phylogenies, however, recent critical contribution have shed much doubt on the phylogenetic significance of these structures, at least on a higher taxonomic level (Jenner 2003, Maslakova et al. 2004). For example, they show that different spiralian cross patterns, which often are considered to be taxon-specific[*], can be identified simultaneously on the same spiralian embryo, or that the cells forming the cross are not homologous between different spiralian embryos (Jenner 2003; Maslakova et al. 2004). Furthermore, a spiralian cross is not essentially present in all species undergoing spiral cleavage; its presence or absence seems to be determined by the relative cells sizes within the embryo as well as the timing of formation of the different micromere quartets (which potentially will give rise to the spiralian cross patterns) (Maslakova et al. 2004). In phoronid embryos, the blastomeres are of roughly equal size, and the cleavage cycles pass approximately synchronous but with some irregular asynchronies in later cleavages. Therefore, phoronid embryos in general are unlikely to display conspicuous spiralian cross like cell patterns. In fact, such cross patterns were not identified in the present study, nor are they described in the literature. This, however, clearly cannot be used as an indication against a spiral cleavage.

In the paragraphs ahead, previous objections against the presence of a spiral cleavage pattern in embryos of *P. pallida* and *P. muelleri* were discussed and rejected. Based on the good evidence from molecule based phylogenetic reconstructions that Phoronida are nested within Spiralia/Lophotrochozoa (see above; Fig. 1D), it seems appropriate to suggested that the correspondences that are found between the early cleavage in *P. pallida* and *P. muelleri* and the pattern of spiral cleavage can serve as morphological support for such a spiralian position of Phoronida.

On the other hand, however, it has to be emphasized that the phoronid early cleavage process – even as it was found in *P. pallida* and *P. muelleri* – differs in one major aspect from typical spiral early cleavage. Spiral cleavage is generally characterized by a precise pattern in respect of blastomere sizes, timing of cleavage divisions, and orientations of cleavage axes; the cleavage divisions pass in a predictable sequence and in a highly stereotypic pattern of alternating oblique orientations. The oblique division pattern is only broken with the sixth or the seventh cleavage cycle, when a particular cell within the embryo divides in a bilateral fashion (see van den Biggelaar et al. 1997; Lambert 2008; Grande 2010).

[*] Often, a so-called “molluscan cross” and an “annelid cross” pattern are distinguished, but also a “nemertean cross” – and even an “entoproct cross” – can be described (reviewed in Maslakova et al. 2004; Merkel et al. 2012).

The phoronid cleavage process, in contrast, involves a degree of variability (and irregularity) with respect to the individual cell divisions that is virtually unknown from typical spiralians. In phoronids, embryos with intermediate cell numbers do occur irregularly, there is no consistent sequence in the individual cell division between different embryos, and even exceptional cases of distinct asynchronies during already the initial cleavage cycles result in normally appearing embryos. It should be noted that already Rattenbury (1951, 1954) mentioned the absence of a consistent sequence of cleavage divisions in *Ph. harmeri* as difference to typical spiral cleavage. In the present investigation, it was also found that different cells differ in the exact inclination of the cleavage axis, divisions in orientations clearly deviating from the alternating oblique cleavage pattern do occur, blastomere arrangements in tiers of four cells are only apparent up to the 16-cell stage, a tier of four blastomeres at each of the embryo's pole is only predominantly present over other patterns, and all this irregularity appears to increase with advancing cleavage cycles. It is due to this variability that the notation system that is commonly used for spiral cleaving embryos does not seem applicable on the phoronid cleavage.

This general variability of the cleavage process was also observed in the third species that was investigated in this study. In addition, however, in contrast to *P. pallida* and *P. muelleri*, the early cleavage in *P. vancouverensis* involves a roughly equatorial orientation of the third division cycle, and subsequent division cycles that tend to pass alternately meridional and equatorial in the vegetal hemispheric cells, but highly irregularly in the animal hemispheric cells. This pattern of cleavage shows evident differences to the spiral cleavage pattern, however, on the other hand, also deviates from a typical radial cleavage pattern (see chapter 4.1.2.). As mentioned, studies on other phoronids rarely paid much attention to variability and irregularities. Although there are some differences between different phoronids, and for some species there are indications that at least the third cleavage passes obliquely, generally a radial pattern of cleavage divisions was reported for phoronids (see chapter 4.1.3.3.).

Based on the good molecule-based phylogenetic evidence for a position of Phoronida within Spiralia/Lophotrochozoa (see above; Fig. 1D), it seems appropriate to suggested that the cleavage pattern present in *P. pallida*, *P. muelleri*, and presumably *Ph. harmeri* – with its correspondences to the pattern of spiral cleavage, but possibly also with its degree of variability unknown from other spiralians – was the ancestral condition of cleavage in Phoronida, while the pattern(s) found in other phoronids are the result of evolutionary

transformations of the cleavage process within the group. Importantly, the reconstructions of the ground pattern of phoronid cleavage, which have been performed on the base of internal phylogenies of phoronids, in parts support this conclusion, while – in no case – they reject this conclusion (see chapter 4.1.3.5.).

In this context, it is important to repeat that also the spiral pattern of early cleavage – despite its high degree of conservativeness in some lineages – within all spiralian lineages is also subject to variation at various levels (see e.g., Boyer and Henry 1998; Henry and Martindale 1999; Hejnol 2010). As was shown in the paragraphs ahead, this refers, for example, to the cell sizes within the embryo, the degree of obliqueness of the cleavage axes, the orientations of the cleavage cycles, the occurrence of cross furrows, or the occurrence and appearance of spiralian cross patterns.

Beyond this, however, there are repeated cases among different spiralian lineages, which show that the spiral pattern of early cleavage can be modified even beyond recognition – and hence, been secondary lost – in the course of evolution. A widely known example is the cephalopods among molluscs, which lost the spiral cleavage and instead evolved a discoidal mode of cleavage (e.g., Arnolds 1974; Marthy 1975; Wadeson and Crawford 2003). This loss of spiral cleavage in cephalopods is presumptively related to the high yolk content of the cephalopod eggs. Notably, among phoronids, most divergences to a spiral pattern of early cleavage are found in those species, which form relatively large and yolk-rich eggs – in opposition to generally smaller and yolk-poorer eggs in *P. pallida*, *P. muelleri*, and *Ph. harmeri* – and which, in addition, undergo early development inside the parental lophophore (see chapter 4.1.3.4.). At present, it is not clear whether yolk-poor or yolk-rich eggs and reproduction via free-spawning or brooding of the embryos was the ancestral mode of phoronid development (see chapters 4.1.3.4., 4.1.3.5.). Yet, it is an appealing thought that the modifications (and losses) of the ancestral cleavage pattern in some phoronid species may be related to the evolution of a longer period of lecithotrophic development, involving yolk-richness of the eggs and brood protection, within the clade Phoronida.

Finally, it has to be noted that also among platyhelminths, the ancestral pattern of spiral cleavage was lost in several lineages. Presumably in relation to the evolution of ectolecithal eggs, it was replaced by very different modes of cleavage in different platyhelminth groups, in some lineages evolving even into a disperse cleavage going without a regular pattern of divisions (so-called “Blastomerenanarchie”) (Martín-Durán and Egger 2012).

4.3.2. Cell fates

In mollusc, annelid, nemertean, platyhelminths, and entoproct embryos, spiral cleavage is – besides its pattern of early cleavage divisions – also characterized by the presence of specific cell fates and a characteristic fate map. Largely consistent between these groups, the same blastomeres – which are individually addressable on base of the cell lineage and the spiralian notation system – will give rise to specific body regions, particular germ layers, and the different morphological structures in the later animal (e.g., Marcus 1939 after Nielsen 2005; Boyer et al. 1998; Henry and Martindale 1998; Henry et al. 2004; Maslakova et al. 2004; Ackermann et al. 2005; Hejnol et al. 2007; Meyer et al. 2010).

For phoronids, data on the cell fates are available for two species: *P. pallida* (present study) and *P. vancouverensis* (Freeman 1991; Freeman and Martindale 2002). Notably, the pattern of early cleavage is very different in these species: while the *P. pallida* cleavage process shows many similarities with the pattern of spiral cleavage, this is not the case for the *P. vancouverensis* cleavage (see chapter 4.3.1.).
For *P. vancouverensis*, it was found that after single cell labelings of unselected blastomeres up to the 16-cell stage, no two identical clones were generated (Freeman and Martindale 2002). This indicates the absence of a specific fate map in the *P. vancouverensis* embryo – very different to the situation in the above-mentioned spiralian groups – and also suggests that the cell fates are not established during the early cleavage process (Freeman and Martindale 2002) (see chapter 4.3.3.).
For *P. pallida*, the present study analyzed the cell fates only for the 2-cell and the 4-cell stages. The results allow a comparison to the situation found in spiralian embryos with respect to the relationship between the first cleavage planes and the later body axes, and the contribution of the individual blastomeres to the germ layers.

4.3.2.1. Relationship between first cleavage planes and later body axes

The first two cleavage divisions pass through the animal-vegetal axis of the egg – in phoronids as well as in spiralian embryos – and generate the four embryonic quadrants of the embryo; respectively named “A” to “D” in the spiralian nomenclature. In spiralian embryos, these four quadrants typically contribute in a specific pattern to the (ectodermal) body regions in the later larval/adult animal. In general terms, the lineages of the quadrants A and C will

give rise to the left and right body regions, respectively, while the lineages of B and D will generate the ventral/anterior and the dorsal/posterior body regions, respectively (e.g., Henry and Martindale 1999; Nielsen 2010, 2012). Although there are some differences in the exact clonal contributions between different spiralian embryos (due to varying sizes and placements of the animal micromere quartets that generate these ectodermal body regions; see Henry and Martindale 1999), this principle alignment of quadrantal cell fates is known from mollusc and annelid embryos (Henry and Martindale 1999; Nielsen 2004; and references therein), and it was also found in a palaeonemertean species (Maslakova et al. 2004), and in platyhelminths (Henry et al. 1995; Boyer et al. 1998).

Importantly, this pattern implies that there is a constant relationship between the first two cleavage planes and the later body axes in spiralian embryos, and moreover, that the dorsoventral (anteroposterior) axis lies in a plane going through the embryonic quadrants B and D (Henry and Martindale 1999; Nielsen 2012). Since the first cleavage division produces the two progenitor blastomeres “AB” and “CD”, respectively, this implies that the later dorsoventral (anteroposterior) axis is always oriented about 45 degree counterclockwise relative to the first cleavage plane, in an animal view of the spiralian embryo (Henry 2002). An interesting exception, however, is known from some nemertean species. There it was found that the dorsoventral axis can take either a counterclockwise or a clockwise 45 degree orientation relative to the first cleavage plane; this is probably related to the absence of cross furrows in these species (Henry and Martindale 1994, 1998; Henry 2002) (see chapter 4.3.3.).

Phoronid embryos undergo a number specific of growth processes during gastrulation, which involve also the displacement of the animal pole from a position opposite of the blastopore toward an anterior position, and thus a bending of the animal-vegetal axis (see chapter 4.2.1.). Due to this, the axial properties in phoronid embryos/larvae are difficult to relate to the body axes in the spiralian embryos.

Nonetheless, the available data on *P. pallida* as well as *P. vancouverensis* show that there is no constant relationship between the first cleavage plane and the later anterior-posterior and left-right axes – and hence, to the later plane of bilateral symmetry – in the phoronid embryo/larva (Freeman 1991; present study). The data were generalized and it was concluded that in both species the plane of the first cleavage division can pass differently oriented either perpendicularly, or along, or – in one of two ways – obliquely relative to the later bilateral

symmetry plane (chapter 4.2.2.). This variability is surprisingly different from the situation in the above-mentioned spiralian embryos*.

One interesting difference was observed between the two phoronids. While in *P. vancouverensis* embryos the prospective anterior-posterior axis is mostly oriented perpendicularly to the first cleavage plane (Freeman 1991), in *P. pallida* also a high percentage of embryos was found in which this axis was oriented clockwise relative to the first cleavage plane. This difference may be related to the different cleavage division patterns in these two species (see chapter 4.2.2.). The finding for *P. pallida* is surprising, as it may indicate the frequent presence of a relationship, which appears to be the opposite, than the one that is found in most spiralian embryos (although, as mentioned, in some nemertean species without cross furrows, a similar orientation may be found; see above). It has to be noted, that the findings are based on a small sample size, and further data are needed to come to a reliable conclusion on the relative abundances of the different orientation patterns in *P. pallida*.

4.3.2.2. Germ layers

4.3.2.2.1. Ectoderm and Endoderm

In most spiralian embryos, all four embryonic quadrants form ectoderm as well as endoderm. The ectoderm (and its derivatives, as for example, apical ganglion/organ or foregut and hindgut) typically is generated by the cells of the first three generations of animal micromere quartets (which are given off from the vegetal macromeres between the third and the fifth cleavage cycles); and the endoderm usually originates from descendants of the four vegetal macromeres after the fifth cleavage cycle (e.g., Henry and Martindale 1998; Henry et al. 2004; Maslakova et al. 2004; Ackermann et al. 2005; Hejnol et al. 2007; Meyer et al. 2010; Nielsen 2012). An exception (that probably is derived from this situation), is known for (polyclad) platyhelminths, in which only one of the four macromeres generates the endoderm (Boyer et al. 1998).

* It should be noted that cases of a variable relationship between the first cleavage plane and the later dorsoventral axis are known from some deuterostome animals, as for example, different species among sea urchins and enteropneust hemichordates (Jeffery 1992; Henry et al. 2001).

Likewise, in phoronids, the ectoderm is formed by all four embryonic quadrants. The position of their individual contribution to the ectoderm, however, does not show the strict correlation with respect to the later body axes, as it is found in spiralian embryos (see previous section).
The data for *P. pallida* indicate that normally also all four cells of the 4-cell stage contribute to the apical plate; however, there might be rare exceptions (data for *P. vancouverensis* are not available) (see chapter 4.2.1.2.). For *P. vancouverensis*, Freeman and Martindale (2002) could show that the hindgut is of ectodermal origin, thus disproving previous descriptions (data for *P. pallida* are not conclusive) (see chapter 4.2.3.1.).
Only for *P. vancouverensis*, the cell fates were studied beyond the 4-cell stage (Freeman and Martindale 2002). It was found that after the marking of an unselected blastomere at the 8-cell stage, 50% of the specimens showed a later labeling of the ectoderm, but not of the endoderm (n = 32; Freeman and Martindale 2002). This is the same ratio one would expect for a spiral fate map. Following the same experiment at the 16-cell stage, however, a similar ratio was observed (51% of n = 57; Freeman and Martindale 2002), while the expected spiralian ratio would be approximately 75% of the specimens. On the other hand, both experiments could also result in rare cases that showed no labeling of the ectoderm (Freeman and Martindale 2002). This is clearly different from the spiralian fate map.

In phoronids, the formation of the endoderm takes place via the invagination of the "vegetal plate" area into the blastocoel, during gastrulation (see chapter 4.2.1.). Hence, this process generally includes the vegetal most blastomeres of the embryo. The observed cell lineages with respect to endoderm, however, differ in important aspects from the typical spiralian fate map.
As mentioned, in *P. vancouverensis* the number of cases in which a cell of the 16-cell stage does not contribute to the endoderm, is higher than one would expect for a spiralian embryo (data for *P. pallida* are not available) (Freeman and Martindale 2002). Yet moreover, although all cells of the 4-cell embryo have the potential to form endoderm (Zimmer 1964), for *P. vancouverensis* there are frequent cases in which a single blastomere of the 2-cell stage or of the 4-cell stage does not contribute to the endoderm (22% of n = 32 2-cell stages in Freeman 1991; 40% of n = 20 4-cell stages in Freeman and Martindale 2002). For *P. pallida*, on the other hand, such cases are not observed for the 2-cell stage, and only very rarely for the 4-cell stage (5 or 10% of n = 20 4-cell stages) (see chapter 4.2.3.2.). Freeman and Martindale (2002) suggested that under some circumstances cell interactions during the early embryogenesis might prevent certain blastomeres from forming endoderm. Although still

different from the typical spiralian fate map, it may be noted that the situation in *P. pallida* – a species more closely resembling the spiral pattern of early cleavage, than *P. vancouverensis* – in the respect of the endodermal cell lineage seems to be more similar to the spiralian fate map, than the situation in *P. vancouverensis*.

4.3.2.2.2. Mesoderm

In spiralian embryos, mesoderm originates from two different sources (Lillie 1895): the two types of mesoderm are called "ectomesoderm" and "endomesoderm", respectively. The origin of the ectomesoderm is somewhat variable between different trochozoan species (it arises from cells of different quadrants as well as of different generations of micromere quartets); the endomesoderm, in contrast, typically stems from the D quadrant cell of the fourth micromere quartet (the cell 4d in the spiralian nomenclature, also called "mesentoblast") (reviewed in Boyer et al. 1996; Meyer et al. 2010). Since ectomesoderm and endomesoderm as well as a mesentoblastic 4d cell also are found in platyhelminths (Boyer et al. 1998), these features are probably plesiomorphic for the entire Spiralia/Lophotrochozoa (see Fig. 1D).

Focusing on the origin of the mesoderm in *P. vancouverensis*, Freeman and Martindale (2002) have found no specific cell lineage-bound origin of the mesoderm up to the 16-cell embryo, and no indications for a single mesentoblast. Their results suggest that the cell lineages that give rise to the mesoderm are not established during these early cleavage cycles. Interestingly, however, the authors found strong indications that the mesoderm in *P. vancouverensis* originates from ectodermal as well as endodermal sources, similar to the situation in spiralians (Freeman and Martindale 2002). These mesodermal cells are established relatively late during development. The two types of mesoderm are generated only after the onset of gastrulation at ectodermal-endodermal boundaries within the embryo (see chapter 4.2.3.3.). The authors suggested the presence of a local signaling system that would be triggered by the contact between ectodermal and endodermal cells at the boundaries, and that would induce cells of both germ layers to differentiate into mesodermal cells (Freeman and Martindale 2002).

In the present study, cell fate tracings on *P. pallida* were only performed up to the 4-cell stage, when in spiralians there is no separation of an ectodermal and an endodermal cell lineage yet. Labeled mesodermal (mesenchymal) cells were found in (almost) all specimens,

suggesting an origin of the mesoderm from all four embryonic quadrants. Although there are single indications that mesodermal cells can originate form ectoderm as well as endoderm (see chapter 4.2.3.3.), as in *P. vancouverensis*, this clearly needs further investigation and cell labelings at more advanced stages.

4.3.3. Cleavage pattern and cell fate establishment

The previous sections have shown that the early cleavage pattern in *P. pallida* and *P. muelleri* (and presumably also in *Ph. harmeri*) in some important points is corresponding to the pattern of spiral cleavage (oblique mitotic spindles relative to the animal-vegetal axis, dextral orientation of third cleavage cycle, alternation of spindle orientations and cleavage divisions after each round of division, identifiable blastomere arrangements in tiers of four cells). On the other hand, it clearly differs from typical spiral cleavage in its degree of variability and the absence of a strict stereotypic spiral cleavage pattern (chapter 4.3.1.). The cleavage pattern of *P. vancouverensis* (and possibly in some other phoronid species) is even greatly different from a typical spiral pattern. The cell fates in the phoronid embryos, on the other hand, are to a large degree similar between *P. pallida* and *P. vancouverensis*; however, they show radical differences to the typical spiralian fate map (for example, in the variable alignments of the initial cleavage planes relative to the later bilateral symmetry plane) (chapter 4.3.2.).
Under the perspective that Phoronida are nested within Spiralia/Lophotrochozoa, for which there is currently good evidence from molecular phylogenetic reconstructions (see above), it seems as if the spiral cleavage mode of development has undergone evolutionary modifications on the lineage to Phoronida (or possibly already to the clade Phoronida + Brachiopoda; see Fig. 1D). The pattern of early cleavage was then possibly further modified within Phoronida (chapters 4.1.3.5., 4.3.1.). One can speculate on the possibility that the variability of the early cleavage process, and the cell fate differences observed to a typical spiral cleavage, are related to the evolution of a different mode of cell fate and axes establishment in Phoronida, than it is present in many spiralian embryos.

In spiralian embryos, the pattern of the cleavage divisions is associated with the specific fate map, via the early establishment of quadrant identities during embryogenesis, and here, in particular, the specification of one quadrant as the D quadrant of the embryo. At least for molluscs and annelids, there are good indications that, once the D quadrant is specified, it will act as the organizer of the dorsoventral axis and of the positional fates of the adjacent

quadrants A, B, and C in the embryo (van den Biggelaar et al. 1997; Boyer and Henry 1998; Lambert 2008; Grande 2010). The cell lineage of the D quadrant will typically form the later dorsal/posterior body regions and, via the mesentoblast, will generate the animal's entire endomesoderm (chapter 4.3.2.). In annelids, molluscs, and (polyclad) platyhelminths, it is also a cell from the D quadrant lineage, which starts the first bilateral division in the embryo (van den Biggelaar et al. 1997; Lambert 2008; Grande 2010) (see chapter 4.3.1.).
The process of D quadrant specification, however, is different in different spiralian embryos, and far from being universally understood. Two principle mechanisms are known: specification by unequal distribution of cytoplasmic determinants, and specification by cell-cell interactions (e.g., Freeman and Lundelius 1992; Henry and Martindale 1999).

The first mechanism appears to be associated with a cleavage process, in which already at the 4-cell stage, one blastomere is markedly larger than the other three. It is known from such mollusc and annelid species (e.g., Guerrier et al. 1978; Dorresteijn et al. 1987; Henry and Martindale 1987; Render 1989). The early inequality is achieved either by an asymmetric shifting of the cleavage spindles, the formation of a temporary cytoplasmic protrusion (a so-called polar lobe) that is inherited by only one cell after the division, or a combination of both these events (Henry and Martindale 1999). The unequal divisions segregate vegetally localized (but still unknown) cytoplasmic factors, which are inherited by the largest blastomere, and specify this cell to become the D quadrant. Different authors have suggested this very early mode of specification to represent the ancestral mechanism, at least for Annelida (Dohle 1999), or to be a derived condition, that evolved several times independently within different mollusc and annelid lineages, from specification via cell interactions (Freeman and Lundelius 1992; van den Biggelaar et al. 1997).

Specification via cell interactions is associated with a spiral cleavage that generates a 4-cell stage with equally sized blastomeres, and it acts only later during cleavage. It is best known for a number of mollusc embryos (e.g., van den Biggelaar and Guerrier 1979; van den Biggelaar 1977, 1996; Martindale et al. 1985; Boring 1989). In these equal-cleaving molluscs, the D quadrant is specified only between the fifth and the sixth cleavage cycles, when the vegetal macromeres intrude far into the embryo's interior, and one of them establishes cell contacts with the derivatives of the first quartet micromeres. These inductive interactions along the animal–vegetal axis specify the macromere to become the D quadrant. Interestingly in these molluscs, this process involves cross furrows, which bias the specification. Although

every macromere has the potential to become the D quadrant, those two that form the vegetal polar furrow are in a more central, and therefore more favorable position to establish the animal cell contacts, and hence, usually one of them becomes specified as the D quadrant (van den Biggelaar and Guerrier 1979; van den Biggelaar 1977; Boring 1989).

By a series of elaborate experiments, the necessity of inductive interactions between the vegetal blastomeres and the progeny of the first quartet animal cells in the embryo, for the specification of the D quadrant was also shown for the equal-cleaving heteronemertean species *Cerebratulus lacteus* (Henry 2002). Also in this species every quadrant can become the D quadrant, however, the embryos lack cross furrows. Apparently, without this sterical predisposition each quadrant has an equal chance of becoming the D quadrant (Henry 2002). This is reflected by the fact that the dorsoventral axis can take two different orientations relative to the first cleavage plane in this nemertean (Henry and Martindale 1994, 1998; Henry 2002) (chapter 4.3.2.1.). However, the exact timing of the inductive interactions is not known for *C. lacteus* (Henry 2002). The author only observed that the blastocoel, which is present up to the 32-cell stage, becomes obliterated by the 64-cell stage, and proposed that the indications may take place between the fifth and the sixth cleavage, similar to the situation in the above molluscs (Henry 2002). Interestingly, for the palaeonemertean species *Carinoma tremaphoros*, the presence of cross furrows, and the same invariant relationship between first cleavage and later dorsoventral axis as in mollusc and annelid embryos, were described (Maslakova et al. 2004) (chapter 4.3.2.1.). However, it is unknown how the cell fates and the quadrants are specified in this species. At least up to the 64-cell stage, the authors found that the embryo remains hollow and the blastocoel separates the animal from the vegetal blastomeres (Maslakova et al. 2004).

To my knowledge, the mechanism of inductive cell interactions was never properly shown for annelid embryos (but see van den Biggelaar et al. 1997). It should be noted that some equal-cleaving annelids have embryos, which possess a large blastocoel that is described to persist at least up to the 64-cell stage (e.g., Woltereck 1904; Smart and von Dassow 2009). It seems as if this central blastocoel would prevent cell contacts between the animal and the vegetal blastomeres, and it is unclear how the mechanism described for equal-cleaving molluscs could work in such embryos.

The differences, which have been found between phoronids and typical spiral cleaving embryos with respect the variability of the cleavage process as well as to the cell fates in the

embryo, seem to indicate that in the phoronid development there is no close association between the early cleavage and the later cell fates.

The present study suggests that the mechanisms of cell fate and axes specification must be to some degree independent of a regular pattern of cleavage divisions or of strict blastomere arrangements in the embryo. However, it is unclear if the mechanisms work via cell interactions or via cytoplasmic factors. The fact that phoronids cleave equally could indicate the former. However, cross furrows – structures that possibly were present and had a function in quadrant establishment in the ancestral trochozoan embryo (see Maslakova et al. 2004) – are of variable occurrence and therefore supposedly of no significance in phoronid development (see chapters 4.1.3.2., 4.3.1.). Furthermore, embryos of all three investigated species form a central blastocoel by the 8-cell stage, which (although it is different in extension) was observed up to the latest analyzed stages (the 64-cell stage in *P. pallida* and *P. muelleri*, and the 32-cell stage for *P. vancouverensis*), and even was described to persist up to the gastrulation (see Zimmer 1964; Herrmann 1986; Santagata 2004a). Cell contact between the animal and the vegetal blastomeres during the cleavage, as they are formed in equal-cleaving mollusc embryos, were never seen, nor reported.

For *P. vancouverensis*, Freeman (1991) could show by an elaborate series of isolation experiments, that the specification of the anterior-posterior axis probably depends on inductive cell interactions during the gastrulation process, although already by (unknown) events during the early cleavage, this axis seems to be set up with reference to the animal-vegetal axis (chapter 4.2.2.). The specification along the animal-vegetal axis, on the other hand, appears to rely on the localization of cytoplasmic factors by the 8-cell stage as well as on inductive interactions between animal and vegetal zones in the embryo (Freeman 1991). The specification of the mesoderm – which, at least with respect to the endomesoderm, is linked to the D quadrant lineage in spiralians – appears to take place only with and post gastrulation in *P. vancouverensis* (Freeman and Martindale 2002).

It is interesting that both mechanisms – the specification of the anterior-posterior axis as well as of the mesodermal cells – apparently act only during gastrulation in *P. vancouverensis*, and both rely on cell interactions at this time. While, however, for the specification of mesodermal cells the presence of a local signaling system, triggered by interactions between endodermal and ectodermal cells at the blastopore and the midgut/hindgut boundary, has been suggested (Freeman and Martindale 2002), it is unclear what interactions cause the axis specification.

For example, it is possible that the two mechanisms are somehow associated. It should be noted that mesodermal cells form asymmetrically – only at the anterior and the anteriolateral regions at the blastopore – in phoronids (chapter 4.2.3.3.), although ectodermal-endodermal cell contacts clearly are present around the whole blastopore circumference. This could suggest the presence of inductive interaction only at the anterior(-lateral) blastopore areas (or of stronger inductive signals at these areas). This asymmetry could either build on an anterior-posterior polarity that is already present in the embryo at this state of gastrulation, but it could represent a polarization that is also involved in the final establishment of the anterior-posterior axis (Freeman 1991). Interestingly, Freeman (1991) found the axis determination to start at the anterior region of the *P. vancouverensis* embryo in gastrulation.
On the other hand, the cell interactions establishing the anterior-posterior axis could be independent of endodermal-ectodermal cell contacts within the epithelium. Notably, for *P. vancouverensis* (as well as for many other phoronid species; see chapter 4.2.1.1.), it is described that the blastocoel becomes obliterated during the gastrulation, when the invaginating archenteron extends far into the embryo and comes in contact with the cells of the opposite (animal/dorsal) ectodermal surface (Zimmer 1964; Freeman 1991). This observation could indicate the presence of cell interactions between invaginating endodermal cells and opposing ectodermal cell along the animal-vegetal axis, and a possible role of such interactions in establishing the body axes and cell fates. In *P. pallida*, an archenteron-ectoderm contact during gastrulation was found in many specimens (however, it is unclear whether it is established in all cases). The hypothesis could be experimentally tested, for example, by injecting an oil drop into the blastocoel prior to gastrulation, which could prevent such animal-vegetal cell contacts.

In total, the available data suggest that the mechanism(s) specifying the cell fates in phoronids are largely different from the different mechanisms known from mollusc, annelid, and nemertean embryos (see above). There are good indications that the establishment of the anterior-posterior axes and of the mesoderm relies on cell interactions that act only during gastrulation, and not during different stages of the cleavage process. If the current phylogenetic placement of Phoronida within Spiralia/Lophotrochozoa, and here in particular nested among Trochozoa, is correct, the modification of the specification mechanism(s) probably evolved on the lineage to Phoronida, or possibly already on the lineage to the clade Phoronida + Brachiopoda (see Fig. 1D) (notably, there are interesting similarities in the general fate map and the timing and mode of axes specification between *P. vancouverensis*

and in particular rhynchonelliforms among brachiopods; see Freeman 2003, 2007). This modification could be interpreted as a heterochronic shift of cell fate specification from a point of time during the cleavage process as in molluscs, annelids, and nemerteans, to a point of time after the initiation of gastrulation. One can speculate on the possibility that this heterochronic shift is related to the variability observed in the early cleavage process in phoronids. The late timing of cell fate specification in phoronids might allow the cleavage process to gain a degree of freedom that is unknown from other spiralians, because a stereotypic early cleavage pattern and strict blastomere arrangements are no longer necessary to generate a "working" embryo. Possibly, this could explain why different patterns of cleavage can be present in the taxon Phoronida (chapters 4.1.3.), and why several phoronid species apparently have lost the characteristic oblique division pattern of spiral cleavage.

5. Zusammenfassung

Gegenstand der vorliegenden Arbeit ist die vergleichende Untersuchung des Furchungsprozesses und der Zellschicksale verschiedener Vertreter der Phoronida (Hufeisenwürmer). Ausgangspunkt der Studie sind einerseits widersprüchliche Literaturangaben, andererseits neue phylogenetische Erkenntnisse. Die Furchung der Phoroniden wird heutzutage meist als Radiärfurchung charakterisiert. In der Literatur finden sich jedoch auch wiederholte – dieser Charakterisierung widersprechende – Berichte von Furchungsteilungen, die schräg zur animal-vegetativ Achse des Keims verlaufend, oder von Embryonen mit nicht-radiären, sondern spiralig angeordneten Blastomeren. Für die Art *Phoronopsis harmeri* wurde sogar Spiralfurchung beschrieben (Rattenbury 1954). Oftmals wurden derartige Beobachtungen jedoch als Unregelmäßigkeiten innerhalb eines radiären Furchungsmusters oder als gar als Artefakt interpretiert. Demgegenüber stehen neue phylogenetische Erkenntnisse. War die Einordnung der Phoronida im phylogenetischen System lange Zeit umstritten, weisen kladistische Analysen auf Basis molekularer Merkmale seit nunmehr zwanzig Jahren übereinstimmend auf eine Stellung in den Protostomia, und dort insbesondere innerhalb der Lophotrochozoa/Spiralia, hin. Diese Befunde legen die Abstammung der Phoronidenentwicklung von der sogenannten Spiralfurchung nahe, einem komplexen Entwicklungsmodus, der sowohl ein charakteristisches frühes Furchungsmuster sowie auch das Vorliegen spezifischer Zellschicksale umfasst.

Die Studie untersucht die frühe Furchung dreier verschiedener Phoronidenarten (*Phoronis pallida*, *Phoronis muelleri* und *Phoronis vancouverensis*) sowie die Schicksale der Einzelblastomeren des 2-Zell und des 4-Zell Stadiums der Art *P. pallida*. Der Furchungsprozess wird sowohl anhand 4D-mikroskopischer Aufnahmen der Entwicklung lebender Embryonen (für *P. pallida* und *P. muelleri*) als auch auf der Basis fixierter Embryonen in unterschiedlichen Furchungsstadien untersucht. Immunzytochemische Fluoreszenzmarkierungen der Mitosespindeln und Färbungen der Zellkerne am fixierten Material werden mittels Konfokaler Laserscanning-Mikroskopie analysiert. Derartige hochauflösende morphologische Methoden wurden bisher noch nie zur Untersuchung der Phoronidenfurchung herangezogen. Verschiedene morphologische Merkmale des Furchungsprozesses (die Neigung der Spindeln bzw. der Zellteilungsachsen relativ zur animal-vegetativ Achse, die Anzahl polständiger Blastomeren, das Auftreten von Polfurchen) werden quantitativ erfasst und vergleichend sowohl innerhalb der untersuchten Arten als auch zwischen den Arten analysiert. Für die Untersuchung der Zellschicksale werden einzelne

Blastomeren des *P. pallida* Embryos mit Fluoreszenzmarker in-vivo injiziert, und die Nachkommen dieser markierten Zelle in Hinblick auf ihre Lage sowie ihren Beitrag zur Bildung der Keimblätter in späteren Gastrulationsstadien ausgewertet.

Die Ergebnisse zeigen einen weitgehend übereinstimmenden Furchungsprozess des Eies von *P. pallida* und *P. muelleri*, jedoch eine davon abweichende Furchung des *P. vancouverensis* Keims. Bei allen drei Arten verlaufen die ersten beiden Furchungsteilungen in der Meridionalebene. Ab der dritten Furchung teilen sich die Zellen in *P. pallida* und *P. muelleri* Embryonen schräg zur animal-vegetativ Achse. Insbesondere die polständigen Blastomeren folgen einem Muster abwechselnd dextraler und sinistraler Furchungsteilungen. Dies steht im deutlichen Widerspruch zum Teilungsmuster der Radiärfurchung sowie zu bisherigen Beschreibungen. Im Gegensatz dazu verläuft die dritte Furchung bei *P. vancouverensis* äquatorial entlang der animal-vegetativ Achse, und nachfolgende Teilungen verlaufen sehr variabel – in den animalen Blastomeren oftmals schräg zur animal-vegetativ Achse, aber in den vegetativen Blastomeren tendenziell in meridionale und äquatoriale Richtungen. Gleichzeitig ist der Furchungsprozess aller drei Arten durch einen gewissen Grad an Variabilität gekennzeichnet. In einem allgemeinen Literaturvergleich werden grundlegende Charakteristika der Phoronidenfurchung sowie Unterschiede zwischen verschiedenen Arten beleuchtet. Die Unterschiede zwischen den hier untersuchten Arten und der Vergleich mit Literaturdaten lassen auf das Vorliegen unterschiedlicher Furchungsmuster innerhalb der Phoronida schließen. Diese scheinen teilweise mit den unterschiedlichen Entwicklungstypen innerhalb der Gruppe zu korrelieren. Rekonstruktionen des Grundmusters der Phoronidenfurchung auf der Basis vorliegender, jedoch widersprüchlicher, Hypothesen über die Verwandtschaften innerhalb der Phoronida erlauben keine abschließende Beurteilung, zeigen jedoch, dass ein Furchungsmuster wie es bei *P. pallida* und *P. muelleri* vorliegt nicht als Grundmuster ausgeschlossen werden kann. Dies und die vorliegenden Beobachtungen stehen im Widerspruch zur gegenwärtigen Auffassung, die Phoronidenfurchung sei zweifelsfrei einem Radiärtypus zuzurechnen.

Die Ergebnisse der Einzelzellmarkierungen lassen sich in diskreten Markierungsmustern beschreiben. Alle Blastomeren des 2-Zell und des 4-Zell Stadiums tragen bei *P. pallida* zur Bildung der drei Keimblätter (Ektoderm inklusive Apikalplatte, endodermaler Urdarm und Mesoderm) bei; jedoch gibt es gelegentliche Ausnahmen. Die Markierungsexperimente bestätigen morphologische Beschreibungen zur Gastrulation der Phoroniden. Die erste Furchungsteilung verläuft durch die spätere Bilateralsymmetrieachse des Embryos, jedoch in keinem kontanten Verhältnis dazu. Die Ergebnisse werden mit vorliegenden Literaturangaben

zu *P. vancouverensis* verglichen. Obwohl die beiden Arten deutliche Unterschiede in ihrem Furchungsmuster aufweisen, stimmen die Zellschicksale in frühen Embryonen weitgehend überein.

Abschließend werden die Ergebnisse mit dem Entwicklungsmodus der Spiralfurchung, wie er insbesondere bei Mollusca, Annelida und Nemertea vorliegt, verglichen. Tatsächlich zeigt die Furchung bei *P. pallida* und *P. muelleri* Übereinstimmungen zum Muster der Spiralfurchung, die bisher nicht wahrgenommen wurden. Auf Basis der breiten molekular-phylogenetischen Unterstützung für eine Stellung der Phoronida innerhalb der Spiralia/Lophotrochozoa, können diese Übereinstimmungen als morphologische Bestätigung interpretiert werden. Die Variabilität des Furchungsprozesses jedoch ist für eine typische Spiralfurchung unbekannt, ein stereotypes Spiralfurchungsmuster liegt nicht vor. Ebenso finden sich bei Phoroniden keine strikten frühen Zellschicksale und auch kein konstantes Orientierungsverhältnis zwischen der ersten Furchungsteilung und den späteren Körperachsen, wie es bei Tieren mit einer typischen Spiralfurchung zu finden ist. Die Übereinstimmungen und die Unterschiede zur Spiralfurchung werden im Lichte unterschiedlicher Mechanismen zur Spezifizierung von Zellschicksalen und Körperachsen bei Embryonen der oben genannten Spiraliagruppen und der Phoroniden diskutiert. Auf Grundlage der gegenwärtigen phylogenetischen Stellung, werden die Unterschiede zu einem klassischen Spiralfurchungsmuster als evolutionäre Modifikationen auf der Stammlinie zu den Phoronida (bzw. zu einem Monophylum Phoronida + Brachiopoda) interpretiert. Eine Veränderung des Zeitpunktes und des Mechanismus der Zellspezifikation in der Evolution der Gruppe wird als Ursache für die ungewöhnliche Variabilität der Phoronidenfurchung diskutiert.

6. References

Ackermann C, Dorresteijn A, Fischer A. 2005. Clonal domains in postlarval *Platynereis dumerilii* (Annelida: Polychaeta). *Journal of Morphology*, 266: 258-280.

Arenas-Mena C. 2007. Sinistral equal-size spiral cleavage of the indirectly developing polychaete *Hydroides elegans*. *Developmental Dynamics*, 236: 1611-1622.

Arnolds JM. 1974. Cleavage furrow formation in a telolecithal egg (*Loligo pealei*) III. Cell surface changes during cytokinesis as observed by scanning microscopy. *Developmental Biology*, 40: 225-232.

Ax P. 1995. Das System der Metazoa I. Ein Lehrbuch der phylogenetischen Systematik. Gustav Fischer: Stuttgart, Jena, New York.

Ax P. 2001. Das System der Metazoa III. Ein Lehrbuch der phylogenetischen Systematik. Spektrum: Heidelberg, Berlin.

Baguñà J, Martinez P, Paps J, Riutort M. 2008. Back in time: a new systematic proposal for the Bilateria. *Philosophical Transactions of the Royal Society B*, 363: 1481-1491.

Bartolomaeus T. 2001. Ultrastructure and formation of the body cavity lining in *Phoronis muelleri* (Phoronida, Lophophorata). *Zoomorphology*, 120: 135-148.

Boring L. 1986. Cell–cell interactions determine the dorsoventral axis in embryos of an equally cleaving opisthobranch mollusc. *Developmental Biology*, 136: 239-253.

Boschetti C, Ricci C, Sotgia C, Fascio U. 2005. The development of a bdelloid egg: a contribution after 100 years. *Hydrobiologia*, 546: 323-331.

Bourlat SJ, Nielsen C, Economou AD, Telford MJ. 2008. Testing the new animal phylogeny: A phylum level molecular analysis of the animal kingdom. *Molecular Phylogenetics and Evolution*, 49: 23-31.

Boyer BC, Henry JQ. 1998. Evolutionary modifications of the spiralian developmental program. *American Zoologist*, 38: 621-633.

Boyer BC, Henry JQ, Martindale MQ. 1996. Dual origins of mesoderm in a basal spiralian: cell lineage analyses in the polyclad turbellarian *Hoploplana inquilina*. *Developmental Biology*, 179: 329-338.

Boyer BC, Henry JJ, Martindale MQ. 1998. The cell lineage of a polyclad turbellarian embryo reveals close similarity to coelomate spiralians. *Developmental Biology*, 204: 111-123.

Brooks WK, Cowles RP. 1905. *Phoronis architecta*: its life history, anatomy, and breeding habits. *Memoirs of the National Academy of Sciences Washington*, 10: 75-113.

Brusca RC, Brusca GJ. 2003. Invertebrates. 2nd edition, Sinauer: Sunderland.

Caldwell WH. 1885. Blastopore, mesoderm and metameric segementation. *Quarterly Journal of Microscopical Science*, 25: 15-28.

Colwin AL, Colwin LH. 1953. The normal embryology of *Saccoglossus kowalevskii* (Enteropneusta). *Journal of Morphology*, 93: 401-453.

Conklin EG. 1897. The embryology of *Crepidula*, a contribution to the cell lineage and early development of some marine gasteropods. *Journal of Morphology*, 13: 1-227.

Conklin EG. 1902. The embryology of a brachiopod, *Terebratulina septentrionalis* Couthouy. *Proceedings of the American Philosophical Society*, 41: 41-76.

Cori CI. 1939. Phoronidea. Akademische Verlagsgesellschaft: Leipzig.

de Rosa R, Grenier JK, Andreeva T, Cookk CE, Adoutte A, Akamk M, Carroll SB, Balavoine G. 1999. Hox genes in brachiopods and priapulids and protostome evolution. *Nature*, 399: 772-776.

de Selys-Longchamps M. 1902. Recherches sur le développement des Phoronis. *Archives de Biologie*, 18: 495-597.

de Selys-Longchamps M. 1903. Über *Phoronis* und *Actinotrocha* bei Helgoland. *Wissenschaftliche Meeresuntersuchungen, Abteilung Helgoland*, 6: 1-55.

de Selys-Longchamps M. 1904. Développement postembryonnaire et affinités des Phoronis. *Académie royale de Belgique, Classe des sciences, collection 4, tome 1, fascule 1*: 1-150.

de Selys-Longchamps M. 1907. Phoronis. *Fauna und Flora des Golfes von Neapel und der angrenzenden Meeres-Abschnitte*, 30: 1-280.

Dohle W. 1999. The ancestral cleavage pattern of the clitellates and its phylogenetic deviations. *Hydrobiologia*, 402: 267-283.

Dohle W. 2013. Spiralia (Lophotrochozoa). In: Westheide W, Rieger G (eds). *Spezielle Zoologie*. 3rd edition, Spinger: Berlin, Heidelberg: 181-185.

Dorresteijn AWC, Borneswasser H, Fischer A. 1987. A correlative study of experimentally changes first cleavage and Janus development in the trunk of *Platynereis dumerilii* (Annelida, Polychaeta). *Roux's Archives of Developmental Biology*, 196: 51-58.

Dunn CW, Hejnol A, Matus DQ, Pang K, Browne WE, Smith SA, Seaver E, Rouse GW, Obst M, Edgecombe GD, Sørensen MV, Haddock SHD, Schmidt-Rhaesa A, Okusu A, Kristensen RM, Wheeler WC, Martindale MQ, Giribet G. 2008. Broad phylogenomic sampling improves resolution of the animal tree of life. *Nature*, 452: 745-749.

Emig CC. 1967. Considérations sur la systématique des Phoronidiens. II. *Phoronopsis harmeri* Pixell, 1912. *Bulletin de Muséum National d'Histoire naturelle*, 39: 984-991.

Emig CC. 1969. Considérations sur la systématique des Phoronidiens. III. *Phoronis psammophila* Cori, 1889, et *Phoronis architecta* Andrews, 1890. *Bulletin de Muséum National d'Histoire naturelle*, 41: 312-327.

Emig CC. 1971. Remarques sur la systématique des Phoronidea. X. Notes sur l'écologie, la morphologie et la taxonomie de *Phoronis ijimai* et de *P. vancouverensis*. *Marine Biology*, 8: 154-159.

Emig CC. 1974a. The systematics and evolution of the phylum Phoronida. *Zeitschrift für zoologische Systematik und Evolutionsforschung*, 12: 128-151.

Emig CC. 1974b. Observation et discussions sur le développement embryonnaire des Phoronida. *Zeitschrift für Morphologie der Tiere*, 77: 317-335.

Emig CC. 1977. Embryology of Phoronida. *American Zoologist*, 17: 21-37.

Emig CC. 1982. The biology of Phoronida. *Advances in Marine Biology*, 19: 1-89.

Emig CC. 1984. On the origin of Lophophorata. *Zeitschrift für zoologische Systematik und Evolutionsforschung*, 22: 91-94.

Emig CC. 1985. Phylogenetic systematics in Phoronida (Lophophorata). *Zeitschrift für zoologische Systematik und Evolutionsforschung*, 23: 184-193.

Emig CC. 1990. Phoronida. In: Adiyodi KG, Adiyodi RG (eds). *Reproductive biology of invertebrates*. John Wiley & Sons: Chichester, New York, Brisbane: 165-184.

Emig CC. 2010. Fossil Phoronida and their inferred ichnotaxa. *Notebooks on Geology*, Letter 2010/03: 1-5.

Emig CC, de Mittelwihr C. 1999. What is a phoronid? <http://paleopolis.rediris.es/Phoronida/; 17.1.2015>.

Emig CC, Marche-Marchad I. 1969. Considérations sur la systématique des Phoronidiens. VII. *Phoronis australis* Haswell, 1883. *Bulletin de Muséum National d'Histoire naturelle*, 41: 1244-1251.

Foettinger A. 1882. Note sur la formation du mésoderme dans la larve de *Phoronis hippocrepia*. *Archives de Biologie*, 3: 679-686.

Freeman G. 1991. The bases for and timing of regional specification during larval development in *Phoronis*. *Developmental Biology*, 147: 157-173.

Freeman G. 1993. Regional specification during embryogenesis in the articulate brachiopod *Terebratalia*. *Developmental Biology*, 160: 196-213.

Freeman G. 1995. Regional specification during embryogenesis in the inarticulate brachiopod *Glottidia*. *Developmental Biology*, 172: 15-36.

Freeman G. 1999. Regional specification during embryogenesis in the inarticulate brachiopod *Discinisca*. *Developmental Biology*, 209: 321-339.

Freeman G. 2000. Regional specification during embryogenesis in the craniiform brachiopod *Crania anomala*. *Developmental Biology*, 227: 219-238.

Freeman G. 2003. Regional specification during embryogenesis in rhynchonelliform brachiopods. *Developmental Biology*, 261: 268-287.

Freeman G. 2007. A developmental basis for the cambrian radiation. *Zoological Science*, 24: 113-122.

Freeman G, Lundelius JW. 1992. Evolutionary implications of the mode of D quadrant specification in coelomates with spiral cleavage. *Journal of Evolutionary Biology*, 5: 205-247.

Freeman G, Martindale MQ. 2002. The origin of mesoderm in phoronids. *Developmental Biology*, 252: 301-311.

Giribet G, Dunn CW, Edgecombe GD, Hejnol A, Martindale MQ, Rouse GW. 2009. Assembling the spiralian tree of life. In: Telford MJ, Littlewood DTJ (eds). *Animal Evolution: Genomes, Fossils, and Trees*. Oxford University: Oxford: 52-64.

Grande C. 2010. Left–Right asymmetries in Spiralia. *Integrative and Comparative Biology*, 50: 744-755.

Grobben K. 1908. Die systematische Einteilung des Tierreiches. *Verhandlungen der Zoologisch-Botanischen Gesellschaft in Wien*, 58: 491-511.

Grobe P. 2007. Larval development, the origin of the coelom and the phylogenetic relationships of the Phoronida. Dissertation, Freie Universität Berlin.

Groepler W. 1986. Die Entwicklung bei *Pomatoceros triqueter* L. (Polychaeta, Serpulidae) vom befruchteten Ei bis zur schwimmenden Blastula. *Zoologische Beiträge, NF* 29: 157-172.

Gruhl A, Grobe P, Bartolomaeus T. 2005. Fine structure of the epistome in *Phoronis ovalis*: significance for the coelomic organization in Phoronida. *Invertebrate Biology*, 124: 332-343.

Gruner E-H. 1980. Einführung. In: Gruner E-H (ed). *Lehrbuch der speziellen Zoologie*. 4th edition, Gustav Fischer: Jena: 15-156.

Guerrier P, van den Biggelaar JAM, van Dongen CAM, Verdonk NH. 1978. Significance of the polar lobe for the determination of dorsoventral polarity in *Dentalium vulgare* (da Costa). *Developmental Biology*, 63: 233-242.

Gundersen GG, Bulinski JC. 1986. Distribution of tyrosinated and nontyrosinated α-tubulin during mitosis. *The Journal of Cell Biology*, 102: 1118-1126.

Halanych KM, Bacheller JD, Aguinaldo AM, Liva SM, Hillis DM, Lake JA. 1995. Evidence from 18S ribosomal DNA that the lophophorates are protostome animals. *Science*, 267: 1641-1643.

Hatschek B. 1888. Lehrbuch der Zoologie. Gustav Fischer: Jena.

Hausdorf B, Helmkampf M, Nesnidal MP, Bruchhaus I. 2010. Phylogenetic relationships within the lophophorate lineages (Ectoprocta, Brachiopoda and Phoronida). *Molecular Phylogenetics and Evolution*, 55: 1121-1127.

Hejnol A. 2010. A twist in time - The evolution of spiral cleavage in the light of animal phylogeny. *Integrative and Comparative Biology*, 50: 695-706.

Hejnol A, Martindale MQ, Henry JQ. 2007. High-resolution fate map of the snail *Crepidula fornicata*: The origins of ciliary bands, nervous system, and muscular elements. *Developmental Biology*, 305: 63-76.

Hejnol A, Obst M, Stamatakis A, Ott M, Rouse GW, Edgecombe GD, Martinez P, Baguñà J, Bailly X, Jondelius U, Wiens M, Müller WEG, Seaver E, Wheeler WC, Martindale MQ, Giribet G, Dunn CW. 2009. Assessing the root of bilaterian animals with scalable phylogenomic methods. *Proceedings of the Royal Society B*, 276: 4261-4270.

Helfenbein KG, Boore JL. 2004. The mitochondrial genome of *Phoronis architecta* - Comparisons demonstrate that phoronids are lophotrochozoan protostomes. *Molecular Biology and Evolution*, 21: 153-157.

Helmkampf M, Bruchhaus I, Hausdorf B. 2008a. Multigene analysis of lophophorate and chaetognath phylogenetic relationships. *Molecular Phylogenetics and Evolution*, 46: 206-214.

Helmkampf M, Bruchhaus I, Hausdorf B. 2008b. Phylogenomic analyses of lophophorates (brachiopods, phoronids and bryozoans) confirm the Lophotrochozoa concept. *Proceedings of the Royal Society B*, 275: 1927-1933.

Henry JJ. 2002. Conserved mechanism of dorsoventral axis determination in equal-cleaving spiralians. *Developmental Biology*, 248: 343-355.

Henry J, Martindale MQ. 1987. The organizing role of the D quadrant as revealed through the phenomenon of twinning in the polychaete *Chaetopterus variopedatus*. *Roux's Archives of Developmental Biology*, 196: 499-510.

Henry JQ, Martindale MQ. 1994. Establishment of the dorsoventral axis in nemertean embryos: evolutionary considerations of spiralian development. *Developmental Genetics*, 15: 64-78.

Henry JJ, Martindale MQ. 1998. Conservation of the spiralian developmental program: cell lineage of the nemertean, *Cerebratulus lacteus*. *Developmental Biology*, 201: 253-269.

Henry JJ, Martindale MQ. 1999. Conservation and innovation in spiralian development. *Hydrobiologia*, 402: 255-265.

Henry JQ, Martindale MQ, Boyer BC. 1995. Axial specification in a basal member of the spiralian clade: lineage relationships of the first four cells to the larval body plan in the polyclad turbellarian *Hoploplana inquilina*. *Biological Bulletin*, 189: 194-195.

Henry JQ, Okusu A, Martindale MQ. 2004. The cell lineage of the polyplacophoran, *Chaetopleura apiculata*: variation in the spiralian program and implications for molluscan evolution. *Developmental Biology*, 272: 145-160.

Henry JQ, Tagawa K, Martindale MQ. 2001. Deuterostome evolution: early development in the enteropneust hemichordate, *Ptychodera flava*. *Evolution & Development*, 3: 375-390.

Herrmann K. 1981. *Phoronis muelleri* (Tentaculata) - Embryonalentwicklung. *Publikationen zu wissenschaftlichen Filmen, Sektion Biologie, Serie 14 (2) / Film E 2563*: 1-13.

Herrmann K. 1986. Die Ontogenese von *Phoronis mülleri* (Tentaculata) unter besonderer Berücksichtigung der Mesodermdifferenzierung und Phylogenese des Coeloms. *Zoologische Jahrbücher, Abteilung für Anatomie und Ontogenie der Tiere*, 114: 441-463.

Herrmann K. 1996. Tentaculata (Lophophorata). In: Westheide W, Rieger R (eds). *Spezielle Zoologie*. *I Einzeller und wirbellose Tiere*, Gustav Fischer: Stuttgart, Jena, New York: 737-754.

Herrmann K, Inst. Wiss. Film. 1980. *Phoronis muelleri* (Tentaculata) – Embryonalentwicklung. Institut für den Wissenschaftlichen Film: Göttingen: Film E 2563, doi: 10.3203/IWF/E-2563.

Hirose M, Fukiage R, Katoh T, Kajihara H. 2014. Description and molecular phylogeny of a new species of *Phoronis* (Phoronida) from Japan, with a redescription of topotypes of *P. ijimai* Oka, 1897. *ZooKeys*, 398: 1-31.

Hyman LH. 1940. The invertebrates: Protozoa through Ctenophora. McGraw-Hill: New York, London.

Hyman LH. 1959. The invertebrates: smaller coelomate groups. McGraw-Hill: New York, London, Toronto.

Ikeda I. 1901. Observations on the development, structure and metamorphosis of Actinotrocha. *The Journal of the College of Science, Imperial University of Tokyo*, 13: 507-592.

Ivanova-Kazas OM. 1977. Comparative embryology of invertebrate animals. Trochophorans, tentaculates, chaetognaths, and pogonophorans. Nauka: Moscow.

Jang KH, Hwang UW. 2009. Complete mitochondrial genome of *Bugula neritina* (Bryozoa, Gymnolaemata, Cheilostomata): phylogenetic position of Bryozoa and phylogeny of lophophorates within the Lophotrochozoa. *BMC Genomics*, 10:167.

Jeffery WR. 1992. Axis determination in sea urchin embryos: from confusion to evolution. *Trends in Genetics*, 8: 223-225.

Jenner RA. 2003. Unleashing the force of cladistics? Metazoan phylogenetics and hypothesis testing. *Integrative and Comparative Biology*, 43: 207-218.

Kaestner A. 1969. Lehrbuch der speziellen Zoologie, Band I: Wirbellose, 1. Teil. 3rd edition, Gustav Fischer: Jena.

Kume M. 1953. Some observations on the fertilization and the early development of *Phoronis australis*. *Natural Science Report of the Ochanomizu University*, 4: 253-256.

Lambert JD. 2008. Mesoderm in spiralians: the organizer and the 4d cell. *Journal of Experimental Zoology (Mol Dev Evol)*, 310B: 15-23.

Lechner M. 1966. Untersuchungen zur Embryonalentwicklung des Rädertieres *Asplanchna girodi* de Guerne. *Roux' Archiv für Entwicklungsmechanik*, 157: 117-173.

Leuckart R. 1869. Bericht über die wissenschaftlichen Leistungen in der Naturgeschichte der niederen Thiere während der Jahre 1866-1867. Nicolaische Verlagsbuchhandlung: Berlin.

Lillie FR. 1895. The embryology of the Unionidae: a study on cell-lineage. *Journal of Morphology*, 10: 1-101.

Luetjens CM, Dorresteijn AWC. 1995. Multiple, alternative cleavage patterns precede uniform larval morphology during normal development of *Dreissena polymorpha* (Mollusca, Lamellibranchia). *Development Genes and Evolution*, 205: 138-149.

Lüter C. 2004. Die Tentaculata im phylogenetischen System der Bilateria - gehören sie zu den Radialia oder den Lophotrochozoa? *Sitzungsberichte der Gesellschaft Naturforschender Freunde zu Berlin*, N.F. 43: 103-122.

Lüter C, Gruhl A, Bartolomaeus T. 2013. Lophophorata (Tentaculata), Tentakulaten. In: Westheide W, Rieger G (eds). *Spezielle Zoologie*. 3rd edition, Spinger: Berlin, Heidelberg: 229-251.

Mackey LY, Winnepenninckx B, de Wachter R, Backeljau T, Emschermann P, Garey JR. 1996. 18S rRNA suggests that Entoprocta are protostomes, unrelated to Ectoprocta. *Journal of Molecular Evolution*, 42: 552-559.

Malakhov VV, Temereva EN. 2000. Embryonic development of the Phoronid *Phoronis ijimai*. *Russian Journal of Marine Biology*, 26: 412-421.

Mallatt J, Winchell CJ. 2002. Testing the new animal phylogeny: first use of combined large-subunit and small-subunit rRNA gene sequences to classify the protostomes. *Molecular Biology and Evolution*, 19: 289-301.

Marcus E. 1958. On the evolution of the animal phyla. *The Quarterly Review of Biology*, 33: 24-58.

Marsden J. 1959. Phoronidea from the Pacific coast of North America. *Canadian Journal of Zoology*, 37: 87-111.

Marthy H-J. 1975. Organogenesis in Cephalopoda: further evidence of blastodisc-bound developmental information. *Journal of Embryology and Experimental Morphology*, 33: 75-83.

Martín-Durán JM, Egger B. 2012. Developmental diversity in free-living flatworms. *EvoDevo*, 3:7.

Maslakova SA, Martindale MQ, Norenburg JL. 2004. Fundamental properties of the spiralian developmental program are displayed by the basal nemertean *Carinoma tremaphoros* (Palaeonemertea, Nemertea). *Developmental Biology*, 267: 342-360.

Masterman AT. 1900. On the Diplochorda. III. The early development and anatomy of *Phoronis buskii*, McI. *Quarterly Journal of Microscopical Science*, 43: 375-418.

Mead AD. 1897. The early development of marine annelids. *Journal of Morphology*, 13: 227-327.

Merkel J, Wollesen T, Lieb B, Wanninger A. 2012. Spiral cleavage and early embryology of a loxosomatid entoproct and the usefulness of spiralian apical cross patterns for phylogenetic inferences. *BMC Developmental Biology*, 12:11.

Meyer NP, Boyle MJ, Martindale MQ, Seaver EC. 2010. A comprehensive fate map by intracellular injection of identified blastomeres in the marine polychaete *Capitella teleta*. *EvoDevo*, 1:8.

Nesnidal MP, Helmkampf M, Bruchhaus I, Hausdorf B. 2010. Compositional heterogeneity and phylogenomic inference of metazoan relationships. *Molecular Biology and Evolution*, 27: 2095-2104.

Nesnidal MP, Helmkampf M, Meyer A, Witek A, Bruchhaus I, Ebersberger I, Hankeln T, Lieb B, Struck TH, Hausdorf B. 2013. New phylogenomic data support the monophyly of Lophophorata and an Ectoproct-Phoronid c.lade and indicate that Polyzoa and Kryptrochozoa are caused by systematic bias. *BMC Evolutionary Biology*, 13:253.

Newby WW. 1932. The early embryology of the echiuroid, *Urechis*. *Biological Bulletin*, 63: 387-399.

Nielsen C. 2001. Animal evolution: Interrelationships of the living phyla. 2nd edition, Oxford University: Oxford, New York.

Nielsen C. 2002. The phylogenetic position of Entoprocta, Ectoprocta, Phoronida, and Brachiopoda. *Integrative and Comparative Biology*, 42: 685-691.

Nielsen C. 2004. Trochophora larvae: cell-lineages, ciliary bands and body regions. 1. Annelida and Mollusca. *Journal of Experimental Zoology (Molecular and Developmental Evolution)*, 302B: 35-68.

Nielsen C. 2005. Trochophora larvae: cell-lineages, ciliary bands and body regions. 2. Other groups and general discussion. *Journal of Experimental Zoology (Molecular and Developmental Evolution)*, 304B: 401-447.

Nielsen C. 2010. Some aspects of spiralian development. *Acta Zoologica*, 91: 20-28.

Nielsen C. 2012. Animal evolution: Interrelationships of the living phyla. 3rd edition, Oxford University: Oxford, New York.

Oka A. 1897. Sur une nouvelle espèce japonaise du genre Phoronis. *Annotationes zoologicae Japonenses*, 1: 147-148.

Paps J, Baguñà J, Riutort M. 2009a. Lophotrochozoa internal phylogeny: new insights from an up-to-date analysis of nuclear ribosomal genes. *Proceedings of the Royal Society B*, 276: 1245-1254.

Paps J, Baguñà J, Riutort M. 2009b. Bilaterian phylogeny: A broad sampling of 13 nuclear genes provides a new Lophotrochozoa phylogeny and supports a paraphyletic basal acoelomorpha. *Molecular Biology and Evolution*, 26: 2397-2406.

Passamaneck YJ, Halanych KM. 2004. Evidence from Hox genes that bryozoans are lophotrochozoans. *Evolution & Development*, 6: 275-281.

Patel NH. 1994. Imaging neuronal subsets and other cell types in whole mount *Drosophila* embryos and larvae using antibody probes. In: Goldstein LSB, Fyrberg EA (eds). *Methods in cell biology, Vol 44 Drosophila melanogaster: Practical uses in cell and molecular biology*. Academic Press: San Diego: 445-487.

Pixell HLM. 1912. Two new species of the Phoronidea from Vancouver Island. *Quarterly Journal of Microscopical Science*, 58: 257-284.

Rattenbury JC. 1951. Studies of embryonic and larval development in California Phoronidea. Dissertation, University of California.

Rattenbury JC. 1954. The embryology of *Phoronopsis viridis*. *Journal of Morphology*, 95: 289-349.

Render JA. 1989. Development of *Ilyanassa obsoleta* embryos after equal distribution of polar lobe material at first cleavage. *Developmental Biology*, 132: 241-250.

Riedl RJ. 1969. Gnathostomulida from America. *Science*, 163: 445-452.

Rimler R. 2013. Early development and spermatophore of the phoronid *Phoronopsis harmeri*. <http://invert-embryo.blogspot.de/2013/05/early-development-and-spermatophore-of.html>.

Roule L. 1900. Sur le développement embryonnaire des Phoronidiens. *Annales des Sciences Naturelles*, 11: 51-247.

Ruppert EE, Fox RS, Barnes RD. 2004. Invertebrate Zoology. 7th edition, Thomson: Belmont.

Sacks M. 1955. Observations on the embryology of an aquatic gastrotrich, *Lepidodermalla squamata* (Dujardin, 1841). *Journal of Morphology*, 96: 473-495.

Sandig M, Dohle W. 1988. The cleavage pattern in the leech *Theromyzon tessulatum* (Hirudinea, Glossiphoniidae). *Journal of Morphology*, 196: 217-252.

Santagata S. 2001. The larval development, settlement, and metamorphosis of *Phoronis pallida*. Dissertation, University of Southern California.

Santagata S. 2002. Structure and metamorphic remodeling of the larval nervous system and musculature of *Phoronis pallida* (Phoronida). *Evolution & Development*, 4: 28-42.

Santagata S. 2004a. Larval development of *Phoronis pallida* (Phoronida): Implications for morphological convergence and divergence among larval body plans. *Journal of Morphology*, 259: 347-358.

Santagata S. 2004b. A waterborne behavioral cue for the actinotroch larva of *Phoronis pallida* (Phoronida) produced by *Upogebia pugettensis* (Decapoda: Thalassinidea). *Biological Bulletin*, 207: 103-115.

Santagata S. 2012. Revaluating spiral-like cell cleavage patterns during the embryonic development of phoronids and brachiopods. *Society for Integrative and Comparative Biology Annual Meeting 2012*, Abstract Book: 26.22.

Santagata S, Cohen BL. 2009. Phoronid phylogenetics (Brachiopoda; Phoronata): evidence from morphological cladistics, small and large subunit rDNA sequences, and mitochondrial *cox1*. *Zoological Journal of the Linnean Society*, 157: 34-50.

Santagata S, Zimmer RL. 2002. Comparison of the neuromuscular systems among actinotroch larvae: systematic and evolutionary implications. *Evolution & Development*, 4: 43-54.

Schiemann S, Hejnol A. 2011. A 4D-microscopic analysis of the cell lineage of the bdelloid rotifer *Adineta vaga*. *2nd International Congress on Invertebrate Morphology*, Abstract Book: 134.

Schleip W. 1929. Die Determination der Primitiventwicklung. Akademische Verlagsgesellschaft: Leipzig.

Schnabel R, Hutter H, Moerman D, Schnabel H. 1997. Assessing normal embryogenesis in *Caenorhabditis elegans* using a 4D microscope: variability of development and regional specification. *Developmental Biology*, 184: 234-265.

Scholtz G. 2010. Deconstructing morphology. *Acta Zoologica*, 91: 44-63.

Schram FR. 1991. Cladistic analysis of metazoan phyla and the placement of fossil problematica. In: Simonetta AM, Conway Morris S (eds). *The early evolution of Metazoa and the significance of problematic taxa*. Cambridge University: Cambridge: 35-46.

Schwartz V. 1973. Vergleichende Entwicklungsgeschichte der Tiere. Georg Thieme: Stuttgart.

Siewing R. 1969. Lehrbuch der vergleichenden Entwicklungsgeschichte der Tiere. Paul Parey: Hamburg, Berlin.

Siewing R. 1980. Das Archicoelomatenkonzept. *Zoologische Jahrbücher, Abteilung für Anatomie und Ontogenie der Tiere*, 103: 439-482.

Silén L. 1952. Researches on Phoronidea of the Gullmar Fiord area (West coast of Sweden). *Arkiv för Zoologi*, 4: 95-140.

Silén L. 1954. Developmental biology of Phoronidea of the Gullmar Fiord area (West coast Sweden). *Acta Zoologica*, 35: 215-257.

Smart TI, von Dassow G. 2009. Unusual development of the Mitraria larva in the polychaete *Owenia collaris*. *Biological Bulletin*, 217: 253-268.

Sonnleitner B, Schwaha T, Wanninger A. 2013. Inter- and intraspecific plasticity in distribution patterns of immunoreactive compounds in actinotroch larvae of Phoronida (Lophotrochozoa). *Journal of Zoological Systematics and Evolutionary Research*, 52: 1-14.

Tannreuther GW. 1920. The development of *Asplanchna ebbesbornii* (Rotifer). *Journal of Morphology*, 33: 388-437.

Tardent P. 1978. Coelenterata, Cnidaria. In: Seidel F (ed). *Morphogenese der Tiere, Lieferung 1: A-I*. Gustav Fischer: Jena.

Temereva EN. 2012. Ventral nerve cord in *Phoronopsis harmeri* larvae. *Journal of Experimental Zoology (Molecular and Developmental Evolution)*, 318: 26-34.

Temereva EN. 2009. New data on distribution, morphology and taxonomy of phoronid larvae (Lophophorata: Phoronida). *Invertebrate Zoology*, 6: 47-64.

Temereva EN, Malakhov VV. 2007. Embryogenesis and larval development of *Phoronopsis harmeri* Pixell, 1912 (Phoronida): dual origin of the coelomic mesoderm. *Invertebrate Reproduction and Development*, 50: 57-66.

Temereva EN, Malakhov VV. 2012. Embryogenesis in phoronids. *Invertebrate Zoology*, 9: 1-39.

Temereva EN, Tsitrin EB. 2013. Development, organization, and remodeling of phoronid muscles from embryo to metamorphosis (Lophotrochozoa: Phoronida). *BMC Developmental Biology*, 13:14.

Temereva E, Wanninger A. 2012. Development of the nervous system in *Phoronopsis harmeri* (Lophotrochozoa, Phoronida) reveals both deuterostome- and trochozoan-like features. *BMC Evolutionary Biology*, 12:121.

Teuchert G. 1968. Zur Fortpflanzung und Entwicklung der Macrodasyoidea (Gastrotricha). *Zeitschrift für Morphologie der Tiere*, 63: 343-418.

Torrey JC. 1903. The early embryology of *Thalassema mellita* (Conn). *Annals of the New York Academy of Sciences*, 14: 165-246.

Treadwell AL. 1901. The cytogeny of *Podarke obscura*. *Journal of Morphology*, 17: 399-486.

Ulrich W. 1972. Die Geschichte des Archicoelomatenbegriffs and die Archicoelomatennatur der Pogonophoren. *Zeitschrift für Systematik und Evolutionsforschung*, 10: 301-320.

van den Biggelaar JAM. 1977. Development of dorsoventral polarity and mesentoblast determination in *Patella vulgata*. *Journal of Morphology*, 154: 157-186.

van den Biggelaar JAM. 1996. Cleavage pattern and mesentoblast formation in *Acanthochiton crinitus* (Polyplacophora, Mollusca). *Developmental Biology*, 174: 423-430.

van den Biggelaar JAM, Dictus WJAG, van Loon AE. 1997. Cleavage pattern, cell-lineages and cell specification are clues to phyletic lineages in Spiralia. *Seminars in Cell & Development Biology*, 8: 367-378.

van den Biggelaar JAM, Guerrier P. 1979. Dorsoventral polarity and mesentoblast determination as concomitant results of cellular interactions in the mollusk *Patella vulgata*. *Developmental Biology*, 68: 462-471.

Vellutini B, Hejnol A. 2014. Remnants of spiral cleavage in bryozoans. *3rd International Congress on Invertebrate Morphology*, Abstract Book: 61.

Voigt E. 1975. Tunnelbaue rezenter und fossiler Phoronidea. *Paläontologische Zeitschrift*, 49: 135-167.

Wadeson PH, Crawford K. 2003. Formation of the blastoderm and yolk syncytial layer in early squid development. *Biological Bulletin*, 205: 179-180.

Woltereck R. 1904. Beiträge zur praktischen Analyse der Polygordius-Entwicklung nach dem »Nordsee-« und dem »Mittelmeer-typus«. I. Der für beide Typen gleich verlaufende Entwicklangsabschnitt: vom Ei bis zum jüngsten Trochophora-Stadium. *Archiv für Entwicklungsmechanik*, 18: 377-403.

Wu B, Chen M, Sun R. 1980. On the occurrence of *Phoronis ijimai* Oka in the Huang Hai, with notes on its larval development. *Studia Marina Sinica*, 16: 101-112.

Zimmer RL. 1964. Reproductive biology and development of Phoronida. Dissertation, University of Washington.

Zimmer RL. 1967. The morphology and function of accessory reproductive glands in the lophophores of *Phoronis vancouverensis* and *Phoronopsis harmeri*. *Journal of Morphology*, 121: 159-178.

Zimmer RL. 1973. Morphological and developmental affinities of the Lophophorates. In: Larwood GP (ed). *Living and fossil Bryozoa: recent advances in research*. Academic Press: London, New York: 593-599.

Zimmer RL. 1980. Mesoderm proliferation and formation of the protocoel and metacoel in early embryos of *Phoronis vancouverensis* (Phoronida). *Zoologische Jahrbücher, Abteilung für Anatomie und Ontogenie der Tiere*, 103: 219-233.

Zimmer RL. 1997. Phoronids, brachiopods, and bryozoans, the lophophorates. In: Gilbert SF, Raunio AM (eds). *Embryology: Constructing the organism*. Sinauer: Sunderland: 279-305.

7. Supplementary Material

Time-lapse videos, which show the early cleavage process in different specimens of *P. pallida* (Video_S1-S6) and of *P. muelleri* (Video_S7-S9), are provided on the attached DVD. All videos are provided as avi-file format and as mov-file format.
The videos are based on the performed 4D microscopic recordings. Video_S1 to S3 and Video_S7 to S9 show the cleavage divisions (beyond the 4-cell stage) in two different focal planes: on the left side of the video the focus is on the animal blastomeres in the embryo, and on the right side the focus is on the vegetal blastomeres. Note, that different embryos were recorded with either the animal pole or the vegetal pole facing toward the camera/the objective (specified in the captions). The video of the pole that was facing to the camera is of course of better quality, while the visibility of the respective opposite pole is obscured by the cells that lie in between the camera-facing pole and that opposite pole. Importantly, this furthermore means that in each embryo the cleavage process is seen from the perspective of that pole that was facing to the camera (thus, both poles are seen from either an animal or a vegetal perspective). Video_S4 to S6 show the divisions only on the one pole that was facing to the camera (see captions). The inserts in the videos give a three-dimensional model of the nuclei in the embryo, in the respective (animal or vegetal) perspective of the video: each dot represents a nucleus, nuclei of the four embryonic quadrants are marked with different colors, and the bigger a dot is the closer to the camera the nucleus is located.

Video_S1: Cleavage in the animal blastomeres (left side) and in the vegetal blastomeres (right side) of a *P. pallida* embryo, from the zygote to the 64-cell stage (recorded with the animal pole facing toward the camera; the polar bodies are visible in the left video). The compactation of the embryo following each division cycle is visible. The twisted cell elongations that precede the dextral third divisions are well recognizable. From the fifth cell cycle on, the divisions pass with some irregularity (and asynchrony) in the animal blastomeres, but with more regularity in the vegetal blastomeres. A vegetal polar furrow is formed at the 64-cell stage (right side).

Video_S2: Same as Video_S1, in a *P. pallida* embryo from the 4-cell stage to the 64-cell stage. In one blastomere of the animal cell tiers (lower left cell on left video), the divisions pass irregular already from the fourth cell cycle on. The cleavage process generally is more regular in the vegetal blastomeres.

Video_S3: Cleavage in the animal blastomeres (left side) and in the vegetal blastomeres (right side) of a *P. pallida* embryo, from the 2-cell stage to the 64-cell stage. This embryo was recorded with the vegetal pole facing toward the camera. The oblique blastomere elongations preceding each cell division are well visible.

Video_S4: Cleavage in the animal blastomeres of a *P. pallida* embryo, from the zygote to the 64-cell stage (recorded with the animal pole facing toward the camera).

Video_S5: Cleavage in the vegetal blastomeres of a *P. pallida* embryo, from the zygote to the 64-cell stage (recorded with the vegetal pole facing toward the camera). At the 32-cell and the 64-cell stage, a vegetal polar furrow is formed.

Video_S6: Same as Video_S5, in a *P. pallida* embryo the 2-cell stage to the 64-cell stage. A vegetal polar furrow already is formed by the 16-cell stage.

Video_S7: Cleavage in the animal blastomeres (left side) and in the vegetal blastomeres (right side) of a *P. muelleri* embryo, from 3-cell stage to the 64-cell stage (recorded with the animal pole facing toward the camera). The polar bodies are visible (left video), and later become intercalated between the four animal blastomeres; the vegetal blastomeres form a polar furrow at the 32-cell and 64-cell stage.

Video_S8: Cleavage in the animal blastomeres (left side) and in the vegetal blastomeres (right side) of a *P. muelleri* embryo, from the 2-cell stage to the 64-cell stage (recorded with the vegetal pole facing toward the camera). The oblique blastomere elongations preceding each cell division are well recognizable. The animal blastomeres appear to form a polar furrow from the 8-cell stage on, the vegetal blastomeres form a polar furrow from the 16-cell stage on.

Video_S9: Same as Video_S8, in a *P. muelleri* embryo from the 2-cell stage to the 64-cell stage. The compactation of the embryo following each division cycle is well recognizable, and established a polar furrow already at the 4-cell stage. The twisted cell elongations that precede the dextral third division are particularly distinct at the vegetal cell apices (right video).

Acknowledgements

I am grateful to my supervisor Prof. Dr. Gerhard Scholtz for introducing me into the field of animal embryology and development, and for providing me with the opportunity to work on my PhD project in his working group “Vergleichende Zoologie” (Comparative Zoology) at the Humboldt-Universität zu Berlin.

Gerhard and all the (former and recent) members of the working group are deeply thanked. Many of them supported this work by calling my attention to new publications, by commenting on my results, by discussing my ideas with me, or by helping me with technical problems. In particular, I want to thank Frederike Alwes, Caterina Biffis, Georg Brenneis, Ekaterina “Katya” Ponomarenko, Petra Ungerer, and Carsten Wolff, who introduced me to the techniques of 4D microscopy, immunocytochemistry, confocal laser-scanning microscopy, single cell in-vivo labeling, and to different computer software. Renate Mbacke is thanked for her help with laboratory procedures, and for cutting semithin sections of embryos. Caterina, Katya, and Carsten helped with the handling of the in-vivo labeling experiments. Georg, Katya, and Carsten took the patience to read and comment on former versions of this manuscript. Katya helped during the stress of the final print production.

I thank Peter Grobe for introducing me to phoronids, and for his help with the localization, the determination, and the keeping of *P. pallida* and *P. muelleri* specimens.
The staff and the ship crews of the Biologische Anstalt Helgoland are thanked for facilitating and supporting my repeated work periods on Heligoland. In particular, I am grateful to Reinhard Saborowski for his support in organizing ship time and sampling trips around Heligoland. Some of his students are thanked for helping in collecting specimens.
Richard Strathmann and the staff of the Friday Harbor Laboratories are thanked for facilitating my work on San Juan Island, and for providing me with the opportunity to present and discuss some of my results at an FHL institute meeting. I am grateful to Richard Strathmann and Fernanda Oyarzun for their help in the localization and the sampling of *P. vancouverensis* specimens.

For financial support, I am thankful to the Deutsche Forschungsgemeinschaft (DFG), which supported this study under the Priority Program “Deep Metazoan Phylogeny”, and to the

Deutscher Akademischer Austausch Dienst (DAAD) and the Humboldt-Universität zu Berlin, which provided my with a stipend at the end of the project.

Last, but not least, I am deeply thankful to my family and to my friends, who supported me and this project with a lot of understanding and encouragement during the past years. Among many other things. This work would not have been possible without them.

Veröffentlichungen

Publikationen

Pennerstorfer M, Scholtz G. 2012. Early cleavage in *Phoronis muelleri* (Phoronida) displays spiral features. *Evolution & Development*, 14: 484-500.

Szucsich NU, Pennerstorfer M, Wirkner CS. 2011. The mouthparts of *Scutigerella immaculata*: Correspondences and variation among serially homologous head appendages. *Arthropod Structure & Development*, 40: 105-121.

Vorträge und Poster

Pennerstorfer M, Scholtz G: Early cleavage in Phoronida shows spiral features. *Deep Metazoan Phylogeny 2011 – new data, new challenges*. Munich, Germany. Zitteliana, B 30: 38.

Pennerstorfer M, Scholtz G: Spiral features in the early cleavage of Phoronida. *Friday Harbor Laboratories Meeting*. 2011. San Juan (WA), USA.

Pennerstorfer M, Scholtz G: Spiral features in the early cleavage of Phoronida. *2nd International Congress on Invertebrate Morphology*. 2011. Cambridge (MA), USA.

Szucsich NU, Pennerstorfer M, Wirkner CS: The myriapod challenge: Evolutionary morphology of the symphylan head. *1st International Congress on Invertebrate Morphology*. 2008. Copenhagen, Denmark. Journal of Morphology, 269: 1476.

Pennerstorfer M, Szucsich NU, Pass G: Leg musculature and thoracic endoskeleton in Symphyla (Myriapoda) – Useful structures for homologization of podomeres? (Poster). *1st International Congress on Invertebrate Morphology*. 2008. Copenhagen, Denmark. Journal of Morphology, 269: 1494.

Hable M, Szucsich NU, Pennerstorfer M, Walzl M, Pass G: 3D-reconstruction in arthropods: advantages and disadvantages of semi-thin section series and tomography. *99. Annual Meeting of the German Zoological Society*. 2006. Münster, Germany.

Pennerstorfer M, Szucsich NU, Pass G: Legs of the symphylan *Scutigerella* sp. in comparison to other myriapods and apterygotes. (Poster). *VIIth International Seminar on Apterygota*. 2006. Texel, Netherlands.

Selbstständigkeitserklärung

Hiermit versichere ich, dass ich die vorliegende Dissertation selbstständig und nur unter Verwendung der angegebenen Quellen und Hilfsmittel erarbeitet und verfasst habe. Diese Arbeit wurde keiner anderen Prüfungsbehörde vorgelegt.

Berlin, den